# The effects of acid sphingomyelinase on endothelial cell function and its role in chronic inflammatory disease

**By**

**Allan Panagiotis Kiprianos**

A thesis submitted to the

University of Birmingham

for the degree of

DOCTOR OF PHILOSOPHY

Rheumatology Research Group

School of Immunity and Infection

Institute of Biomedical Research

College of Medical and Dental Sciences

University of Birmingham

February 2011

UNIVERSITY OF
BIRMINGHAM

## University of Birmingham Research Archive

### e-theses repository

This unpublished thesis/dissertation is copyright of the author and/or third parties. The intellectual property rights of the author or third parties in respect of this work are as defined by The Copyright Designs and Patents Act 1988 or as modified by any successor legislation.

Any use made of information contained in this thesis/dissertation must be in accordance with that legislation and must be properly acknowledged. Further distribution or reproduction in any format is prohibited without the permission of the copyright holder.

## Abstract

Accelerated atherosclerosis and cardiovascular disease are seen in patients with primary vasculitis (PSV) and rheumatoid arthritis (RA). The mechanisms behind this remain unclear, but recent studies have linked it to endothelial cell dysfunction (ECD), which may result from the vasculitis also seen in RA, secondary to the joint disease. TNFα has been shown to induce ECD *in vitro* and *in vivo* through poorly understood mechanisms, but other pro-inflammatory cytokines can induce secretion of acid sphingomyelinase (ASM) from EC. ASM has been shown to induce reduced intracellular $Ca^{2+}$ ($_{i}Ca^{2+}$) signalling responses in lymphocytes through ceramide generation. Since NO production in EC is tightly coupled to agonist-induced $_{i}Ca^{2+}$ responses, this thesis set out to investigate whether inflammatory mediator-induced secretion of ASM (S-SMase) could regulate EC function through changes in $_{i}Ca^{2+}$ responses. The activity of S-SMase in blood from patients with RA and primary vasculitis was also assessed to underline the clinical relevance of the hypothesis.

Patients (n=20) with ANCA-associated systemic vasculitis (AASV) had high levels of S-SMase (114.8 ± 41 pmol/mL/$h^{-1}$) in their blood compared to 13 healthy controls (52.3 ± 35 pmol/mL/$h^{-1}$). These levels fell following induction of remission by 14 weeks (96.7 ± 41 pmol/mL/$h^{-1}$) and remained low at 6 months (33.7 ± 14 pmol/mL/$h^{-1}$). Raised active blood S-SMase was also confirmed in 35 patients with RA (84.1 ± 35 pmol/mL/$h^{-1}$) where enzyme activity correlated with several CV risk factors. TNFα directly induced the secretion of a redox-sensitive and enzymatically active S-SMase from human umbilical vein EC (HUVEC), a process blocked by antibody-mediated inhibition of TNFα. Exposure of HUVEC to ASM inhibited $_{i}Ca^{2+}$ signals in response to bradykinin. Subsequent studies on endothelial nitric oxide synthase (eNOS) suggested that exogenous ASM could alter eNOS phosphorylation at $Ser^{1177}$ responsible for its activation, while ASM may also decrease NO production in HUVEC.

We propose that TNFα and the prevalent oxidative environment at sites of vascular inflammation could promote increased activation and secretion of S-SMase that would act systemically on EC causing diffuse, widespread ECD promoting the development of atherosclerosis in inflammatory disease.

**Dedicated to my family**

## Acknowledgments

First and foremost I would like to thank my supervisors Dr. Stephen Young and Professor Paul Bacon for the opportunity to work with them and undertake a Ph.D. in their laboratory. I have been fortunate to gain much under their guidance. The work outlined in this thesis was supported and funded by the Elkin Foundation and the Birmingham Arthritis Appeals Trust for which I am very grateful.

Critically I am ever grateful to Professor Caroline Savage, Dr. Mark little, Dr. Matt Morgan and Professor Loraine Harper for the supply of clinical samples from patients with primary vasculitis and importantly for always being available. I would also like to thank Professor George Kitas and the team at Russell's Hall Hospital, Dudley, for their supply and assistance with clinical samples from rheumatoid arthritis patients. Finally, I am grateful to Professor Janet Lord for supplying healthy control samples and for her help throughout. Without the supply of this material from all the above, none of the outcomes of this study would have been possible.

I would like to extend to my gratitude to Dr. John Curnow, Dr Andrew Filer, Dr. Karim Raza and Dr. Dagmar Scheel-Toellner for their guidance, support and critique of my work. I would still like to express my appreciation to Professor Chris Buckley for being a great person to work with. I would like to thank Professor Bryan Turner and Dr. Karl Nightingale for their support and friendship. A great thank you is owed to Katherine Howlett for her endless help in the laboratory and for somehow always having an answer/solution to my problems. This also applies to Hema Chahal who in similar fashion was always available. Dr. Peter Hampson, like so many on this page, was a great person to work with and am indebted for his consultation on my work and day-to-day antics. I would like to thank Dr. Jason Wing Lee for his help and guidance in the lab whenever needed. Similarly this extends Dr. Nigel Francis for his friendship and advice at on my work. I owe a special thank you to my friend and flatmate Elsa Boudadi, whose patience and advice helped me through much of the past four years. I am indebted to Teresa for her endless, continuing support and inspiration during my Ph.D. I would also like to extend my gratitude to individuals on the 3$^{rd}$ floor of the IBR, past and present, including Alistair, Fern, Sarah, Geraint, Annelise, Steve, Ester, Loraine, Sherine, Jawaher, Caroline, Marianne, Celia, Sian, Ewan and Narrinder in no particular order for being wonderful colleagues.

Generally, I am very grateful to all my friends and colleagues for making my time very enjoyable. I would like to thank the staff at the Institute for Biomedical Research for all of their help. Over the past four years I was fortunate to take part in many great seminars and meetings within the College of Medical and Dental Sciences, which I believe allowed me to gain a comprehensive insight into biomedical and clinical research. Finally I would like to thank my dad George, mother Janet and brother Jason for their continuous support throughout my life leading to this point.

A special acknowledgment must go to the donors of umbilical cords from Birmingham Women's hospital. Again, without this none of the above would have been possible.

# Table of Contents

## CHAPTER 1

## 1 GENERAL INTRODUCTION

## Abbreviations

| | |
|---|---|
| Ab | AntiBody |
| ACPA | Anti-Cyclic citrullinated Peptide Antibody |
| ACC | Acetyl Coenzyme (A) Carboxylase |
| AEBSF | [4-(2-aminoethyl)benzenesulfonyl fluoride hydrochloride] |
| AICAR | 5-Aminoimidazole-4-carboxamide-1-βribofuranoside |
| AMPK | Adenosine MonoPhosphate-activated protein Kinase |
| AMP/ATP | Adenosine MonoPhosphate/Adenosine TriPhosphate |
| ANCA | Anti-Neutrophil Cytoplasm Antibodies |
| AASV | ANCA Associated Systemic Vasculitis |
| AAPH | 2,2-azobis (2-amidinopropane) dihydrochloride |
| ASMase (ASM) | Acid Sphingomyelinase |
| bSMase | bacterial Sphingomyelinase |
| BCAEC | Bovine Coronary Artery Endothelial Cell |
| bFGF | Basal Fibroblast Growth Factor |
| BVAS | Birmingham Vasculitis Activity Score |
| $_{i}Ca^{2+}$ | Intra-cellular molecular calcium; $_{i}[Ca^{2+}]$ |
| $Ca^{2+}$ | Calcium |
| CaM | Calmodulin |
| CaMKII | Calcium/Calmodulin-dependent Kinase II (CaMK2) |
| CCA | Common Carotid Artery |
| CD | Cluster of Differentiation |
| Cer | Ceramide |
| CHCC | Chapel Hill Consensus Conference |
| CHO | Chinese Hampster Ovary cells |
| CNS | Central Nervous System |
| CSS | Churg-Strauss Syndrome |
| CSP | Constitutive Secretory Pathway |
| CYC | CYcloPhosphamide |
| DAN | 2,3-DiAminoNaphthalene |
| DAF-2 | DiAminoFluorescein-2 |
| DAG | DiAcylGlycerol |
| DD | Death Domain |
| DMEM | Dulbeco's Modified Eagles Medium |
| DMSO | DiMethyl SulfOxide |
| DTT | DiThioThreitol |
| EC | Endothelial Cell |
| ECD | Endothelial Cell Dysfunction |
| EGF | Endothelial Growth Factor |
| EGTA | Ethylene Glycol Tetraacetic Acid |
| EL | Endothelial Lipase |
| eNOS | Endothelial Nitric Oxide Synthase |
| EPC | Endothelial Progenitor Cell |
| ER | Endoplasmic Reticulum |

| | |
|---|---|
| ERK | Extracellular signal Regulated Kinase |
| FAN | Factor-Associated with Neutral sphingomyelinase |
| FCS | Fetal Calf Serum |
| GCA | Giant Cell Arteritis |
| GPA | Granulomatosis with PolyAngiitis |
| GPCR | G-Protein Coupled Receptor |
| GSH | Glutathione (reduced) |
| GSSG | Glutathione (oxidised) |
| $H_2O_2$ | Hydrogen eroxide |
| HBSS | Hank's Buffered Saline Solution (not loaded with $Mg^{2+}$ and $Ca^{2+}$) |
| HBSS-$Ca^{2+}$ | HBSS loaded with $Mg^{2+}$ and $Ca^{2+}$ |
| HEPES | 4-(2-hydroxyethyl)-1-piperazine ethane sulphonic acid |
| HESFM | Human Endothelial Serum-Free Medium |
| HIFCS | Heat Inactivated Fetal Calf Serum |
| HPLC | High Performance/Pressure Liquid Chromatography |
| HSP | Henoch-Schonlein Purpura |
| hSerum | Human Serum |
| hEGF | Human Endothelial Growth Factor |
| hSMase | Human SMase (sphingomyelinase) |
| HRP | Horseradish Peroxidise |
| $_{i}Ca^{2+}$ | intracellular Molecular Calcium |
| Ig | ImmunoGlobulin |
| IL | Interleukin |
| $IP_3$ | Inositol triPhosphate |
| kDa | Kilo Dalton |
| KLH | Keyhole Limpet Hemocyanin |
| LKB1 | Liver Kinase B1 |
| LR | Lipid Raft |
| L-SMase | Lysosomal SphingoMyelinase (ASM splice variant) |
| MCF-7 | Michigan Cancer Foundation 7, breast carcinoma cell line |
| MHC | Major Histocompatibility Complex |
| MI | Myocardial Infarction |
| MMP | Matrix MetalloProteinase |
| MPA | Microscopic PolyAngiitis |
| MPO | MyeloPerOxidase |
| MTS | (3-(4,5-Dimethylthiazol-2-yl)-5-(3-carboxymethoxyphenyl)-2-(4-sulfophenyl)-2H-tetrazolium) |
| MTX | MeThotreXate |
| M199 | Medium 199 |
| M-6-P | Mannose-6-Phosphate |
| NADH | reduced Nicotinamide Adenine Dinucleotide |
| NBD | 7-Nitro-2,1,3-BenzoxaDiazol-4-yl |
| NBD-SM | (NBD-sphingomyelin); NBD $C_6$-sphingomyelin (6-((*N*-(7-nitrobenz-2-oxa-1,3-diazol-4-yl)amino)hexanoyl) sphingosyl phosphocholine) |
| NF kB | Nuclear Factor Kappa B |
| NO | Nitric Oxide |

| | |
|---|---|
| NPD | Niemann-Pick Disease |
| NSMase | (nSMase) Neutra SphingoMyeliase |
| PAN | Polyarteritis Nodosa |
| PB | Peripheral Blood |
| PBS | Phosphate-Buffered Saline |
| PCR | Polymerase Chain Reaction |
| $PIP_2$ | PhosphatidylInositol 4,5-biPhosphate |
| PKCδ | Protein kinase C delta |
| PKG | cGMP-dependent protein kinase G (Protein Kinase G) |
| PLC | PhosphoLipase C |
| PMCA | Plasma Membrane Calcium ATPase (pump) |
| PMR | Polymyalgia Nodosa |
| PR3 | Proteinase 3 |
| PSV | Primary Systemic Vasculitis |
| PTP | Protein Tyrosine Phosphatase |
| RA | Rheumatoid Arthritis |
| rhASM | Recombinant Human Acid Sphingomyelinase |
| Rho | Rho family of GTPases |
| ROS | Reactive Oxygen Species |
| RPMI | Roswell Park Memorial Institute (medium) |
| RIPA | RadioImmunoPrecipitation Assay (buffer) |
| SD | Standard Deviation |
| SDS PAGE | Sodium Dodecyl Sulphate PolyAcrylamide Gel Electrophoresis |
| SEM | Standard Error of the Mean |
| SERCA | Sarco/Endoplasmic Reticulum Calcium ATPase (pump) |
| SF | Synovial Fluid |
| SM | Sphingomyelin |
| SMase | Sphingomyelinase |
| S-SMase | Secretory Sphingomyelinase (ASM splice variant) |
| STIM | STromal Interacting Molecule |
| S1P | Sphingosine-1-Phosphate |
| TAK | Takayasu's Arteritis |
| TBS | Tris-buffered Saline |
| TEMED | N,N,N',N'-Tetramethylethylenediamine |
| TGF | Transforming Growth Factor |
| TLC | Thin Layer Chromatography |
| TNFα | Tumour Necrosis Factor Alpha |
| TRAIL | TNF-Related Apoptosis Inducing Ligand |
| v/v | Volume over Volume (volume/volume) |
| VDI | Vasculitis Damage Index |
| WG | Wegener's Granulomatosis |
| x 3 | Three times (referring to repetition of a procedure) |

* The terms ASM/S-SMase/L-SMase are used interchangeably. ASM refers to the pre-cursor protein, a generic term for the acid fraction of sphingomyelinase. Secreted protein (S-SMase) can be referred to as secretory ASM. L-SMase refers to the lysosomal fraction.

# List of figures

## Chapter 1



## Chapter 2



## Chapter 3

## Chapter 4



## Chapter 5



## Chapter 6



## Appendices

# List of tables

## Chapter 2



## Chapter 3

# Chapter 1

# General Introduction

# 1 General introduction

## 1.1 Rheumatoid arthritis

Rheumatoid arthritis (RA) is an autoimmune inflammatory disease that affects approximately 1% of the population, it typically occurs in those between 40-70 years old (Harris, 1990, Hochberg, 1981). Its cardinal features include chronic inflammation and synovial hyperplasia characterised by infiltration of blood-derived inflammatory cells into the synovial space. The clinical course of RA varies from early self-limiting disease to chronic, destructive multisystem inflammation (Lee and Weinblatt, 2001) often associated with excess morbidity, mortality and decreased life expectancy (Pincus and Callahan, 1993, Gonzalez-Gay et al., 2005a).

### 1.1.1 Diagnosis of RA

Inflammatory markers used in RA diagnosis include C-reactive protein (CRP), an acute phase protein and the erythrocyte sedimentation rate (ESR). More specific markers include rheumatoid factor (RF), an autoantibody against IgG and anti-cyclic citrullinated peptide antibodies (ACPA) (Scott, 2000). There is no single diagnostic test for RA and diagnosis relies on the presence of RF, ACPA, raised CRP and ESR (American College of Rheumatology Subcommitte on Rheumatoid Arthritis, 2002, Scott, 2000, Avouac et al., 2006, Aletaha et al., 2010). Formal diagnosis of RA is made according to the American Rheumatism Association 1987 revised criteria, which require four of the following to be presented including 1) morning stiffness (> 1 hour), 2) soft tissue swelling in three or more joints, 3) swelling of the proximal interphalangeal, metacarpophalangeal or wrist

joints, 4) symmetric swelling, 5) presence of rheumatoid nodules, 6) presence of RF, and 7) radiographic evidence of erosions in hands or wrists with criteria 1 to 4 evident for at least six weeks (Arnett et al., 1988). The new criteria were recently revised and validated (Aletaha et al., 2010).

### 1.1.2 Pathophysiology of RA

The healthy joint is composed of epiphyseal bone covered by hyaline cartilage and an overlaying synovial membrane while the joint space is filled with synovial fluid (SF). The SF is composed of oligosaccharides, proteins and glucosaminoglycans such as hyaluronic acid produced by fibroblast-like synoviocytes, which helps lubricate the joint. Joint swelling in early RA is a result of tissue oedema and fibrin deposition. Synovial hyperplasia then takes place with macrophage (MΦ)-like and fibroblast-like synoviocyte proliferation. This is closely followed by further mononuclear cell infiltrate including B cells, $CD4^+$ and $CD8^+$ T cells, NK cells, and neutrophils found mostly in the SF while the joint becomes a site for increased angiogenesis with generation of endothelial venules supporting hyperplastic growth (Lee and Weinblatt, 2001, Bugatti et al., 2007, Cope, 2008, Cascao et al., 2010). The hyperplastic synovial tissue (pannus) composed of MΦ and synovial fibroblasts is rich in matrix metalloproteinases (MMP) invades the cartilage and mediates its destruction through activation of osteoclasts, chondrocytes and synovial fibroblasts themselves. In persistent RA, destructive joint erosion during pannus formation leads to ankylosis (bone fusion) clinically presented as joint deformities (Lee and Weinblatt, 2001).

The production of RF and anti-CCP antibodies contribute to an autoimmune aspect of RA known as the pre-articular phase. The precise mechanism behind articular

inflammatory cell recruitment remains unclear (McInnes and Schett, 2007). The existing synovial inflammation is thought to give rise to, or propagate rheumatic disease. RA is characterised by a cytokine disequilibrium whereby the effects of pro-inflammatory cytokines and chemokines (e.g. TNF$\alpha$, IL-1$\beta$, IL-6, IL-8, GM-CSF) outweigh those of anti-inflammatory cytokines (e.g. sTNFR, IL-10, IL-1ra, IL-4) (Feldmann et al., 1996). M$\Phi$ and fibroblasts are considered the richest source of pro-inflammatory cytokine production in RA, while T cells and adipocytes also support the multi-cellular response (McInnes and Schett, 2007, Feldmann et al., 1996).

### 1.1.3 Extraarticular manifestations in RA

Extraarticular disease is prevalent in established RA (ExRA). Common sites include the skin, lungs, eyes and peripheral nerves (Turesson et al., 2002, Vollertsen and Conn, 1990). Vascular involvement in RA, known as rheumatoid vasculitis (RV) is now recognised as an important aspect of RA pathology (Turesson and Matteson, 2009, Bacon and Kitas, 1994). Inflammatory RV affects mostly small and medium-sized vessels and has been associated with increased premature mortality (Turesson et al., 2002). However, diagnosis of RV still relies on ruling out the presence other diseases such as diabetes, atherosclerosis, infection and primary vasculitides.

It is often difficult to diagnose or characterise RV and this may reflect perseverance or guided systematic approach. However, if assessed post-mortem it is almost always present in RA (Bacon and Kitas, 1994). The pathogenesis of RV is often associated with RF presence (Westedt et al., 1985), anti-endothelial cell and anti-CCP antibodies, (Turesson et al., 2007, van der Zee et al., 1991). Histologically in RV there is evidence of fibrinoid

vessel necrosis and immune cell infiltrate through the vessel wall (Voskuyl et al., 1998a, Voskuyl et al., 1998b) while the resulting thrombus formation may lead to ischaemic events and infarcts often present in the myocardium and fingertips (Genta et al., 2006).

RV was proposed to significantly contribute to the accelerated atherosclerosis often observed in RA (Bacon and Kitas, 1994). Rheumatoid heart disease is often a sub-clinical manifestation that is rarely recognised however, upon closer echocardiographic assessment its diagnosis is indeed increased and is best confirmed only by autopsy (Kitas et al., 2001). Cutaneous vasculitis and pleuritis were initially shown to be the most common presentations of ExRA and were associated with increased mortality related to heart disease (Turesson et al., 1999). It was later confirmed however, that cutaneous vasculitis was a major determinant of mortality second to neuropathy and followed by pericarditis (Turesson et al., 2002). Since vasculitis can present as a pathology secondary to a disease such RA and as a number of conditions where vascular inflammation is the primary pathology, a comparison with RV may provide useful insights for both conditions.

## 1.2 Primary Systemic Vasculitis (PSV)

Primary Systemic Vasculitis describes the inflammation of blood vessels in a group of chronic systemic inflammatory diseases affecting the whole arterial tree from the aorta to the capillaries. They feature leukocyte activation and infiltration, endothelial activation and vascular necrosis (Savage, 2002, Watts et al., 2007, Watts et al., 2010). In PSV, vessel stenosis and occlusion can lead to tissue ischaemia and although the vasculitides are a

histologically well-characterised group of disorders, the precise mechanism initiating their pathology remains undefined.

### 1.2.1 Classification and diagnosis of PSV

Diagnosis of the primary vasculitides generally relies on identifying a clinical phenotype coupled with a laboratory diagnostic test or supported by histological findings through biopsy. Confirmation of a particular PSV is made through exclusion of mimics of vasculitic disease (e.g. atheromatous vascular disease, multiple myeloma) and secondary causes such as RA (Jayne, 2009). The PSVs are a heterogeneous group of disorders often distinguished by the presence of granulomatous disease and auto-antibodies such as anti-neutrophil cytoplasmic antibodies (ANCA). PSVs are currently defined according to the Chapel Hill Consensus Conference definitions (1994) and are broadly categorised into conditions affecting small, medium or large vessels (Jennette et al., 1994) A recent report from the European League against Rheumatism (EULAR) brought forward an international consensus for alteration of their classification criteria and definitions (Basu et al., 2010).

The large vessel PSVs not associated with ANCA presence include giant cell arteritis (GCA) and Takayasu's arteritis (TAK). GCA or temporal arteritis is a granulomatous disease of large and medium sized vessels and is the most common form of PSV affecting branches of the carotid artery, with an incidence up to 35 per 100,000 over 50 years old (Watts and Scott, 2004, Mohan and Kerr, 2000). Takayasu's arteritis (TAK) is another granulomatous large vessel disease with a prevalence of up to 2.6/million/year in the northern hemisphere (Hall et al., 1985, Reinhold-Keller et al., 2005). TAK is a rare disorder

that predominantly affects the aorta, carotid, subclavian and associated branches featuring stenotic lesions and aneurysms (Maksimowicz-McKinnon et al., 2007). Polyarteritis nodosa (PAN) was the first described form of PSV in 1866 (Kussmaul and Maier, 1866) affecting medium or small size vessels and clinically manifests as hypertension, fever, myalgia, and systemic vasculitis of skin, heart and renal vessels. It is also associated with Hepatitis B infection (HBV-PAN) (Guillevin et al., 2005, Pagnoux et al., 2010). The last of the non-ANCA associated PSVs is Kawasaki's disease (KD), a form of idiopathic juvenile vasculitis that affects medium sized vessels usually in children below five years old, and more often in boys. KD in severe cases features coronary artery aneurysms, which account for the increased morbidity and mortality in these patients (Lytwyn et al., 2010, Jennette et al., 1994).

### 1.2.2 ANCA-associated systemic vasculitis (AASV)

There are two types of ANCA; these are cytoplasmic proteinase 3(PR3) antibodies, termed cANCA, and the perinuclear enzyme myeloperoxidase (MPO) antibodies, termed pANCA. ANCA are disease specific and are thought to contribute to disease progression in AASV (Savage, 2002). Patients with AASV are often considered for plasmapheresis (plasma exchange, PEX), and can be used for those with renal failure (Jayne et al., 2007). The most extensively studied AASV is Wegener's Granulomatosis (WG), affecting capillaries, venules, arterioles and arteries. WG is a granulomatous disease that presents mostly in the respiratory tract and renal vessels, while necrotizing glomerulonephritis develops during the course of the disease (Jennette et al., 1994). Churg-Strauss syndrome (GSS) is a small vessel disease that features asthma, hypereosinophilia and necrotizing

vasculitis manifesting with disease progression. It is a poorly understood disease with pANCA presence in 40-75% of patients (Keogh and Specks, 2006, Guillevin et al., 1999a). Microscopic polyangiitis (MPA) is a PSV that was initially classified as a type of PAN however, is distinguished by the presence of small vessel involvement including capillaries, venules or arterioles (Jennette et al., 1994, Guillevin et al., 1999b). Most patients with MPA have renal impairment (78%). MPA also has a high frequency of ANCA (>70%) and is characterised by a 74% 5-year survival rate (Guillevin et al., 1999b). Other small vessel vasculitides include cutaneous vasculitis, cryoglobulinemic vasculitis and Henoch-Schonlein purpura (HSP) all of which have not been shown to feature ANCA (Gibson, 2001, Saulsbury, 1999). On rare occasions, PAN may be ANCA positive (Cohen et al., 1995). Clinical disease activity in AASV is determined by the Birmingham Vasculitis Activity Score (BVAS), a numerical system that weighs organ involvement according to severity (Luqmani et al., 1994), while organ/tissue damage is expressed using the Vasculitis Damage Index (VDI) which scores non-healing scars (Exley et al., 1997, Exley et al., 1998).

### 1.2.3 Pathogenesis of AASV

AASV are known as pauci-immune necrotizing vasculitides that show relatively little Ig immune deposits. Granulomatous disease is evident in two of the three AASV (WG, CSS). This features tertiary lymphoid like structure formation with T and B cells, and follicular dendritic cells (DC), suggesting an immune association (Mueller et al., 2008). Furthermore, AASV is also characterised by inflammatory lesions distal to the primary inflammation, such as seen in the lung (Bosch et al., 2006, Kradin and Mark, 2002).

Neutrophil activation and endothelial cell (EC) damage are hallmarks of AASV pathogenesis. ANCA-induced EC apoptosis is evident in AASV (Yang et al., 2001). This can lead to EC dissociation from the basement membrane, platelet aggregation, subsequent thrombosis and vessel occlusion (Williams et al., 2005). Immune involvement is also evident through the presence of TNFα, IL-1β, IL-6 and IL-8 in renal biopsies and plasma of AASV patients (Noronha et al., 1993, Tesar et al., 1998). ANCA can bind to MPO or PR3 of TNFα-primed neutrophils that also require Fcγ receptor ligation for full activation (Reumaux et al., 2003) producing pro-inflammatory cytokines, generating reactive oxygen species (ROS), and degranulating to release proteolytic enzymes. Furthermore, ANCA may accelerate neutrophil apoptosis and phagocytosis by MΦ which, then secrete IL-1, IL-8 and TNFα adding to the inflammatory burden (Harper et al., 2001, Harper et al., 2000). ANCA also induce neutrophil adhesion, enhancing transmigration thus potentially contributing to lesion development (Savage, 2002).

## 1.3 Cardiovascular disease in inflammatory rheumatic diseases

Cardiovascular disease (CVD) is the collective term for a group of disorders with multifactorial aetiology and remains one of the leading causes of death in the Western world (Adams and Celermajer, 1999). The risk of developing cardiovascular disease (CVD) amongst the healthy population increases with age, obesity and male gender, all of which are often associated with heart failure (Listing et al., 2008). Over the past 10-15 years the prevalence of CVD such as atherosclerosis, in chronic rheumatic diseases including RA, PSV, systemic lupus erythematosous (SLE), Behcet's disease and psoriatic arthritis (PsA) has been highlighted (Bacon and Kitas, 1994, Manzi et al., 1997, Von Feldt, 2008,

Gladman et al., 2009, Del Rincon, 2009, de Leeuw et al., 2005, Chambers et al., 2001, Suppiah, 2011).

### 1.3.1 Atherosclerosis

Atherosclerosis is a multifactorial, inflammatory disease of the vascular system characterised by hyperlipidemia, endothelial dysfunction (ECD) and immune cell activation at the site of initiation (Ross, 1999, Del Rincon et al., 2003). This leads to the formation of atherosclerotic plaques called fatty streaks in their infancy, stemmed through an initial process called diffuse intimal thickening, an enlargement of the inner arterial layer lined with EC (Nakashima et al., 2002). The initial growth is outwards into the vessel lumen however lesion size does not pre-dispose to plaque rupture (Haskard, 2004).

Atherosclerosis has been increasingly referred to as a disease of the immune system and examination of plaques reveals the presence of pro-inflammatory cytokines (IFN$\gamma$, TNF$\alpha$) and activated M$\Phi$, B and T cells, expanded smooth muscle cells (SMC) and EC (Jonasson et al., 1986, Hansson and Libby, 2006). The mature plaque, an atheroma, has a collagen-rich matrix fibrous cap that is lined with SMC and EC enclosing a lipid core. This is largely composed of lipid droplets and M$\Phi$, termed foam cells due to increased uptake of low-density lipoprotein (LDL) (Jonasson et al., 1986). One of the proposed roles of EC is to initiate the retention of apolipoprotein-B-containing LDL and sub-endothelial deposition (Tabas et al., 2007). Inflammation is considered to propagate the development of atherosclerosis and the initiating mechanism behind this disease is now considered to

arise from a dysfunctional endothelium (Bacon et al., 2002, Zeiher et al., 1991, Bonetti et al., 2003). There is accumulating evidence for accelerated atherosclerosis in rheumatic diseases and the precise mechanism behind this development still remains unclear (Shoenfeld et al., 2005).

### 1.3.2 CVD in rheumatoid arthritis

Early investigations revealed a familial component for shortened life expectancy in RA (Kaplan, 1986, Kaplan and Feldman, 1991). These raised mortality rates are accompanied by a standardised mortality ratio (SMR) between 0.87-3.0 and an average decreased life span of 3-18 years in RA patients using data gathered from 21 studies reviewed in Van Doornum et al., (2002). It is now established that RA patients have an excess all-cause CVD mortality (Goodson et al., 2005, Watson et al., 2003). These patients were twice as likely to suffer myocardial infarcts and developing congestive heart failure (CHF) (Solomon et al., 2003). The increased mortality and morbidity in RA (Wolfe and Michaud, 2004, Naranjo et al., 2008) could not be explained by traditional risk factors such as smoking, familial history, increased BMI, age, dyslipidemia and diabetes (Nicola et al., 2005, Crowson et al., 2005).

Systemic inflammation in RA adds to the increased risk of CV mortality in RA patients whose 10-year absolute risk of developing CVD at incidence of RA reflects similar prevalence in non-RA individuals 5-10 years older (Kremers et al., 2008). This suggests that CVD onset may start in early RA. Furthermore, in some patients, myocardial infarctions (MI) are thought to precede the diagnosis of RA (Maradit-Kremers et al., 2005a). Comorbidities such as RV are independent risk factors for CV mortality in RA

(Maradit-Kremers et al., 2005b). The synovitis in RA is the primary source of inflammation thought to cause diffuse perturbation of vascular function. Small and large vessel inflammation manifests in a high percentage of cases and RV presence has been shown to occur irrespective of therapy (Bacon and Kitas, 1994).

RA patients also show a higher prevalence of atherosclerosis (Han et al., 2006, Gonzalez-Gay et al., 2005a) which shares similar characteristics with RA itself including raised endothelial cell and leukocyte adhesion molecule expression, increased immune cell activation and raised levels of IL-1$\beta$, TNF$\alpha$ and IFN$\gamma$ (Pasceri and Yeh, 1999, Ross, 1999, Van Doornum et al., 2002). Immune activation is believed to contribute to atherogenesis in RA. One possible cause for this is thought to be a $CD4^+/CD28^-$ T cell phenotype found present in plaques of patients with unstable angina. In RA patients, expansion of this T cell subset was later associated with increased IMT and lower vasodilator capacity (Liuzzo et al., 2000, Gerli et al., 2004) suggesting these cells may contribute to atherogenesis in RA.

Several factors may predispose those with RA to accelerated atherosclerosis including the raised TNF$\alpha$, CRP and homocysteine levels, an altered lipid profile, and factors not derived from RA pathogenesis such as prolonged inactivity and smoking status (Bacon and Townend, 2001, Gonzalez-Gay et al., 2005b). Projecting from this, endothelial injury is now also considered an initiating mechanism in the development of atherosclerosis. Contributing factors to cardiovascular disease in RA and PSV are summarised in **figure 1.1)** (Gonzalez-Gay et al., 2008, Kerekes et al., 2008).

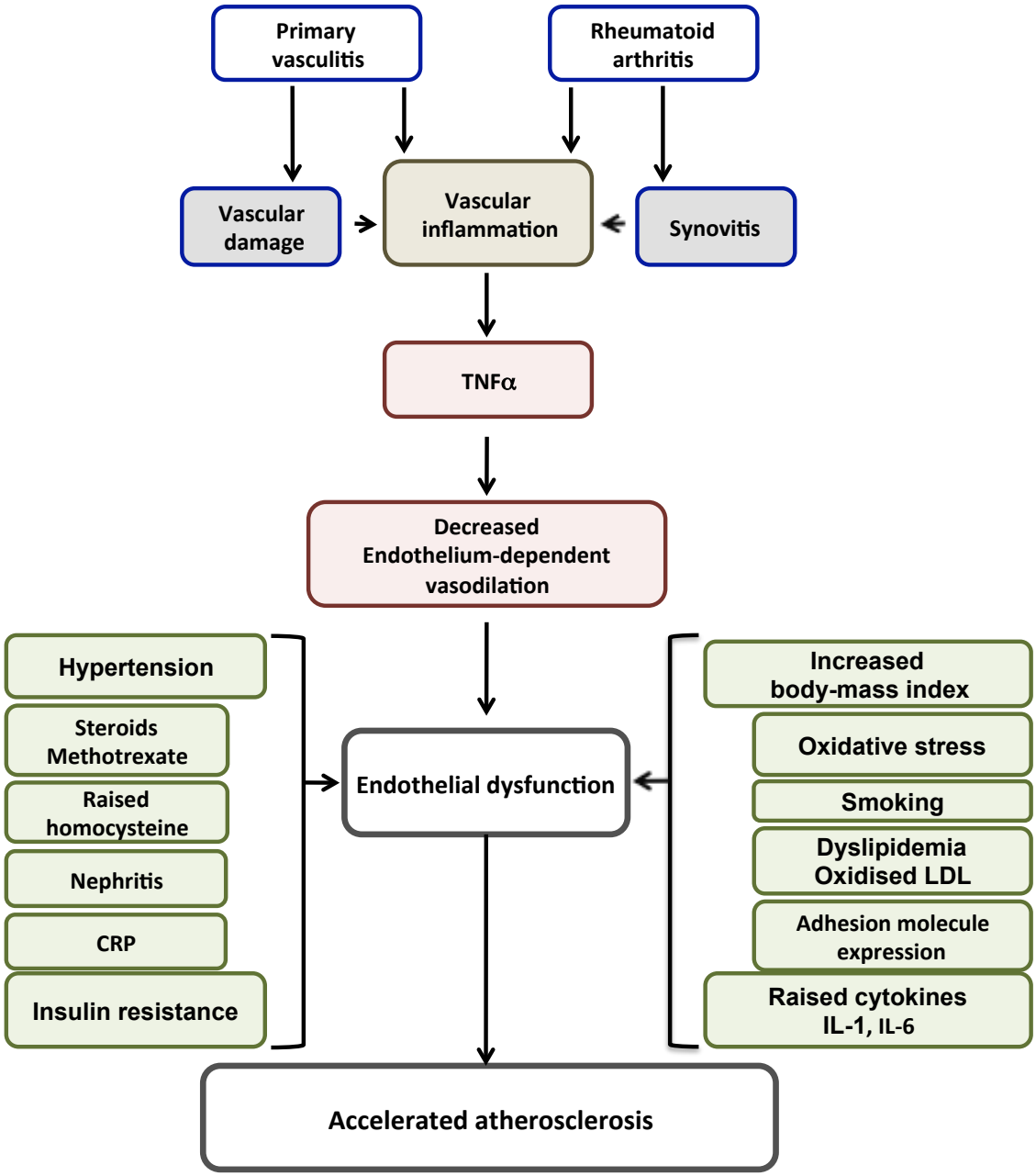


**Figure 1.1 TNFα and other contributors to ECD in chronic inflammatory disease**

This figure shows the presence of vascular inflammation in two different diseases, primary systemic vasculitis (PSV) and rheumatoid arthritis (RA) with vascular damage and synovitis respectively contributing to the inflammatory burden. Both diseases have elevated TNFα levels, which can lead to decreased endothelium-dependent vasodilation and endothelial dysfunction. Several other factors may initiate or contribute to endothelial dysfunction in these diseases and examples include oxidative stress, raised CRP and cytokines, tobacco smoking and oxidised LDL. Both PSV and RA feature accelerated atherosclerosis and endothelial cell dysfunction is thought to be an initiating step in atherosclerosis. Developed and adapted from Bacon et al. (2002), Van doornum et al. (2005) and Haskard (2004).

### 1.3.3 CVD in primary systemic vasculitis

Sufferers of PSV are thought to be at increased CV risk due to the vascular complications that come secondary to the underlying inflammation. In AASV and PAN, patients showed decreased arterial and dermal microvascular endothelium-dependent vasodilation compared to controls (Filer et al., 2003). The ankle-brachial pressure index (ABPI), a tool for detecting peripheral arterial vascular disease, has been used in a wide range of systemic vasculitides revealing abnormal vascular function compared to controls. The same patients were also hypertensive and showed an increased number of CV events compared to control individuals (Sangle et al., 2008). Furthermore patients with AASV also presented impaired renal function, which in the elderly especially was shown to predispose to CVD carrying similar CV risk to MI (Rashidi et al., 2008).

Arterial stiffness is a determinant for CV risk and was shown to increase in AASV patients with active disease compared to those in remission and controls. Recently, arterial stiffness positively correlated with CRP levels in AASV suggesting a link with inflammation (Booth et al., 2004c), which is linked to impaired vascular function, an early marker for atherosclerosis, also evident in PSV. The first such evidence in AASV came from WG patients who had increased IMT compared to healthy controls unexplained by traditional risk factors (de Leeuw et al., 2005). Accordingly, Chironi and colleagues then showed that subclinical atherosclerosis was more frequent in PSV patients compared to controls. High-risk status determined by CVD history, type 2 diabetes or a Framingham risk score above 20% was more frequent in patients with three plaques (carotid, aortic, femoral) and the presence of the three combined was associated with raised CRP levels and vasculitis (Chironi et al., 2007). Prevalence of CVD in AASV was recently confirmed

highlighting the importance of long-term CVD management of these patients (Morgan et al., 2009). Importantly, there is evidence of CV events in large vessel PSV such as TAK, which features accelerated atherosclerosis (Seyahi et al., 2006). However, prevalence in GCA remains unclear (Ray et al., 2005, Gonzalez-Juanatey et al., 2007).

## 1.4 The inflammatory environment

### 1.4.1 Pro-inflammatory cytokines - TNFα, IL-1β, IFNγ, IL-6

Pro-inflammatory cytokines aid the immune response, playing an important role in atherosclerosis and chronic inflammation. IFNγ is a pro-inflammatory cytokine with established anti-viral properties, also known to have immuno-modulatory characteristics increasing the expression of MHC class I and II. Although present in lesions, its role in the atherosclerotic process remains unclear (Hansson and Libby, 2006, Haskard, 2004, McInnes and Schett, 2007). IL-6 is a pleiotropic pro-inflammatory cytokine also considered to have some anti-inflammatory activity. It is involved in the maturation and activation of MΦ, osteoclasts, chondrocytes, EC, B and T cells (Kishimoto, 2005, Xing et al., 1998). IL-6 is secreted from T cells and MΦ while although raised in RA alongside IL-1, its role also remains in the balance (Sivalingam et al., 2007, Feldmann et al., 1996). Recently, antibody-mediated suppression of IL-6 has been suggested to dampen disease activity in RA (Smolen et al., 2008). IL-1β is a pro-inflammatory cytokine that has several housekeeping roles in sleep, feeding and temperature regulation but also contributes to heart disease and RA, where it is raised in the synovium (Dinarello, 1996, Dayer, 2003, Hussein et al., 2008, Bujak and Frangogiannis, 2009, Feldmann et al., 1996). Neutralising

IL-1β was shown to significantly impair joint destruction (Joosten et al., 1999, Dayer, 2003).

Tumor necrosis factor (TNF) was first described as a neoplastic cell death inducer, later differentiated as TNFα (Carswell et al., 1975, Kolb and Granger, 1968). A member of the TNF superfamily, TNFα is a pleiotropic cytokine capable of inducing apoptosis and regulating cell-mediated immunity. Furthermore TNFα has anti-viral properties, and mediates acute and chronic inflammation (Popa et al., 2007, Cassatella et al., 2007). TNFα, which is found raised in chronic inflammatory diseases such as RA (Petrovic-Rackov and Pejnovic, 2006), is mostly produced by MΦ but also by T cells, EC, SMC, adipocytes and fibroblasts (Popa et al., 2007). On EC it acts through ligation to TNF receptors (TNFR), designated TNF receptor 1 (TNFR1, CD120a) and TNF receptor 2 (TNFR2, CD120b) enabling it to induce the secretion of other soluble mediators such as cytokines and tissue factors whilst also increasing oxidative stress (Nawroth et al., 1986, Ferrero et al., 2001, Paleolog et al., 1994, Corda et al., 2001).

#### *1.4.1.1 TNFα blockade in RA and PSV pathogenesis*

In RA, TNFα mediates joint damage through osteocyte, chondrocyte and fibroblast activation, which facilitate cartilage and bone damage (Dayer et al., 1985, Bertolini et al., 1986). TNFα receptor expression in stromal RA synovial cells is increased in comparison to healthy individuals, while TNFα itself is raised in RA serum and synovial fluid correlating with disease activity (DAS-28) (Petrovic-Rackov and Pejnovic, 2006, Deleuran et al., 1992). An important cytokine network appeared to be dependent on TNFα bioactivity since its blockade *in vitro* led to the decreased activity and expression of other cytokines and

chemokines such as IL-1, IL-6, IL-8 and GM-CSF (Haworth et al., 1991, Butler et al., 1995, Brennan et al., 1989). A central role for TNFα in RA was first highlighted in mice *in vivo* whereby monoclonal antibodies (mAb) against TNFα dampened the inflammatory process and halted joint damage (Keffer et al., 1991, Williams et al., 1992). Subsequently, TNFα blockade using the anti-TNFα mAb infliximab ameliorated clinical symptoms and decreased CRP and ESR levels (Elliott et al., 1993). These effects may also be replicated in PSV (Hurlimann et al., 2002, Booth et al., 2004a, Raza et al., 2006).

### 1.4.2 Oxidative stress

#### *1.4.2.1 Reactive oxygen species (ROS)*

Free radicals are atoms or molecules that have at least one unpaired electron ($e^-$). The most common of these are the nucleophile superoxide anion ($O_2^-$) and the hydroxyl radical ($^{\cdot}OH$). Oxygen can be reduced to form superoxide ($O_2^-$), and in the presence of another $O_2^-$ molecule and two protons forms hydrogen peroxide ($H_2O_2$). Similarly $O_2^-$ can be protonated to form a hydroperoxyl radical or peroxynitrite in the presence of nitric oxide (NO).

Intracellular generation of ROS can arise from the mitochondrial transport chain, oxidative bursts from phagocytic cells, and enzymes such as xanthine oxidase, nitric oxide synthase (NOS), cytochrome P450's and NADPH oxidases (Cai and Harrison, 2000). ROS can be toxic to cells and can oxidise macromolecules such RNA/DNA, lipids, proteins causing DNA base adducts, DNA strand breaks and oxidative protein damage (Kohen and Nyska, 2002, Wiseman and Halliwell, 1996). Under inflammatory conditions EC are exposed to ROS as a result of phagocyte activation, enzyme systems (NOS, xanthine

oxidase), but also due to their presence in oxidative microenvironments such as the RA synovium (Harrison, 1997). In ECD, diminished NO production has been shown to result from ROS generation and peroxynitrite formation following TNFα treatment (Zhang et al., 2009a).

#### *1.4.2.2 Antioxidant systems*

There are several antioxidant systems including superoxide dismutase (SOD), catalase, the thioredoxin (TRX) and glutathione (GSH) systems, whilst there are also low weight antioxidants such as vitamin C (ascorbic acid), vitamin E, flavonoids, melatonin and carotenoids (Kemp et al., 2008). Thioredoxin alongside GSH arguably form the most important cellular antioxidant systems (Kemp et al., 2008, Nakamura et al., 1997). GSH is involved in xenobiotic metabolism (Boesterli, 2003). GSH is highly compartmentalised found in the ER, nucleus, cytoplasm and mitochondria (Markovic et al., 2007, Jessop and Bulleid, 2004, Soderdahl et al., 2003). Glutathione is mostly found in a reduced state as GSH, and can be itself oxidised by ROS to GSSG, protecting proteins from oxidative damage. The concentration of GSH depends on the rate-limiting enzyme glutamate cysteine ligase (GCL) (Meister and Anderson, 1983). GCL can be blocked with the GCL inhibitor L-buthionine-(S,R)-sulfoximine (BSO) thus mimicking a low GSH environment. This facilitates a pro-oxidant state while GSH levels can be augmented with the GSH precursor *N*-acetylcysteine (NAC) (Heng-Long Hu et al., 2000, Tsou et al., 2007, Lu, 1999).

#### *1.4.2.3 ROS in chronic inflammation*

ROS secondary to disease have been shown to play a significant role in RA, thought to arise from the hypoxic synovial environment and oxidative bursts from activated phagocytes such as neutrophils and MΦ (Seven et al., 2008). This is coupled with lower GSH, GSH peroxidase, catalase and vitamin E in these patients thought to maintain or exacerbate the pro-oxidant environment (Hassan et al., 2001, Kamanli et al., 2004). Indeed increasing GSH levels by NAC was shown to decrease $H_2O_2$ and lipid peroxidation in post-myocardial infarction rats (Adamy et al., 2007). Evidence also exists for ROS in chronic heart failure (CHF) featuring raised serum and plasma myeloperoxidase and malondialdehyde, the latter a product of lipid peroxidation is also evident in RA (McMurray et al., 1993, Hassan et al., 2001, Tang et al., 2007). Interestingly, decreased EDV in CHF can be improved with vitamin C supplementation suggesting that maintenance of redox balance facilitates EC function (Landmesser et al., 2002)

## 1.5 Endothelial cells

Endothelial cells (EC) line the interior face of blood vessels, or luminal aspect, principally interacting with smooth muscle cells (SMC) in the vessel wall behind them, and circulating blood-derived cells. The endothelium controls vascular homeostasis by 1. Regulating vascular tone and blood flow, 2. Acting as a barrier between luminal aspects of vessels and the sub-endothelial matrix (Schnittler, 1998), 3. Maintaining a dormant coagulation cascade (Michiels, 2003) and 4. Regulating leucokcyte transmigration (Dejana, 1996, Michiels, 2003, Kevil, 2003). Under basal conditions EC create an antithrombotic, anticoagulant environment by releasing nitric oxide.

When stimulated by IL-1β and TNFα, EC have been shown to produce a wide array of cytokines including IL-1α, IL-3, IL-6, IL-7, IL-8, IL-11, IL-14, IL-15, TNFα and TGFβ suggesting that inflammation itself could even be propagated through EC (Nilsen et al., 1998). Upon stimulation with vasoactive agonists, EC regulate vascular tone by producing NO, inducing smooth muscle relaxation (Michiels, 2003, Shireman and Pearce, 1996).

### 1.5.1 Endothelial cells in rheumatoid arthritis and primary systemic vasculitis

EC expression of adhesion molecules aid in recruitment and transmigration of leukocytes, a process tonically maintained during chronic inflammation and upregulated by increased expression of TNFα, IL-1β and IFNγ in RA (Middleton et al., 2004, Ferrero et al., 2001). Blockade of TNFα in RA has been shown to decrease disease activity, improving endothelial function and anti-oxidant capacity leading to lower incidence of first CV events in RA patients (Jacobsson et al., 2005, Hurlimann et al., 2002, Popa et al., 2009). The raised expression of adhesion molecules, in particular VCAM-1, was shown to correlate with common carotid artery (CCA) atherosclerosis by increased IMT suggesting that EC activation may contribute to atherogenesis in RA (Dessein et al., 2005).

Angiogenesis in RA is particularly prevalent as it allows oxygenation and nutrient supplementation in a hypertrophic synovium (Koch, 2003, Szekanecz et al., 2010). Endothelial necrosis in AASV can lead to thrombosis and possible vessel occlusion (Williams et al., 2005). Mature Endothelial Progenitor Cells (EPC) can replenish dysfunctional EC and become involved in neo-vascularisation. EPC are found raised in the RA synovium (Ruger et al., 2004) however, their precise role is often contradictory due to their inaccurate definition in RA (Grisar et al., 2005, Jodon de Villeroche et al., 2010,

Wrigley et al., 2010, Yiu et al., 2010) and AASV (Zavada et al., 2008, Santana, 2009, Westerweel and Verhaar, 2009, Zavada et al., 2009). Healthy endothelia in RA and PSV following repair or resolve of endothelial dysfunction may help decrease the chances of accelerated atherosclerosis.

### 1.5.2 Endothelial cell dysfunction

#### *1.5.2.1 Definition and assessment*

Endothelial cell dysfunction (ECD) may be an important initiating step in the promotion of atherosclerosis. A critical characteristic of ECD is the impaired ability of a vessel to dilate due to diminished NO production in response to physical or biochemical stimuli (Bonetti et al., 2003). Several methods exist to measure vascular function *in vivo*. Post-occlusion flow mediated dilatation (FMD) is measured by induction of reactive hyperemia (increased blood flow). This causes endothelial sheer stress, release of NO and muscle relaxation thus measuring endothelium-dependent vasodilation (EDV) (Corretti et al., 2002). Endothelium independent vasodilation (EIV) can be assessed in response to glyceryl trinitrate. In microvascular tissue (e.g. skin), Laser Doppler flowmetry records the flow of red blood cells and EDV responses can be measured in response to acetycholine (ACh), through iontophoresis, while sodium nitroprusside (direct NO donor) records EIV (Khan et al., 2010). *In vitro*, ECD can be assessed by measuring several EC markers such as endothelial nitric oxide synthase (eNOS) activity, NO and cyclic guanosine monophosphate production.

### *1.5.2.2 ECD In rheumatoid arthritis and primary systemic vasculitis*

RA features vascular inflammation (vasculitis) secondary to the disease and coupled with PSV has been shown to be at risk of ECD. In PSV, ECD was first demonstrated in Kawasaki's disease (KD) (Dhillon et al., 1996) while recent studies showed decreased change in brachial artery diameter and impaired myocardial blood flow in response to reactive hyperemia in KD (Deng et al., 2003, Furuyama et al., 2003, Noto et al., 2009). The involvement of ECD in AASV was highlighted when patients with WG and PAN (non-AASV) exhibited decreased EDV capacity compared to healthy controls and that EDV improved following induction of remission (Raza et al., 2000). This was later independently confirmed in AASV (WG, CCS) and PAN patients. The same study showed evidence of diffuse ECD in different vascular beds supported by the fact that these patients did not have brachial artery pathology but exhibited decreased microvascular EDV (Filer et al., 2003). The role of TNF$\alpha$ in ECD in PSV was highlighted in two subsequent studies where following anti-TNF$\alpha$ (Infliximab) treatment patients exhibited marked improvement in forearm and microvascular EDV responses compared to EIV (Booth et al., 2004b, Raza et al., 2006). Thus, anti-TNF$\alpha$ was able to improve endothelium-dependent vascular responses suggesting that PSV might be a potential archetypal model for the study of vascular inflammation (Booth et al., 2004b, Booth et al., 2004c).

ECD is also considered a contributing factor for accelerated atherosclerosis in RA (Gonzalez-Gay et al., 2008). Young to middle aged RA patients with no CV involvement were shown to have decreased brachial artery FMD compared to controls, which inversely correlated with CRP and LDL-cholesterol levels (Vaudo et al., 2004). Even newly diagnosed patients with RA exhibited vascular dysfunction measured by impaired EDV

responses to ACh (Bergholm et al., 2002), although this was not the case in patients with established RA (Foster et al., 2010). In established RA patients, TNFα blockade also caused a transient improvement in FMD over 14 weeks but led to a steady increase in mean arterial diameter (Bosello et al., 2008), however in a study by Sidiropoulos et al., anti-TNFα was shown to induce sustained increases in FMD over 18 months (Sidiropoulos et al., 2009). Subsequently, Gonzalez-Juanatey et al., highlighted that infliximab could induce a rapid increase in EDV post-infusion, compared to EIV coinciding with a significant decrease in the DAS-28 by day 7 post-infusion (Gonzalez-Juanatey et al., 2004). Alleviating the inflammatory burden with anti-TNFα therapy has been associated with a lower CVD risk in patients with RA (Jacobsson et al., 2005) and may be effective in preventing the development of heart failure in RA, although the data remains contradictory (Wolfe and Michaud, 2004, Gonzalez-Juanatey et al., 2006, Dixon et al., 2007).

#### *1.5.2.3 ECD In vitro*

Although effective blockade of TNFα alleviates ECD suggests an active role for the cytokine, there is yet to be a convincing direct causal effect. Perhaps bridging this gap comes a recent study that showed TNFα was able to decrease eNOS protein expression (Anderson et al., 2004). TNFα was first shown to inhibit EDV responses *in vivo* in mice (Wang et al., 1994) and similarly in human volunteers decreasing venous responses (Bhagat and Vallance, 1997). This was later also confirmed in arterial beds (Chia et al., 2003). Induction of ECD was shown *ex vivo* in rat mesenteric arteries where TNFα inhibited NO-dependent EDV but was abolished in the presence of superoxide dismutase (SOD). This suggested a role for $O_2^-$ and peroxynitrite formation, which inhibit eNOS

activity (Wimalasundera et al., 2003) and is particularly important since TNFα has been shown to increase endothelial ROS production (Corda et al., 2001, Gao et al., 2007, Zhang et al., 2009a). Thus, although TNFα is a potential candidate for ECD during inflammation the mechanisms are likely to be multifactorial (Kim et al., 2001, Nakamura et al., 2000).

#### *1.5.2.4 Proposed mechanisms of TNFα as a mediator of ECD*

In previous studies from our laboratory on cultured lymphocytes, we showed that the enzyme acid sphingomyelinase (ASM) and ceramide (Cer) generated by activation of ASM via TNFα, profoundly attenuated the activation of T cells through their antigen receptor by impairing $Ca^{2+}$ influx across the plasma membrane (PM). This was attributable to an effect on store-operated $Ca^{2+}$ channels (SOCs), and exogenous Cer itself was found to reduce $Ca^{2+}$ influx through SOC within one minute of application (Church et al., 2005). Agonist-evoked generation of NO by eNOS is also tightly regulated by $Ca^{2+}$ and release from intracellular stores, influx across the PM playing a dominant role (Nilius and Droogmans, 2001). This raises the possibility that SMase and Cer have an relatively rapid inhibitory effect on agonist-stimulated NO synthesis and release from EC, by interfering with $Ca^{2+}$ handling, thus providing a mechanism by which TNFα could induce ECD and loss of NO production.

## 1.6 Endothelial cell signalling

### 1.6.1 Receptor mediated $Ca^{2+}$ mobilisation

Guanine nucleotide-binding protein (G-protein) coupled receptors (GPCR) receive a wide range of $Ca^{2+}$-mobilising ligands including bradykinin, acetylcholine and thrombin (Dudzinski and Michel, 2007). Following receptor stimulation, phospholipase C (PLC) located on the intracellular leaflet of the PM is activated and hydrolyses phosphotidylinositol 4,5 biphosphate ($PIP_2$) to inositol 1,4,5 triphosphate ($IP_3$) and diacylglycerol (DAG). $IP_3$ then translocates through the cytosol and binds to the $IP_3$ receptor ($IP_3R$) on the ER causing the release of intracellular ER store $Ca^{2+}$. This resulting depletion of luminal ER store $Ca^{2+}$ is detected from $Ca^{2+}$-sensitive proteins in the ER membrane which cross-talk with plasmalemmal partners inducing the influx of extracellular $Ca^{2+}$ (Lewis, 2007). These processes are discussed below.

#### *1.6.1.1 $Ca^{2+}$ entry channels in EC*

$Ca^{2+}$ signalling in EC can occur in various ways by means of a broad range of multifunctional, selective and non-selective ion channels. Several $Ca^{2+}$ entry channels exist including purinergic ligand-gated receptor channels ($P_{2x}4$), which are non-selective cation channels (NSC), the transient receptor potential channels (TRPC) and $Na^{2+}/Ca^{2+}$exchange (NCX) transporters (Nilius and Droogmans, 2001). In 1986, Putney proposed the concept of *'capacitative $Ca^{2+}$ influx'* or capacitative $Ca^{2+}$ entry (CCE) in excitable cells, the process now referred to as store operated calcium entry (SOCE) (Putney, 1986). Store operated calcium (SOC) channels are regulated by the concentration of intracellular $Ca^{2+}$ ions and in EC represent the major pathway for $Ca^{2+}$ influx (Nilius and Droogmans, 2001). The basis of SOCE can be observed by depleting

intracellular $Ca^{2+}$ ($_{i}Ca^{2+}$) stores (ER/SER) by A) using $Ca^{2+}$ chelators, B) blocking $Ca^{2+}$ reuptake through sarco/endoplasmic reticulum $Ca^{2+}$-ATPase (SERCA) pumps or C) stimulating $Ca^{2+}$ release from intracellular stores (Parekh, 2008b). Physiologically, stimulation of agonist-sensitive $_{i}Ca^{2+}$ stores by agonists such as bradykinin leads to store emptying of $Ca^{2+}$ and the opening of PM SOC channels. The most widely studied prototype SOC channels are the *$Ca^{2+}$-released-activated $Ca^{2+}$ channels* ($I_{CRAC}$) identified due to a calcium-specific current directly evident following intracellular $Ca^{2+}$ store emptying. $I_{CRAC}$ have a single channel conductance which is highly $Ca^{2+}$-selective and could be activated irrespective of the mechanism of store emptying (Hoth and Penner, 1992, Takemura et al., 1989, Parekh and Penner, 1997).

### *1.6.1.2 Regulation and control of $Ca^{2+}$ entry in EC*

Direct ER-PM crosstalk is considered to mediate the governance of $Ca^{2+}$ entry thought to involve two key components, the stromal interaction molecule (STIM), an ER/SER membrane embedded $Ca^{2+}$ sensor and Orai, component of CRAC channel pores on the PM (Putney and Bird, 2008). *In vitro*, ER $Ca^{2+}$ stores can be pharmacologically depleted using the SERCA re-uptake pump blocker thapsigargin or the $Ca^{2+}$ ionophore ionomycin which ensures emptying of ER stores (Hofer et al., 1998). STIM are highly abundant transmembrane ER proteins that sense luminal-ER $Ca^{2+}$ levels and translocate close to the plasmalemmal interface (*puncta*) to relay this signal and begin the process of SOCE. At the same time, Orai proteins translocate to a locus proximal to the PM-ER interface opposite STIM proteins in the ER membrane (Lewis, 2007, Liou et al., 2005, Bird et al., 2009, Wu et al., 2006). These processes are depicted in **figure 1.2.**

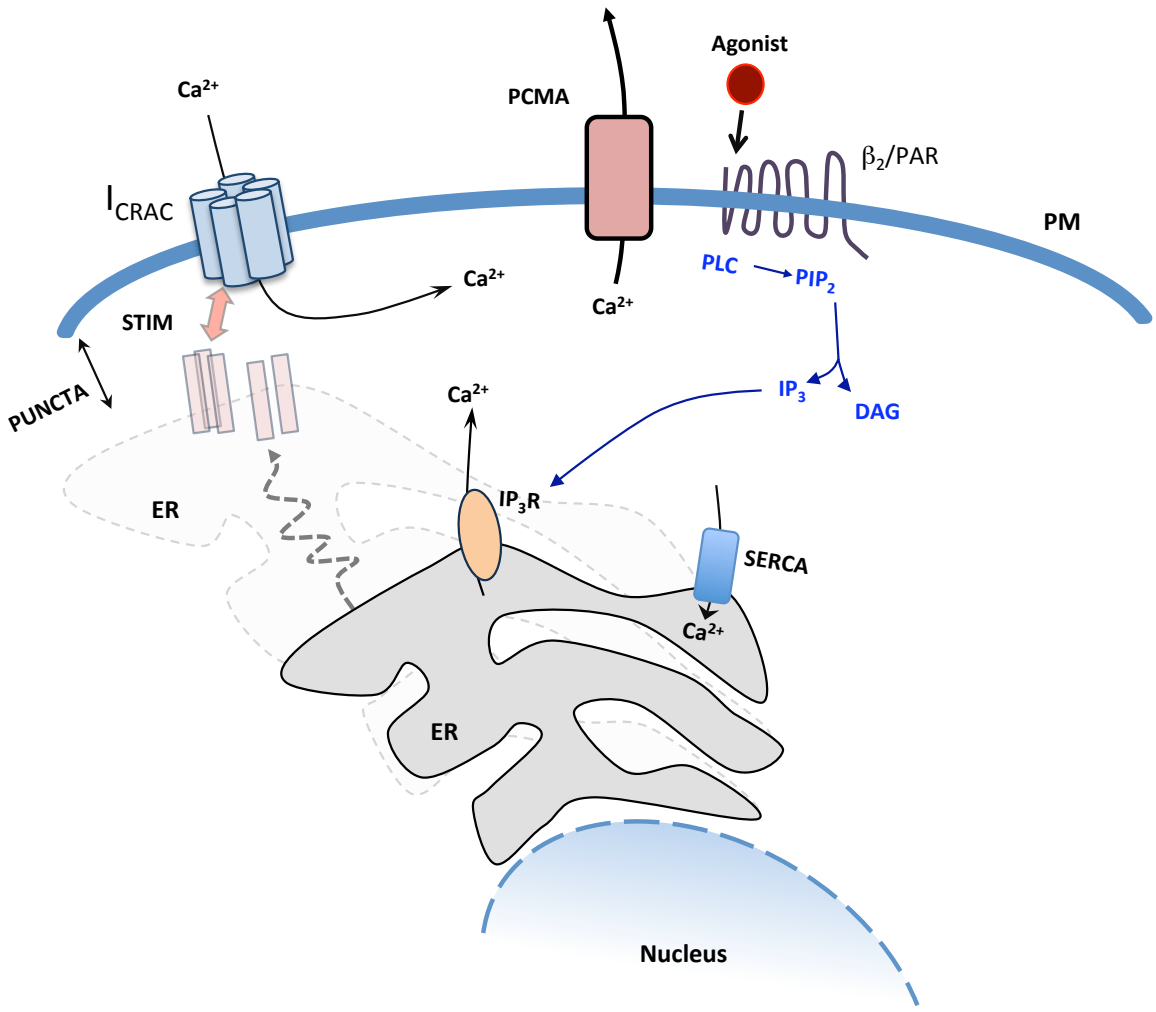


**Figure 1.2 Calcium signalling in endothelial cells**

Agonist stimulation (bradykinin, thrombin, acetylcholine) leads to phospholipase C (PLC) activation which hydrolyses phosphatidylinositol 4,5 biphosphate ($PIP_2$) to inositol 3,4,5 triphosphate ($IP_3$) and diacylglycerol (DAG). To maintain intracellular store $Ca^{2+}$ levels, the sarco/endoplasmic reticulum $Ca^{2+}$ ATPase (SERCA) transfers $Ca^{2+}$ from the cytosol to the luman of the endoplasmic reticulum (ER). $IP_3$ signals endoplasmic reticulum $Ca^{2+}$ store release which triggers $Ca^{2+}$ influx through store-operated $Ca^{2+}$ (SOC) channels in the plasma membrane. This is mediated through direct cross-talk of stromal interacting molecule (STIM) proteins on the ER which migrate towards the PM opposite calcium release-activated calcium (CRAC) channels. Interaction with CRAC proteins Orai results in $Ca^{2+}$ influx into the cell. The plasma membrane $Ca^{2+}$ ATPase (PCMA) regulates $Ca^{2+}$ efflux from the cytosol.

Of two splice variants, it is STIM-1 that is associated with $Ca^{2+}$ entry, while STIM-2 is believed to regulate Orai-1 activation and have limited activation itself (Zhou et al., 2009). STIM translocation to the puncta leads to Orai-3 recruit at the PM close to the $I_{CRAC}$ locus. This been shown to parallel $Ca^{2+}$ spikes suggesting these observations reflect SOCE through $I_{CRAC}$ as a result of intracellular $Ca^{2+}$ depletion (Putney and Bird, 2008). Conformational changes of STIM-1 promote oligomerisation and aggregation to form the puncta (Stathopulos et al., 2008). The luminal N-terminals of STIM-1 proteins are thought to recognize $Ca^{2+}$ while the C-terminal end reaches across the ER-PM gap to interact with Orai proteins (Liou et al., 2005, Williams et al., 2002, Zhang et al., 2005b, Liou et al., 2007, Wu et al., 2006), opening $I_{CRAC}$ facilitating SOCE (Bolotina, 2008, Park et al., 2009a, Csutora et al., 2008). Upon ER store $Ca^{2+}$ refill, the processes are reversed.

#### *1.6.1.3 $Ca^{2+}$ mobilisation and nitric oxide production*

Production of nitric oxide NO in EC is mediated by endothelial nitric oxide synthase (eNOS). Regulation of NO is a complex process and can result from various stimuli that can be $Ca^{2+}$-independent (Fisslthaler et al., 2000) or $Ca^{2+}$-dependent and GPCR agonist-mediated (Harris et al., 2001). The origin of stimulation through GPCRs occurs proximal to caveolae (Isshiki et al., 1998) which, have been shown to bind eNOS (Shaul et al., 1996) and have a functional relevance to NO output (Lin et al., 2000).

One of the remarkable features of $Ca^{2+}$ signalling is its temporal and spatial orientation, which ensures that $Ca^{2+}$ activates only pathways related to the upstream stimulus. This means that influx of $Ca^{2+}$ occurs close to or itself creates *$Ca^{2+}$ microdomains*, cytoplasmic areas of high-$Ca^{2+}$ concentration that are activated only by

specific targets; eNOS is one of these, shown to co-localise with caveolae (Feron et al., 1996). In support of these observations, NO production was greater in PM-targeted eNOS than its cytosolic homologue, which was less sensitive to SOCE (Lin et al., 2000). This suggests that SOCE-derived $Ca^{2+}$ microdomains, in close proximity to eNOS and caveolae, may expose eNOS to high $Ca^{2+}$ concentrations by ensuing efficient activation and rapid responses.

### 1.6.2 Endothelial nitric oxide synthase

Three NOS isoforms exist in mammalian cells, neuronal NOS (nNOS, NOS I), inducible NOS (iNOS, NOS II) and endothelial NOS (eNOS, NOS III) found in vascular EC, cardiac myocytes and blood platelets. eNOS is composed of a C-terminal end reductase domain and an N-terminal end oxygenase domain whilst between the two exists an allosteric small sequence binding site for Calmodulin (CaM), which is essential for the enzymatic functioning of eNOS **(Figure 1.3)** (Dudzinski et al., 2006).

#### *1.6.2.1 Stimulants of eNOS activation*

The $Ca^{2+}$-dependence of eNOS activation varies according to the type of stimulant which may be a physical (liquid flow, shear stress), pharmacological (statins), energy production (ATP), oxidative stress ($H_2O_2$), endocrine (estrogen), pathological (ischaemia) or a wide variety of physiological vasoactive compounds including thrombin, bradykinin, histamine and VEGF (Balligand et al., 2009, Fleming, 2010, Fulton et al., 2008).

### 1.6.2.2 Cofactors of eNOS

eNOS activation is dependent of the presence of a number of cofactors including substrate L-arginine. The requirement for $Ca^{2+}$ was considered essential for *all or nothing* activation however, fluid shear stress can cause $Ca^{2+}$ transients (series of momentary cytoplasmic $Ca^{2+}$ oscillations) leading to eNOS activation in a $Ca^{2+}$-independent manner (Dimmeler et al., 1999, Fleming, 2010). In most other examples however, eNOS activation is tightly $Ca^{2+}$-dependent (Park et al., 2009b) and sustained activation of membrane-bound eNOS has been shown to require CCE or SOCE discussed above (Lin et al., 2000). Therefore the $Ca^{2+}$ requirement varies depending on the stimulus. CaM is an essential cofactor of eNOS activation, a $Ca^{2+}$ regulatory protein, binds to eNOS and facilitates electron ($e^-$) transfer and dissociation from caveolae, preventing the inhibitory binding of eNOS to the PM (Abu-Soud et al., 1994, Michel and Vanhoutte, 2010).

### 1.6.2.3 Dimerisation and Caveolin-1 association of eNOS

The importance of eNOS is highlighted by the great level of control exerted over its activity at a number of levels. Binding of tetrahydrobiopterin ($BH_4$) to the eNOS N-terminal oxygenase domain facilitates eNOS dimerisation (Berka et al., 2004a, Berka et al., 2004b). This allows binding of L-arginine to the oxygenase domain close to heme and $BH_4$ and molecular oxygen to the ferrous iron (Crane et al., 1998, Raman et al., 1998). In a quiescent state, eNOS is targeted and bound to caveolae by specific association with caveolin-1 (Shaul et al., 1996) in EC which is believed to inhibit the binding of $Ca^{2+}$/CaM to eNOS thus blocking part of its activation cascade (Ghosh et al., 1998, Bucci et al., 2000, Feron et al., 1996). eNOS association with caveolae at the PM is also maintained through *N*-myristoylation at $Gly^2$ and palmitoylation at $Cys^{15}$ and $Cys^{26}$ (Feron and Balligand, 2006).

When EC are stimulated with agonist, eNOS becomes rapidly depalmitoylated, binds $Ca^{2+}$/CaM and dissociates from the PM (Michiels, 2003). Similarly, eNOS is tonically *S*-nitrosylated in resting cells shown to be associated with eNOS monomerisation, thus appears to be an inhibitory mechanism of eNOS regulation (Erwin et al., 2006, Ravi et al., 2004).

#### *1.6.2.4 Phosphorylation of eNOS*

eNOS activation can be regulated by the differential phosphorylation of tyrosine (Tyr), serine (Ser) and threonine (Thr) amino acids (Mount et al., 2007). Phosphorylation of Ser residues is mostly associated with increased activation whereas phosphorylation of a threonine residue at $Thr^{495}$ inhibits eNOS activation and dephosphorylation of this site accordingly increases enzyme activity (Fleming et al., 2001). Phosphorylation of eNOS is mediated through various kinases discussed below (David-Dufilho et al., 2005, Stahmann et al., 2006, Thors et al., 2008, Thors et al., 2004, Fleming et al., 2001). The specificity of kinase depends on the stimulus target amino acid. The increasing number of eNOS phosphorylation sites being identified includes $Tyr^{81}$ (Fulton et al., 2008), $Ser^{633}$ (Michell et al., 2002, Harris et al., 2004), $Ser^{615}$ (Bauer et al., 2003, Michell et al., 2002) and $Ser^{114}$ (Kou et al., 2002, Drew et al., 2004). However, the two most studied eNOS residues are located at $Thr^{495}$ and $Ser^{1177}$ outlined in **figure 1.3**.

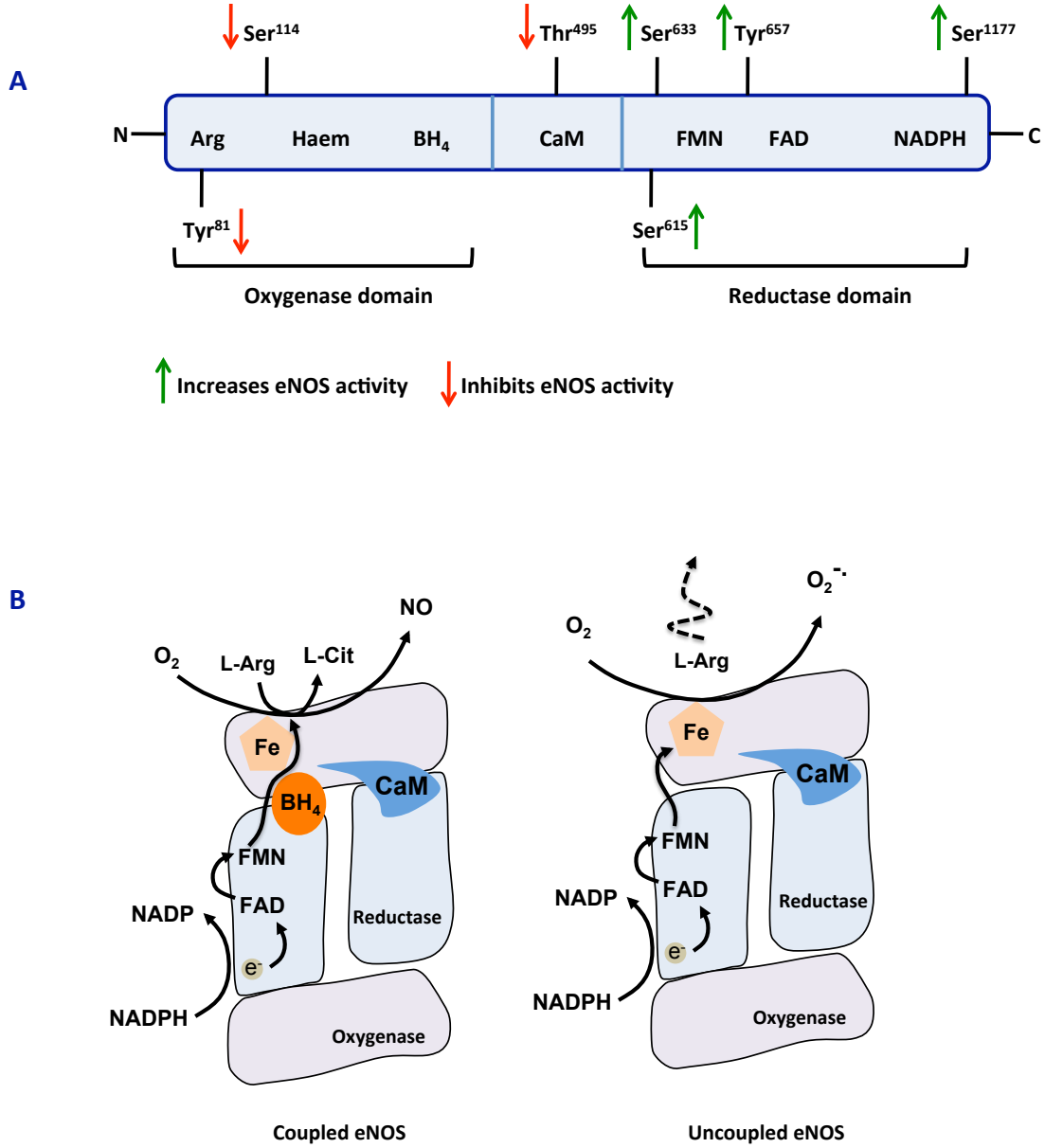


**Figure 1.3 Structure and function of endothelial nitric oxide synthase**

**(A)** Schematic representation of endothelial nitric oxide synthase (eNOS) showing the different binding motifs including the calmodulin (CaM) binding region (inside) and various phosphorylation sites (outside). Figure adapted from Mount et al., (2007) and Fleming et al., (2010). **(B)** eNOS dimer showing electron flow from NADPH (Nicotinamide adenine dinucleotide phosphate) through FAD (Flavin adenine dinucleotide), FMN (flavin mononucleotide) and $BH_4$ (tetrahydrobiopterin) to the tetrahedral haem enabling the formation of L-arginine (L-Arg) from L-citrulline (L-Cit). Coupled eNOS describes the dimerised protein with normal electron flow through the flavins to $BH_4$ and haem resulting in L-arginine formation and NO formation rather than superoxide generation. Figure adapted from Schmidt and Alp (2007).

Thr$^{495}$, found in the $Ca^{2+}$/CaM domain, is the only threonine residue shown to regulate eNOS activation to date. Thr$^{495}$ dephosphorylation leads to eNOS activation, regulating CaM binding (Harris et al., 2001, Chen et al., 1999, Greif et al., 2002, Fleming et al., 2001). It is generally believed that eNOS is activated through concomitant Thr$^{495}$ dephosphorylation and phosphorylation at Ser$^{1177}$ (Michell et al., 2001, Harris et al., 2001, Fleming et al., 2001). The C-terminal Ser$^{1177}$ residue in the reductase domain, is arguably the most studied of all eNOS regulatory sites and phosphorylation here leads to increased eNOS activation (Chen et al., 1999, Thors et al., 2004, Fleming et al., 2001).

#### *1.6.2.5 Bradykinin and thrombin mediated regulation of eNOS Thr$^{495}$ and Ser$^{1177}$*

$Ca^{2+}$/CaM and $Ca^{2+}$/CaM-dependent protein kinase II (CaMKII) have been tightly associated with rapid eNOS activation (Cai et al., 2008). Bradykinin (Bk) and thrombin relay their stimulatory signal through G-protein coupled receptors (GPCR) and have both been shown to induce $Ca^{2+}$-dependent phosphorylation of eNOS at Ser$^{1177}$ and dephosphorylation of the inhibitory Thr$^{495}$ (Motley et al., 2007, Harris et al., 2001, Fleming et al., 2001).

##### 1.6.2.5.1 Bradykinin regulation of Thr$^{495}$ and Ser$^{1177}$

Bradykinin signals through the $\beta_2$ adrenergic receptor, a GPCR which houses the pertussis-toxin-insensitive $G_{aq}$ protein subtype (Vanhoutte et al., 2009). Bradykinin induces phosphorylation of Ser$^{1177}$ in a $Ca^{2+}$-dependent manner even at low concentrations of the agonist (100 nmol/L), through rapid CaMKII activation. Furthermore, bradykinin has been shown to activate eNOS in a bimodal fashion by phosphorylation at Ser$^{1177}$ and dephosphorylation of the inhibitory Thr$^{495}$ site (Fleming et

al., 2001). Phosphorylation of $Ser^{1177}$ is considered to be a transient procedure involving kinases such as AMP-activated protein kinase (AMPK) and protein kinase A (PKA) (Michell et al., 2002, Fleming et al., 2001, Chen et al., 1999, Boo et al., 2002a). Akt has been implicated with $Ser^{1177}$ phosphorylation, however this has been in $Ca^{2+}$-independent mechanisms following shear stress (Boo et al., 2002b). Phosphorylation of $Ser^{1177}$ by Bk is $Ca^{2+}$-dependent and therefore thought not to occur through Akt/PKB activation (Fleming et al., 2001), which takes place following $Ser^{1177}$ phosphorylation (Harris et al., 2001). Use of CaMKII inhibitor KN-93 was able to block Bk-induced $Ser^{1177}$ phosphorylation suggesting that CaMKII is a key kinase involved in this process (Fleming et al., 2001) **(Figure 1.4)**. Bk also leads to a rapid dephosphorylation of $Thr^{495}$ probably through protein phosphatase 1 (PP1). Although evidence for PP1 involvement remains circumstantial, it is believed that pharmacological inhibition of PP1 abrogates the Bk-induced dephosphorylation of $Thr^{495}$, preventing CaM binding (Fleming et al., 2001). Conversely, Bk has also been suggested to perform auto-inhibitory functions on its own activation of eNOS by phosphorylating eNOS at $Thr^{495}$ (Watts and Motley, 2009).

#### 1.6.2.5.2 Thrombin regulation of $Ser^{1177}$

Thrombin signals through the protease-activated receptor (PAR), a GPCR, specifically the PAR-1 subtype on the PM (Coughlin, 2000, Hirano et al., 2007) although recently PAR-2 was also suggested to be a target (Watts and Motley, 2009). This is thought to occur through the pertussis-toxin-sensitive $G_{al}$ or $G_{aq}$ subunits (Coughlin, 2000, Michel and Vanhoutte, 2010). The thrombin signalling pathway is complex and the kinases involved are still under debate **(Figure 1.4)**. It was initially shown that thrombin tightly regulated CaMKII activation (Borbiev et al., 2001, David-Dufilho et al., 2005). Furthermore, like

histamine thrombin has been shown to phosphorylate $Ser^{1177}$ via an AMPK-dependent, Akt/PKB-independent manner. This process is considered to be $Ca^{2+}$-dependent, however without the involvement of CaMKII or protein kinase C (PKC) (Thors et al., 2004). More recently AMPK was shown not to be a downstream target of thrombin stimulation since inhibition of the upstream AMPK kinase (CaMKII) using the CaMKII-specific inhibitor STO-609 or by inhibition AMPK itself had no effect on $Ser^{1177}$ phosphorylation (Stahmann et al., 2006). Thrombin phosphorylation of $Ser^{1177}$ was completely dependent on $Ca^{2+}$, suggesting a role for CaMKII but a different downstream kinase to AMPK (Stahmann et al., 2006). This contradicts the findings by Thors et al. (2004) above who used a generic protein kinase inhibitor (H89) to inhibit AMPK activation rather than one specific to CaMKII. This may highlight a role for two independent pathways involving CaMKII and AMPK both requiring the presence of $Ca^{2+}$.

Thrombin has been linked to $Ca^{2+}$ store release and SOCE (Sandoval et al., 2001) working independently of Akt/PKB and PI3K, increasing $Ser^{1177}$ phosphorylation and the NO surrogate marker cGMP levels in the presence of $Ca^{2+}$ (Motley et al., 2007). This process was suggested to be regulated by PKCδ (Motley et al., 2007). Thrombin, like Bk, is believed to have an auto-inhibitory function on eNOS activation. It was recently shown to phosphorylate the inhibitory eNOS residue $Thr^{495}$, which is associated with decreased eNOS activation (Watts and Motley, 2009). Here it was able to induce a rapid, but transient PAR-2 mediated phosphorylation of $Ser^{1177}$ and upon its cessation was met by increased PAR-1 induced $Thr^{495}$ phosphorylation suggesting that thrombin transiently increases eNOS phosphorylation but regulates its temporal activation (Watts and Motley, 2009).

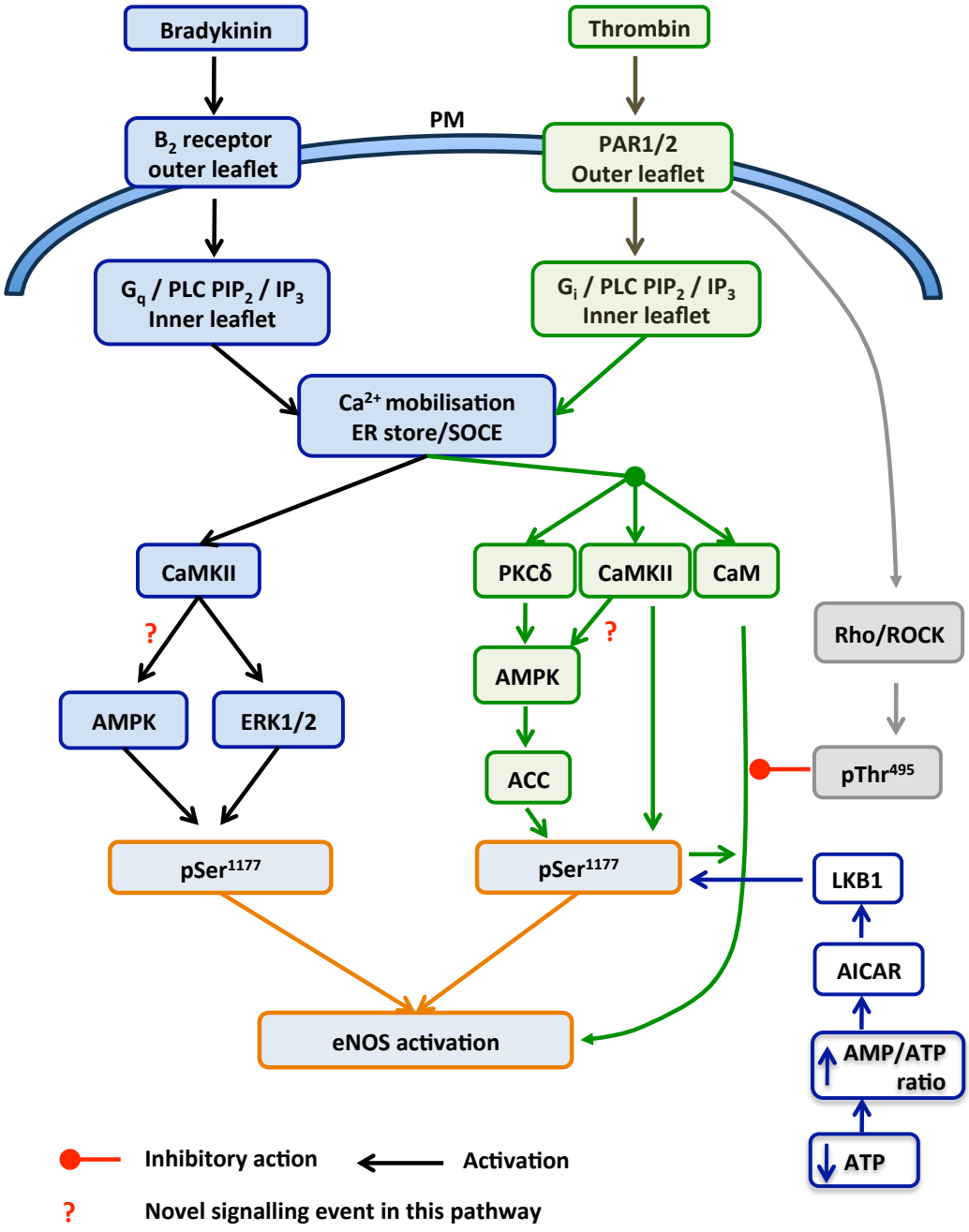


**Figure 1.4 Bradykinin and thrombin-induced eNOS Ser$^{1177}$ phosphorylation**

The figure outlines the pathways involved in bradykinin and thrombin-induced phosphorylation of eNOS, leading to eNOS activation. The blue filled panels represent the bradykinin pathway and the green filled panels show the thrombin pathway. Both pathways lead to phosphorylation of eNOS (pSer$^{1177}$). The clear panels (blue outline) represent the regulation of eNOS phosphorylation by adenosine triphosphate levels. PM, plasma membrane; pSer$^{1177}$, phosphorylation of eNOS at Ser$^{1177}$; The pathways are outlined in Stahmann et al., (2006), David-Dufilho et al., (2005), Watts & Motley, (2009), Thors et al., (2008), Fleming et al., (2003), Fleming et al., (2010).

### 1.6.3 Nitric oxide production

Nitric oxide (NO) is a potent signalling molecule in many cell types and is generated through the conversion of amino acid L-arginine, in the presence of NADPH and oxygen ($O_2$), to L-citrulline and NO (Fleming and Busse, 1999). Synthesis of NO is believed to occur following the shuttle of electrons ($e^-$) through the C-terminal end reductase domain from NADPH to flavine adenine dinucleotide (FAD) and flavin mononucleotide (FMN) targeting heme located in the N-terminal end oxygenase domain. Generation of NO sees a two-step monooxygenation process whereby NADPH donates $e^-$ to molecular oxygen ($O_2$), which reacts with bound substrate L-arginine forming L-omega-*N*-hydroxyarginine (LHA). A further single $e^-$ transfer from NADPH to $O_2$ is required for a nucleophilic attack of the LHA guanidino carbon to form a tetrahedral compound that eventually yields L-citrulline and NO production. CaM is believed to play a critical role in this process by allowing the flow of $e^-$ between the reductase and oxygenase domains (Abu-Soud et al., 1994, Presta et al., 1997) while dimerisation of eNOS is considered vital for NO production as $e^-$ flow through the flavins in the reductase domain of one monomer to the oxygenase domain of another (Siddhanta et al., 1998).

### 1.6.4 Vasodilation

Endothelium-dependent vasodilation (EDV) is mediated through smooth muscle (SM) relaxation, which dilates the vessel itself **(Figure 1.5)**. Nitric oxide exerts its effects through guanosine 3′, 5′-cyclic monophosphate (cGMP) generation and cyclic GMP-dependent protein kinase (PKG) activation, leading to SM relaxation through decreased ${}_{i}Ca^{2+}$ signalling in SMC. Nitric oxide release from EC diffuses through to the proximal

underlying smooth muscle layer and binds to its only known receptor to date, soluble guanylate cyclase. Soluble guanylate cyclase is a homodimeric protein with an N-terminal ferrous-binding domain, whereas the C-terminal end possess its catalytic ability (Dudzinski et al., 2006, Capece et al., 2008, Nimmegeers et al., 2007). Soluble guanylate cyclase is responsible for the generation of cGMP from GTP which occurs upon ligation of soluble guanylate cyclase with NO (Dudzinski et al., 2006). The primary target for cGMP is the cGMP-dependent protein kinase or protein kinase G (PKG), which is thought to decrease contractility by inhibiting store-operated $Ca^{2+}$ entry and sarco/endoplasmic reticulum $Ca^{2+}$ release (Gao, 2010). PKG however, may also prevent actin/myosin association by preventing the phosphorylation of myosin regulatory light chains (Ito et al., 2004, Surks et al., 1999).

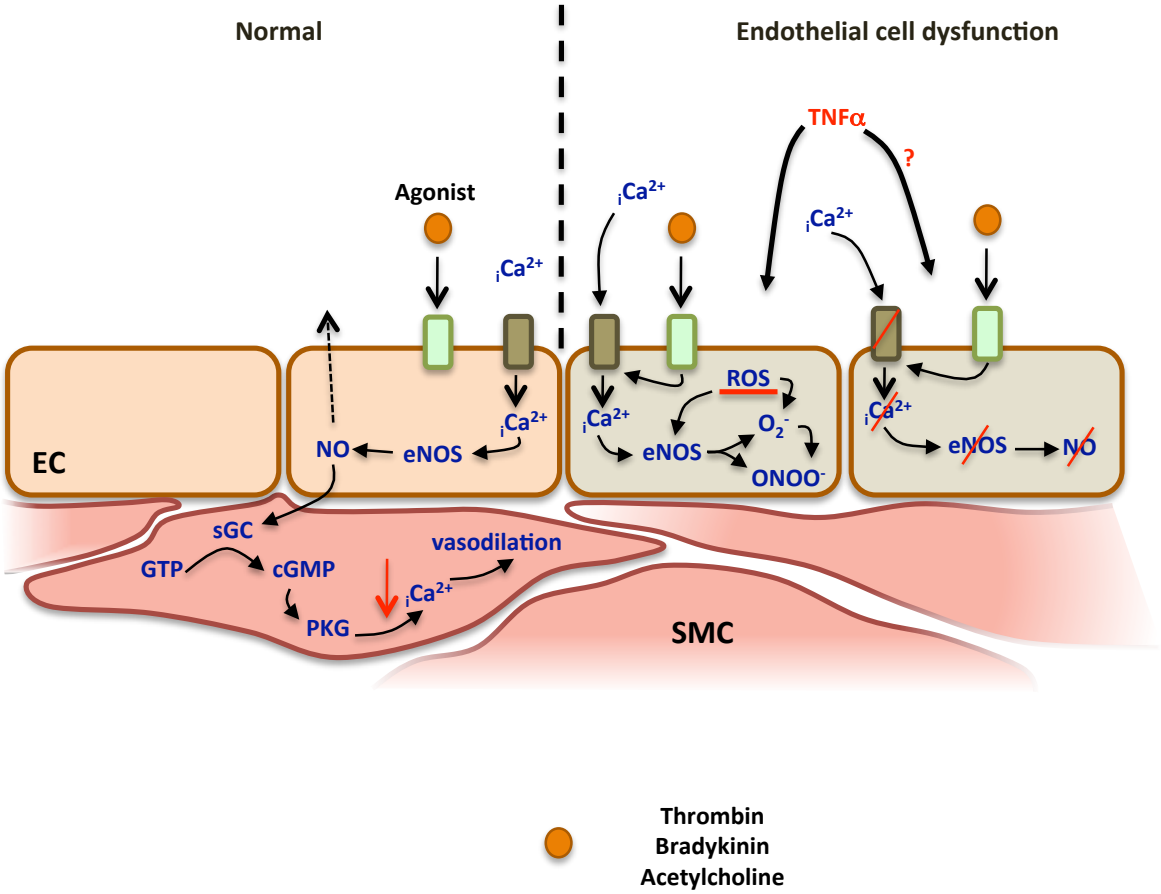


**Figure 1.5 Vasodilation and endothelial cell dysfunction**

One of the main mechanisms of nitric oxide (NO)-dependent vasodilation occurs by decreasing smooth muscle cell (SMC) intracellular calcium ($_{i}Ca^{2+}$). Endothelial cell (EC) $Ca^{2+}$ leads to activation of endothelial nitric oxide synthase (eNOS). This generates nitric oxide (NO) that diffuses to the underlying smooth muscle binding to soluble guanylate cyclase (sGC) which mediates the conversion of GTP (guanosine triphosphate) to cGMP (cyclic guanosine monophosphate). cGMP targets cGMP-dependent protein kinase (PKG) decreasing $_{i}Ca^{2+}$, essential for muscular contraction in SMC. Endothelial cell dysfunction (ECD) in this context describes the loss of NO and impaired vasodilation. In the presence of endothelial cell (EC) $Ca^{2+}$ but during increased oxidative stress, eNOS uncoupling can take place, which favours peroxynitrite ($ONOO^-$) formation as opposed to NO generation and vasodilation. In the absence of EC $Ca^{2+}$, there is an inhibition of upstream NO production. The symbol [?] in the 'endothelial cell dysfunction' panel represents a hypothetical role for TNFα in the regulation of $Ca^{2+}$ influx into endothelial cells.

## 1.7 The sphingolipid signalling pathway

### 1.7.1 Sphingomyelin

Sphingolipids have become increasingly recognised as important mediators of signal transduction mechanisms, facilitating intracellular messages through their lipid by-products. Serine palmitoyl CoA transferase is the rate-limiting enzyme in sphingolipid biosynthesis (Merrill and Jones, 1990). Plasma membranes consist mainly of cholesterol, phospholipids and sphingolipids, (Dumitru et al., 2007) of which sphingomyelin (SM) is the most abundant on the extracellular leaflet (Merrill and Jones, 1990). The sphingoid bases are long chain aliphatic amines that contain two or three hydroxyl groups and often a *trans* double bond at C4. The most common sphingoid base is sphingosine or [2*S*,3*R*,4*E*]-2-amino-4-octadecen-1,3-diol), a $C_{18}$ molecule which has hydroxyl groups at positions 1 and 3, and an amine group at $C_2$. This is coupled with a ceramide moiety, which is an acylated sphingosine at the 2-amino position (Huwiler et al., 2000). Sphingolipids are thought to have atherogenic potential and plasma SM is considered an independent risk factor for coronary heart disease (Nelson et al., 2006). Accordingly myriocin, an SM synthesis inhibitor, has shown to have possible anti-atherogenic effects by decreasing plasma SM and Cer levels highlighting their importance in cardiovascular biology (Hojjati et al., 2005).

### 1.7.2 Sphingomyelinase

Sphingomyelin phosphodiesterase (EC 3.1.4.12), otherwise known as sphingomyelinase (SMase) catalyses the hydrolysis of sphingomyelin (SM) to ceramide (Cer) and phosphorylcholine **(Figure 1.6)** (Kanfer et al., 1966). SMases were identified

nearly 50 years ago and have increasingly gained importance in cell biology (Kanfer et al., 1966, Brady et al., 1966, Schneider and Kennedy, 1967).

SMases exist in various splice variants that generally differ in terms of their primary structure, cation dependence and sub-cellular localisation (Pavoine and Pecker, 2009). Broadly speaking SMases were divided into three general categories according to their pH optima and called acid, neutral or alkaline SMase (Goni and Alonso, 2002). These enzymes derive from distinct genes termed *sphingomyelin phosphodiesterase* (*SMPD*). The acid SMase (ASM) gene *SMPD1*, was the first to be cloned from human urine in 1989 giving two splice variants (Quintern et al., 1989a, Schuchman et al., 1991, Schuchman et al., 1992, Quintern et al., 1989b). It was later confirmed that *SMPD1* gave rise to a lysosomal and secretory fraction of the enzyme termed accordingly and now known as lysosomal SMase (L-SMase) and secretory SMase (S-SMase). Neutral sphingomyelinases (nSMases) arise from three distinct genes termed *SMPD2-4* following SMPD1 described above. The neutral SMase genes give rise to a protein product each termed nSMase1 (from *SMPD2*) (Hofmann et al., 2000), nSMase2 (*SPMD3*) (Tomiuk et al., 1998) and nSMase3 (*SMPD4*) (Krut et al., 2006). The nSMases are $Mg^{2+}$-dependent enzymes with an optimum hydrolytic capacity of pH 7.4 (Goni and Alonso, 2002). They are sub-cellular enzymes localising to the ER, golgi apparatus and inner plasmalemmal face (Krut et al., 2006, Hofmann et al., 2000, Tomiuk et al., 1998, Tani et al., 2007). Alkaline SMase is a $Mg^{2+}$ independent enzyme involved in cancer biology, however it is beyond the scope of this thesis (Goni and Alonso, 2002, Duan, 2006).

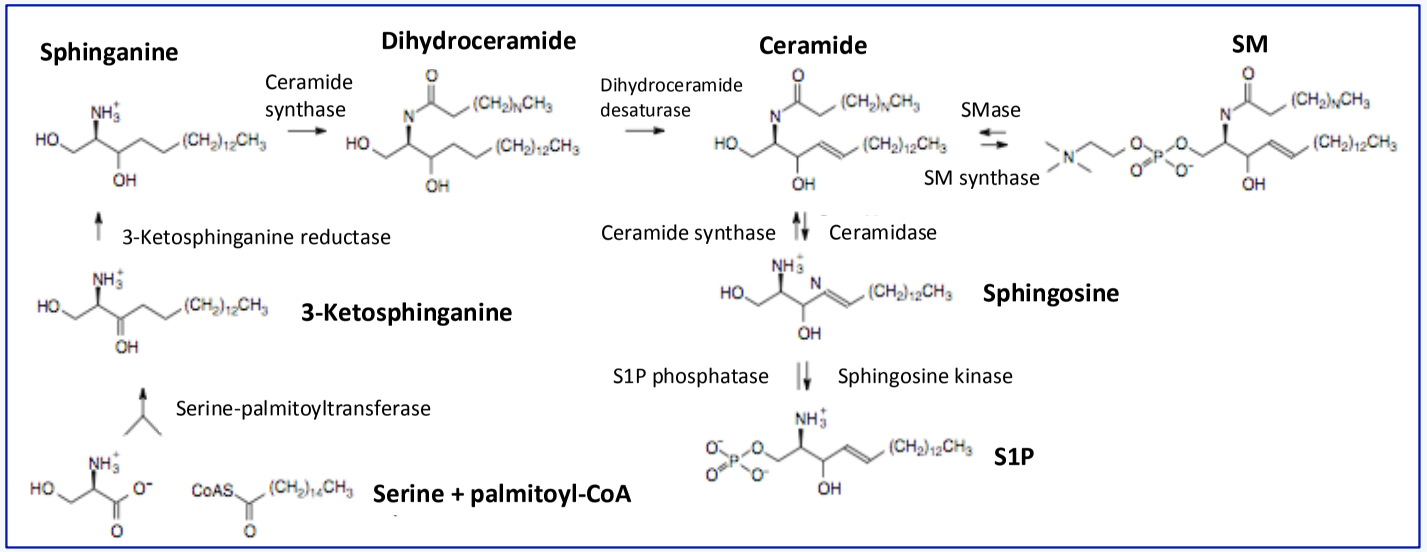


**Figure 1.6 Sphingomyelin metabolism**

This figure shows the pathways involved in sphingomyelin (SM) hydrolysis and synthesis. SM is synthesised from serine and palmitoyl-Coenzyme A by serine palmitoyl transferase. This sequence yields 3-ketosphingosine, sphinganine, dihydroceramide, ceramide and finally SM. Conversely, SM is catabolised by sphingomyelinases (SMases) to the bioactive lipid ceramide which can be further broken down by ceramidase to sphingosine. Subsequently, sphingosine kinase can produce sphingosine-1-phosphate (S1P) from sphinganine itself. The reverse reaction can also yield SM from S1P. Where SM, sphingomyelin; SMase, sphingomyelinase; S1P, sphingosine-1-phosphate; Adapted from Kolesnick & Fuks (2003).

### 1.7.2.1 Neutral sphingomyelinase (nSMase)

The biological roles of nSMases have been extensively studied over the past 15 years and have been associated with cell growth, proliferation, apoptosis and senescence (Hannun and Obeid, 2008). nSMases are ubiquitously expressed and all three enzymes share similar biochemical characteristics (Stoffel et al., 2007, Levade et al., 1991, Krut et al., 2006). nSMase1 and nSMase2 are present in significant amounts in the brain, have a high affinity for $Mg^{2+}$ and are activated by fatty acids and phosphatidylserine (PS) (Hofmann et al., 2000). nSMase3 is a member of the C-tail-anchored integral membrane proteins and forms part of the TNFR1 membrane receptor and 'factor-associated with nSMase activation' (FAN) signalling which is essential for nSMase activation (Krut et al., 2006). nSMase3 (*SMPD4*) was shown to be abundant in striated smooth muscle responsive to TNFα (Krut et al., 2006). As the only nSMase to be highly expressed in cardiac myocytes, it begs the question as to whether it has a role in cardiac pathobiology (Krut et al., 2006).

nSMases have also been associated with apoptotic and proliferative processes (Krown et al., 1996, Kolmakova et al., 2004, Tellier et al., 2007). Much of our current understanding of nSMases in cell signalling has come from work on cardiomyocytes and vascular smooth muscle cells (VSMC). Indeed nSMase has been closely associated with pro-inflammatory markers such as TNFα and apolipoprotein A-1 suggesting a link with atherosclerosis (Oral et al., 1997, Tellier et al., 2007, De Palma et al., 2006, Auge et al., 1996, Kolmakova et al., 2004). Interestingly, nSMase has shown a sensitivity to changes in oxidative stress induced by TNFα following a decrease in GSH (Liu et al., 1998, Liu and

Hannun, 1997). Accordingly, GSH repletion using NAC was shown to inhibit ROS production and nSMase activation in response to TNFα (Cailleret et al., 2004).

### *1.7.2.2 Acid sphingomyelinase (ASM)*

#### 1.7.2.2.1 Cellular processing

Acid sphingomyelinase (ASM), is a zinc-dependent enzyme with a predominantly acid pH optimum, the schematic structure of which is shown in **figure 1.7.** ASM has also been shown to work at neutral pH by hydrolysing lesional LDL-associated SM, suggesting its lipase activity it is not limited to acidic microenvironments thus may be applicable in disease (Schissel et al., 1996b). As mentioned above, the two products of the *SMPD1* gene were termed lysosomal SMase (L-SMase) and secretory SMase (S-SMase) on the basis of their topology. Pulse-chase radiolabelling of the protein precursor in normal and I-cell fibroblasts (cells lacking the capability to traffic proteins to lysosomes), revealed ASM to be subject to proteolytic processing from an initial 75 kDa protein to a 70-72 kDa mature enzyme which can be digested to a 57 kDa protein (Ferlinz et al., 1994, Hurwitz et al., 1994b, Marathe et al., 1998, Hurwitz et al., 1994a). Assessed by matrix-assisted laser desorption/ionization (MALDI) mass spectrometry, the placental ASM showed eight intra-molecular disulfide bridges spanning the length of the protein (Lansmann et al., 2003). The importance of the cysteine residues in ASM was highlighted in a study by Qiu et al., (2003), who showed that deletion or mutation of the carboxy terminal $Cys^{629}$ significantly increased enzymatic activity (Qiu et al., 2003). ASM also has several predicted *N*-glycosylation sites, which are considered important for the maturation of ASM especially in the lysosomal environments (Ferlinz et al., 1994).

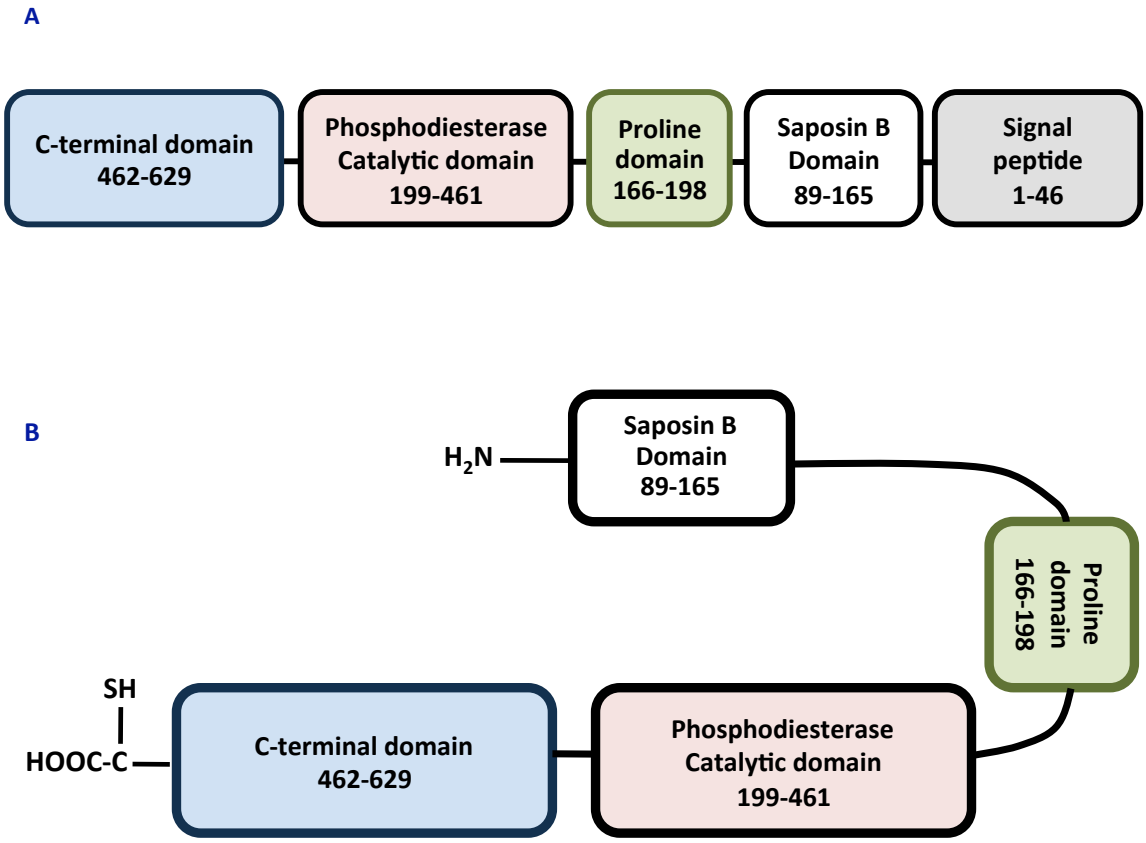


**Figure 1.7 Structure of acid sphingomyelinase**

**(A)** The primary polypeptide form of acid sphingomyelinase (ASM) showing its different structural domains prior to signal peptide digestion. The saposin domain is thought to be involved in substrate presentation to the phosphodiesterase domain. **(B)** Conformational structure of the mature ASM protein showing the C-carboxyl terminal end involved in activation of ASM and the location of the catalytic phosphodiesterase domain. Figure generated and adapted from Jenkins et al., (2009), and Qiu et al. (2003) Kolter et al. (2005) Jenkins et al. (2010b).

The *SMPD1* product is subject to post-translational modification and mannose-6-phosphate (M6P) trafficking (Ferlinz et al., 1994). Lysosomes are acidic intracellular vesicles that contain hydrolytic enzymes taking part in phagocytosed bacterial killing, autophagy and transport of proteins (Kornfeld, 1987). It has been suggested that L-SMase and S-SMase derive from differential intracellular trafficking with L-SMase trafficked through the M6P shuttle system to endo-lysosomes or the PM, while S-SMase takes the default Golgi secretory pathway and is either secreted or shuttled to the PM (**Figure 1.8)** (Tabas, 1999, Hurwitz et al., 1994b).

Alternative oligosaccharide processing in the Golgi apparatus is believed to target the ASM precursor to the default secretory pathway. The precise targeting of lysosomal hydrolases depends on M6P binding residues recognised by M6P receptors and pre-lysosomal shuttling. The key enzyme catalysing this M6P tagging is N-acetyl glucosamine phosphotransferase (NAGPT) in the Golgi apparatus (Marathe et al., 1998). Differential trafficking between L-SMase and S-SMase was evident when raised S-SMase levels in EC medium came about with concomitant decrease of L-SMase in cell lysates. Furthermore, mutation in the lysine residue $Lys^{93}$ which is important in NAGTP recognition of ASM led to decreased intracellular activity and raised secretory activity of ASM (Takahashi et al., 2005). An alternative trafficking pathway has been proposed whereby sortilin, a membrane neuromediator receptor, was directly associated with ASM delivery to phagosomes in MΦ (Wahe et al., 2010, Jin et al., 2008).

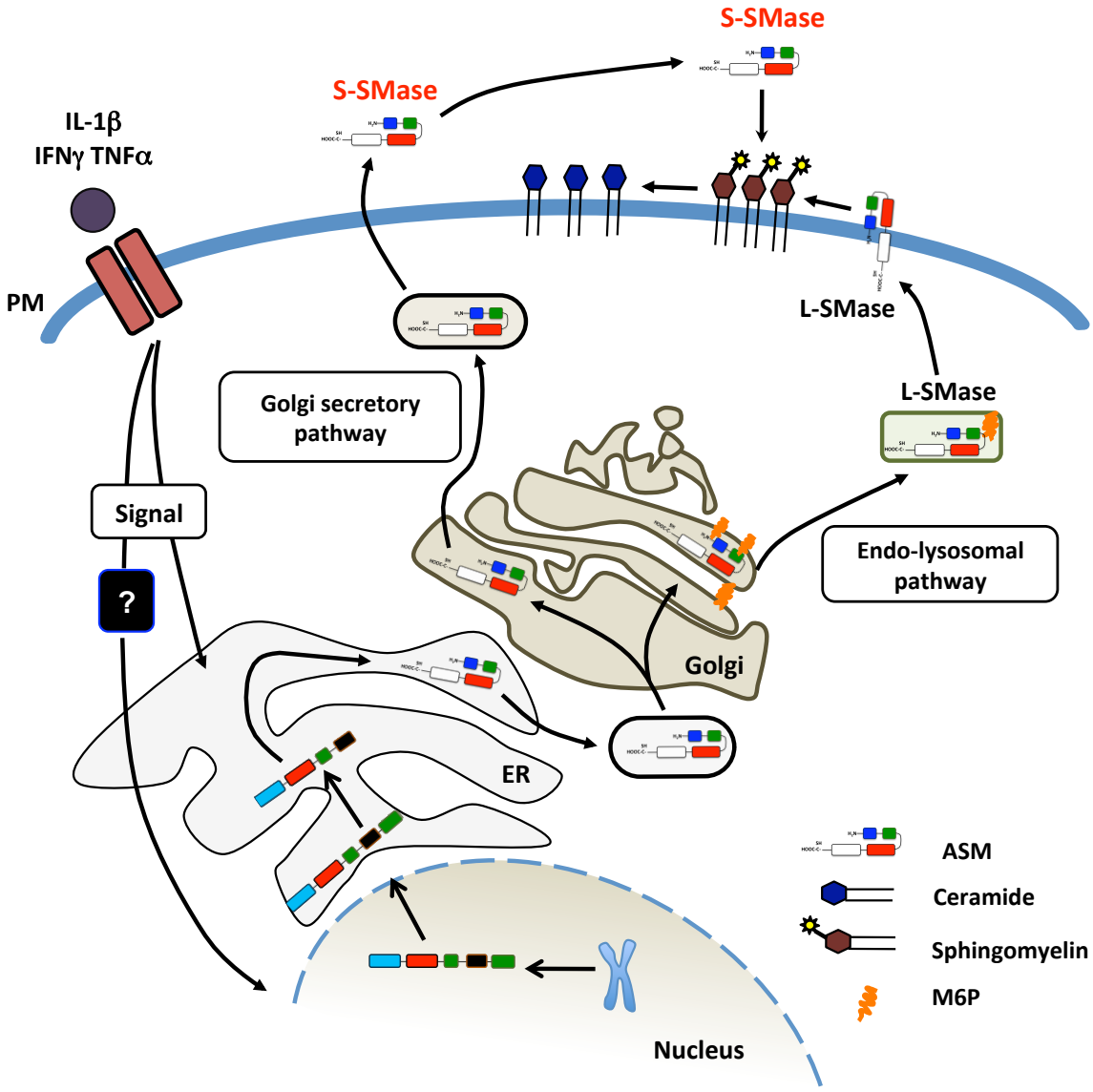


**Figure 1.8 Regulation of acid sphingomyelinase trafficking and secretion**

Alternative splicing gives rise to an active acid sphingomyelinase (ASM) pre-cursor which undergoes post-translational modification in the endoplasmic reticulum **(ER)**. The mature protein is trafficked to the golgi where if mannose-6-phosphate **(M6P)** tagged, it is targeted to lysosomes where it is activated by $Zn^{2+}$ binding. Alternatively, the proASM takes the default golgi secretory pathway where it is released from the cell and requires $Zn^{2+}$ for activation. Secretion of S-SMase can be stimulated by pro-inflammatory mediators such as IL-1β, IFNγ and TNFα.

#### 1.7.2.2.2 Lysosomal acid sphingomyelinase (L-SMase)

Lysosomal acid sphingomyelinase (L-SMase) is best known for its involvement in Niemann-Pick disease (NPD) a lysosomal storage disorder that features abnormally high levels of SM due to *SMPD1* deficiency (Schneider and Kennedy, 1967). Localisation of L-SMase however is not only limited to lysosomes but can be PM-associated, possibly in lipid rafts (LR) (Grassme et al., 2001). L-SMase encounters cellular pools of $Zn^{2+}$ during trafficking and maturation thus is a $Zn^{2+}$-independent enzyme (Jenkins et al., 2010b).

##### 1.7.2.2.2.1 L-SMase and apoptosis

L-SMase is ubiquitously expressed in most cells and like nSMases is considered to have housekeeping roles. In fact the best evidence for its involvement in apoptosis comes from the protection gained in its absence in ASM knockout ($ASM^{-/-}$) cells. Defective TNF$\alpha$-induced apoptosis has been witnessed in $ASM^{-/-}$ EC and hepatocytes (Haimovitz-Friedman et al., 1997, Garcia-Ruiz et al., 2003). Similarly, apoptosis was also averted following radiation treatment in $ASM^{-/-}$ human lymphoblasts (Santana et al., 1996), after phototoxicity in $ASM^{-/-}$ lymphoblasts (Separovic et al., 1999) and following ischemia reperfusion injury (Llacuna et al., 2006).

##### 1.7.2.2.2.2 Regulation of L-SMase

There is no known biological inhibitor of L-SMase to date, however it is sensitive to the reducing agent DTT but was not directly affected by GSH (Liu and Hannun, 1997). Accordingly, observations by Qiu et al., (2003) support a role for oxidative stress in the activation of L-SMase. A recent account described ROS involvement in ASM-mediated, Cer-induced neutrophil apoptosis that could be inhibited using the antioxidant

desferrioxamine in cultured neutrophils (Scheel-Toellner et al., 2004). The Gulbins group recently reported that sensitization of glioma cells to chemotherapy was due to expression of ASM and increased Cer levels, which could be prevented by neutralizing ROS (Grammatikos et al., 2007). Other activators of L-SMase include Fas/Fas ligand (Zhang et al., 2007, Jin et al., 2008) and endostatin (Zhang et al., 2005a). Intriguingly, TNFα has been shown to cause rapid activation of L-SMase in bovine coronary artery endothelial cells (BCAEC) raising Cer levels within 2 minutes leading to decreased EDV. This was suggested to occur through Cer-induced $O_2^-$ production and eNOS uncoupling with no direct causal effect of Cer (Zhang et al., 2002).

#### 1.7.2.2.2.3 L-SMase and disease

L-SMase has been linked to various pathologies including gastrointestinal syndrome, cystic fibrosis and hepatic injury recently reviewed in Zeidan and Hannun, (2010). Recent advances have highlighted a role in regulation of vascular tone. It is here that stimulation of CD95 led to L-SMase translocation to the PM and generation of extracellular orientated Cer, followed by clustering of CD95 itself (Grassme et al., 2003). This supports a role for Cer in potentiating intracellular signals suggested to occur through receptor clustering in lipid rafts (LR) and membrane platform formation (Gulbins, 2003, Jin et al., 2008). Fas ligand (FasL)-induced inhibition of EDV could be prevented by disrupting L-SMase transport to the plasma membrane in coronary artery EC (CAEC) (Jin et al., 2008). Zhang et al., demonstrated that these events may be regulated through a redox mechanism. Accordingly, superoxide production was able to increase L-SMase activity and lead to the formation of LR redox signalling platforms, inhibited by superoxide dismutase (SOD) (Zhang et al., 2007).

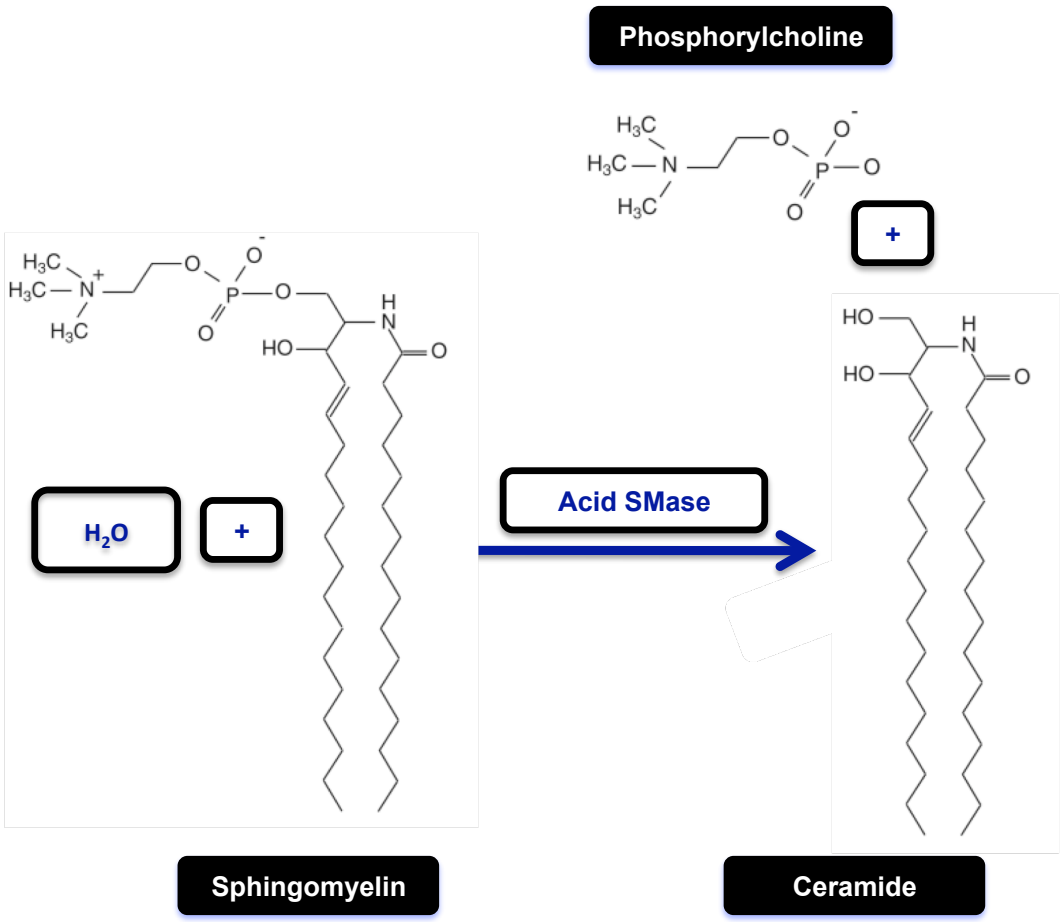


**Figure 1.9 Hydrolysis of sphingomyelin to ceramide by acid sphingomyelinase**

The figure shows the chemical structures of sphingomyelin, ceramide and phosphorylcholine. Acid sphingomyelinase (Acid SMase) hydrolyses sphingomyelin, cleaving the phosphorylcholine head-group to yield free phosphorylcholine and the bioactive lipid ceramide. Adapted from Smith & Schuchman (2008b).

L-SMase has been shown to regulate vascular dilatation and has been linked to ROS-mediated phagocytic killing, evident by decreased anti-bacterial activity against *Salmonella* in $ASM^{-/-}$ MΦ (McCollister et al., 2007). This suggests that it may play a role in atherosclerosis and functioning of the innate immune response.

#### 1.7.2.2.3 Secretory acid sphingomyelinase (S-SMase)

Spence et al. (1989) is considered the first to have described active S-SMase in bovine serum. S-SMase does not encounter intracellular $Zn^{2+}$ thus is a $Zn^{2+}$-dependent hydrolase (Schissel et al., 1996a) with an acid pH optimum (Schissel et al., 1998a). S-SMase is the only SMase described to date found active in soluble media (Tabas, 1999) and it has only been found active in media cultured with stimulated stromal cells or platelets (Romiti et al., 2000). Macrophages and fibroblasts can release active S-SMase however the most abundant source are EC (Marathe et al., 1998, Schissel et al., 1996a), while Chinese Hamster Ovary (CHO) cells are often used for recombinant human ASM transfections (Schissel et al., 1996a, Qiu et al., 2003).

##### 1.7.2.2.3.1 Regulation of S-SMase

Most notably, pro-inflammatory cytokines have been shown to induce S-SMase release. In particular, IL1β, IFN-γ and to a lesser extent IFN–β caused active S-SMase to be detected in HUVEC medium by 18 hours (Marathe et al., 1998). Lipopolysaccharide (LPS) and TNFα have been linked with S-SMase release (Wong et al., 2000) and though this evidence suggests a role for TNFα in L-SMase activation in EC *in vitro*, its effect on S-SMase activation has only been demonstrated *in vivo* (Wong et al., 2000). At the same time TNFα and IL-1β appear to have a synergistic effect on S-SMase release *in vivo* (Wong

et al., 2000). These data suggest a potential role for local stimulation of S-SMase release by pro-inflammatory mediators, possibly increasing systemic levels of the enzyme. S-SMase activity from human serum was shown to increase following the addition of pro-oxidant 2,2'-azobis-2-amidinopropane (AAPH) and could be halted using the anti-oxidant ascorbic acid (Claus et al., 2005). In the study described above by McCollister et al., S-SMase was found to increase by 4 hours in MΦ medium after being challenged with *Salmonella* or *E. coli.* In support for the role of ROS in S-SMase activation, ASM-mediated bacterial killing was ROS-dependent, however it was not clear whether this involved S-SMase (McCollister et al., 2007).

#### 1.7.2.2.3.2 S-SMase in vascular pathophysiology

As with L-SMase, S-SMase has also been linked with atherosclerosis (Marathe et al., 1999, Marathe et al., 2000) and proposed to regulate subendothelial LDL retention in early atherogenesis (Tabas et al., 2007). Several lines of evidence support its role in atherogenesis. Increased SMC proliferation is evident in atheromatous lesions (Ross, 1999) and early studies showed that the mitogenic effects of oxidised LDL on SMC proliferation could be reproduced using exogenous bacterial SMase (nSMase) and short chain ceramides (Auge et al., 1996). Work from the Tabas group later showed that S-SMase can hydrolyse lesional (not plasma) LDL bound SM at neutral pH outside its pH optimum. Furthermore, they confirmed immuno-reactivity of anti-ASM antibodies to antigen in the intima of atherosclerotic lesions, while sodium-[$^{124}$]-iodide labeled S-SMase bound to the extracellular matrix of aortic SMC and EC (Marathe et al., 1999, Schissel et al., 1998a). In a recent study ASM, possibly as S-SMase, was associated with increased LDL retention, a mechanism in early atherogenesis, whereby ASM$^{-/-}$ mice showed significantly

decreased aortic root lesion area and as much as 87% less lipoprotein trapping compared with wild type (WT) mice, similar to LDL receptor deficient mice (Devlin et al., 2008).

#### 1.7.2.2.3.3 Evidence for S-SMase in clinical disease

Recently S-SMase has been found elevated in several clinical disease states including sepsis (Claus et al., 2005), cardiac cachexia (Doehner et al., 2007), hypercytokinaemia in haemophagocytic lymphohistiocytosis (HLH) (Takahashi et al., 2002), type 2 diabetes (Gorska et al., 2003) and following ionizing radiation treatment in cancer patients (Sathishkumar et al., 2005). ASM is known to be sensitive to ROS-mediated activation as shown in sepsis patients while raised pro-inflammatory cytokine profiles may underlie the increased S-SMase levels in HLH. In chronic heart failure (CHF), correlation analysis revealed a negative association between S-SMase activity and peripheral vasodilator capacity and an association with circulating TNF$\alpha$ levels suggesting S-SMase activity suggesting S-SMase activity may rise with TNF$\alpha$ (Doehner et al., 2007). What all SMases have in common is the hydrolysis of SM generating the downstream mediator ceramide.

### 1.7.3 Ceramide

Ceramide (Cer) is the major product of sphingolipid metabolism that has a central role in intracellular signalling. Cer is a bioactive sphingolipid implicated in apoptosis, cell cycle arrest and cell senescence (Kitatani et al., 2008). It can be principally synthesized in four ways including *de novo* in the ER, recycling of exogenous Cer (short chain $C_6$-Cer), SM catabolism (by SMase), and the salvage pathway from endo-lysosomal sphingolipids (Kitatani et al., 2008). Cer can also be formed by reversible synthesis from its downstream by-products such as ganglioside, glucosylceramide and sphingosine reviewed in Levade et

al., (2001). The most studied routes of Cer synthesis are the *de novo* and SMase pathways and for the purposes of this thesis, the latter is of principal interest. Cer is composed of a sphingosine base and a long fatty acid chain **(Figure 1.9**). Sphingosine linkage to the fatty acid occurs via an amido group at C2, whilst carbons at C1 and C3 are hydroxylated. The head group of sphingosine is complete with a double bond between C4 and C5.

The SM/Cer pathway generates different cellular responses depending on the topology of SM hydrolysis and availability of SMases responsible (Huwiler et al., 2000). Accordingly, Cer has been associated with both necrotic and apoptotic independent pathways (Villena et al., 2008, Colell et al., 2002, Kolesnick and Fuks, 2003). Perhaps the best evidence of ASM-derived Cer in cellular stress responses comes in its absence from studies using ASM $^{-/-}$ mice since ASM null mice appear to be protected from apoptosis described in L-SMase and apoptosis. Cer has also been linked with CD40-induced Factor associated with neutral sphingomyelinase (FAN)-mediated apoptosis through nSMase activation (Segui et al., 1999). Conversely, Cer involvement has been described in cell proliferation and associated with MAPK-dependent mitogenic effects in response to TNF$\alpha$, bacterial nSMase and oxidised LDL (Auge et al., 1996, Raines et al., 1993, Sasaki et al., 1995).

#### *1.7.3.1 Topology of Cer generation by ASM*

One of the leading questions surrounding the mechanism of S-SMase-mediated Cer generation is its access to SM. SM is highly abundant in the outer leaflet of the PM giving S-SMase likely access to large pools (Merrill and Jones, 1990). Generation of Cer on the outer plasmalemmal face has been shown to lead to alteration of PM architecture and dynamics, cause LR formation, receptor clustering and intracellular signal propagation (Grassme et al., 2001, Jin et al., 2008). Thus, it is feasible that Cer can be generated by L-

SMase and S-SMase at the cell surface, however to date there is no evidence of S-SMase association at the outer PM leaflet due to the technical difficulties that surround this exercise.

### *1.7.3.2 Ceramide, endothelial dysfunction and ROS production*

Cer generation has been shown to occur downstream of ROS production (Hernandez et al., 2000) and also to stimulate the release of oxygen radicals in EC itself (Li et al., 2002). These are believed to be mitochondrial-derived, which can be blocked by ASM inhibitors and mitochondrial complex III inhibitors (Therade-Matharan et al., 2005, Corda et al., 2001). ASM-generated Cer was suggested to inhibit EDV in a process instigated by TNF$\alpha$. This led to ROS generation through the membrane-bound NADPH oxidase system leading to $O_2^-$ production and $ONOO^-$ formation but was blocked by the NAPDH oxidase inhibitor N-vanillynonanamide in EC (Zhang et al., 2001, Zhang et al., 2002, Zhang et al., 2003). In light of the recent observation that oxidation of the C-terminal $Cys^{629}$ activates ASM (Qiu et al., 2003), it is possible that increased ROS generation could activate ASM generating Cer-enriched LR, clustering of NADPH subunits propagating ROS formation and amplifying redox signalling in EC (Zhang et al., 2008). The above highlight the potential involvement of Cer in ECD and favour a pro-atherogenic role for Cer. To complement these observations, there have been several reports of Cer interfering with $Ca^{2+}$ signalling.

### *1.7.3.3 Ceramide, membrane platform formation and $Ca^{2+}$ signalling*

Cer is involved in the formation of PM microdomains through Cer-Cer interactions (Sot et al., 2006). Due to its biophysical nature, Cer indeed favours the formation of Cer-enriched microdomains, which vary in comparison to phosphatidylcholine membranes.

This is believed to occur through tight interactions between Cer molecules that associate closely due to their polar headgroups (Megha and London, 2004, Kolesnick et al., 2000).

In similar fashion, these microdomains may also fuse creating larger Cer-enriched macrodomains (platforms) (Grassme et al., 2001). Membrane platforms are known to cluster and aggregate surface receptors which are thought to create a highly dense area of receptor signalling units, facilitating efficient signal transduction (Grassme et al., 2001, Gulbins and Grassme, 2002, Grassme et al., 2003). Accordingly evidence exists for Cer-mediated clustering of CD95 and CD40 at the PM surface, an event thought to be crucial for CD95 signalling (Grassme et al., 2001, Grassme et al., 2002). Similarly, lateral association of Cer in the PM can lead to its aggregation which may potentiate cell signals by oligomerising receptor sub-units and causing protein dimerisation (Deaglio et al., 2007). To this end, ASM translocation to the cell surface can lead to Cer-dependent formation of LR redox signalling platforms (Jin et al., 2008).

Although Cer was also reported to prevent caveolin-1 inhibition of eNOS, proximal to to LR, planar lateral association of Cer molecules is thought to affect ion channel formation such as $I_{CRAC}$ **(Figure 1.10)** (Der et al., 2006). Accordingly Cer has been shown to interfere with $Ca^{2+}$ signalling in various cell types including rat pinealocytes, rat thyroid FRTL-5 cells and cardiac myocytes (Negishi et al., 1998, Condrescu and Reeves, 2001, Tornquist et al., 1999). Similarly, In T lymphocytes, nSMase and Cer led to decreased SOCE, which was abrogated in $ASM^{-/-}$ cells (Church et al., 2005). Therefore Cer generation at the PM by S-SMase could induce Cer-enriched platform formation, thus altering ion channel dynamics and affecting $Ca^{2+}$-dependent signalling cascades such as NO production **(Figure 1.10)**.

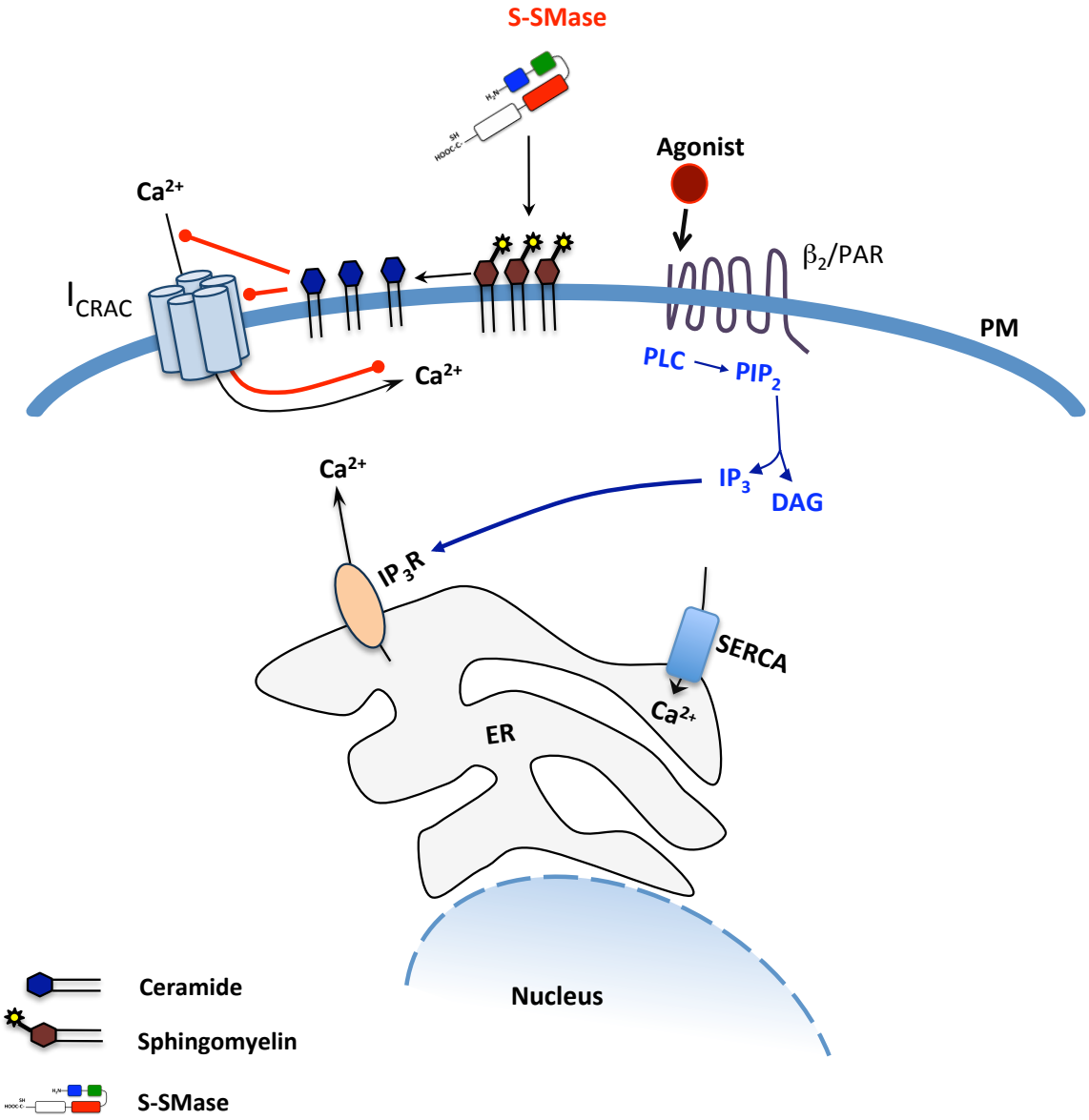


**Figure 1.10 Hypothetical role of ceramide in disruption of $Ca^{2+}$ signalling in EC**

Secretory sphingomyelinase (S-SMase)-induced ceramide (Cer) generation on the outer leaflet of the plasma membrane may disrupt protein relationships such as those of $Ca^{2+}$ channels $I_{CRAC}$ leading to decreased $Ca^{2+}$ influx.

## 1.8 Summary

Both RA and PSV have been linked with enhanced CVD in particular accelerated atherosclerosis. What both these diseases have in common with atherosclerosis is endothelial dysfunction supported by observations in clinical disease. ECD in this setting is best described as impaired EDV brought about by decreased NO production. The process of NO production is carried out by eNOS activation, an enzyme tightly $Ca^{2+}$-dependent. Previous work from our laboratory has found that Cer can regulate the major source of cell $Ca^{2+}$ by blocking SOCE. Cer is a ubiquitous downstream lipid messenger produced following SM catabolism by SMases. A particular fraction of SMase is soluble and readily secreted by EC (S-SMase) in response to pro-inflammatory cytokines found raised in RA and PSV. S-SMase therefore could access multi-site endothelia and alter EC signalling, causing ECD and deregulating vascular function considered an early event in atherosclerosis.

## 1.9 Hypothesis and aims of the thesis

### Hypothesis

Vascular inflammation in RA and vasculitis leads to persistent exposure of endothelial cells to TNFα and ROS that may act synergistically to alter signalling in these cells. TNFα and ROS activate sphingomyelinase, which may be a key mediator of endothelial cell dysfunction through ceramide generation causing a decrease in $_{i}Ca^{2+}$ signalling and subsequent inhibition of $Ca^{2+}$-dependent eNOS activation and loss of nitric oxide production.

### Aims of the thesis

1. To investigate the presence, activity and role of S-SMase in vasculitis and RA
2. To establish a model for the exploration of S-SMase-induced endothelial dysfunction
3. To determine whether TNFα and oxidative stress induce the secretion and modulate the activity of native endothelial-derived S-SMase
4. To examine the mechanism by which S-SMase may cause endothelial cell dysfunction.

# Chapter 2

# Materials and Methods

# 2 Materials & Methods

## 2.1 Materials

All materials were purchased from Sigma-Aldrich UK, unless otherwise stated

| | |
|---|---|
| ASM specific Peptide-CPG beads | **Alta Bioscience** |
| Benchtop microcentrifuge | **Eppendorf 5415R** |
| ECL solution | **GE Healthcare** |
| E.L.I.S.A. 96 well plates | **Maxisorp, *Nunc* Technologies** |
| Exposure Film (X-ray) | **Kodak** |
| Fluorometric Nitric Oxide Assay kit | **Calbiochem, Molecular Probes** |
| Foetal calf serum | **Biosera** |
| FURA-2 AM | **Invitrogen, Paisley, UK** |
| Hanks Buffered Salt Solution | **Gibco Scientific** |
| Heparin | **Multiparin** |
| Human Serum | **HD Supplies** |
| Hydrochloric Acid | **Fisher Scientific** |
| Microplate Fluorescence reader - | **Fluoroskan Ascent, Labsystems** |
| Microplate photometer | **Anthos ht II** |
| Medium 199 | **Gibco (Invitrogen)** |
| NBD-SM | **Molecular Probes** |
| Parafilm | **Pechiley Plastic Pack'g, Menasha, US.** |
| PVDF Membrane | **Geneflow** |
| Sodium Nitrate | **Fisher Scientific** |
| Solvents (Methanol, ethanol, Chloroform) | **Fisher Scientific** |
| Tris/Glysine/SDS (10x) | **Geneflow** |
| Tris/Glycine (10x) | **Geneflow** |
| TLC plates | **Alugram® Macherey-Nagel, Germany** |
| Trypsin-EDTA | **Gibco (Invitrogen)** |
| Vacuum Pump (Speed Vac SC100 Savant) | **Divac, 2.4 L, Leybold** |
| Vivaspin-30 concentrators | **GE Healthcare** |
| Well plates | **Sarstedt** |

## 2.2 Methods

### 2.2.1 Methodological notes

| | | |
|---|---|---|
| **1** | **Growth medium** | Fully supplemented medium routinely used for cell growth prior to experimentation (in the case that other media were used during an assay) |
| **2** | **Centrifugations** | Unless stated otherwise, all centrifugations were performed at room temperature in a Mistral 3000i centrifuge, MSE at 322 *x g* (1200 rpm) |
| **3** | ***In vitro* treatments** | For each treatment, an appropriate solvent control was used (v/v, w/v). This typically included $dH_2O$, PBS, HBSS, DMSO, buffered aqueous glycerol solution, ethanol. |
| **4** | **Tissue culture** | Unless stated otherwise, all tissue culture incubations forming part of normal growth culture conditions or experimental incubations, were performed at $37^0$C, 5% $CO_2$ in a humidified atmosphere. |

Table 2. 1 General laboratory notes

#### *2.2.1.1 Media formulations*

| Medium | Use | Supplementation |
|---|---|---|
| **M199 fully supple/ed** | General tissue culture, HUVEC $Ca^{2+}$ signalling assays | Penicillin (100 U/mL), Streptomycin (100 μg/mL), HIFCS (15%), Human serum (5%), Heparin (10 U/mL), EGF (10 ng/mL) |
| **M199 (P/S alone)** | Serum starvation, acute serum-free treatments | Penicillin (100 U/mL), streptomycin (100 μg/mL) |
| **HESFM** | ( ≤24h) serum-free ASM secretion assays NO production assays | Penicillin (100 U/mL), streptomycin (100 μg/mL), bFGF (20 ng/mL), heparin (10 U/mL), EGF (20 ng/mL), BSA (0.2%). |
| **DMEM** | ( ≤24h) serum free ASM secretion assays | Penicillin (100 U/mL), streptomycin (100 μg/mL), ), EGF (20 ng/mL), BSA (0.2%) |
| **HBSS** | HUVEC $Ca^{2+}$ signalling assays | Prepared in $dH_2O$ with 7.5% sodium bicarbonate ($NaHCO_3$), 1.0 mmol/L HEPES |

Table 2. 2 List of cell culture supplementations

### 2.2.1.2 Tissue culture & heat-inactivation

Molten LaminAir Model 1.2 Class II biological safety cabinets were used for sterile conditions and maintaining sterile solutions and equipment. Non-sterile solutions were filtered through a 0.2 μm filter. Serum, plasma and media were heated to 57$^0$C for 30 minutes. Samples were cooled to room temperature and stored appropriately.

### 2.2.1.3 Patient samples

| | Material | PEX | Source | Storage |
|---|---|---|---|---|
| **AASV cohort 1**[4] | Plasma | Yes | Renal Immunobiology group [1] | -80$^0$C |
| **AASV cohort 2**[4,5] | Serum | No | Wellcome clnical trials unit [3] | -80$^0$C |
| **AASV cohort 3**[4] | Plasma | Yes | Renal Immunobiology group [1] | -80$^0$C |
| **AASV cohort 4**[4,7] | Plasma | Yes | Renal Immunobiology group [1] | -80$^0$C |
| **AASV cohort 5**[3,5] | Serum | No | Renal Immunobiology group [1] | -80$^0$C |
| **RA**[6] | Serum | No | Russell's Hall Hospital [2] | -80$^0$C |

Table 2. 3 Clinical patient sample cohorts

Patient plasma and serum collected from the above research groups were used to measure ASM levels by TLC and using the Amplex Red sphingomyelinase assay.

[1] Prof. Caroline Savage, Dr. Mark Little, Dr. Matt Morgan, Renal Immunobiology Group, College of medical and dental sciences, University of Birmingham, Birmingham, West Midlands.
[2] Prof. George Kitas Rheumatology Clinical trials unit, Russells Hall hospital, Dudley, West Midlands.
[3] Wellcome Trust Clinical Research Facility, Queen Elizabeth II Hospital, Birmingham, West Midlands
[4] PEX all patients – plasma exchange/plasmapheresis; patients previously underwent
[5] Some PEX patients
[6] Peripheral blood samples
[7] This cohort included ANCA negative non-vasculitis patients with: anti-GBM disease, transplant rejection (x2), myeloma, unknown cause end-stage renal failure, mesangiocapillary (membrenoprolipherative) glomerulonephritis and focal segmental glomerulosclerosis.

### 2.2.1.4 Patient confidentiality & Ethics

Clinical samples were assayed anonymously. Patient clinical data was not released until all experiments had been carried out. Patient information and clinical parameters remained confidential between the clinicians in charge and principle investigators.

| Sample | Local Research ethics committee (LREC) | LREC number |
|---|---|---|
| **HUC*** | South Birmingham Research Ethics Committee | 2002/277 |
| **Healthy controls** | Solihull local research ethics committee | 07/Q2706/2 |
| **AASV cohort 1** | South Birmingham Research Ethics Committee | 5779 |
| **AASV cohort 2** | South Birmingham Research Ethics Committee | 5779 |
| **AASV cohort 3** | South Birmingham Research Ethics Committee | 5779 |
| **AASV cohort 4** | South Birmingham Research Ethics Committee | 5779 |
| **AASV cohort 5** | South Birmingham Research Ethics Committee | 2001/0722 |
| **RA** | Dudley Research ethics committee | 04/Q2702/18 |

**Table 2.4 Study ethical approval numbers**

HUC, human umbilical cord endothelial cell extraction and culture use.

#### *2.2.1.5 Preparation of human plasma and serum*

Blood was taken from consented human healthy control individuals with no known chronic ailment. Peripheral whole blood (10 mL) was extracted and placed into 50 mL centrifuge tubes. For plasma preparations, 100 μL of 25,000 U heparin (Multiparin) was added to the tube prior to the blood. The heparin was mixed by gentle inversion. Blood was centrifuged 895 x *g* (2500 rpm) for 10 minutes at room temperature. Plasma was aspirated and aliquoted in working aliquots of 25 μL and stored at -20$^0$C whilst in use or at -80$^0$C for long-term storage. For serum preparations, blood was left to clot without anti-coagulant for 1 hour at room temperature and centrifuged at 895 *x g* (2500 rpm) for 10 minutes at room temperature.

### 2.2.2 Cell Culture

#### *2.2.2.1 Human Umbilical Vein Endothelial Cell (HUVEC) isolation*

*HBSS washing buffer ($CaCl_2$ & $MgCl_2$-loaded)*: see 2.2.1.1
*Collagenase Solution:* 1 mg/mL in HBSS-$Ca^{2+}$
*Human endothelial cell growth factor* (hEGF) (10 ng/mL; final) *solution* in HBSS-$Ca^{2+}$
*Culture media:* see 2.2.1.1
*Gelatin solution:* 0.2% gelatin in $dH_2O$, prepared from 2% gelatin stock solution (Sigma)

Human umbilical cords were collected up to 6 hours after donor neonatal delivery from the Birmingham Women's Hospital delivery suite department, Birmingham. This procedure followed an ethically approved protocol (Sth. B'ham; 2002/277) and anonymity was ensured. Prior to HUVEC extraction, 25 $cm^2$ vented tissue culture flasks were coated with a film of 0.2% gelatin. Umbilical cords were kept within containers, sterilised by 70% alcohol swabbing prior to entry into culture hoods. Umbilical cords still attached to the placenta were selected wherever possible for maximum sterility. Umbilical cords were wiped with ethanol and initially cannulated unilaterally using a glass cannula into the umbilical vein available. Sterile PBS (20 mL) was syringed through the umbilical vein to wash out any blood and blood clots. The cord was bilaterally cannulated and 10 mL of 1.0 mg/mL collagenase in HBSS-$Ca^{2+}$ was syringed in and the cords were incubated for 15 minutes at $37^0$C, 5% $CO_2$. During this time, the excess gelatin solution was apirated from the tissue culture flasks. Following incubation, the umbilical cords were lightly massaged to ensure the detachment of HUVECs. Syringing approximately 25 $cm^3$ of air through each cord eluted the collagenase solution. A further 20 mL of HBSS-$Ca^{2+}$ was syringed through the umbilical cord. Eluate was poured directly into sterile 50 mL centrifuge tubes. The samples were then centrifuged for 8 minutes at 322 *x g* (1200 rpm) ($20^0$C). The supernatant was removed and the pelleted cells re-suspended in 1.0 mL of fresh growth M199 to ensure comprehensive dispersion of cells. A further 1.0 mL M199 per allocated flask was added and the cell suspension was loaded into each gelatin-coated flask in 1.0 mL aliquots. To each flask containing 1.0 mL of cell suspension, a further 4.0 mL of growth M199 was added, the flask gently rocked to ensure even spread of cells across the culture plastic. The cells were cultured for 3 hours at $37^0$C, 5% $CO_2$. The

medium was then removed and cells were washed up to three times with pre-warmed sterile PBS. Fresh growth M199 (5 mL) was added to each 25 $cm^2$ flask and cells were incubated for 24 hours at $37^0$C, 5% $CO_2$. M199 was once again aspirated, the cells washed three times with pre-warmed sterile PBS to ensue the removal of any remaining non-adherent cells. A further 5 mL of pre-warmed M199 was added and the cells incubated at $37^0$C until the medium required changing 48 hours later.

#### *2.2.2.2 HUVEC maintenance culture*

*See media formulations*
*Trypsin-EDTA:* 0.05% (0.5 mL/25 $cm^2$)

All media were used within than 4 weeks of making up. HUVEC medium was changed every 48 hours during normal culture conditions. Primary cultures of HUVEC seeded from an umbilical cord underwent medium the first medium change within 3 hours of seeding and 1 mL of centrifuged (322 *x g*, 1200 rpm) original medium was replaced. A second medium change followed 24 hours after seeding and repeated every 48 hours. HUVEC were cultured using 0.2 mL/$cm^2$ of medium. For a two-fold cell subculture, plastic culture flasks were pre-coated with 0.2% gelatin:$dH_2O$ solution. Cultured HUVEC were washed three times with sterile pre-warmed PBS (2 mL/25 $cm^2$). PBS was removed and 1x pre-warmed 0.05% trypsin/EDTA (Gibco) (0.5 mL/25 $cm^2$) was added and incubated for 1-2 minutes. The cells were dislodged by gentle tapping of the culture flask. The trypsin solution was neutralised with 5 mL growth M199. The cell suspension was aspirated and centrifuged at 322 *x g* (1200 rpm) for 8 minutes at 20-$23^0$C. The supernatant was removed and the pellet re-suspended in 1 mL growth M199. A further 1 mL of growth M199 was added to the cell suspension and mixed. Cell suspension (1 mL) plus a further 4

mL of growth M199 was added to each sub-culture. The cells were incubated for 48 hours prior to media change.

### 2.2.3 Measuring ASM activity using thin layer chromatography

*Assay buffer*: 0.1% NP-40 (Igepal) / sodium acetate (62 mmol/L) (pH 5.0); $ZnSO_4$ (2.0 mmol/L)
*NBD-Sphingomyelin*: 1.0 nmol
*Human placental Acid Sphingomyelinase*: 1 μL stock (0.7-1.2 U)
*TLC Solvent:* Chloroform/methanol/ammonium hydroxide [2.0 *N*] (65:25:4 v/v/v)
*Reaction stop solvent:* 400 μL chloroform:methanol (2:1 v/v)
*Sample (plasma, serum, media):* 20 μL

#### *2.2.3.1 Preparation of TLC solvent*

Methanol (100%) (25 mL) was added to 65 mL (100%) chloroform in a glass bottle. To the chloroform:methanol solution, 4 mL ammonium hydroxide (2 *N*) was added using a volumetric pipette ensuring a slow dispensing rate without mixing the solution in the bottle. Upon addition of all the ammonium hydroxide, the whole solution was mixed by slow inversion until the ammonium hydroxide was dissolved. This procedure was necessary to ensure a homogenous solution resulted.

#### *2.2.3.2 Assay reaction*

Assay buffer (359.0 μL) was added to a 1.5 mL microcentrifuge tube alongside 1.0 μL (1.0 nmol) substrate (NBD-SM), 20 mL $ZnSO_4$ (2 mmol/L) followed by 20.0 μL of sample. Samples were either clinical material (serum/plasma) or media supernatants produced from *in vitro* experiments. A positive control of ASM was prepared by incubating the 1 nmol of NBD-SM (Abbreviations list) with 1 μL (approx. 260 mU) of purified ASM (Sigma). Samples were incubated in the dark at $37^0$C for 2 hours. The reaction was stopped by the addition of 400 μL of a chloroform:methanol (2:1) solution. The mixture was vortexed 3 times and centrifuged at 9300 *x g* (10000 rpm) using an Eppendorf 5415R benchtop

centrifuge for 1 minute. Of the two layers formed, 200 μL of the bottom organic layer was carefully aspirated and loaded into a new microcentrifuge tube. The organic layer was evaporated under vacuum (Divac, Leybold) whilst being centrifuged (SpeedEvac SC100, Savant) for 15 minutes. A solid pellet resulted which contained cleaved NBD-ceramide (NBD-Cer) and non-cleaved NBD-sphingomyelin (NBD-SM). The total pellet was reconstituted in 10 μL chloroform (100%) and to ensure uniform loading amongst samples, 9 μL was pipetted onto a glass silica TLC plate 2 cm from the origin. TLC solvent (25.0 mL) chloroform/methanol/ammonium hydroxide [2.0 *N*] (65:25:4 v/v/v) was added to a glass tank 2 minutes prior to extraction to allow for the saturation of the tank atmosphere. A solvent saturated piece of cardboard covering the height of the tank was also added standing against the side of the tank to ensure atmospheric saturation. The tank lid was carefully removed and the TLC plate was inserted in vertically in a plate holder. A layer of Vaseline was applied onto the rim. Solvent was allowed to migrate sufficiently to allow separation of NBD-SM and NBD-Cer. When the front reached a few millimetres below the plate top edge, the plate was removed and dried in a fume cupboard. The plate was immediately wrapped in foil to protect from light. Analyses of the plates were performed on a (Fluoroscan, Labystems) microplate reader and Ascent Research Ed. Software (V.1.2.3.1) **(Figure 2.1)**. The plate was scanned over a period of 10 minutes to produce a fluorescence matrix 5x10 cm and 3750 individual data points.

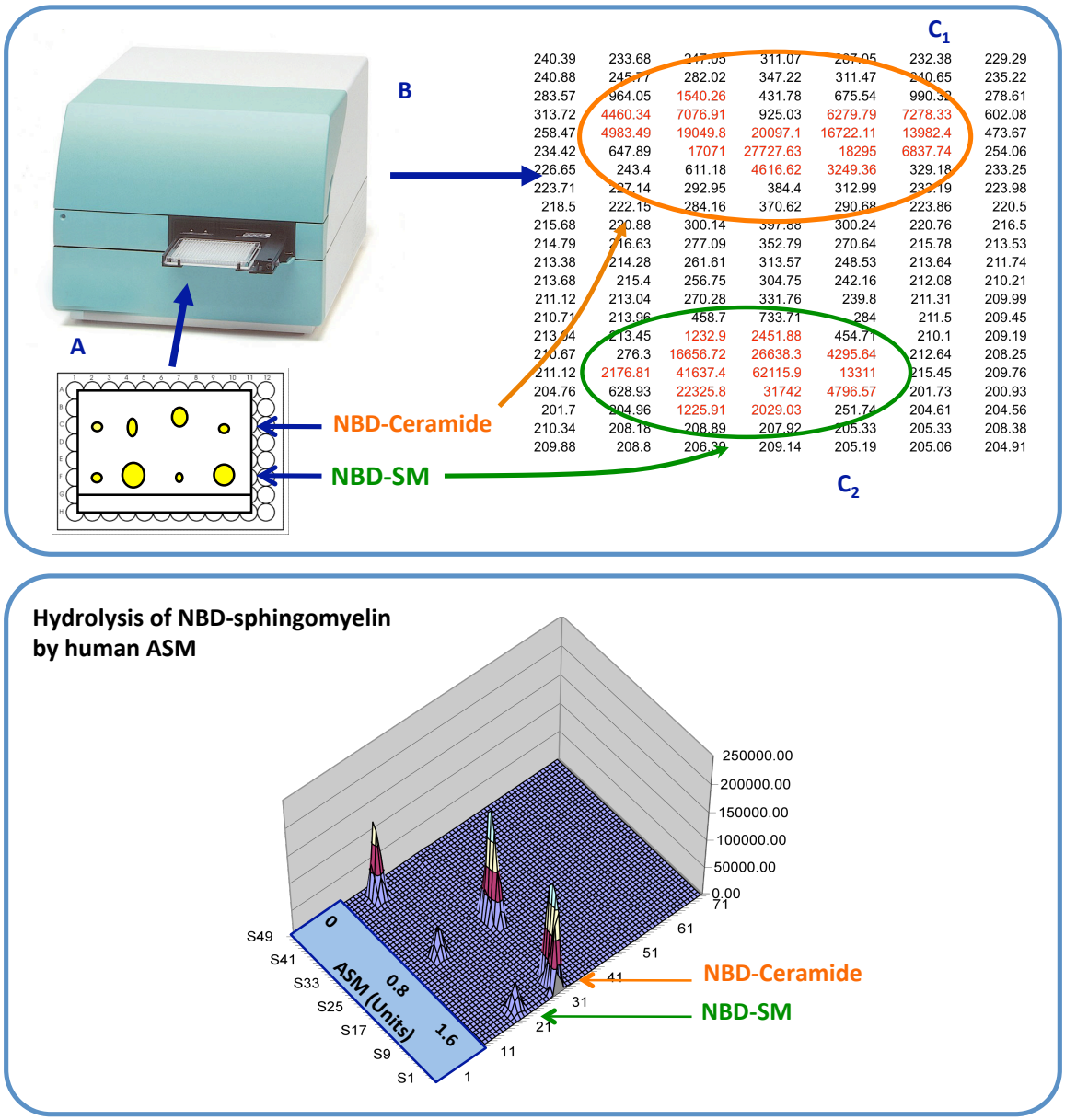


**Figure 2.1 Measuring fluorescence of NBD-sphingomyelin/ceramide**

**Upper panel,** samples were spotted onto TLC plates. Following TLC separation, the TLC plates were loaded onto a lid of a 96-well tissue culture microplates **(A)** and placed in the reading tray of a fluorescence microplate reader for analysis **(B)**. Spots on each plate resulting in a fluorescence matrix **(C).** Following analysis of fluorescence from the TLC plates was exported from the Ascent Software onto an Microsoft Excel spreadsheet showing NBD-SM **($C_2$)** and NBD-Cer **($C_1$). Lower panel,** NBD-sphingomyelin found in the lower peaks. The migrated peaks at '31' represent NBD-ceramide. Analysis performed on Microsoft Excel (2004) and Ascent Research Ed. Software (V.1.2.3.1).

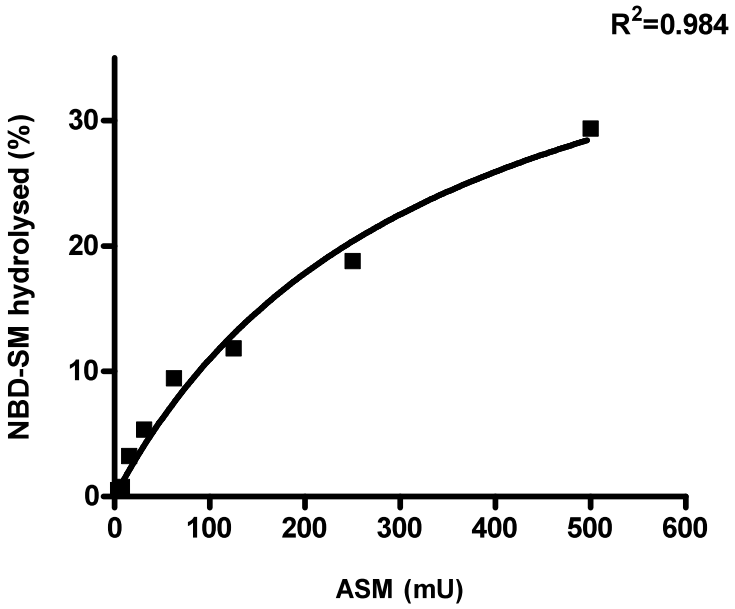


**Figure 2.2 ASM standard curve for thin layer chromatography ASM assay**

Fluorescence detection of ASM activity using NBD-labelled sphingomyelin substrate (NBD-SM). Purified ASM (Sigma) was incubated with 1 nmol NBD-SM in an acid buffer with zinc sulphate for 2 hours at $37^0$C. The reaction was stopped upon the addition of chloroform/methanol (2:1). The solution was centrifuged and the lower organic layer was aspirated and freeze-dried to evaporate and yield a substrate (NBD-SM) pellet. The pellet was re-suspended in chloroform, spotted onto a TLC plate and allowed to migrate. The percentage hydrolysis of NBD-SM to NBD-ceramide was calculated through fluorescent visualisation of the substrates using a fluorescence microplate scanner at 485 nm excitation and 530 nm emission.

Background fluorescence of 1000 AU was subtracted and the fluorescence in the SM and Cer spots assessed **(Figure 2.2)**. Fluorescence detection of NBD-SM/Cer was achieved at the following wavelengths, excitation 485 nm; emission 530 nm. Display fluorescence of NBD-Cer was calculated as a percentage of the total NBD fluorescence of both Cer and SM fractions. Intra and inter-assay statistics were performed.

### 2.2.4 Measuring ASM activity by high-performance liquid chromatography (HPLC)

The *in vitro* reaction was performed as in section (2.2.3) (TLC method). A pelleted solid phase of NBD-SM and NBD-Cer was achieved. The pellet was reconstituted in 100 μL of ethanol (100%) and transferred to a glass sampling vial (Chromacol, UK) and 5 μL of the reaction mixture was auto-sampled WPS-3000-RS (Dionex, UK) onto a HPLC system (Dionex, UK) equipped with a reverse-phase $C_{18}$ column (Phenomex, UK) and the sample was eluted at a flow rate of 1.0 mL/min using an isocratic buffer consisting of methanol:Tris-HCl (96:4, 0.5 mol/L Tris-HCl, pH 9.0). NBD fluorescence was detected using a fluorescence detector RF-2000 (Dionex, UK) set at excitation (485 nm) and emission (530 nm). The peak products were identified by retention time, which was compared to a known standard. The amount of product was calculated using a regression equation established by an ASM treated NBD-SM standard curve. Sample peak analysis was performed using Chromeleon softaware (v6.8) (Dionex, UK) establishing area under the curve for each sample as a percentage of the total sample. Specific ASM activity was calculated as the amount of SM hydrolysed (pmol/mL/$h^{-1}$).

### 2.2.5 Measuring ASM activity using an Amplex Red SMase assay(R)

This assay indirectly measures SMase activity monitored by 10-acetyl-3,7-dihydroxyphenoxazine (Amplex(R) Red, Molecular probes/Invitrogen), a sensitive fluorochrome (assay cocktail 2.2.5.2). The assay reactions are shown in **figure 2.3.**

#### *2.2.5.1 Development of the Amplex Red Sphingomyelinase assay*

This SMase activity assay was altered to measure S-SMase levels in clinical samples. The aim was to develop a high-throughput method for the detection of ASM activity. This also served as an independent method to confirm findings recorded by TLC within this chapter. Until now most colorimetric or fluorimetric methods used for the detection of ASM are labour intensive or are not readily available in most laboratories, such as using liquid scintillation counting of [$^3$H]-SM substrate (Loidl et al., 2002). The assay had to be performed in a two-step method. Initially ASM was incubated with SM in acid buffer (62 mM sodium acetate pH 5.0, supplemented with ZnSO4 2mM [5% v/v]). The second step involved the addition of an alkaline (pH 9.5) Amplex red reaction cocktail to neutralise the pH and allow the final reaction sequence to take place **(Figure 2.3a).** The main issue with using human serum or plasma in this method was the presence of confounding factors such as phosphorylcholine and choline **(Figure 2.3b)** (Ilcol et al., 2004, Hidaka et al., 2008). The interference of choline in the assay sample may act as a false positive and therefore we tried to eliminate this by modifying the kit protocol. By assaying two aliquots of the same sample in parallel, of which one is heat inactivated (HI) and deducted from the activity of the non-HI sample yielding specific ASM activity **(Figure 2.4)**.

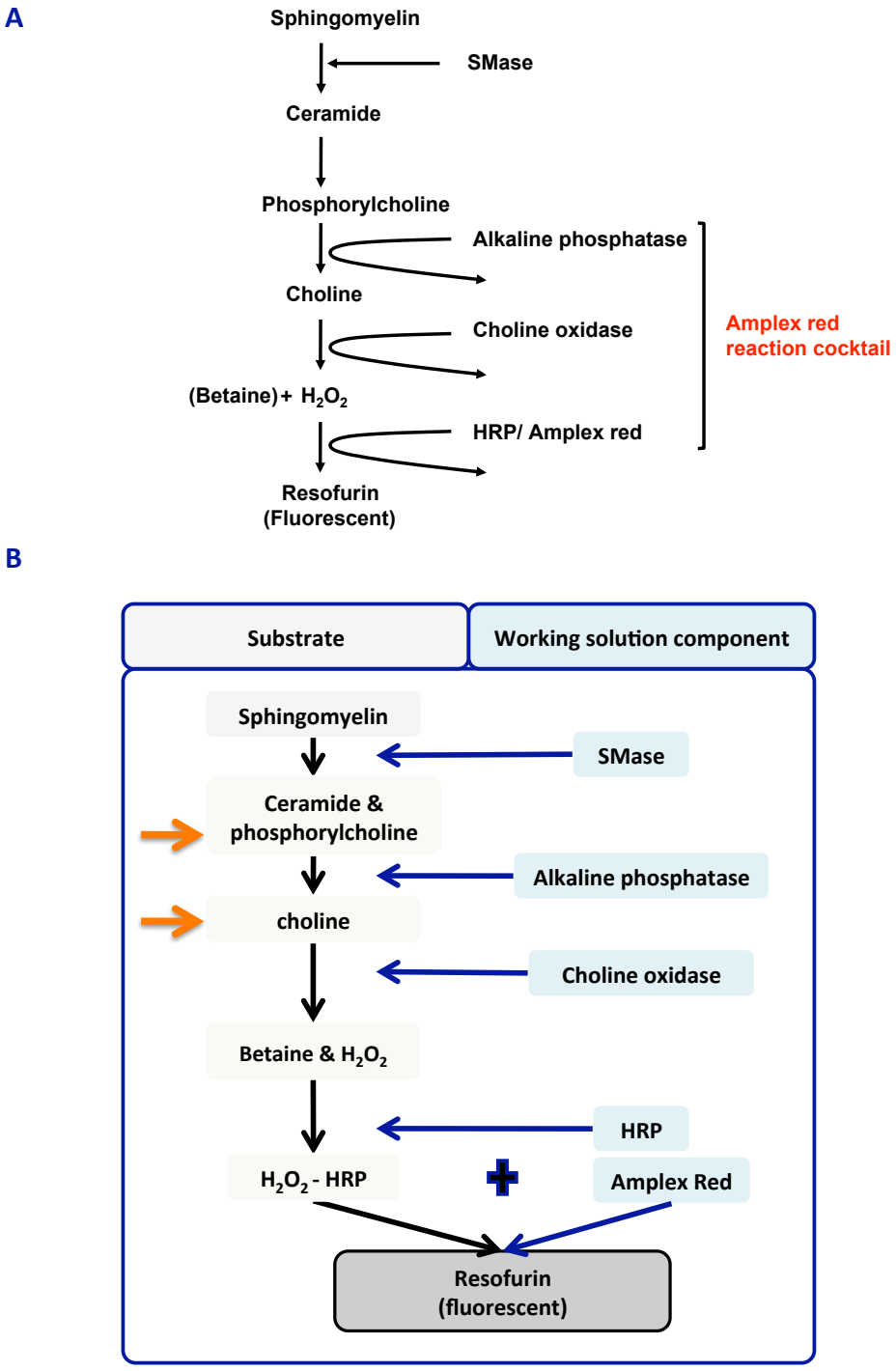


**Figure 2.3 The Amplex Red SMase assay kit pathway**

Amplex Red SMase assay kit by Molecular Probes. **(A)** Schematic diagram of the SMase assay kit reaction pathway following sphingomyelin hydrolysis by SMase. **(B)** Assay confounders present in blood (orange). Reaction solution provided in the assay kit (blue boxes) catalyses each step of sphingomyelin breakdown through to fluorescence detection of resofurin.

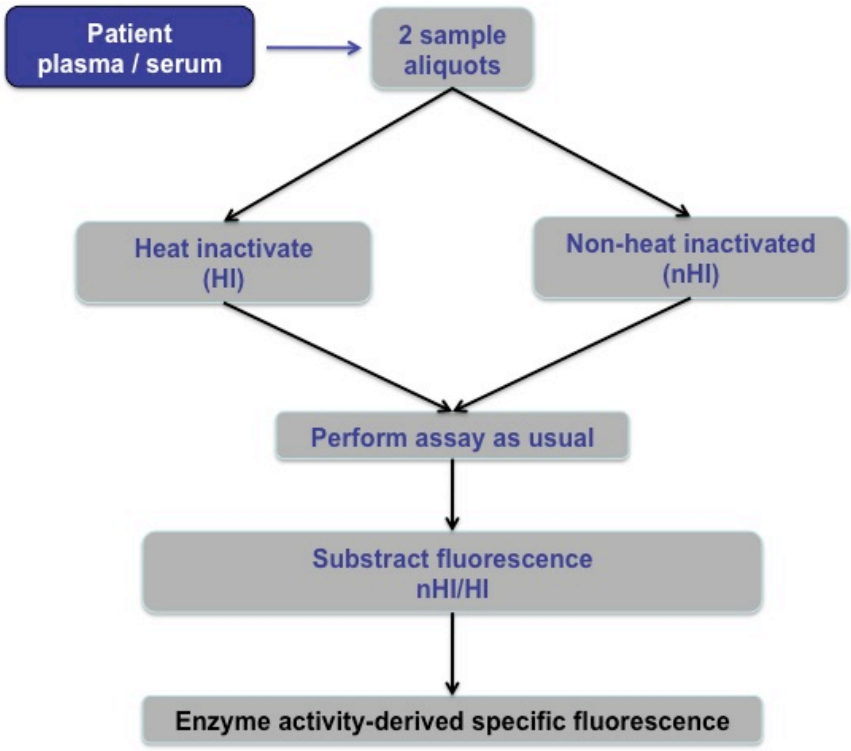


**Figure 2.4 Schematic representation of the altered Amplex Red SMase assay strategy.**

Double aliquots of patient plasma are prepared and one is heat inactivated for 30 minutes at $57^0$C. Both samples are added to acid buffer (62 mmol/L sodium acetate, 0.1% Igepal NP-40 type, 5% v/v 2mmol/L zinc sulphate, pH 5.0) in the presence of 0.5 mmol/L sphingomyelin and incubated for 2 hours at $37^0$C. Amplex Red reaction cocktail is added and incubated for 180 minutes at $37^0$C. Fluorescence intensity of the heat-inactivated sample is subtracted from that of the non-heat-inactivated sample. Fluorescence was measured by single measure at 550 nm (excit.) and 615 nm (emm.)

Purified placental ASM (Sigma-Aldrich) was used to determine the suitability of measuring enzyme activity in acidic conditions. Initial experiments indicated that early resolution incubation time with the Amplex red reagent was not sufficient to distinguish between enzyme activity and background fluorescence **(Figure 2.5a).** In an attempt to enhance sensitivity, we increased the enzyme:substrate reaction time (from 1 hour to 2 hours) and substrate incubation time with the amplex red working reagent for up to 3 hours. This enhanced the assay sensitivity 2-fold **(Figure 2.5b).**

The pH of plasma/serum tends to vary around pH 7.3. Increasing volumes of plasma in acid buffer (pH 5.0) shifted towards a more basic pH, not suitable for the assay **(Figure 2.6a).** To determine the suitable volume of plasma/serum, two PSV patients with differing ASM activity were used; one with low S-SMase activity and one with high activity, previously determined by the TLC activity assay. Using duplicate samples from each patient, one HI and one normal, the plasma was added to acid buffer as 10, 20 and 30% mixtures (v/v) **(Figure 2.6b-d)**. The greatest resolution was provided from samples using 10% (v/v) plasma and to a lesser extent with 20% plasma (**Figure 2.6b-c)**. The initial fluorescence is thought arise from the background fluorescence of Amplex Red reagent typically observed up to 60 minutes. After this time, the cleaved choline in non-HI samples would react with choline oxidase whereas samples affected by ASM inactivation would not produce any choline and the data would plateau earlier (**Figure 2.6b, red line)** than those with active ASM **(Figure 2.6b, black line)**. This is in contrast to samples from a patient with low ASM activity that showed no difference between HI and non-HI plasma indicating the lack of active ASM **(Figure 2.6b-d, blue & green lines)**.

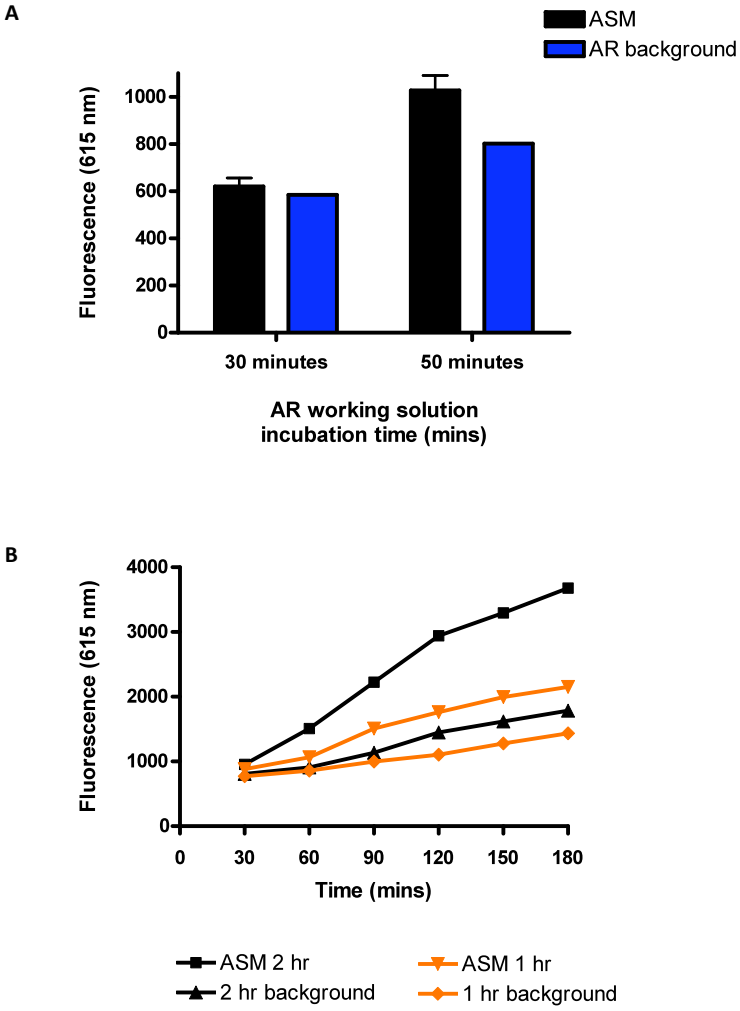


**Figure 2.5 Increasing enzyme-substrate and Amplex Red cocktail incubation time**

**(A)** Purified ASM (Sigma) was incubated with 0.5 mmol/L sphingomyelin in acid buffer (62 mmol/L sodium acetate, 0.1% Igepal NP-40 type, 5% v/v 2mmol/L zinc sulphate, pH 5.0) for 1 hour $37^0$C. Samples were then incubated with the Amplex Red reaction cocktail for 30 and 50 minutes at $37^0$C. Fluorescence was measured by single measure at 550 nm (excit.) and 615 nm (emm.). **(B)** Purified ASM (Sigma) was incubated as in (A) for 1 and 2 hours at $37^0$C. Samples were then incubated with the Amplex Red reaction cocktail for up to 180 minutes at $37^0$C. Fluorescence was measured as in (A)

A

| Plasma (%) In acid buffer (v/v) | pH | Composition |
|---|---|---|
| 0 | 4.90 | Acid buffer alone |
| 10 | 5.00 | Plasma:acid buffer |
| 20 | 5.30 | Plasma:acid buffer |
| 30 | 5.75 | Plasma:acid buffer |
| 40 | 6.20 | Plasma:acid buffer |
| 100 (native plasma) | 7.5 | Plasma alone |

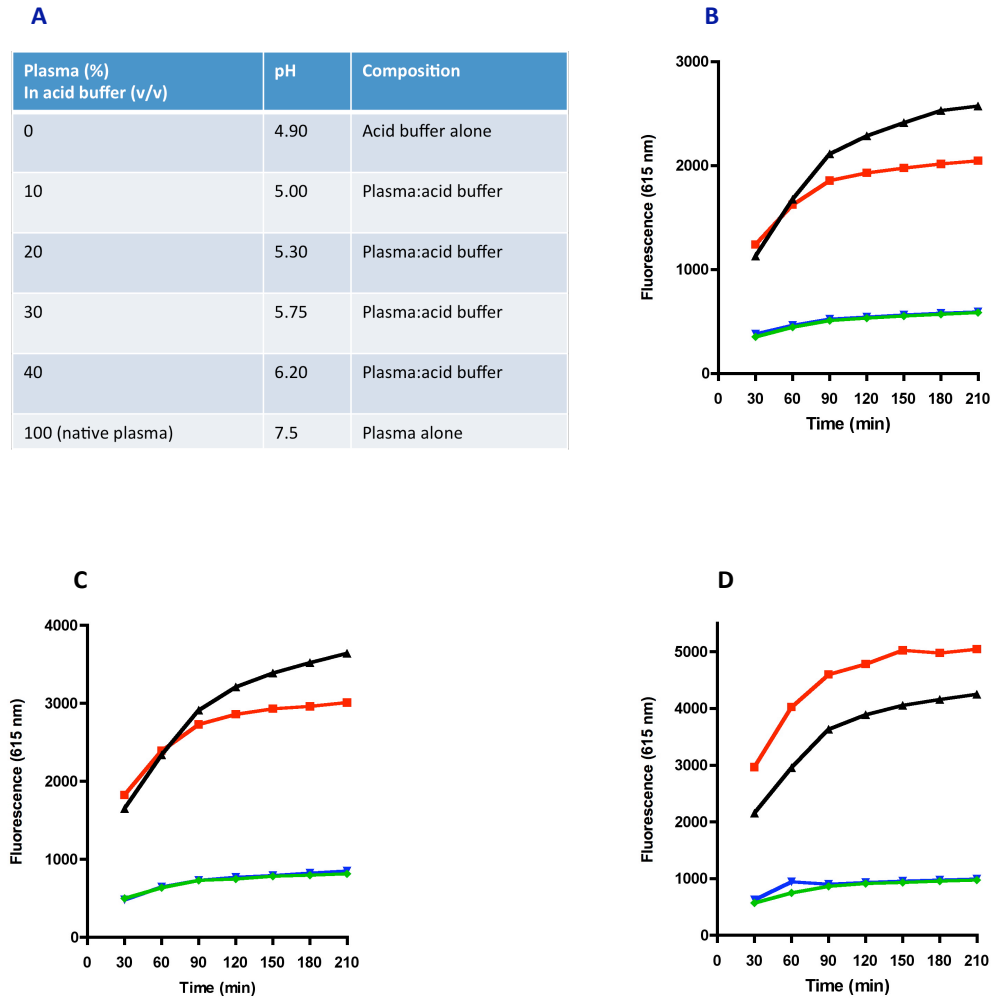


**Figure 2.6 Low plasma volume is optimal for greater assay sensitivity**

**(A)** Differing volumes of pooled human plasma were added to acid buffer (62 mmol/L sodium acetate, 0.1% Igepal NP-40 type, pH 5.0) to represent the percentage indicated above and the pH was measured. Samples are added to acid buffer (62 mmol/L sodium acetate, 0.1% Igepal NP-40 type, 5% v/v 2mmol/L zinc sulphate, pH 5.0) in the presence of 0.5 mmol/L sphingomyelin and incubated for 2 hours at $37^0$C. Amplex Red reaction cocktail is added and incubated for 180 minutes at $37^0$C. **(B)** 10%, **(C)** 20%, **(D)** 30% plasma:buffer (v/v). High S-SMase activity patient (black/red lines) was compared against a low S-SMase activity patient (blue/green lines) (determined by the TLC SMase assay). Fluorescence intensity measure at 550 nm (excit.) and 615 nm (emm.) from heat-inactivated plasma (red, High SMase activity patient; green, low SMase activity patient) was subtracted from non-heat-inactivated fluorescence intensity values (black, high SMase activity patient; blue, low SMase activity patient) to yield specific S-SMase activity.

These assays demonstrated the need to use small volumes of plasma/serum in this method, which are in line with the amount of sample used for the TLC activity assay. Optimisation of the sample volumes led to the need to examine the effect of different HI times assay sensitivity. A PSV patient with high ASM activity was used and **Figure 2.7** suggested that different HI times (> 30 min.) did not enhance assay sensitivity. To confirm the suitability of this method for use with clinical samples it was important to validate that the source of fluorescence was directly derived from ASM activity. To delineate the requirement of choline in the assay, a high ASM activity patient sample was again assayed as normal in a reaction cocktail with and without choline oxidase **(Figure 2.8)**. These two samples were HI and one was spiked with purified ASM (pASM, Sigma). The data here confirmed that not denaturing the enzyme led to a significantly higher fluorescence intensity (FI) compared to HI samples whilst spiked pASM substituted the lack of native ASM in HI samples in the presence of choline oxidase (lines with squares). Furthermore, in samples incubated without choline oxidase, all fluorescence was omitted **(Figure 2.8, lines with inverted triangles)** suggesting that the change ($\Delta$) observed between HI and non-HI samples was attributed to ASM activity. Thus, we concluded from these observations that by heat inactivating a plasma/serum sample and comparing its fluorescence against a non-HI counterpart we could determine specific ASM-derived enzymatic activity. Intra and inter-assay variability was estimated to be between 3-6% examined using HIFCS and FCS (data not shown). Having established this altered method for measuring ASM in patient plasma/serum, it was utilised to assay S-SMase activity in selected patients with ANCA positive and ANCA negative disease and healthy controls (HC). **Figure 2.9** shows 5 HC individuals with modest levels of S-SMase in their plasma.

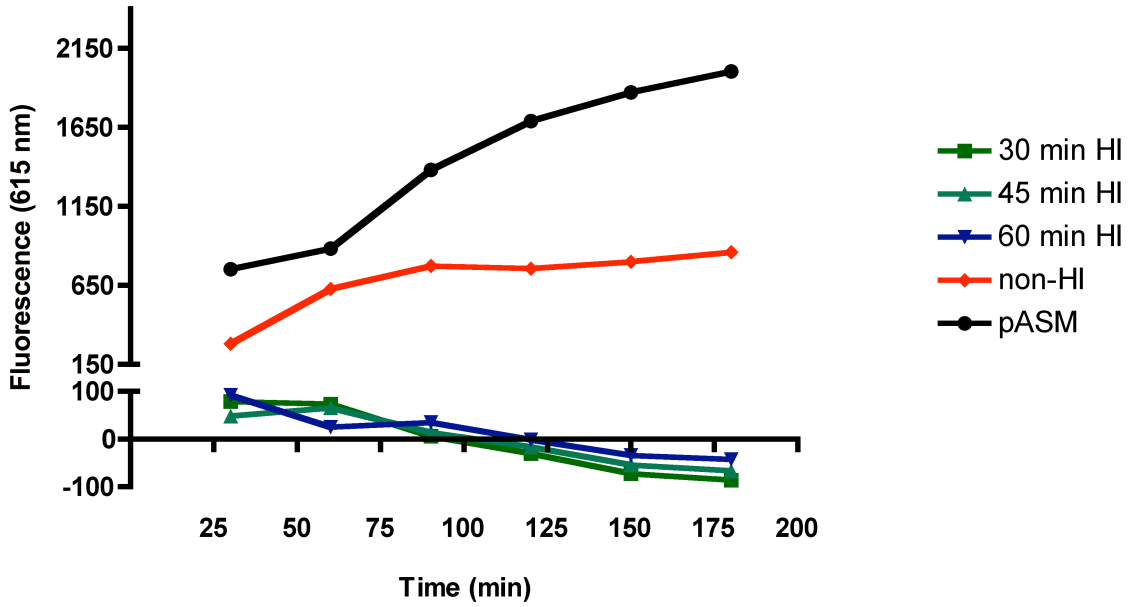


**Figure 2.7 Increasing heat-inactivation time does not lead to increased assay sensitivity**

Patient plasma was heat inactivated for 30, 45 and 60 minutes at $57^0$C. Samples are added to acid buffer (62 mmol/L sodium acetate, 0.1% Igepal NP-40 type, 5% v/v 2mmol/L zinc sulphate, pH 5.0) in the presence of 0.5 mmol/L sphingomyelin and incubated for 2 hours at $37^0$C. Amplex Red reaction cocktail is added and incubated for 180 minutes at $37^0$C. Activity was compared against non-heat-inactivated plasma **('non-HI')** and non-heat-inactivated plasma spiked with purified ASM (Sigma) **('pASM').** Fluorescence was measured by single measure at 550 nm (excit.) and 615 nm (emm.)**.** Data corresponding to the 30, 45 and 60 minute HI times are closely related and cannot be distinguished easily.

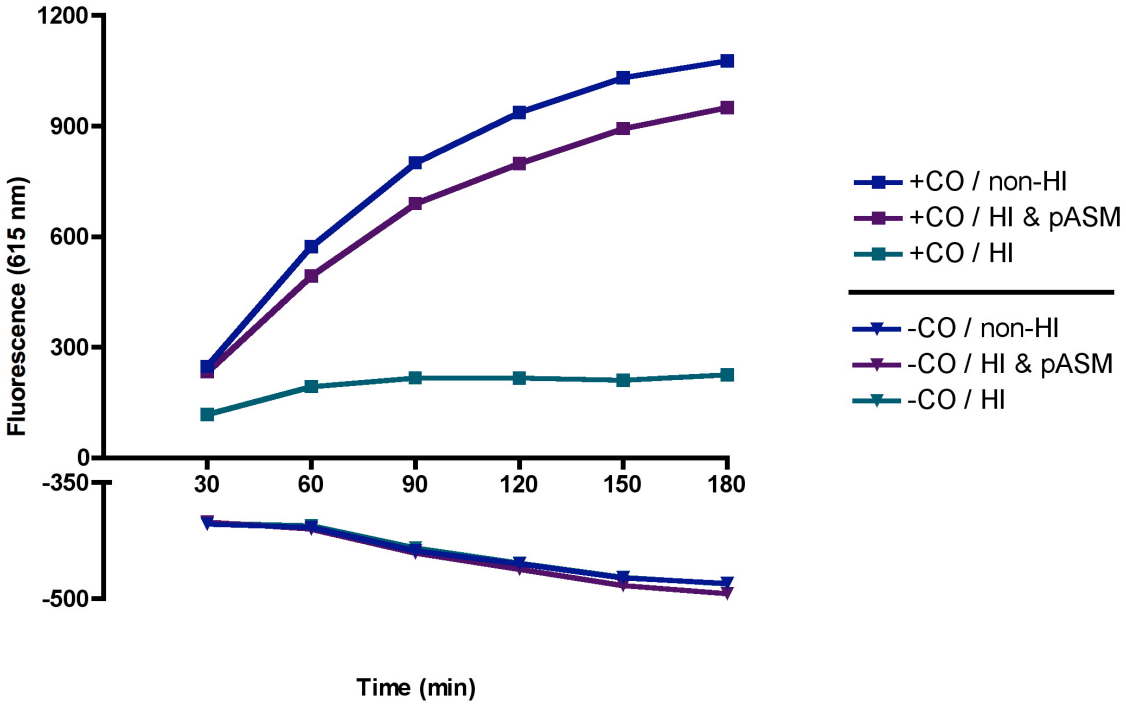


**Figure 2.8 Removal of choline oxidase from the Amplex Red reaction cocktail prevents a rise fluorescence intensity**

Two groups of parameters were examined with patient plasma was heat inactivated for 30 minutes at $57^0$C and compared against non-heat-inactivated plasma **('non-HI')** and heat-inactivated plasma spiked with purified ASM (Sigma) **('HI & pASM').** Samples are added to acid buffer (62 mmol/L sodium acetate, 0.1% Igepal NP-40 type, 5% v/v 2mmol/L zinc sulphate, pH 5.0) in the presence of 0.5 mmol/L sphingomyelin and incubated for 2 hours at $37^0$C. One group of parameters was incubated with Amplex Red reaction cocktail inclusive of choline oxidase **('+CO') (filled stubbed squares).** The second group was incubated with Amplex Red reaction cocktail excluding choline oxidase **('-CO')**. All were incubated for 180 minutes. Fluorescence was measured by single measure at 550 nm (excit.) and 615 nm (emm.). Data corresponding to reaction cocktail without CO are closely related and cannot be distinguished easily.

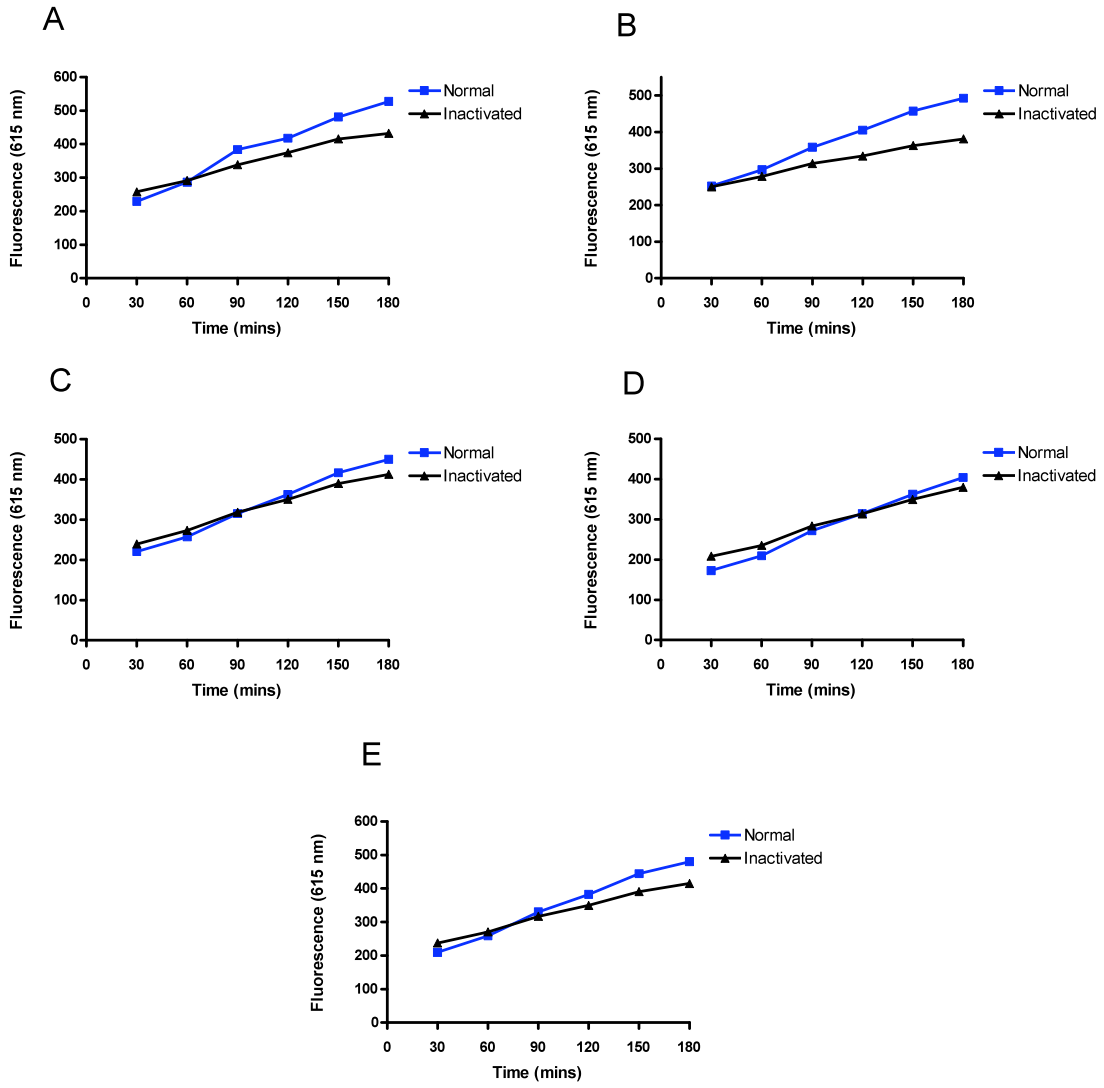


Healthy controls; (A) 4, (B) 6. (C) 7, (D) 8, (E) 9

**Figure 2.9 S-SMase activity in healthy control individuals using the Amplex Red activity assay**

Healthy control plasma samples were heat-inactivated for 30 minutes at $57^0$C. Healthy control plasma (10 μL) was added to acid buffer (62 mmol/L sodium acetate, 0.1% Igepal NP-40 type, 5% v/v 2mmol/L zinc sulphate, pH 5.0) in the presence of 0.5 mmol/L sphingomyelin and incubated for 2 hours at $37^0$C. Amplex Red reaction cocktail is added and incubated for 180 minutes at $37^0$C. **(A)** healthy control 4, **(B)** healthy control 6 etc. Fluorescence was measured by single measure at 550 nm (excit.) and 615 nm (emm.). Healthy control numbers 4, 6, 7, 8 and 9 refer to laboratory codes.

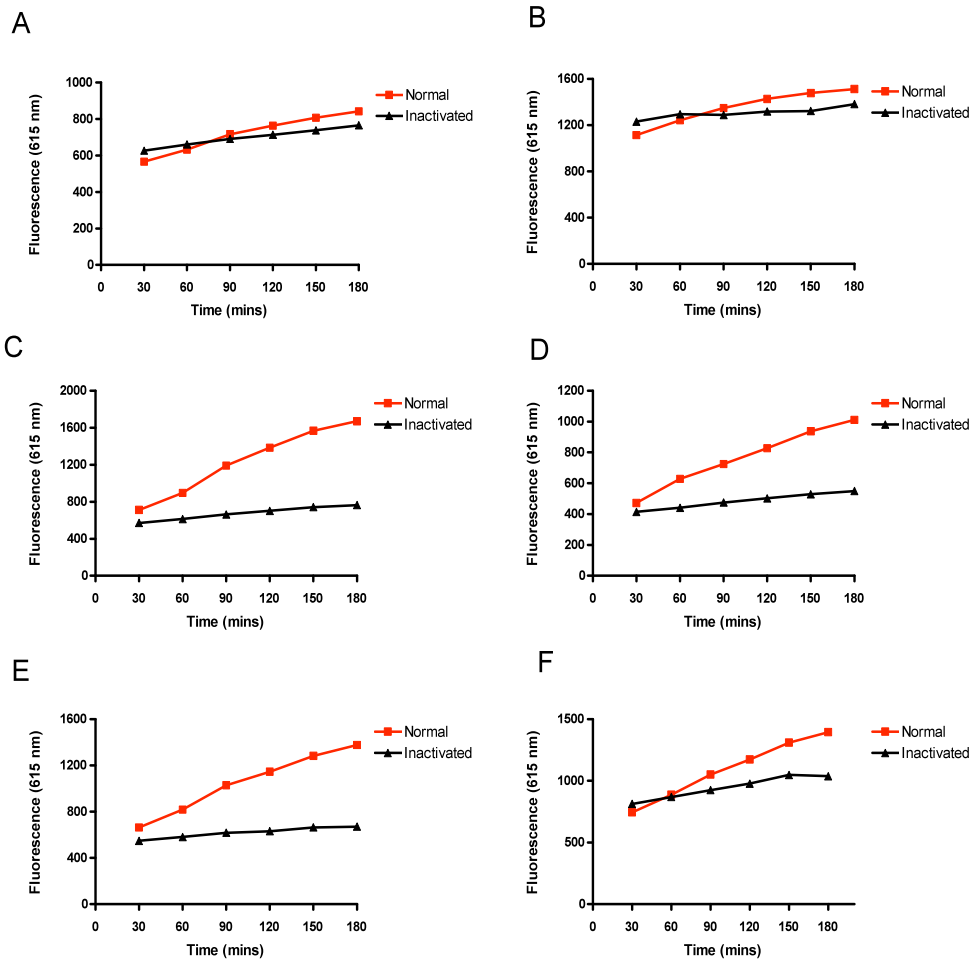


(A) patient 89, (B) patient 96, (C) patient 114
(D) patient 122, (E) patient 137, (F) patient 145

**Figure 2.10 S-SMase activity in AASV patient plasma using the Amplex Red activity assay**

AASV plasma samples were heat-inactivated for 30 minutes at 57$^0$C. Patient plasma (10 µL) was added to acid buffer (62 mmol/L sodium acetate, 0.1% Igepal NP-40 type, 5% v/v 2mmol/L zinc sulphate, pH 5.0) in the presence of 0.5 mmol/L sphingomyelin and incubated for 2 hours at 37$^0$C. Amplex Red reaction cocktail is added and incubated for 180 minutes at 37$^0$C. Patients with low activity **(A-B)** and patients with high activity **(C-F)**. Fluorescence was measured by single measure at 550 nm (excit.) and 615 nm (emm.). Patient numbers 89, 96, 114, 122, 137 and 145 refer to laboratory codes.

The cohort in **figure 2.10** shows a selection of patients with low **(Figure 2.10a-b)** and high **(Figure 2.10c-f)** S-SMase activity. For patients with high activity this is evident by the increased Δ between HI and non-HI samples at 180 minutes, which differs from those with low activity. To accurately compare independent data between the Amplex red assay and the established TLC activity assay, enzyme activity was standardised and expressed in international units of activity (1 unit of pASM hydrolyses 1 nmol of SM/hour, pH 5.0, $37^0$C; Sigma-Aldrich). To do this, standards curves were constructed for both assays using the pASM **(Figures 2.2, 2.11).** The Amplex red assay was used in Chapter 3 to confirm data retrieved from the TLC based method.

### *2.2.5.2 Methodology of the Amplex Red® SMase assay*

*SMase detection assay kit*: Amplex Red® SMase Assay Kit (Molecular Probes, Paisley, UK)
*Amplex Red reaction cocktail:* 100 μL of Amplex Red reagent (10 mmol/L), 100 μL HRP (200 U/mL), 100 μL choline oxidase (20 U/mL); 200 μL alkaline phosphatase (400 U/mL) in 9.5 mL Tris-HCl (100 mM, pH 8.0].
*Acid Buffer:* 62 mmol/L sodium acetate, pH 5.0, $ZnSO_4$ 2 mmol/L (5% v/v)

Human plasma was prepared in duplicate and one was heat inactivated (HI). Both HI and normal plasma were assayed and S-SMase activity was deduced by subtracting the fluorescence of the HI plasma from that of the normal plasma. Each sample (10 μL) was incubated with 10 μL (5 mmol/L) SM and 90 μL acid buffer in each well of a 96 well plate for 2 hours at $37^0$C. Amplex red reaction cocktail (100 μL/well) was added to each well and incubated for 180 minutes, $37^0$C. Fluorescence was measured by single measure at 550 nm (excit.) and 615 nm (emm.) using a Fluoroskan Ascent microplate reader (Lab systems) and Ascent Research Ed. Software (V.1.2.3.1). Background fluorescence was subtracted from each sample.

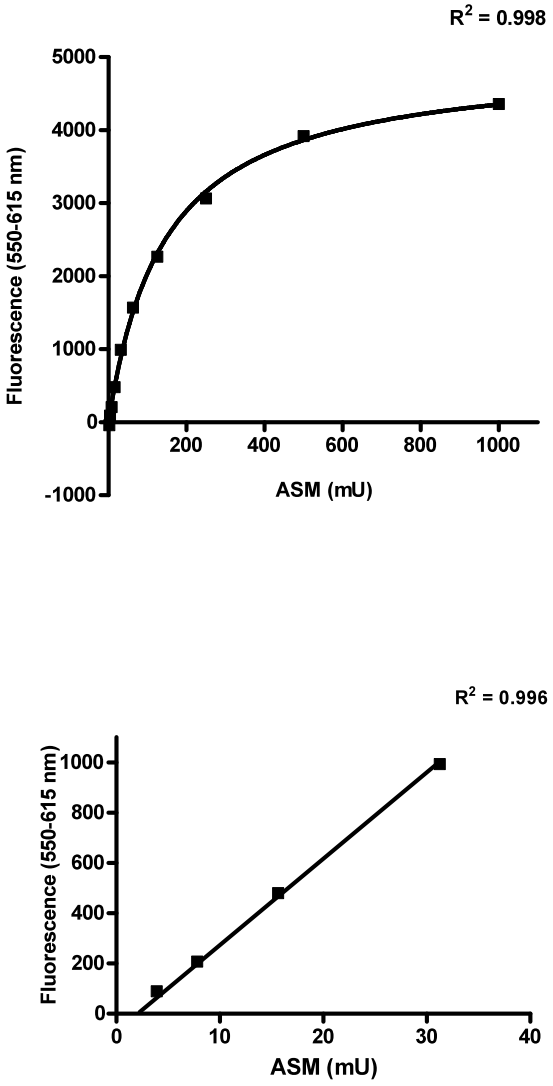


**Figure 2.11 ASM standard curve for the Amplex red SMase assay**

Dose-response curve and fluorescent detection of ASM activity. Purified ASM (Sigma) was incubated with 0.5 mmol/L sphingomyelin in acid buffer with zinc sulphate and incubated for 2 hours at $37^0$C. Amplex Red reaction cocktail is added and incubated for 180 minutes at $37^0$C. Fluorescence was measured by single measure at 550 nm (excit.) and 615 nm (emm.).

### 2.2.6 Assessing cell death by the MTS reduction assay

*Media:* M199 fully supplemented, HESFM. See 2.2.1.1
*Treatments* TNFα (R&D) (0-100 ng/mL), ASM (Sigma-Aldrich) (0-500 mU/mL)
*MTS*:* One stop reaction (Promega)

The MTS reduction assay is a colorimetric method used to determine cell viability. MTS is reduced in viable cells to a formazan product by dehydrogenase enzymes in viable cells. The assay is sensitive enough to be performed in a 96 well plate and the amount of formazan detected is directly proportional to the number of viable cells. HUVEC were cultured to 90% confluence in 25 $cm^2$ gelatin coated (0.2%) tissue culture flasks. They were sub-cultured and $1.5x10^3$ cell/well were re-seeded in gelatin coated (0.2%) 96 well plates grown for 24 hours after which culture medium was replaced with growth M199. HUVEC were cultured for a further 24 hours to achieve confluence or up to 72 hours for slow growing lines. At confluence, medium was replaced with ASM (Sigma) containing fresh growth M199 and HUVEC were incubated for 1 hour at $37^0$C. For TNFα, medium was replaced with TNFα-containing fresh HESFM and HUVEC incubated for 18 hours at $37^0$C. Following incubation, 20 μL of MTS solution was added to each well and the cells were incubated for a further 4 hours at $37^0$C. Absorbance was measured directly at 490 nm.

### 2.2.7 Assessing HUVEC apoptotis by mitochondrial depolarisation using flow cytometry

*$DiOC_6$:* 40 nmol/L (Final) (Invitrogen, UK)
*Treatments* TNFα (R&D) (0-100 ng/mL), ASM (Sigma-Aldrich) (0-500 mU/mL)

Mitochondrial transmembrane potential (ΔΨm) can be studied by observing the incorporation of 3,3'-dihexyloxacarbocyanine iodide ($DiOC_6$) (Sigma-Aldrich). Disruption of mitochondrial transmembrane potential is a late marker of apoptosis. This assay was

employed to study the effects of TNFα and ASM on HUVEC apoptosis. Confluent HUVEC were sub-cultured and $6x10^4$ cells re-seeded in gelatin coated (0.2%) 24-well tissue culture plates. HUVEC were cultured until confluence (48-72 hours). For TNFα treatments, growth M199 was removed and HUVEC were washed once with pre-warmed HBBS-$Ca^{2+}$ (0.2 mL/well) to remove serum. Control or conditioned HESFM (1.0 mL) was added to each well. HUVEC were incubated for 18 hours, $37^0$C. For ASM treatments, growth M199 was removed and replaced with fresh control or conditioned growth M199 for 1 hour, $37^0$C. For both treatments the method is the same following treatment. Control and conditioned media were removed and placed into plastic flow cytometry tubes (Falcon) in order to retain any dead HUVEC. Adherent HUVEC were washed once with HBSS-$Ca^{2+}$ (0.2 mL/well) and washing buffer was also added to corresponding flow cytometry tubes (Falcon). Pre-warmed 1x trypsin-EDTA (0.05%, 0.2 mL/well) was added and HUVEC were incubated for 1 minute at $37^0$C. Fully supplemented growth M199 (2 mL/well) was quickly added to each well to neutralise the trypsin. The HUVEC suspension was aspirated and added to the corresponding FACS tube. HUVEC were centrifuged at 322 *x g* (1200 rpm) for 10 minutes at room temperature. Supernatants were removed and HUVEC were washed with HBSS-$Ca^{2+}$ (0.5 mL/tube), re-suspended and centrifuged once more at 322 *x g* (1200 rpm) for 10 minutes at room temperature. Supernatants were removed and HUVEC were incubated with 40 nmol/L $DiOC_6$ in HBSS-$Ca^{2+}$ for 15 minutes at $37^0$C. HUVEC were then analysed by flow cytometry. At least 10,000 events (cells) were recorded and analysed. The percentage of $DiOC_6^{high}$ (non-apoptotic) and $DiOC_6^{low}$ (apoptotic) HUVEC were calculated using Summit software (Dako Cytomation).

### 2.2.8 S-SMase secretion assay

Media from cells treated with TNFα were harvested for S-SMase content. The ultra-filtrates were collected following media concentration (2.2.8.4) to increase the S-SMase yield. Prior to concentration, TNFα was removed from solution by adding anti-TNFα antibody infliximab (1 mg/mL, 2 hours, $4^0$C). Antibody:antigen complexes were extracted using agarose A/G beads (20 μL/mL), incubated for 30 minutes and centrifuged (600 *x g* [2600 rpm], 30 seconds, $4^0$C). The supernates were used for S-SMase redox manipulation (2.2.9), $Ca^{2+}$ flux assays on HUVEC (2.2.10) and can be used in NO studies **(Figure 2.15).**

#### *2.2.8.1 Multi-well plate model*

Approximately $6x10^4$ cells were seeded into 0.2% gelatin coated wells in 24 well plates for 48-72 hours. Upon confluence the medium was removed, cells were washed once with HBSS-$Ca^{2+}$ (0.5 mL/well) and M199 or DMEM (0.5 mL/well) containing vehicle (PBS) or TNFα (10 ng/mL) or IL-1β (5 ng/mL) was added to each well and incubated for different time periods. Media were harvested, centrifuged to remove dead cells and frozen (-$80^0$C).

#### *2.2.8.2 Scale-up 25 & 75 $cm^{2-}$ models*

Briefly, HUVEC were grown and treated in 25 $cm^2$ tissue culture flasks in order to increase the yield of secreted SMase from HUVEC treated in HESFM. At 90% confluence in growth M199, the medium was removed and the cells were washed once with HBSS-$Ca^{2+}$ (2 mL). Immediately upon removal of the wash buffer, 5 mL/25 $cm^2$ HESFM (Gibco; Invitrogen; see 2.2.1.1) with solvent control or loaded with 10 ng/mL TNFα, both supplemented BSA (0.2%) was added and HUVEC were incubated at $37^0$C for 30 minutes, 3, 6, 12 and 24 hours. HUVEC in 25 $cm^2$ flasks were seeded at a density of $1.5x10^6$ in 75 $cm^2$ flasks, treated as above but with 15 mL/75 $cm^2$ in HESFM for appropriate times (2.2.8.3.1-2).

#### 2.2.8.3.1 TNFα treatments

Upon 90% confluence in 75 $cm^2$ culture flasks HUVEC were washed as above once with HBSS-$Ca^{2+}$ (4 mL) and incubated with solvent control, TNFα (10 ng/mL) or IL-1β (5 ng/mL) conditioned HESFM (Gibco, Invitrogen; 10.5 mL/75 $cm^2$ flask) for 18 hours. After 18 hours, 10 mL media were aspirated from each flask and spun at 322 *x g* (1200 rpm) at $4^0$C for 8 minutes to pellet any cells. The supernatant was aspirated and placed into a Vivaspin-30 (GE Healthcare) for concentration (2.2.8.4) and the cells were lysed (2.2.8.5).

#### 2.2.8.3.2 Treatment with BSO and NAC

Growth M199 (Sigma-Aldrich) was removed and HUVEC were washed once with HBSS-$Ca^{2+}$ (4 mL) and supplemented with 10.5 mL control unconditioned, BSO (100 μmol/L) or NAC 1 mmol/L) loaded M199 for 16 hours at $37^0$C (Table 2.6). After 16 hours, all media were removed, cells were washed once as above and 10.5 mL of HESFM with solvent control, IL-1β (5 ng/mL) or TNFα (10 ng/mL) was added to appropriate flasks. BSO and NAC pre-treated cells were further treated with TNFα (10 ng/mL) and incubated for 18 hours. TNFα (10 ng/mL) alone and IL-1β (5 ng/mL) controls were performed. After 18 hours, media were collected (2.2.8.3.1), concentrated (2.2.8.4) and cells lysed for protein content as described below (2.2.8.5). The same concentrations were used for all treatments. For co-treatment of BSO and NAC with TNFα, HUVEC were cultured as in 2.2.8.3.1, the growth M199 replaced with 10.5 mL HESFM containing solvent control, BSO + TNFα, NAC + TNFα, TNFα or IL-1β alone for 18 hours at $37^0$C (Table 2.6). The media were collected (2.2.8.3.1), concentrated (2.2.8.4) and the cells lysed for protein content

as described below (2.2.8.5). For pre-treatment and co-treatment of BSO and NAC with TNFα, procedures performed as above for the times indicated (16 + 18 hours).

### *2.2.8.4 Media concentration*

Media was centrifuged to remove cells and concentrated 20-fold using a 50 mL Vivaspin-30 (Millipore, UK). Media (10 mL) was centrifuged at 895 *x g* (2000 rpm) in a pre-chilled ($4^0$C) centrifuge twice for 20 minutes checking the volumes in between. Media was centrifuged at the same speed once more for approximately 5 minutes to reach a final volume of 500 μL. The concentrated media was aliquoted immediately. For 5 mL media aliquots (2.2.8.2; Scale-up 25 $cm^2$ model), media was also concentrated 20-fold to 250 μL.

### *2.2.8.5 Cell lysis for protein estimation*

Cells still attached in culture flasks were washed once with PBS and 1x trypsin-EDTA (1.5 mL/75 $cm^2$) was added to each flask. Cells were incubated for 1 minute and dislodged following gentle agitation. M199 (15 mL) was added to each flask to neutralise the trypsin. The cell suspension was aspirated, placed into a 50 mL universal centrifuge tube and centrifuged at 322 *x g* (1200 rpm) for 8 minutes. All medium was removed by aspiration with a 5 mL serological pipette (Corning) and a 200 μL pipette (Gilson) for residual volumes. Ice-cold RIPA lysis buffer (50 μL) supplemented with protease and phosphatase inhibitors (Table 2.7). The cells were placed into a 1.5 μL microcentrifuge tube on ice and lysed by sheer-stress aspirating the cell pellet 30 times using a fine tip 200 μL pipette. The cells were then incubated on ice for 30 minutes. Following incubation, the cell lysate was aspirated a further 10 times and centrifuged at 15700 *x g* (13,000 rpm) at $4^0$C for 2 minutes. The supernatant was aspirated, aliquoted into fresh 0.5 mL microcentrifuge tubes and frozen at -$20^0$C until use for protein content estimation.

### 2.2.9 Redox manipulation of S-SMase activity

We wanted to examine the activity of newly secreted ASM (S-SMase) in a redox sensitive environment. To do this we examined the catabolic capacity of S-SMase by rendering endothelial harvested S-SMase to an oxidative or reduced state using the reducing agent dithiothreitol and pro-oxidant hydrogen peroxide ($H_2O_2$). Excess $H_2O_2$ was neutralised by the addition of catalase. HESFM from TNF$\alpha$ (10 ng/mL) treated HUVEC were harvested, concentrated (2.2.8.4) and assayed for S-SMase activity by the TLC assay (2.2.3.2). The harvested supernatants were aliquoted and stored at -80$^0$C until use. To assess whether $H_2O_2$ can increase S-SMase activity, supernatants were thawed at room temperature and placed in fresh micro-centrifuge tubes. DTT (10 mmol/L) or vehicle (PBS) were added to the supernatants containing S-SMase. Each aliquot was vortexed well and incubated for 15 minutes at 37$^0$C. The samples (20 $\mu$L of the total) were then added to a normal TLC reaction mixture (2.2.3.2) and subjected to chloroform/methanol extraction as described in (2.2.3.2**).** To examine whether $H_2O_2$ can re-establish the oxidised, activated state of the S-SMase, supernatants containing S-SMase were pre-incubated with DTT (0.1 mmol/L; 1 mmol/L) for 15 minutes at 37$^0$C. To the same supernatant aliquots, 1 mmol/L $H_2O_2$ was added and incubated for a further 15 minutes at 37$^0$C. To neutralise the $H_2O_2$, 10 U/mL catalase was added to each aliquot and incubated for 30 minutes at 37$^0$C. The samples were assayed as above in section 2.2.3.2.

### 2.2.10 Measuring intracellular $Ca^{2+}$ responses in HUVEC

*Agonist* Bradykinin: 1.0 μmol/L final)
*Treatments*:$C_2$ ceramide: 500 μmol/L in HBSS-$Ca^{2+}$, ASM: see 2.2.1
*FURA-2-AM*: 50 μg aliquots, made to 2.0 mmol/L stock in 25 μL DMSO
Media*:* Medium 199, see 2.2.1.1; HBSS buffer, see 2.2.1.1

#### *2.2.10.1 HUVEC seeding & culture*

HUVEC calcium ($Ca^{2+}$) responses were measured using the fluorescent $Ca^{2+}$-sensitive chelator dye FURA-2 AM. HUVEC were cultured to confluence in gelatin-coated 25 $cm^2$ tissue culture flasks. Cells were trypsinised and re-seeded onto gelatin pre-coated (0.2%) 8-well chambered glass coverslides at a density of $6x10^4$ cells/well for a minimum of 24 hours in growth M199 (2.2.1.1).

#### *2.2.10.2 HUVEC treatment and FURA-2 AM dye loading*

Culture medium was removed by careful, slow aspiration using a 50-300 μL pipette tip. Cells were washed with pre-warmed HBSS-$Ca^{2+}$ buffer (100 μL/well) by adding slowly down the chamber wall. Cells were treated with ASM (purified placental, Sigma-Aldrich) or TNFα at $37^0$C in growth M199. The solvent control, ASM or TNFα loaded media were removed and FURA-2 AM-containing (4 μmol/L) medium (M199-ASM; HESFM-TNFα) was added to each well (200 μL/well), and foil-wrapped coverslides incubated at room temperature for 30 minutes. Room temperature was used to help prevent leakage of FURA-2 AM into intracellular organelles. FURA-2 AM-loaded medium was removed and cells were washed once with HBSS-$Ca^{2+}$ (100 μL/well) at room temperature to remove un-incorporated dye. Cells were incubated in 200 μL HBSS-$Ca^{2+}$ for a further 15 minutes to complete the cleavage of the ester AM moiety from the FURA-2 AM dye to its active FURA-2 form. HBSS-$Ca^{2+}$ was removed and cells washed as before. Fresh HBSS-$Ca^{2+}$ (100

μL) was added to each well and the coverslide was taken to a dark microscope room. Coverslides were loaded onto the stage of a fluorescence microscope, the lens was focused and baseline fluorescence was recorded for 30 seconds. Cells were then stimulated one well at a time with 100 μL 2x concentrated (2.0 μmol/L) bradykinin or 2 U/mL thrombin in HBSS-$Ca^{2+}$, diluted to 1x with the 100 μL HBSS-$Ca^{2+}$ already in each well. Video montage using SimplePCI (v5.3.1.091305, Compix Inc. USA) was recorded for 5 minutes and pictorial representation is seen in Chapter 5. Intracellular FURA-2 fluorescence was measured by excitation at 340 nm and 380 nm allowing for ratiometric derivation of $Ca^{2+}$ flux. Briefly, resting un-stimulated cells fluoresce green, progressing to a red/orange spectrum upon $Ca^{2+}$-FURA-2 association. Fluorescence from as many cells as possible is recorded by annotation of cells that respond to agonist stimulation, while the background fluorescence of the field is also recorded and subtracted from the cell FI.

#### *2.2.10.3 Patient plasma and media supernatant transfer*

HUVEC were seeded as above (2.2.10.1) and cultured for 24 hours in M199. The medium was removed and replaced with 200 μL, 1:1 dilution of plasma:M199 using plasma from a high ASM activity patient for 1 hour. FURA-2 AM loading and $Ca^{2+}$ mobilisation was performed as above (2.2.10.2). For supernatant transfer, HUVEC were seeded as above for 24 hours (2.2.10.2). Cells were treated with M199 containing S-SMase or HI S-SMase. To obtain this, media from 18 hour TNFα (10 ng/mL) treated cells were collected and concentrated (2.2.8.5). Concentrated media were assayed for ASM activity by the TLC assay (2.2.3) to show a specific activity of 150 mU calculated from an ASM standard curve **(Figure 2.14)**. For $Ca^{2+}$ flux studies, cells were treated with an equivalent of 750 mU/mL ASM for 1 hour at $37^0$C. Media were then removed and FURA-2 AM loading was

performed as above. Comparisons included S-SMase against HI S-SMase and solvent control media (HESFM).

#### *2.2.10.4 Post-treatment recovery*

HUVEC were given the chance to recover in growth M199 following the removal of ASM-loaded media. Briefly, cells were treated as above with ASM (2.2.10.2). Half of the cells were allowed to recover for 1 hour prior to FURA-2 AM loading by means of removing ASM-spiked media and replacing with M199 for 1 hour at $37^0$C. FURA-2 AM loading and cell responses were measured as above (2.2.10.2).

### 2.2.11 Assessment of eNOS regulation

*Media:* 2.2.1.1
*Bradykinin*: 1.0 μmol/L final, (Sigma-Aldrich)
*Treatments*: Thrombin (1 U/mL final) (Sigma-Aldrich), ASM (Sigma-Aldrich) see 2.2.1
*Ionomycin*: 5.60 μmol/L (Sigma-Aldrich)

To assess eNOS activation, bradykinin and thrombin were used as agonists to stimulate a $Ca^{2+}$ dependent-phosphorylation of eNOS at $Ser^{1177}$ and de-phosphorylation at $Thr^{495}$. HUVEC at low passage were re-seeded onto 6 well plates at a density of $2.5x10^5$/well and cultured for 48 hours in growth M199. Medium was replaced with fresh growth M199 at 48 hours and cells were cultured for a further 24-48 hours. On the day of experimentation, cells were serum starved for 1 hour by replacing the growth medium with M199 (P/S only). Medium change was performed slowly by pipetting 1.0 mL down the wall of each well as not cause shear stress. Following serum starvation, the medium was removed by slow aspiration and replaced with 1.0 mL ASM-loaded (1.25 U/mL) M199 (P/S only), whilst control well were incubated with solvent control in fresh M199-P/S.

Cells were incubated for either 30 or 60 minutes. Following treatment with ASM, 2x concentrated bradykinin (2 μmol/L) or thrombin (2 U/mL) were added to reach a final concentration of 1 μmol/L and 1 U/mL respectively. To ASM loaded and control wells, ionomycin (5.60 μmol/L) was also added. Agonists were added whilst the 6 well plates were still in the incubator for 2 minutes at $37^0$C. All actions were performed with minimal interference to medium flow in order to not induce sheer stress-induced eNOS activation. Following agonist stimulation, cells were placed on ice, the medium was removed and 50 μL ice-cold RIPA buffer containing phosphatase and protease inhibitors (Table 2.7) added to each well. Cells were scraped, placed into 0.5 mL microcentrifuge tubes and lysed using a small Dounce homogeniser (30 strokes). Cell lysates were incubated on ice for 15 minutes and centrifuged at 9300 *x g* (10000 rpm) using an Eppendorf 5415R benchtop centrifuge at $4^0$C for 2 minutes. The supernatant was placed into a new 0.5 mL microcentrigufe centrigued tube and the pellet discarded. Of the cell lysates prepared, 5 μL was aliquoted for protein estimation (2.2.14), stored at $-20^0$C and used within 1 month. Electrophoresis and immunoblotting of eNOS is described below (2.2.12.2).

### 2.2.12 Immunoprecipitation & immunoblotting

Immunoblotting was used to confirm the presence of ASM in clinical samples and phosphorylation status of endothelial nitric oxide synthase (eNOS).

| Antibody | Species | Source | Dilution | Conc./Weight |
|---|---|---|---|---|
| **Primary antibodies** | | | | |
| **anti-ASM** | Rabbit | Santa-Cruz Biotech. | 1:200 (IB*) | 1 mg/mL |
| **anti-ASM** | Rabbit | Santa-Cruz Biotech. | IP** | 2mg |
| **anti-eNOS** | Mouse | BD Biosciences | 1:1000 | 0.55 mg/mL |
| **anti-peNOS** | Rabbit | Cell Signalling | 1:500 | - |
| **anti-b-actin** | Mouse | Sigma-Aldrich | 1:5000 | - |
| **Secondary HRP-conjugated antibodies** | | | | |
| **anti-rabbit (ASM)** | Donkey | GE Healthcare | 1:5000 | |
| **anti-mouse (eNOS)** | Sheep | GE Healthcare | 1:5000 | |
| **anti-rabbit (peNOS)** | Donkey | GE Healthcare | 1:3000 | |
| **anti-mouse (b-actin)** | Sheep | GE Healthcare | 1:5000 | |

**Table 2.5 Antibodies used for immunoblotting and immunoprecipitation****

| Inhibitor | Source | Ingredients | Dilution |
|---|---|---|---|
| **Phosphatase inhibitor cocktail 1** | Sigma (P2850) | microcystin LR, cantharidin, p-bromotetramisole | 1:100 |
| **Phosphatase inhibitor cocktail 2** | Sigma (P5726) | Sodium orthovanadate, Sodium molybdate, Sodium tartate, Imidazole | 1:100 |
| **Protease inhibitor cocktail** | Sigma (P8340) | AEBSF, aprotinin, E-64, bestatin hydrochloride, leupeptin hemisulfate salt, pepstatin-A | 1:100 |

**Table 2.6 Protease and phosphatase inhibitor cocktails**

Used for additive to RIPA lysis buffer In HUVEC lysates used for protein estimate of experimental samples and for the creation of lysates for immunobloting. E-64, [N-(trans-epoxysuccinyl)-L-leucine 4-guanidino butylamide.

### *2.2.12.1 Immunoprecipitation*

*Lysis buffer*: RIPA (150 mmol/L NaCl, 1% Igepal®, 0.5% sodium deoxycholate, 0.1% SDS, 50 mmol/L Tris, pH 8.0)
*Loading buffer (1x):* distilled water; SDS (10%, w/v); glycerol (20% ); 0.5 mol/L Tris buffer (pH 6.8); bromophenol blue (10 mg), DTT 40 (mmol/L)
*Agarose protein A/G beads*: 25 % w/v, Santa Cruz Biotechnology, UK

For lysate preparations, HUVEC were grown to confluence and $6x10^6$ of cells were lysed in

200 μL lysis buffer (RIPA) with protease and phosphatase inhibitors (Table 2.7) on ice for

15 minutes. Lysates were then centrifuged at 13400 *x g* (12000 rpm) for 10 minutes at $4^0$C. The supernatant was aspirated and the pellet discarded. Lysates (200 μL) or plasma (0.5 mL, PSV or healthy control) were pre-cleared with anti-rabbit IgG fraction (1 μg) and 10 μL agarose A/G protein beads for 30 minutes rotating at $4^0$C. Binding of non-specific proteins to the IgG fraction were removed by centrifugation at 600 *x g* (2600 rpm) 30 seconds in a pre-chilled bench-top microcentrifuge (Eppendorf) at $4^0$C. The supernatant was incubated for 2 hours at $4^0$C with 1 μg anti-ASM antibody (Santa-Cruz Biotech. UK). Protein A/G agarose beads (10 μL) were added to the lysate to precipitate the antibody:antigen complex and incubated overnight at $4^0$C. The samples were centrifuged at 600 *x g* (2600 rpm) for 30 seconds at $4^0$C. The new supernatant was discarded and the pellet (bead/antibody/antigen complex) was re-suspended in ice cold sterile PBS (100 μL) and centrifuged at 600 *x g* (2600 rpm) for 30 seconds at $4^0$C. This washing process was repeated a further 3 times. After the final wash, the supernatant was discarded and 30 μL loading buffer (above) was added. The samples were heated for 10 minutes and loaded onto the appropriate percentage SDS-polyacrylamide gel for electrophoresis.

| Percentage Gel | Protogel (Acrylamide) | $dH_2O$ | Tris, 1.5 M (pH 8.8) | 10% SDS | 10% APS | TEMED |
|---|---|---|---|---|---|---|
| **8% (250-120 kDa)** | 8.0 mL | 14.5 mL | 7.5 mL | 300 μL | 150 μL | 30 μL |
| **10% (120-40 kDa)** | 10 mL | 12.5 mL | 7.5 mL | 300 μL | 150 μL | 30 μL |
| **12% (40-15 kDa)** | 12 mL | 10.5 mL | 7.5 mL | 300 μL | 150 μL | 30 μL |
| **20% (< 20 kDa)** | 20 mL | 2.5 mL | 7.5 mL | 300 μL | 150 μL | 30 μL |
| **5%** | 2.6 mL | 12.2 mL | 5.0 mL (0.5 M pH 6.8) | 200 μL | 100 μL | 20 μL |

**Table 2.7 Formulation reagents of SDS-PAGE gels**

### *2.2.12.2 SDS-PAGE & immunoblotting*

*Running buffer:* Tris (25 mmol/L), glycine (192 mmol/L), SDS (0.1%) 10% v/v/v in $dH_2O$
*Blotting buffer:* Tris (20 mmol/L), glycine (150 mmol/L) 10% v/v, methanol (100%) 10% v/v.
*Resolving SDS PAGE gel (10 %) :* Table 2.8
*Stacking SDS PAGE gel (5 %) :* Table 2.8
*RIPA:* see 2.2.11.1
*Loading buffer:* see 2.2.11.1
*Blocking solution:* BSA (5%) in (1x) TBS/Tween-20
*Antibody loading solution:* BSA (2 %) in (1x) TBS/Tween-20
*Enhanced chemiluminescence solution:* GE healthcare, Amersham Bioscience)

SDS-PAGE was performed in 8% (eNOS) or 10% (ASM) resolving gels (Table 2.8) using a running buffer (above) prepared from a 10x concentrate (GeneFlow, National diagnostics, UK) as 10% (v/v/v) in distilled $H_2O$. Gels were prepared in casting cassettes (Invitrogen) creating wells using plastic combs (Invitrogen). For eNOS, lysates were thawed and kept on ice while the protein content was calculated using a BSA standard curve from absorbance estimates obtained previously in a BCA assay (2.2.14). Protein antigen was loaded onto each lane of a 5% stacking gel (Table 2.8), alongside 5 μL protein markers (SeeBlue, Invitrogen) in an independent lane. For eNOS, protein loading was normalised across samples and an equal amount of protein was loaded per lane (10-50 mg) in concentrated loading buffer (5x) to prevent excessive protein dilution. An appropriate amount of 5x loading buffer was added to each sample alongside DTT (40 mmol/L, final). For ASM, immunoprecipitated protein was resuspended in 20 μL of 1x loading buffer. The proteins were allowed to migrate for approximately 90 – 100 minutes with a current ranging between 95-105 V. A blotting sandwich was assembled **(Figure 2.12**) using PVDF membrane (Geneflow, UK), which had been previously activated by soaking in methanol (100%). Transfer of proteins onto the PVDF membrane was performed at 47 mA resistance. Protein transfer was performed for 1 hour and 45 minutes in blotting buffer

(above) prepared using from a 10x concentrate of Tris/glycine and methanol (100%) (GeneFlow, National diagnostics, UK) and 10% (v/v) in distilled water.

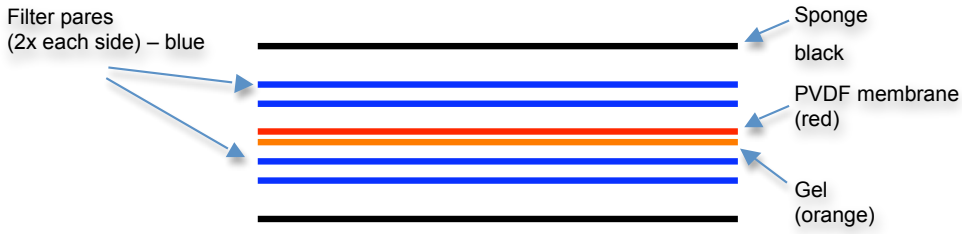


**Figure 2.12 Blotting sandwich**

To ensure transfer of protein from the SDS-PA gel, the PVDF membrane was placed close to the anode electrode and the SDS-PA gel close to the cathode electrode.

Following protein transfer, the PVDF membrane was blocked in a 1x TBS/Tween-20 (0.1%) 5% BSA solution on a rocker for 1 hour at room temperature. For eNOS blots, each membrane from the corresponding gels was cut and separated from its β-actin control **(Figure 2.13).**


**Figure 2.13 PVDF seperation for loading control (β-actin)**

Lysates were probed simultaneously for antigen of choice and loading control.

The blocking solution (above) was removed and primary antibody (anti-ASM or anti-eNOS, anti-β-actin, eNOS loading control) at the concentrations indicated (Table 2.6) in antibody loading solution (above) was added. The membrane was incubated overnight at $4^0$C on a rocker. Membranes were then washed three times with 1x TBS/Tween-20 (0.1%). Secondary HRP-conjugated secondary antibody (Table 2.6) in TBS/Tween-20 (0.1%) 2% BSA was added and the membranes incubated for 1 hour at room temperature. Membranes were washed 3 times with 1x TBS/Tween-20 (0.1%) at room temperature enhanced chemiluminescence detection solution (ECL, GE Healthcare) was prepared and washed over the membranes for 2 minutes lifting the membrane and touching against a paper towel removed excess ECL solution. The membranes were wrapped in cling film and proteins visualised on X-ray film (Kodak).

#### *2.2.12.3 Quantification of protein bands*

Protein quantification was performed by densitometry. X-ray film images were captured by GeneSnap and the GeneGenius gel imaging system (Syngene, UK). X-ray film background and protein band intensity was estimated by GeneTools (Syngene, UK) in arbitary units. The background was subtracted from each protein band. Bands for eNOS and p-eNOS were normalised to their β–actin control and expressed as fold changes of p-eNOS over total eNOS between treated and un-treated cells.

### 2.2.13 Measuring nitric oxide production from HUVEC

#### *2.2.13.1 Recording nitric oxide release using diaminofluorescein-2 (DAF-2)*

*Bradykinin:* 1.0 μmol/L (final)
*DAF-2:* 0.1 mmol/L (final)
*Media & HBSS:* see 2.2.1.1

HUVEC from one confluent 25 $cm^2$ tissue culture were seeded onto one gelatin (0.2%) coated 6 well plate at a density of $2.5x10^5$ cells/well. HUVEC were grown for 72-96 hours using growth M199. On the day of experimentation, HUVEC were washed once with pre-warmed HBSS-$Ca^{2+}$ (0.25 mL/well). HUVEC were serum starved in phenol red-free DMEM supplemented with 2% BSA, L-ascorbate (100 mmol/L) (0.5 mL/well) for 1 hour at $37^0$C. DMEM was removed and HUVEC were incubated with HBSS-$Ca^{2+}$ supplemented with 1.0 mmol/L bradykinin and DAF-2 (0.1 mmol/L; 0.5 mL/well) for 10 minutes at $37^0$C. Supernatants were removed, centrifuged for 8 min at 322 *x g* (1200 rpm). Supernatants were analysed using a spectrofluorimeter at 495 nm excitation and 515 nm emission both at 10 nm slits.

#### *2.2.13.2 Chemiluminescent analysis for the detection of nitrites*

*Treatment*: Cer, 500 μmol/L (Sigma-Aldrich); ASM 1.25 U/mL (Sigma-Aldrich); nSMase 25 mU/mL (Sigma-Aldrich)
*Bradykinin:* 1.0 μmol/L
*HESFM:* 2.2.1.1
*Gelatin:* (Sigma-Aldrich) 0.2% in $dH_2O$

Analysis of nitric oxide (NO) can be performed using a Sievers Chemiluminescence NO Analyser (GE Power and Water, UK). This is a very sensitive technique that measures nitrites in solution as low as $10^{-12}$ mol/L. Briefly, the reaction formed depends on the reduction of nitrites ($NO_2$) to NO when present in a reducing solution containing glacial acetic acid/sodium iodide (Na/I) (1%). The NO produced directly proportional to the $NO_2$

in the solution sampled. The generated NO is purged by nitrogen under vacuum into a cooled (-10$^0$C until -20$^0$C) reaction chamber where it reacts with ozone ($O_3$) to form nitrogen dioxide ($NO_2^*$) depicted as ($2NO + 2O_3 \rightarrow 2NO_2^* + 2O_2$).

Detection is made possible through the fluorescence of activated $NO_2^*$ which, fluoresces in the far red to infrared spectra and releases a single photon for every $NO_2$ molecule produced. The number of photons detected is directly proportional to the total amount of NO present in the sample. Light is detected by a photomultiplier and recorded as a change in voltage (mV). The amount of NO in each sample is calculated from a sodium nitrite standard curve dividing the area of the peak of each sample in mV by the sodium nitrite standard curve gradient using the Sievers NO Analysis Software v3.21 (GE, Power & Water, UK). Quiescent HUVEC cultured in a 25 cm$^2$ flask were re-seeded at a density of 6x10$^4$ cells/well into 0.2% gelatin coated 24 well plates and cultured for 48-72 hours until confluence. On the day of experimentation, growth M199 was removed and replaced with HESFM for 1 hour to ensure serum starvation. Cells were stimulated with agonists 1 μmol/L bradykinin or 1 U/mL thrombin for 30 minutes, 37$^0$C, 5% $CO_2$. The conditioned medium was collected in 1.5 mL microcentrifuge tubes and centrifuged for 8 min at 322*xg* (1200 rpm) to pellet any dead cells. Supernatants were removed and frozen alongside fresh medium for background control at -80$^0$C until analysis. Conditioned media were slowly thawed on ice. Nitrite analysis was performed by injecting 100 μL of conditioned culture medium into a glass purge vessel containing 1% Sodium Iodide/glacial acetic acid creating gaseous NO detected as described above. Experimental triplicate wells were assayed in technical triplicates of 100 μL.

#### *2.2.13.3 Recording nitric oxide release using an ISO-NOP electrode*

*Agonists:* Bradykinin (1 μmol/L), thrombin (1 U/mL)
*ASM:* 1.25 U/mL
*Media*: HESFM see 2.2.1.1; HBSS buffer: HBSS-$Ca2^{+}$ see 2.2.1.1
*ISO NOP electrode:* World precision instruments (WPI)

Confluent HUVEC were re-seeded onto gelatin (0.2%) coated 6 well plates (Sarstedt, UK) at a density of $2.5x10^{5}$ cells/well and cultured in growth M199 for 72-96 hours until a confluent monolayer was formed. On the day of experimentation, growth M199 was removed and replaced for 1 hour with M199 (P/S only) for serum starvation. M199 was removed and replaced with 1 mL solvent control M199 or ASM loaded M199 (P/S only) for 30 or 60 minutes. A magnetic 2-3 mm stirrer ensured adequate agonist dispersion. A background was established by placing the ISO-NOP electrode (WPI, UK) a few millimetres above the cell monolayer distal to the magnetic stirrer. Cells were stimulated with agonist and immediate responses were recorded. Recording is performed with an NO selective permeable membrane to generate an electrical current recognised by the electrode, which creates a reading measured in mA using the Apollo 4000 multi-channel free radical analyser (WPI, UK).

### 2.2.14 BCA assay for protein content

The BCA assay is a colorimetric method and was used to measure protein concentration of whole cell lysates and human plasma samples. Copper ($Cu^{2+}$) reduction by protein to cuprous ions ($Cu^{1+}$) in an alkaline environment can be observed by colorimetric detection. Briefly, bicinchoninic acid (BCA) reacts with the reduced cuprous cations to produce a purple colour at 562 nm of which intensity increases linearly with protein content. To measure the protein concentration of cell extracts and human plasma, 3 μL of sample was

added to BCA reagent, mixed well and incubated for 30 minutes at $37^0$C. Absorbance was measured directly at 550 nm using an Anthos ht II microplate photometer. Analysis of the absorbance was performed using StingRay software v1.5 (DazDaq, UK). Protein concentration was estimated by calculation against a BSA calibration curve (2000-7.8 mg/mL). BSA for standard curves related to human plasma protein estimation was constructed by dissolving BSA in PBS and serially dilutions. BSA standard curve related to HUVEC lysates were constructed by dissolving BSA in RIPA cell lysis buffer supplemented with protease and phosphatase inhibitor cocktails (Table 2.7), then serially diluted.

### 2.2.15 Statistical analysis

Statistical analysis of data was performed using GraphPad Prism 4 software. Variation is expressed as standard deviation (S.D.) or standard error of the mean wherever stated. The minimum confidence level at which data were considered significantly different was indicated as $p \leq 0.05$. Normality tests for Gaussian distribution of data populations were determined by assessing the kurtosis and skewness of the data and by the D'Agostino-Pearson normality test. For parametric analyses the Student's unpaired t-test was used, and Student's paired t-test for parametric paired data. Non-parametric data from un-paired populations were analysed with Mann-Whitney U test. Non-parametric data expressed in paired observations were analysed using the Wilcoxon signed ranked test and Kruskal-Wallis one-way ANOVA with Dunn's post-hoc comparison. Non-parametric clinical correlations were analysed by Spearman rank correlation test.

# Chapter 3

# ASM in clinical inflammatory disease

# 3 ASM in clinical inflammatory disease

## 3.1 Introduction

Inflammatory rheumatic diseases are increasingly linked with cardiovascular disease (CVD) development and decreased life expectancy (**section 1.3; p8)**. Primary Systemic Vasculitis (PSV) and Rheumatoid Arthritis (RA) are examples of these diseases with CV involvement (Jacobsson et al., 1993, Filer et al., 2003) (**1.3.2-3; p11-13**). Controlling systemic inflammation leads to improved outcome, decreased risk of developing a first cardiovascular event and thus decreased mortality in RA (Jacobsson et al., 2005, Listing et al., 2008, Popa et al., 2009). Atherosclerosis is an inflammatory disease and likely underlying pathology behind the CVD in PSV and RA (Chironi et al., 2007, Pasceri and Yeh, 1999, Van Doornum et al., 2002). The initiating factors are believed to involve endothelial cell dysfunction (ECD), which leads to decreased endothelium-dependent vasodilation (EDV) (**1.5.2.1-2; p20-21**) (Haskard, 2004, Gonzalez-Gay et al., 2008) reviewed in Bacon, (2005).

EDV is mediated by eNOS-derived nitric oxide (NO) production, depletion of which is a hallmark of ECD. In coronary vessels, ECD has been used to successfully predict atherosclerotic disease progression and CV events (Schachinger et al., 2000) and is now a recognised feature of autoimmune inflammatory diseases (Behcet's and SLE) (Lima et al., 2002, Von Feldt, 2008, Chambers et al., 2001). ECD is also established in PSV (Booth et al., 2004b, Dhillon et al., 1996, Filer et al., 2003, Sangle et al., 2008) and RA, where the latter features secondary rheumatoid vasculitis (**1.5.2.2; p21**) (Bosello et al., 2008, Metsios et

al., 2010). Vascular endothelial function has been shown to improve following treatment of inflammation with anti-TNFα therapy (Hurlimann et al., 2002, Gonzalez-Juanatey et al., 2004, Sidiropoulos et al., 2009, Raza et al., 2000). TNFα has contrasting effects on endothelial function by a) inducing eNOS activation (De Palma et al., 2006), and b) causing ECD by decreasing endothelial NO availability (Kim et al., 2001) and impaired NO-dependent vasodilatation (Bhagat and Vallance, 1997, Zhang et al., 2002, Chia et al., 2003). This dysregulation of vascular homeostasis has detrimental effects on endothelial signalling in inflammatory conditions and the details of its role on subsequent atherosclerotic development remains unclear.

One signaling pathway that has started to receive more attention over the past decade is the sphingomyelin-ceramide (SM-Cer) pathway. Pro-inflammatory cytokines (IL-1β, IFNγ) induce the secretion of ASM (S-SMase) generating Cer and TNFα has been reported to promote rapid but transient activation of intracellular ASM (L-SMase) (**1.7.2.2.2-3; p47-51**) (Marathe et al., 1998, Zhang et al., 2002, Wong et al., 2000). Elevated S-SMase has been documented in clinical diseases (**p52**) in particular chronic heart failure (CHF) (Doehner et al., 2007). In CHF it was associated with decreased peripheral blood flow, positively correlating with TNFα and disease severity (NYHA class) however, the precise role of S-SMase in pathophysiological processes remains unclear. One mechanism involves reorganisation of plasma membrane (PM) architecture. Cer-induced lipid raft (LR) aggregation affects store-operated $Ca^{2+}$ entry (SOCE) into the cell (Lepple-Wienhues et al., 1999, Tornquist et al., 1999) while Cer also blocks $Ca^{2+}$ influx and efflux through interference with the $Na^{+}/Ca^{2+}$ exchanger in cardiac myocytes (Condrescu

and Reeves, 2001). Similarly, TNF$\alpha$-induced Cer-mediated inhibition of $Ca^{2+}$ influx through SOC channels is completely abrogated in $ASM^{-/-}$ T-lymphocytes (Church et al., 2005) suggesting a role for Cer in ion channel regulation.

EDV featuring eNOS-generated NO is a process tightly regulated by $_{i}Ca^{2+}$ signaling (Fleming et al., 2001) from the ER stores and influx across the PM through SOCE. Deregulation of this signalling pathway by S-SMase and Cer may lead to inhibition of $Ca^{2+}$-dependent EDV and ECD. The progress of atherosclerosis in PSV (Chironi et al., 2007) and RA (Gonzalez-Gay et al., 2005a, Shoenfeld et al., 2005) is likely to be a multi-factorial process. Diffuse ECD is evident in PSV occurring distally to the primary inflammatory site (Raza et al., 2000) suggesting a role for inflammatory mediators driven by systemic extraarticular disease featuring TNF$\alpha$.

We propose a mechanism whereby vascular inflammation leads to activation and secretion of S-SMase generating Cer and inhibiting SOCE. Decreased $_{i}Ca^{2+}$ signaling can lead to dysregulation of NO production through impairment of $Ca^{2+}$-dependent eNOS activation viewed as an early step in ECD, a mechanism for accelerated atherosclerosis. This hypothesis regarding the role of S-SMase in vascular dysfunction in chronic inflammatory autoimmune diseases predicts that the active enzyme should be present in blood of patients. The objectives of this study were to investigate S-SMase in diseased patients against healthy controls and to correlate S-SMase activity with anthropometric, clinical and laboratory parameters. Data from selected diseased patients and healthy controls were confirmed using a two further independent S-SMase assays, a fluorometric Amplex Red activity assay (Molecular Probes, Invitrogen) and a fluorescence HPLC-based method.

## 3.2 Results

### 3.2.1 TLC based S-SMase activity assay

Patient serum and plasma S-SMase activity was determined using a TLC based assay from which the percentage NBD-SM substrate catabolised reflected enzymatic activity. For analytical methodology see 2.2.3.

### 3.2.2 Active S-SMase is raised in plasma of patients with primary systemic vasculitis

S-SMase was found elevated in patients with primary systemic vasculitis. A small pilot cohort of 11 non-clinically phenotyped patients with ANCA associated primary systemic vasculitis (AASV) **(cohort 1, Table 2.3)** was initially used. These were patients that all underwent therapeutic plasmapheresis (plasma exchange, PEX) during their management. In total, 11 PEX AASV patient samples were compared against healthy control plasma that was not age or sex-matched (*n* = 9) for S-SMase activity **(Figure 3.1a)**. S-SMase levels in PEX AASV patients were increased more than 3-fold (29.40 ± 24.04 pmol/mL/$h^{-1}$) compared to healthy controls (9.131 ± 10.29 pmol/mL/$h^{-1}$) (*p < 0.03).* We sought to replicate our findings by expanding the current PEX AASV cohort. The second cohort of PEX AASV **(cohort 2, Table 2.1)** patients (n = 10) also exhibited higher mean S-SMase activity (34.42 ± 29.30 pmol/mL/$h^{-1}$) compared to non-matched healthy control plasma (n = 9; 9.13 ± 10.29 pmol/mL/$h^{-1}$) (*p < 0.02*) **(Figure. 3.1b).** The identity of ASM was confirmed by immunoprecipitation of the enzyme from patient plasma using an anti-ASM antibody from Santa Cruz Biotech. USA, **(Table 2.5).** These data demonstrated for the first time that AASV patients undergoing plasmapheresis have higher levels of active S-SMase in their circulation compared to healthy control individuals.

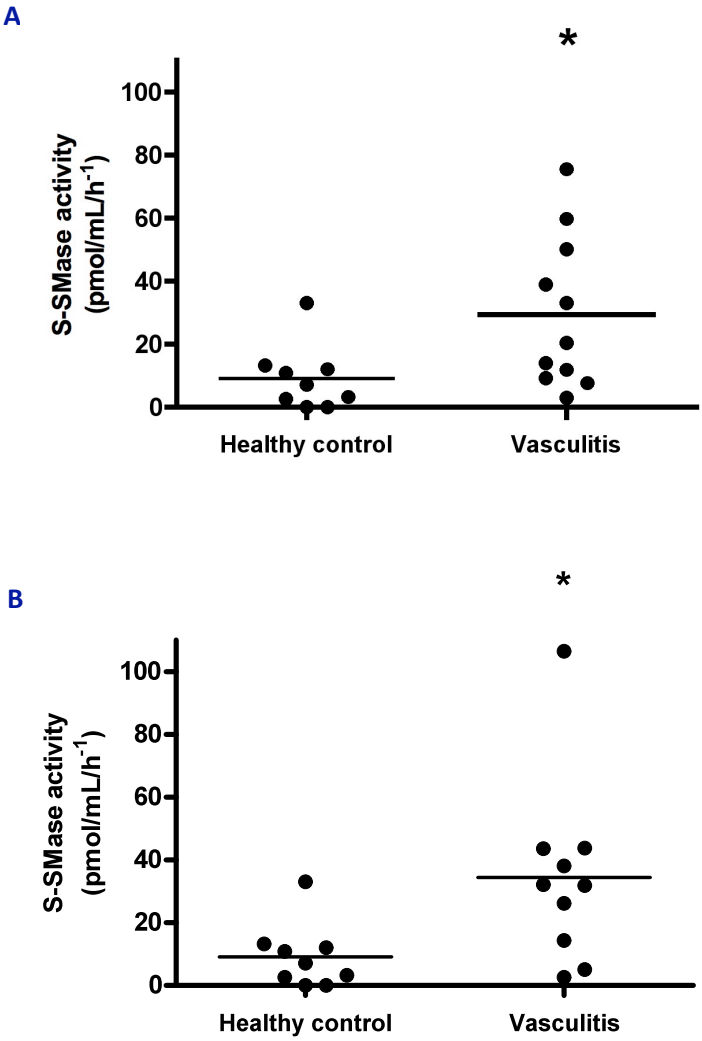


**Figure 3.1 AASV patients undergoing plasmapheresis exhibit higher active S-SMase compared to healthy controls**

S-SMase activity in ANCA-associated systemic vasculitis (AASV). AASV patients were not sub-grouped. Plasma S-SMase activity was determined *in vitro* by the TLC activity assay. **(A)** Plasma from patients (n=11) undergoing plasma-exchange (PEX, cohort 1) were compared with healthy control (HC) (n=9) plasma. HC vs AASV; *$p < 0.03$. Data represent means of four independent experiments (n=4). **(B)** Patient plasma (n=10) undergoing PEX (PEX, cohort 2) was compared with healthy control (HC) (n=9) plasma. HC vs AASV; *$p < 0.02$. Data represent means of three independent assays (n=3). Statistical analysis was performed using the Mann-Whitney U-test.

### 3.2.3 S-SMase levels in plasma of clinically phenotyped AASV patients

A third cohort of clinically phenotyped patients undergoing PEX was used to further characterise levels of S-SMase in AASV, **(Figure 3.2)**. This cohort also included a small inflammatory disease control group, which included ANCA negative disease control patients associated with impaired kidney function (See 2.2.1.5). This provided an insight as to whether active S-SMase is present in diseases with overt vascular inflammation or if higher S-SMase activity is associated more closely with ANCA positive small vessel vasculitides. Plasmapheresis may dilute patient plasma with similar effects on S-SMase. To account for this, plasma from disease patients and controls was assayed for protein content and S-SMase activity normalized accordingly. In total, 18 AASV patients were used in this study alongside 7 ANCA-negative inflammatory disease control individuals. These two cohorts were compared to 9 age but not sex-matched, healthy controls with a median age of 58 years (IQR 55 – 68.5 years; mean 61.3 years), compared to 65.5 years (IQR 53.5 – 75 years; mean 62.4 years) in the AASV group. Again we found elevated active S-SMase levels in patients with active AASV (1.4 ± 0.98 pmol/mg/$h^{-1}$) compared to healthy controls (0.15 ± 0.14 pmol/mg/$h^{-1}$) ($p < 0.0005$) **(Figure 3.2a)** while ANCA negative inflammatory disease control patients also showed raised enzyme activity suggesting a dissociation of S-SMase activity with ANCA status (1.47 ± 0.90 pmol/mg/$h^{-1}$) ($p < 0.0005$). Plasma S-SMase activity was similar between ANCA positive and ANCA negative patients. This suggests that elevated S-SMase is not exclusive to ANCA associated vasculitides and may be a broad marker of vascular inflammation

Immunoblot analysis of diseased patient plasma confirmed the presence of S-SMase in these samples. This was used to determine whether S-SMase presence correlated with

increased activity of the enzyme or whether it could be secreted in an inactive form. **Figure 3.2b** shows that S-SMase, when secreted, is likely to be active since prominent protein bands visualized by immunoblotting **(Figure 3.2b)** correspond to higher enzymatic activity whereas the absence of protein bands is coupled with significantly lower activity.

This AASV cohort was clinically characterised and non-healing scars were recorded using vasculitis damage index (VDI). Our data revealed a positive correlation between S-SMase and the VDI ($r^2 = 0.47; p < 0.003$) suggesting that increased S-SMase activity may relate to accumulated vascular damage through chronic ECD **(Figure 3.3d)**. Disease activity was assessed according to the Birmingham Vasculitis Activity Score (BVAS) (Luqmani et al., 1994)**.** In univariant regression analysis S-SMase did not correlate with the BVAS of patients at the time of plasma exchange ($r^2 = 0.087$) **(Figure 3.3a).** Induction of clinical remission is largely described as a BVAS of below 1 (Booth et al., 2004a). None of the patients in this cohort exhibited a BVAS < 9 (Figure 3.4a), whilst all patients had highly active disease with a median BVAS of 17.5 (IQR 14 – 20; mean 16.6) (data not shown). Since a BVAS above 5 is regarded as active disease and given the patients' high scores here, the lack of a significant S-SMase/BVAS relationship it is not surprising, rather it is predicted and may be due to the lack of low BVAS scores. A split of BVAS into 2 groups is evident with scores either below or above 15. This did not reveal a significant difference in S-SMase activity. S-SMase activity did not relate to the duration of follow-up between patients ($r^2 = -0.011$) nor with creatinine levels ($r^2 = -0.13$) and age at PEX ($r^2 = 0.0001$) **(Figure 3.3b,c,f)**. S-SMase activity also did not relate to the number of organs involved ($r^2 = 0.166$) in these patients **(Figure 3.3e)**. This is supported by the lack of correlation of BVAS with S-SMase activity **(Figure 3.3a, 3.3a)**.

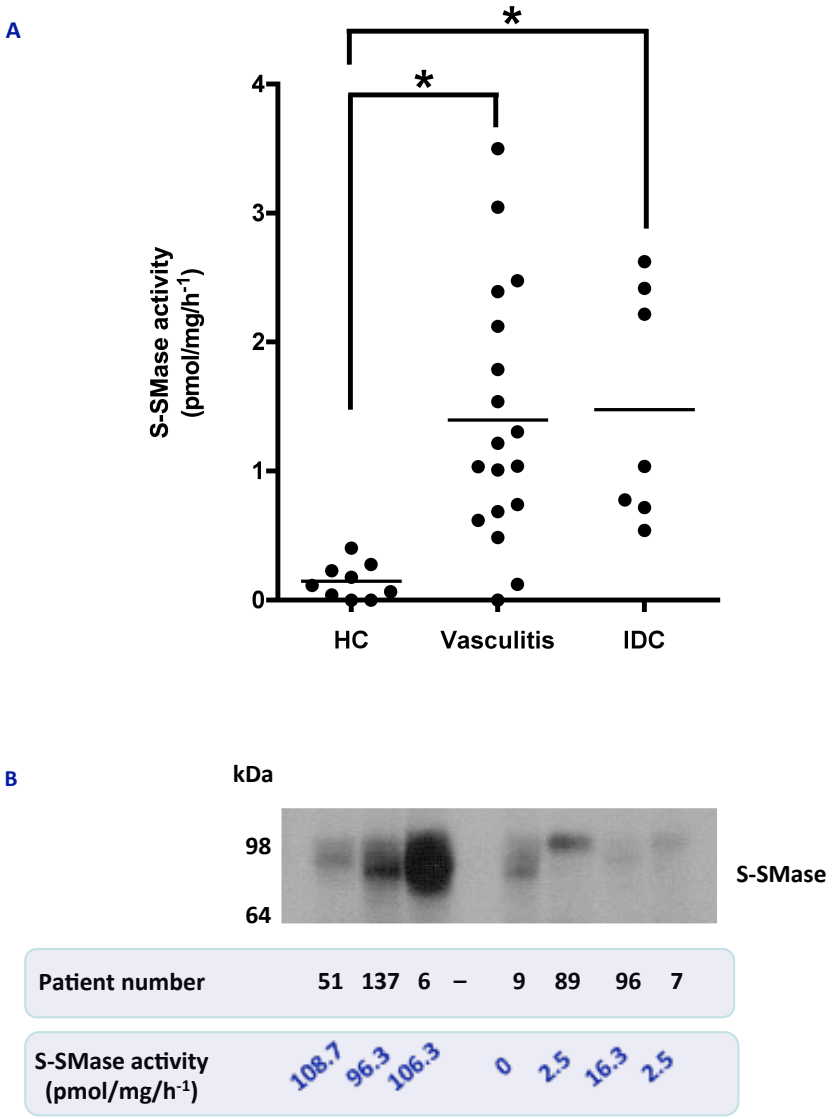


**Figure 3.2 Clinically phenotyped AASV plasma exchange patients exhibit higher active S-SMase compared to healthy controls.**

**(A)** S-SMase activity is raised in clinically phenotyped AASV (n=18) patient plasma undergoing plasma-exchange (PEX, cohort 3) compared with age-matched healthy control (HC) (n=9) plasma. S-SMase is higher n inflammatory disease control (IDC, ANCA-negative) patient plasma (PEX) compared to healthy control plasma. Plasma S-SMase activity was determined *in vitro* by the TLC activity assay. IDC patients exhibited various stages of renal failure and were ANCA negative. Plasma S-SMase activity was normalised to total plasma protein **(B)** S-SMase presence in high-activity patient plasma (51, 137, 6), compared to low activity patient plasma. Protein detected by immunoprecipitation of S-SMase using a polyclonal anti-ASM antibody (Santa-Cruz Biotech. USA). HC vs Vasculitis; *$p < 0.0005$, *HC vs IDC;* *$p < 0.0005$. Data represent means of three independent assays of each sample (n=3). Statistical significance assessed using the Mann-Whitney U-test.

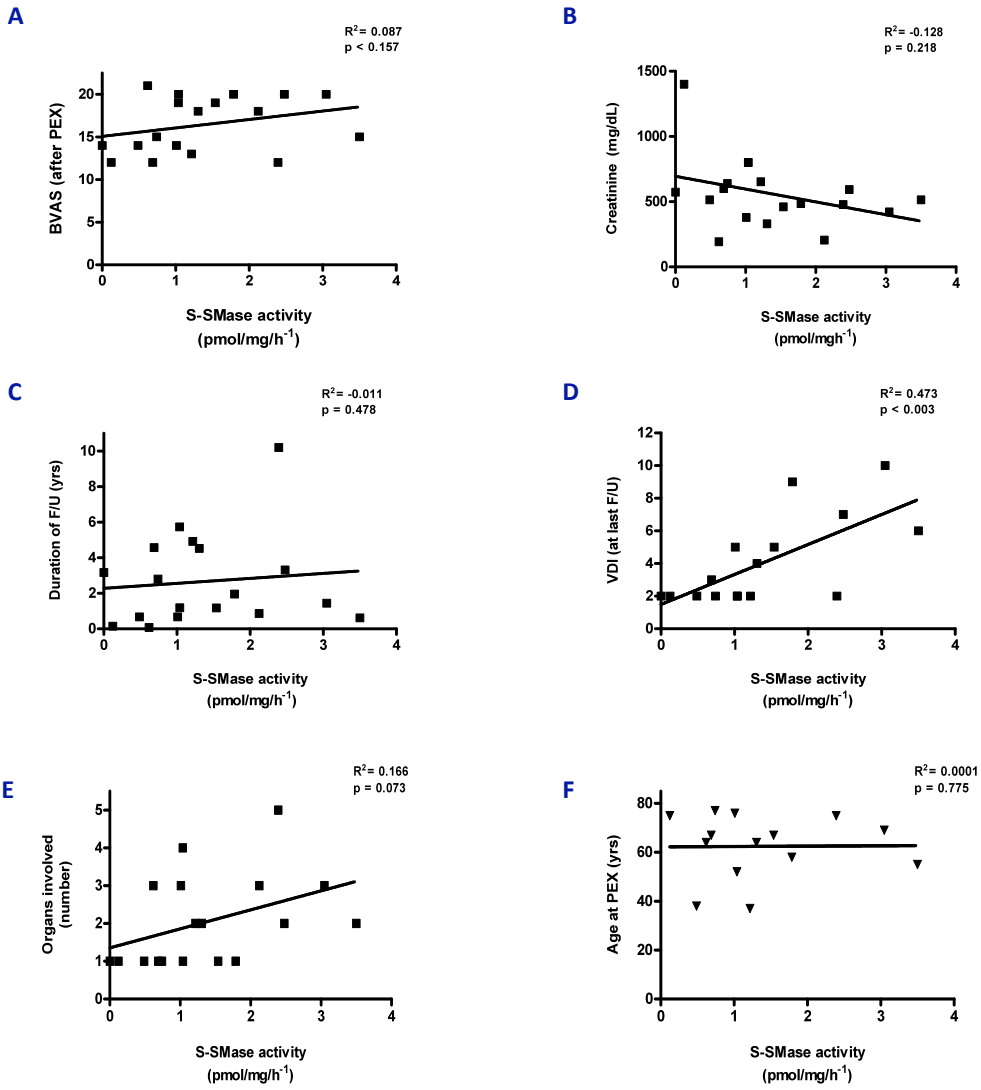


**Figure 3.3 S-SMase activity relates to vascular damage in AASV PEX patients**

S-SMase activity in plasma of AASV (n=18 total) patients undergoing plasma-exchange (PEX) positively correlates with **(D)** accumulated vascular damage (VDI) ($p < 0.003$) but not with **(A-C, E-F)** BVAS, age, creatinine levels, duration of follow up and number of organs involved clinically. Plasma S-SMase activity was determined *in vitro* by the TLC assay. Data for S-SMase activity represent means of three independent assays of each sample (n=3). Statistical significance was determined using the Spearman rank correlation test.

### 3.2.4 Serum S-SMase activity levels decrease following resolving treatment in AASV

Plasmapheresis is mentally and physiologically stressful for the patient and may affect S-SMase levels, thus serum from a small pilot cohort of AASV patients was examined **(Figure 3.4).** Data confirmed the presence of S-SMase in PSV separate from the effects of plasmapheresis. This cohort included its own healthy control individuals, and patients with active or inactive disease and remission patients according to BVAS. These included patients with Wegener's granulomatosis (n=8) and microscopic polyangiitis (n=8). Healthy controls (n=4) exhibited lower active S-SMase levels (3.56 ± 7.16 pmol/mL/$h^{-1}$) than patients with active disease (n=5) (23.69 ± 15.30 pmol/mL/$h^{-1}$) (*p < 0.04*) **(Figure 3.4)**. There was no significant increase between healthy controls (3.56 ± 7.16) and patients with inactive disease (n=9) (10.62 ± 12.71 pmol/mL/$h^{-1}$) or those in remission (n=2) (4.79 ± 1.90 pmol/mL/$h^{-1}$). The small numbers did not allow for accurate conclusions between subgroups.

To confirm the findings above, a second, larger cohort of AASV patient sera was compiled. Serum from these patients was collected prior to and following 14 weeks of active treatment. Pro-inflammatory cytokines are known to induce S-SMase secretion thus our secondary question was to ask whether decreasing the inflammatory response affected S-SMase levels in these patients. The cohort was composed of 20 patients, WG (n=14), MPA (n=4) and renal limited vasculitis (n=2). Of the total, 45% (9) were female and the cohort had a median age of 64.7 years (mean 60.9 ± 15.3). These patients were compared against a group (n=7) of early remission AASV patients (6-12 months), (median age 61.2, mean 59.1 ± 4.6) and healthy controls (n=13) with a median age of 59 years (mean 58.6 ± 8.4).

### *3.2.4.1 S-SMase in AASV before and after resolving treatment*

TNFα blockade leads to decreased CV mortality in RA (Popa et al., 2009) and suppression of inflammation restores endothelial function, at least temporarily (Raza et al., 2000). Since pro-inflammatory cytokines are known to induce secretion of S-SMase we hypothesised that clinical remission in AASV may lead to an altered S-SMase profile. S-SMase activity was elevated in AASV patients (114.8 ± 40.58 pmol/mL/$h^{-1}$) compared to healthy controls (52.3 pmol/mL/$h^{-1}$) ($p < 0.005$) **(Figure 3.5a)** confirming previous findings **(Figure 3.4).**

Importantly, S-SMase levels were significantly lower in 6/12 month remission patients (33.67 ± 13.85 pmol/mL/$h^{-1}$) ($p < 0.0004$) **(Figure 3.5a)**. These effects may be evident very early in the remission process. Following induction of treatment a significant fall in S-SMase activity was seen by week 14 **(Figure 3.5b)**. Prior to the commencement of treatment (week 0), mean S-SMase levels were 114.8 ± 40.6 pmol/mL/$h^{-1}$ falling by 15.7 % to 96.7 ± 40.76 pmol/mL/$h^{-1}$ ($p < 0.001$) **(Figure 3.5b).** By week 14, from the total of 20 patients, S-SMase activity fell in 16 patients (80%), increased in 3 patients (15%) and remained the same in 1 patient (5%). Patients responded differently to treatment with regards to S-SMase. Specifically, S-SMase activity decreased more than 40% in 2 patients (n=2), more than > 30% (n=3), >20% (n=3), >10% (n=3) and less than 10% (n=3). S-SMase activity increased in 3 patients while in 1 patient it remained the same. These data confirm results from the smaller independent serum AASV cohort **(Figure 3.4**) and suggest that S-SMase *in vivo* is regulated by inflammation and disease processes.

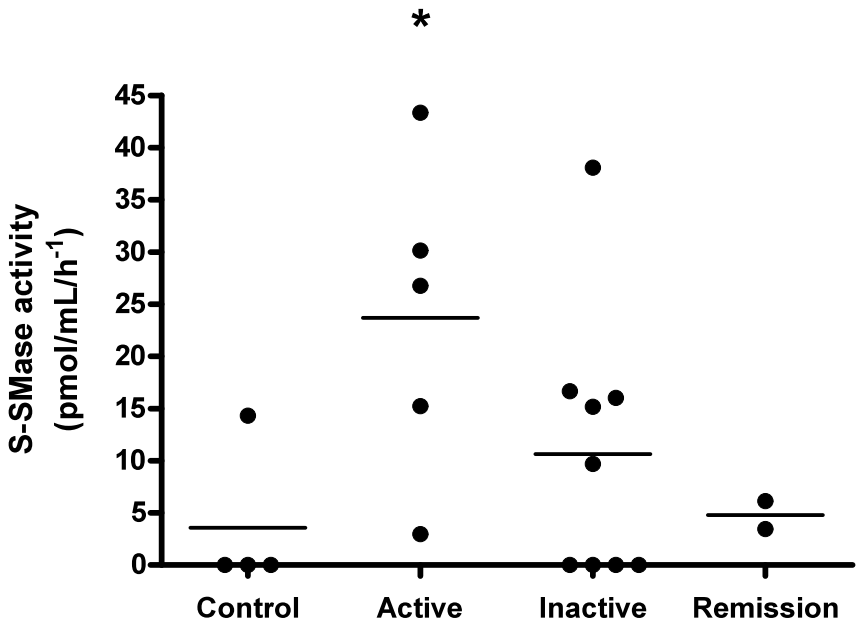


**Figure 3.4 S-SMase activity is raised in AASV patient serum**

AASV serum cohort 1, S-SMase activity in serum of patients with clinically active AASV (n=5) is higher compared to healthy control (HC) (n=4) individuals (internal HC cohort). S-SMase analysis was performed *in vitro* by the TLC activity assay. Data represent means from three independent assays of each sample (n=3). HC vs Active *$p < 0.04$. Statistical significance was determined using the Mann-Whitney U-test.

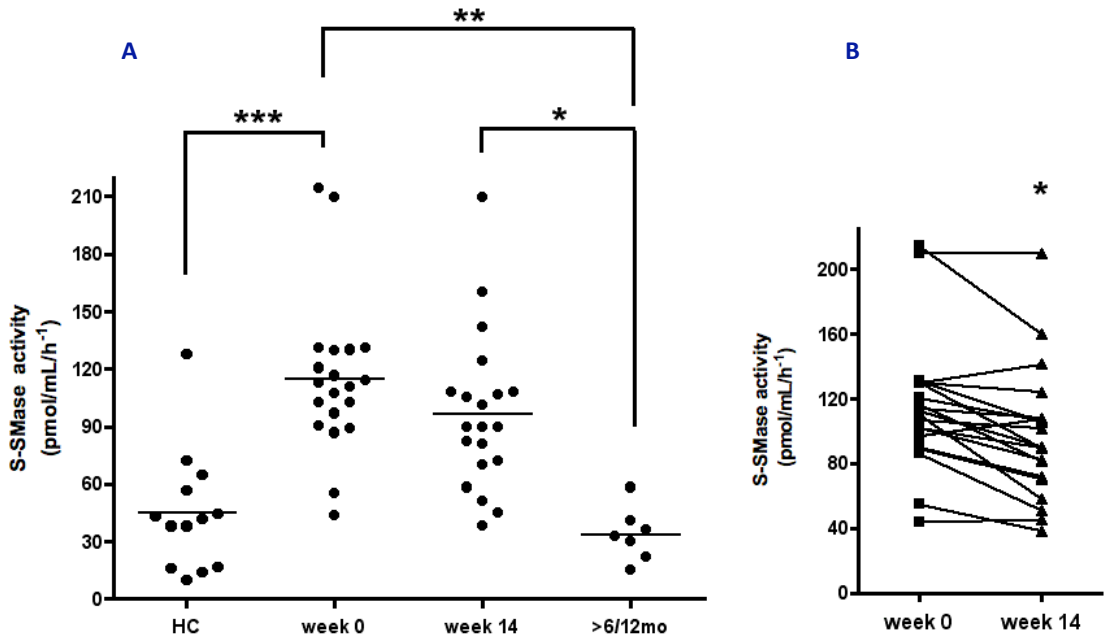


**Figure 3.5 S-SMase in active AASV falls with treatment and induction of remission**

**(A)** S-Smase activity in AASV serum (serum cohort 2) compared with healthy control age matched serum and early remission patient serum. Serum from AASV patients was extracted prior to commencement of resolving treatment (Week 0) and 14 weeks after resolving treatment (Week 14). AASV patients (n=20 total) included Microscopic polyangiitis (n=4), Wegener's granulomatosis (n=14), renal limited vasculitis (n=2). Healthy controls (n=13). AASV Remission patients (6/12 months) (n=7). HC vs Week 0; ****p < 0.0001,* Week 0 vs Remission; ***p < 0.0002,* Week 14 vs Remission; * *p < 0.0004.* Data represent means of three independent measurement of each sample (n=3). Statistical analysis was performed using the Mann-Whitney U-test. **(B)** S-Smase activity in AASV serum (serum cohort 2) falls following resolving treatment. Serum from AASV patients was extracted prior to commencement of resolving treatment (Week 0) and 14 weeks after treatment (Week 14). AASV patients as in (A). Week 0 vs Week 14; *$p < 0.0008$. Data represent means of three independent measurements of each sample (n=3). Statistical significance was determined using the Wilcoxon signed rank test. Serum S-SMase activity was determined *in vitro* by the TLC activity assay.

### *3.2.4.2 S-SMase in relation to disease parameters in AASV*

Levels of S-SMase were compared to a number of clinical disease parameters and established clinical laboratory markers of PSV summarised in **table 3.1**. In univariate regression analysis S-SMase activity levels at week zero (0) did not relate to immune cell counts including total white cell counts, lymphocyte and neutrophil levels **(Table 3.1).** There was also no relation with haemoglobin, VEGF and renal function such as glomerular filtration rate (MDRD eGFR) **(Table 3.1).** Univariate analysis also indicated a negative relationship between cytokines and S-SMase in most cases**.** There was no correlation between S-SMase activity IL-6, IL-8 and IL-10**.** TNF$\alpha$, IL-1$\beta$ and IFN$\gamma$ are known to induce S-SMase secretion from EC (Marathe et al., 1998, Wong et al., 2000) and therefore alterations in levels of these cytokines may affect circulating S-SMase levels. However, neither related to S-SMase activity in these patients **(Figure 3.6).** This is in contrast with the study by Doehner *et al.* (2007) who revealed a positive correlation between TNF$\alpha$ and S-SMase ($r^2 = 0.22$; $p = 0.02$) in patients with CHF. TNF$\alpha$ levels are raised in renal vasculitis (Tesar et al., 1998, Noronha et al., 1993, Feldmann and Pusey, 2006) and one might have expected TNF$\alpha$ to therefore correlate with S-SMase levels in these patients. We also found a negative correlation between S-SMase levels and IL-1ra ($p < 0.03$) however, this lone association comes with certain caveats. Given the number of parameters tested above (20) and low R output value (-0.27), It is likely that this correlation ($p < 0.03$) occurred by chance. Thus, this finding must be considered in the context of the number of parameters tested in table 3.1 and is likely to be an anomaly.

Furthermore, S-SMase activity did not relate with other inflammatory markers such as CRP, ESR or creatinine levels **(Figure 3.6, Table 3.1).** Interestingly S-SMase did not relate to accumulated damage (VDI) **(Figure 3.6b)**, which contrasts previous findings in AASV PEX patients (3.2.3) **(Figure 3.3d).** This may have been due to inconsistent VDI scoring for these patients and missing data points which was also the case with age and BVAS **(Figure 3.3)**. Longitudinal studies are required to delineate the role of S-SMase in active clinical disease.

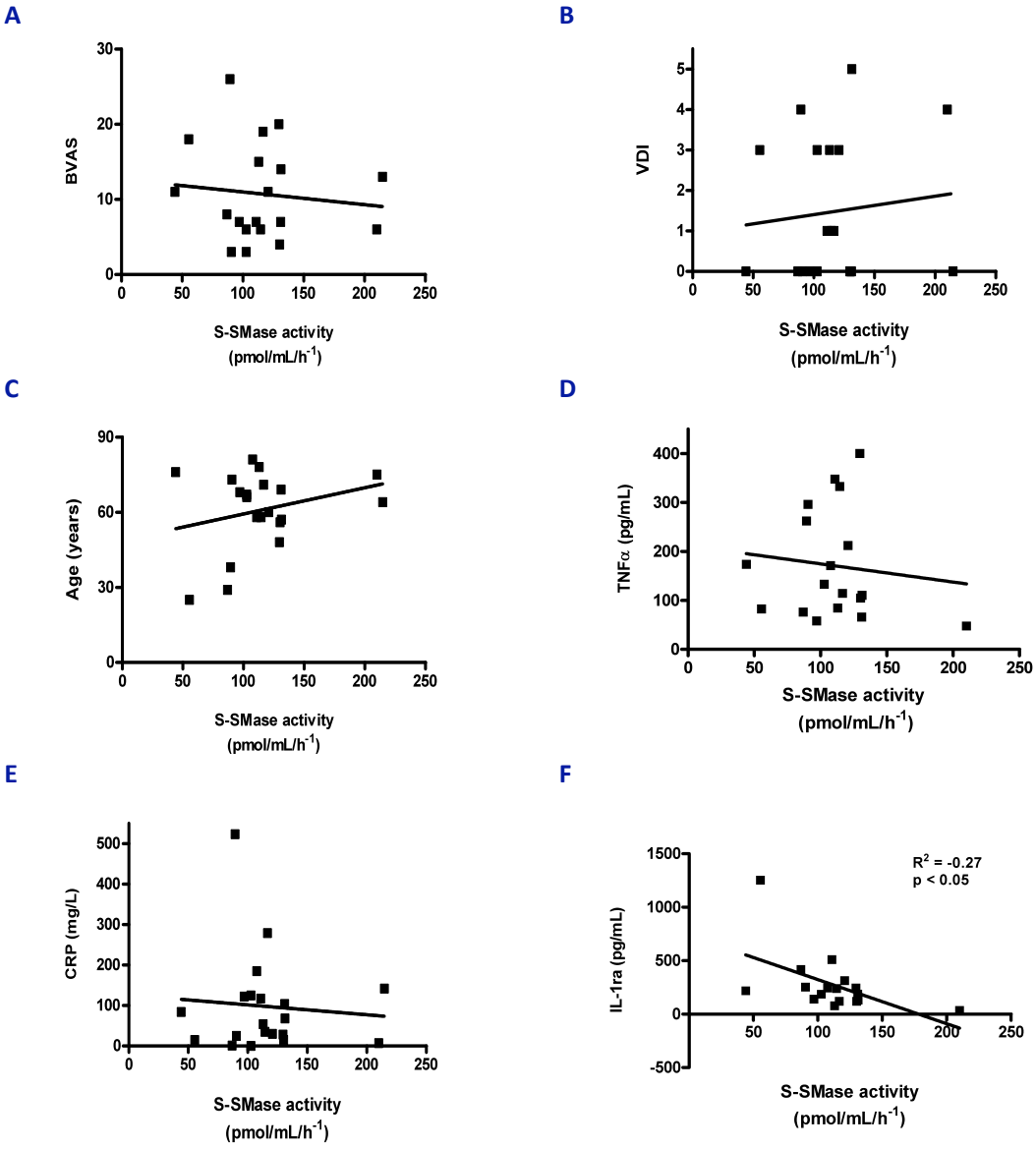


**Figure 3.6 Correlation of S-SMase levels with disease indices, and inflammatory markers in AASV patient serum**

S-SMase activity in serum of AASV patients does not correlate with disease activity (BVAS), accumulated damage index (VDI) and age **(A-C)**. There was no relation of S-SMase with CRP, and TNFα levels in AASV patients **(D-E)**. S-SMase activity negatively correlated with IL-1ra levels in AASV ($p < 0.05$) **(F)**. Serum in these patients was extracted prior to the commencement of treatment (Week 0). AASV patients included microscopic polyangiitis (n=4), Wegener's granulomatosis (n=14), renal limited vasculitis (n=2). Statistical analysis was performed using the Spearman rank correlation test.

| Univariate correlation analysis of S-SMase in AASV | | | |
|---|---|---|---|
| **S-SMase Vs** | | ***R-value*** | ***P-value*** |
| **VEGF** | **(pg/mL)** | -0.1992 | 0.43 |
| **Wcc** | **($x10^9$/L)** | -0.0001 | 0.99 |
| **Hb** | **(g/dL)** | -0.1882 | 0.43 |
| **Creatinine** | **(mmol/L)** | 0.2798 | 0.23 |
| **ANCA titre (generic)** | **A.U** | 0.3160 | 0.17 |
| **Lymphocytes** | **($x10^9$/L)** | -0.0747 | 0.75 |
| **Neutrophils** | **($x10^9$/L)** | 0.0617 | 0.80 |
| **MDRD eGFR** | **A.U** | -0.1992 | 0.42 |
| **VDI** | **A.U** | 0.1102 | 0.65 |
| **BVAS** | **A.U** | -0.0308 | 0.90 |
| **Age** | **(Years)** | 0.0740 | 0.76 |
| **ESR** | **($mm/hr^{-1}$)** | 0.1922 | 0.43 |
| **CRP** | **(mg/mL)** | 0.0436 | 0.86 |
| **TNFα** | **(pg/mL)** | -0.1331 | 0.59 |
| **IFNγ** | **(pg/mL)** | -0.3024 | 0.22 |
| **IL-1ra** | **(pg/mL** | **-0.2700** | **< 0.03** |
| **IL-1β** | **(pg/mL)** | -0.2611 | 0.29 |
| **IL-6** | **(pg/mL)** | -0.4386 | 0.06 |
| **IL-8** | **(pg/mL)** | 0.0010 | 0.99 |
| **IL-10** | **(pg/mL)** | -0.0588 | 0.82 |

**Table 3.1 Univariate correlation analysis of S-SMase with clinical and laboratory parameters of AASV patients**

### *3.2.4.3 Clinical disease status in the AASV cohort at 14 weeks*

Clinical assessment data indicated that the majority of these patients reached early clinical response according to their BVAS. S-SMase activity did not relate to this response status. Of the 20 patients, 1 was not accounted for in terms of BVAS (no data). Prior to treatment, the cohort showed a median BVAS of 8 (mean 8 ± 6.48) while by week 14 this fell to a median of 1 (mean 1.79 ± 2.72) ($p = 0.0001$). Most of the patients were deemed to be in early clinical remission. Of these, 7 had a BVAS of zero (0) **(Figure 3.7a)** while 60% of patients (n=12) had a BVAS of ≤ 1 and 80% (n = 16) had a BVAS of ≤ 2 suggesting that the progression of disease was successfully halted, however, this does not mean that the underlying inflammation was suppressed. Three to four months is established as the time taken to induce a response to initial aggressive therapy in SV – but this is far from a real remission, which requires at least a year of active immunosuppressive therapy and even then, relapse is common unless active treatment is longer maintained (De Groot et al., 2005). This assumption of continuing sub-clinical vascular inflammation was supported by the continued high cytokine levels **(Figure 3.7).** The VDI increased significantly from a median of 1 (mean 1.47 ± 1.74) at week zero (0) to median of 2 (mean 2.34 ± 1.94) ($p < 0.004$) by week 14 suggesting continuous cumulative damage. Inflammatory markers CRP and ESR fell following treatment by week 14. Median patient CRP levels prior to treatment were 61 mg/L (mean 97.9 ± 123 mg/L) and fell to a median of zero (0) mg/L (mean 4.2 ± 8.24 mg/L) by week 14 ($p = 0.0002$) **(Figure 3.7d)**. Although analysis of ESR values should be performed on a single patient basis, at presentation median ESR was 80.5 $mm/h^{-1}$ (mean 71.8 ± 41.71) and decreased significantly by week 14 to a median 11.5 $mm/h^{-1}$ (mean 17.9 ± 14.62) ($p < 0.004$) (50% of patient data available) **(Figure 3.7c)**.

### *3.2.4.4 Pro-inflammatory cytokine status in the AASV cohort at 14 weeks*

Despite the induction of clinical response and decrease in CRP and ESR levels in most of these patients, TNFα, IFNγ and IL-1β levels were not significantly altered following treatment **(Figure 3.7e-i)**. This was expected for TNFα as not all patients from this cohort received anti-TNF (infliximab). Of the total (20), 12 patients received infliximab while there was no data for one of these patients. TNFα levels were not significantly altered in those receiving infliximab, nor those not receiving treatment **(Figure 3.7g-i)**. Patients receiving infliximab showed a non-significant decrease in median levels of TNFα by week 14 (median 123.9 pg/mL, range 50.16-224.3; mean 121.6 ± 49.93) compared to week zero (0) (median 140.8 pg/mL, range 47.96-440.2; mean 169.7 ± 116) **(Figure 3.7g-i)**. This could be because the reversibility of TNFα levels may require prolonged treatment beyond 14 weeks. Cytokine production can be transient and so can be the effect of infliximab. For example, infliximab can rapidly improve EC function however, this effect is short-lived and endothelial responses return to baseline by 2 weeks, following a single-only infusion of the antibody (Raza et al., 2006). Importantly in a separate study, although infliximab was shown to improve endothelial responses by 12 weeks, TNFα levels in the same patients did not fall significantly (Booth et al., 2004b). This supports the lack of effect of infliximab see in our AASV patients (**Figure 3.7g-i**). Levels of IFNγ and IL-1β in the patients from our cohort also remained unchanged **(Figure 3.7e-f)**.

### 3.2.5 S-SMase in AASV summary

We showed for the first time that S-SMase was raised in AASV. This was confirmed in plasma and serum of diseased AASV patients compared to healthy controls. S-SMase did not correlate with anthropometric parameters as previously shown in CHF (Doehner et al., 2007). S-SMase correlated with the VDI in patients who underwent plasmapheresis compared to patients whom had not, suggesting that highly active vascular disease may associate with raised plasma S-SMase activity. Furthermore, serum S-SMase fell significantly 14 weeks through to 6 months following the commencement of resolving treatment. To further examine the role of S-SMase as a mediator of vascular dysfunction we next investigated S-SMase activity in RA that features rheumatoid vasculitis, arising secondary to the rheumatoid disease process.

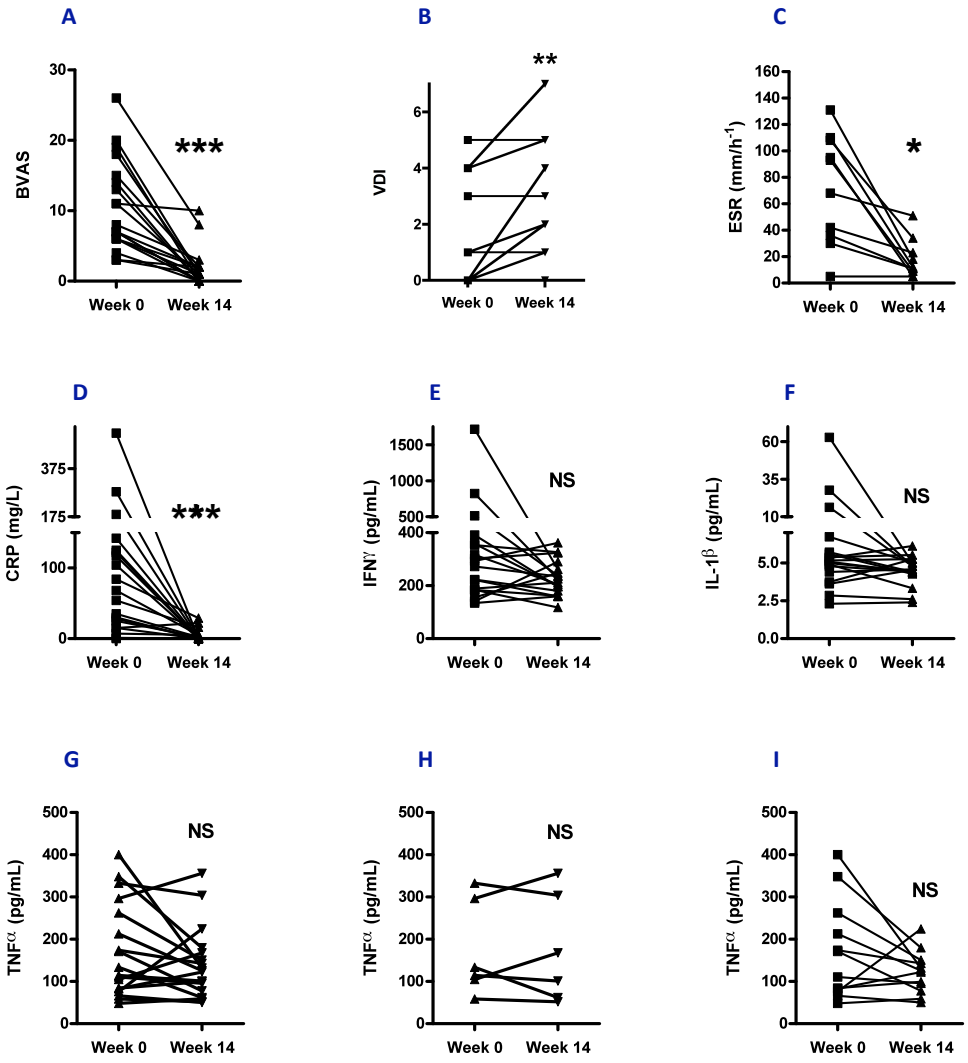


**Figure 3.7 Disease activity and inflammatory marker status following resolving treatment In AASV serum used for S-SMase assays**

Scoring before and after treatment for disease activity was assessed by Birmingham Vasculitis Activity Score (BVAS) **(A)**, accumulated vascular damage assessed using the vasculitis damage index (VDI), **(B)** erythrocyte sedimentation rate and C-reactive protein (CRP) levels **(C-D)** in patients with AASV. BVAS and CRP are significantly lower by 14 weeks. Pro-inflammatory cytokines showed no difference by 14 weeks **(E-I)**. IFNγ and IL-1β levels **(E-F).** TNFα levels in all patients **(G)**, TNFα levels in patients not receiving anti-TNFα (Infliximab) treatment **(H)**, TNFα levels in patients receiving anti-TNFα (Infliximab) treatment **(I)**. Week 0 vs Week 14, *$p < 0.004$, **$p < 0.005$, ***$p < 0.0005$. Statistical significance was determined using the Wilcoxon signed rank test.

### 3.2.6 S-SMase is elevated in patients with RA

ECD in vasculitis is a strong candidate mechanism believed to mediate accelerated atherosclerosis in secondary vasculitis such as seen in RA and SLE (Raza et al., 2000). Patients with early RA have dysfunctional endothelia and exhibit decreased EDV consistent with other evidence for widespread vascular inflammation in these patients (Bergholm et al., 2002). We wanted to see if the increased S-SMase activity seen in AASV was also mirrored in RA. To do this, serum from 35 patients with established RA was compared to that of healthy controls (n = 13) due to limited availability of samples from patients and healthy individuals **(Figure 3.8)**. Our data revealed that RA patients also exhibited elevated S-SMase levels (84.10 ± 34.50 pmol/mL/$h^{-1}$), more than 1.5-fold greater than age-matched healthy controls (52.30 ± 34.85 pmol/mL/$h^{-1}$) ($p < 0.02$) **(Figure 3.8)**. This finding confirms that S-SMase is not only raised in inflammatory primary vasculitis but is also evident in other chronic inflammatory diseases that feature secondary vasculitis. Since EC are the only major source of S-SMase this suggests that it may be another hallmark of the activated endothelium, linked to its dysfunction as manifested by decreased vasodilatory responses frequently also seen in PSV. Another marker of endothelial injury or activation is von Willebrand factor (vWF). vWF however is also associated with EC detachment not dysfunction while it has been previously shown to not correlate with endothelial-dependent vasodilation (Filer et al., 2003). Thus it was not considered as this may have distracted from the focus of our hypothesis. Moreover, although decreased sample availability did not allow us to assay for other EC markers we were able to observe the relationship of S-SMase with vascular endothelial growth factor (VEGF) and vascular cell adhesion molecule 1 (VCAM1) (**Table 3.3**).

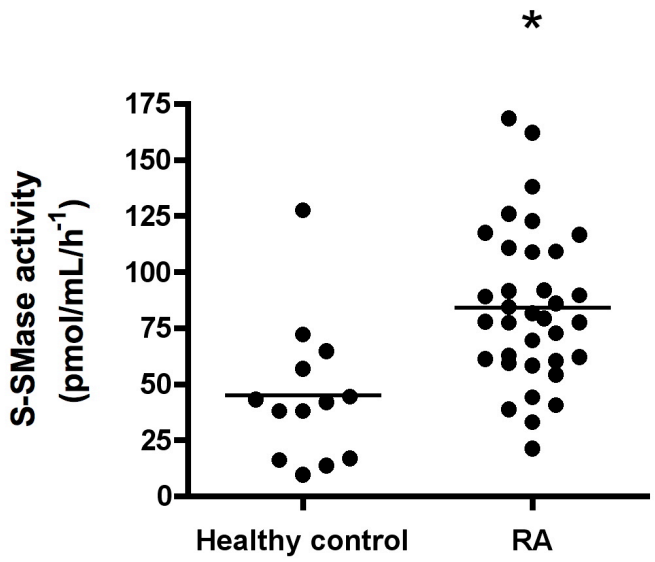


**Figure 3.8 S-SMase activity is raised in patients with RA**

S-SMase activity is raised in serum of rheumatoid arthritis (RA) patients (n=35 total) compared to age-matched healthy control (HC) individuals (n=13 total) serum as confirmed by the TLC activity assay. Data represent means from three independent assays (n=3). HC vs RA; *$p < 0.01$. Statistical significance was determined using the Mann-Whitney U-test

### *3.2.6.1 S-SMase in serum of RA patients correlates with cardiovascular endpoints*

Data in this chapter show that S-SMase was raised in AASV but did not correlate with current disease activity or cytokine profiles (at the time). S-SMase in RA was also compared to a panel of clinical disease parameters.

S-SMase has been linked to LDL retention in the sub-endothelium of atheromatous lesions whilst LDL is also considered a carrier of S-SMase (Schissel et al., 1998a, Marathe et al., 1999) and **figure 3.9a** confirms that S-SMase correlates well with the increasing levels of LDL in RA serum ($p < 0.0007$). Furthermore, there was a strong relationship with the LDL:HDL ratio (**Figure 3.9b)** but not with HDL itself **(Figure 3.9c)**. Interestingly, S-SMase did relate to ApoB **(Figure 3.9d)**, which makes sense given the relationship between LDL and S-SMase as ApoB is a component of LDL. There was no correlation between the HDL component ApoA and S-SMase **(Figure 3.9e)** supporting the lack of association between S-SMase and HDL **(Figure 3.9c).** There was also no correlation with total cholesterol levels **(Table 3.3)**. Furthermore, S-SMase showed a positive correlation with triglyceride levels but patients with a history of hypercholesterolemia had lower levels than those who did not **(Figure 3.9g-h)**. These data suggest that the association of S-SMase with the lipid parameters above may not occur by chance. S-SMase positively correlated with white cell count (Wcc) but negatively correlated with homocysteine levels both of which are considered traditional CV risk factors **(Figure 3.10f-g)**. S-SMase levels in RA were compared against clinical disease severity indicators as had been done in AASV **(Figure 3.3; 3.6; table 3.1 [BVAS])**. In RA, S-SMase showed no correlation with DAS or the duration of disease in RA **(Figure 3.10a**). Furthermore, S-SMase levels did not differ in patients with ExRA compared to those without **(Figure 3.10b)**.

Pulse pressure (PP) is a measure of arterial stiffness and combined with heart rate (HR) is considered a positive indicator of cardiovascular mortality in healthy individuals (Thomas et al., 2001). Accordingly, S-SMase levels were compared against PP and the PP x HR index, which is a measure of pulsatile stress. We found a positive correlation with PP which, was deemed marginally insignificant (R: 035; $p = 0.052$) **(Figure 3.10d)** whereas there was a stronger correlation with PP x HR (R: 0.47; $p < 0.009$) **(Figure 3.10e)**.

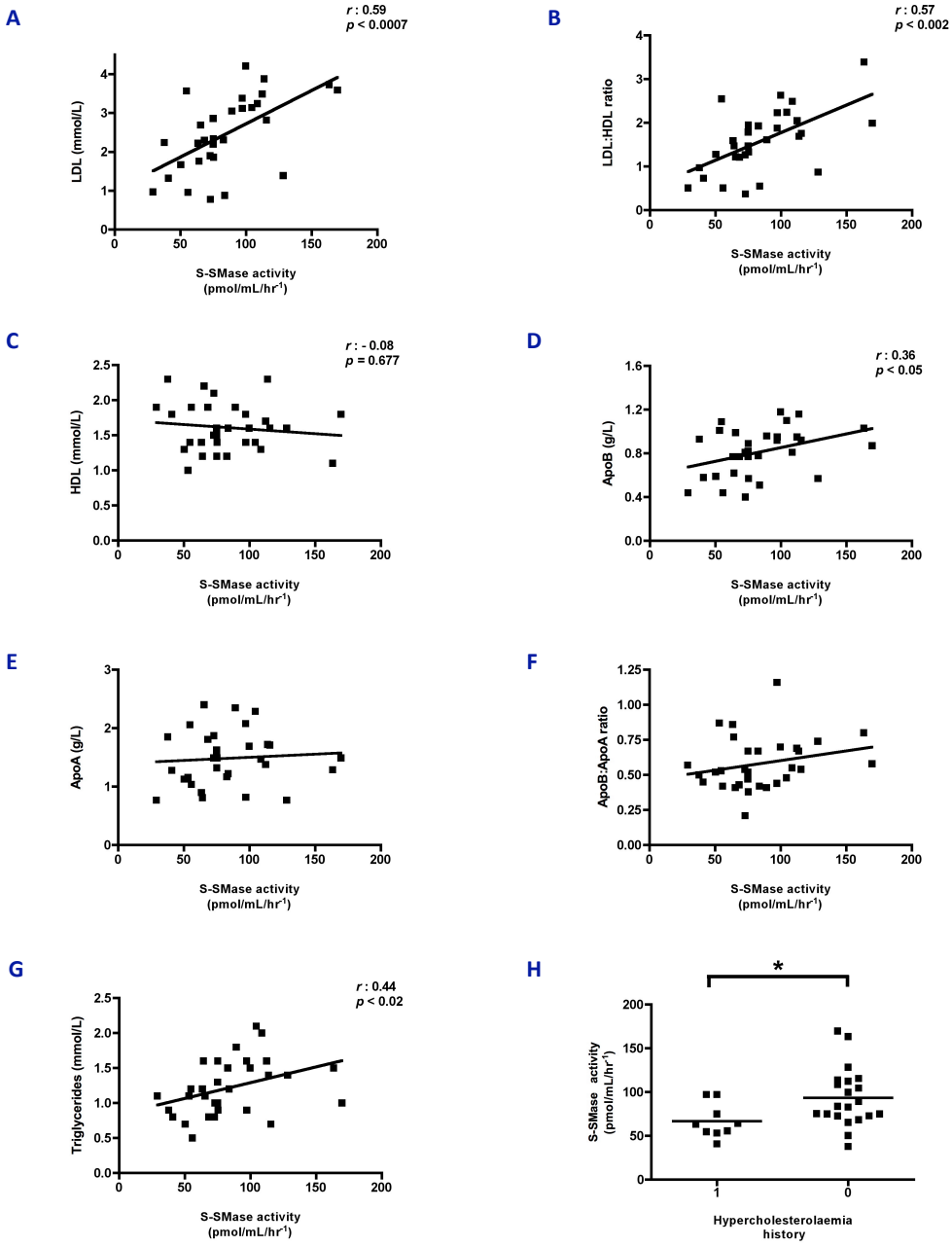


**Figure 3.9 S-SMase activity compared to lipid profiles in RA patient sera**

S-SMase activity positively correlates with **(B)** LDL:HDL ratio, **(A)** LDL and **(D)** ApoB and **(G)** triglyceride levels in RA patient serum. No correlation was seen between S-SMase activity and **(C)** HDL**, (E)** ApoA and **(F)** ApoB:ApoA ratio. **(H)** Patients with a history of hypercholesterolaemia (1) had decreased serum S-SMase compared to those without (0). Statistical significance was determined using the Spearman rank correlation test and the Mann-Witney U-test. *$p < 0.05$

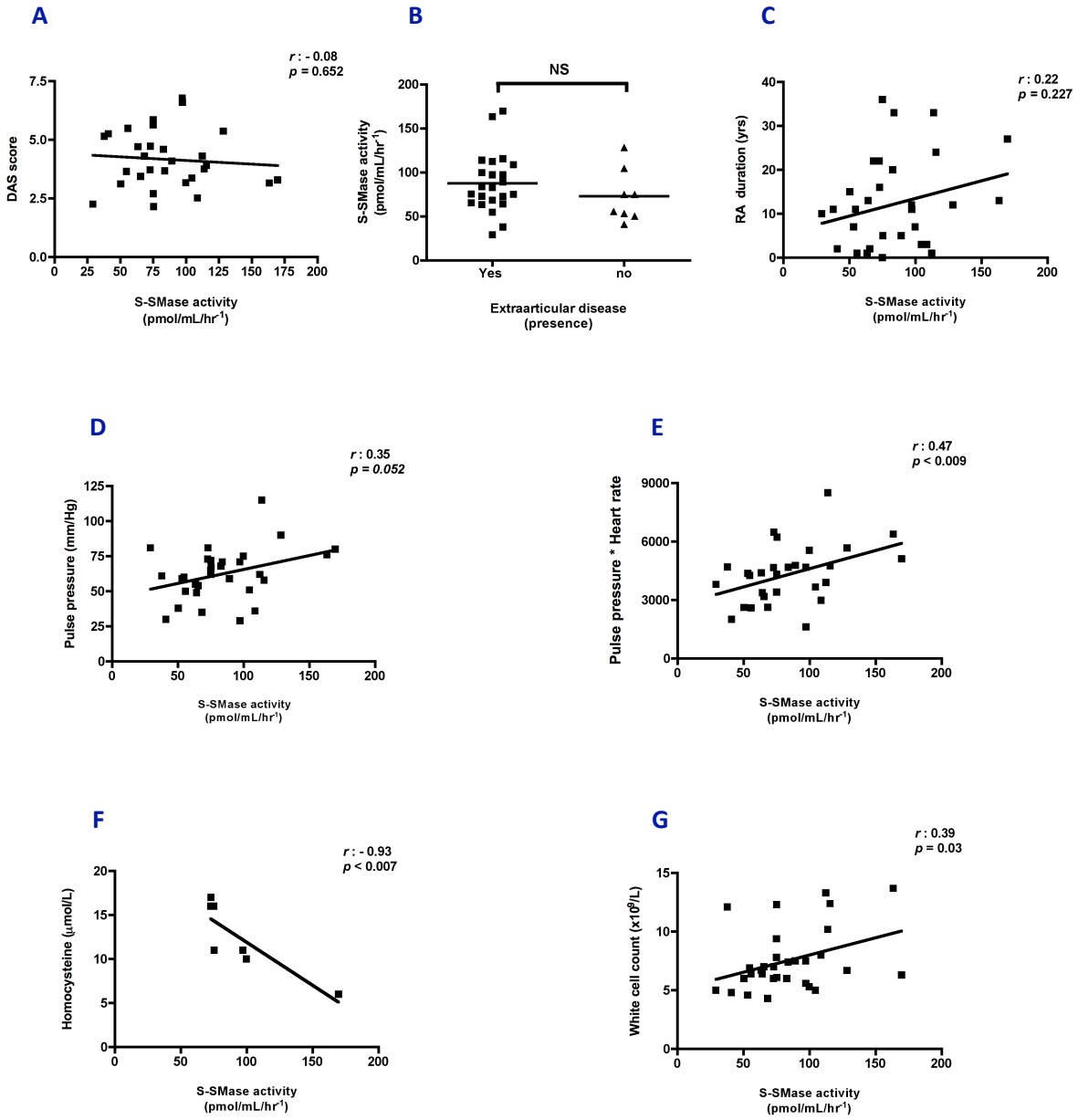


**Figure 3.10 S-SMase activity compared to disease parameters in RA patient sera**

S-SMase activity positively correlated with **(E)** arterial tensile stress (pulse pressure*heart rate) and **(G)** white cell counts but not with the disease activity score-28 (DAS-28) **(A)**, RA disease duration **(C)** or pulse pressure **(D)**. There was no difference in S-SMase activity between patients with extraarticular disease and those with not **(B)**. Homocysteine levels negatively correlated with S-SMase activity **(F)**. Statistical significance was determined using the Spearman rank correlation test for univariate correlation analysis and the Mann-Whitney U test for 2-sample population differences.

S-SMase did not correlate with systolic and diastolic blood pressure **(Figure 3.11a-b)** whilst hypertensive patients showed no difference in their S-SMase levels compared to non-hypertensive RA patients **(Table 3.5).** We therefore looked for other traditional CV risk factors. Smoking is a strong independent CV risk factor and contributor to the pathogenesis of RA. Patients that were active smokers showed higher S-SMase levels than those who had never smoked ($p < 0.05$) and they also had higher but insignificant S-SMase levels compared to ex-smokers **(Figure 3.11c)**. Smoking described as pack-years, is the cumulative smoking burden and defined as the number of years one pack (20) of cigarettes was smoked every day. As shown in **figure 3.11d**, the number of pack years correlated strongly with increasing S-SMase levels in these RA patients ($r$: 0.46; $p < 0.009$) supporting data from **figure 3.11c.** With the above in mind we examined the association of S-SMase with various CV parameters. Initially the presence of CVD and those patients whose primary cause of death was CV-related was assessed. S-SMase levels in patients with all-cause CVD were mildly elevated compared to those without CVD and similar results were obtained for RA patients that died of CVD **(Figure 3.11e-f)**.

RA patients with elevated S-SMase were at higher risk of coronary heart disease **(Figure 3.12a)**, which is in agreement with the finding of increased S-SMase levels in CHF (Doehner et al., 2007). CVD risk in RA strongly correlates with S-SMase levels. Patients with RA have a high 10 year CV risk, which may be more profound in women (Kremers et al., 2008) and **figure 3.12b** shows a positive correlation between S-SMase activity and CV 10 year risk in these patients. This absolute 10 year risk of developing CVD in RA is evident even at onset of arthritis and is similar to non-RA subjects 5-10 years older. Furthermore, this phenomenon is more profound in women (Kremers et al., 2008). As a result a

comparison between S-SMase and the 10-year CVD risk was made for females and males separately and no difference in S-SMase levels was observed **(data not shown).**

S-SMase levels also correlated with the Framingham risk score for the prediction of an absolute 10-year CHD risk **(Figure 3.12d),** which corroborates the relationship between S-SMase and CHD risk **(Figure 3.12a).** Importantly, we also found a positive correlation of S-SMase with the Reynolds risk score, a recent alteration to the Framingham risk score, that takes into account CRP levels and parental CVD history **(Figure 3.12e).** The observation of independent risk analyses above make it unlikely that these associations have occurred by chance. In support of this, other parameters such as lipid profiles and smoking have shown a relationship with S-SMase and are independent risk factors for CVD. However, not all the clinical parameters showed a correlation with S-SMase, strengthening the concept that the positives were not a chance finding related to the large number of correlations performed. SCORE risk analysis did not show any correlation with S-SMase levels and neither did the health assessment questionnaire scores **(Table 3.4)**. Levels of S-SMase in patients were not different when sub-grouped according to chest X-ray (CXR) analysis, a method used to assess extraarticular disease identifying lung fibrosis and heart size **(Table 3.5)**.

As in the AASV patients in this chapter **(Figure 3.7)**, S-SMase levels did not correlate with cytokine profiles in RA patients **(Table 3.3)**. Furthermore, there was no correlation of S-SMase with CRP, ESR, Hb and creatinine nor with markers of endothelial activation **(Table 3.3)**. Finally, there was no association between S-SMase and any of the 5 anthropometric parameters **(Table 3.2)**.

An important point should be taken into consideration here regarding the impact of the statistical significance of S-SMase correlations with RA patient parameters. In order to account for the increased number of statistical tests (Spearman's rank) performed in this RA cohort, it may be appropriate to take into consideration post-hoc analysis by performing corrections to some of the data sets. This could prevent over-interpretation of the significance of these tests. Although S-SMase correlated highly with several parameters here including lipids and CV risk algorithms, increasing statistical tests also increases the chances of generating type I errors, or false positive statistical significance, when in fact this was not true in the first place. Applying Bonferroni's corrections in this instance would provide control over the generation of type I errors however, this application is also prone to type II errors (over-looking true statistical significance). Although such adjustments should not be used hastily, the chances of gaining statistical significance will naturally increase with multiple comparisons. Thus conclusions from these data should be taken with the above points in mind. These are considered in this chapter's discussion (**section 3.4**).

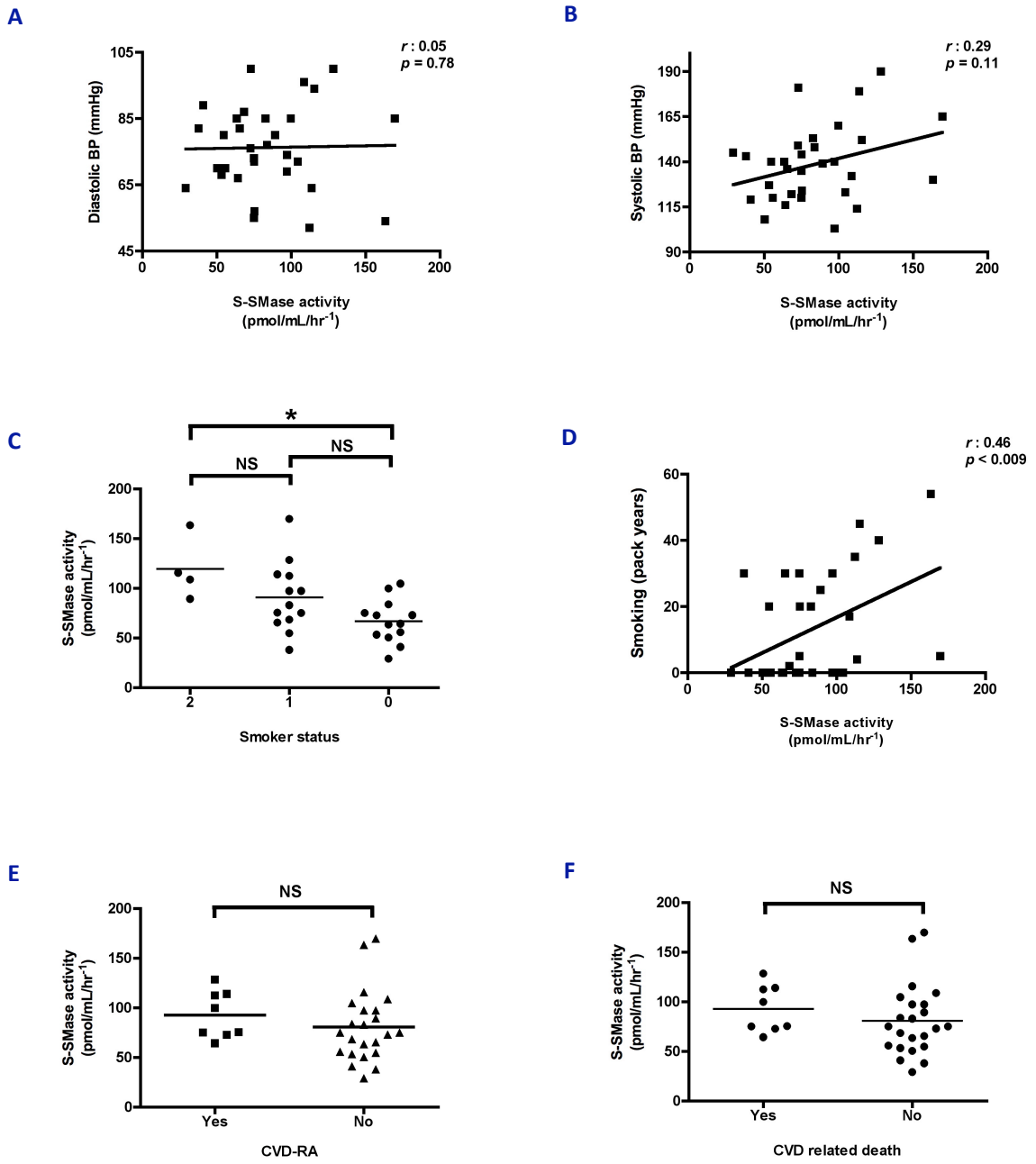


**Figure 3.11 S-SMase activity compared to blood pressure and smoking status in RA**

S-SMase activity did not correlate with diastolic or systolic blood pressure **(A-B)** but positively correlated with **(D)** smoking (pack-years). **(C)** Current smokers have higher S-SMase levels than those who had never smoked. Where 2, current smokers, 1, have previously smoked, 0, have never smoked before. **(F)** There was no difference in S-SMase activity in patients who had died of CVD. Statistical significance was determined using the Spearman rank correlation test univariate correlation analysis and the Mann-Whitney U test for 2-sample population differences.

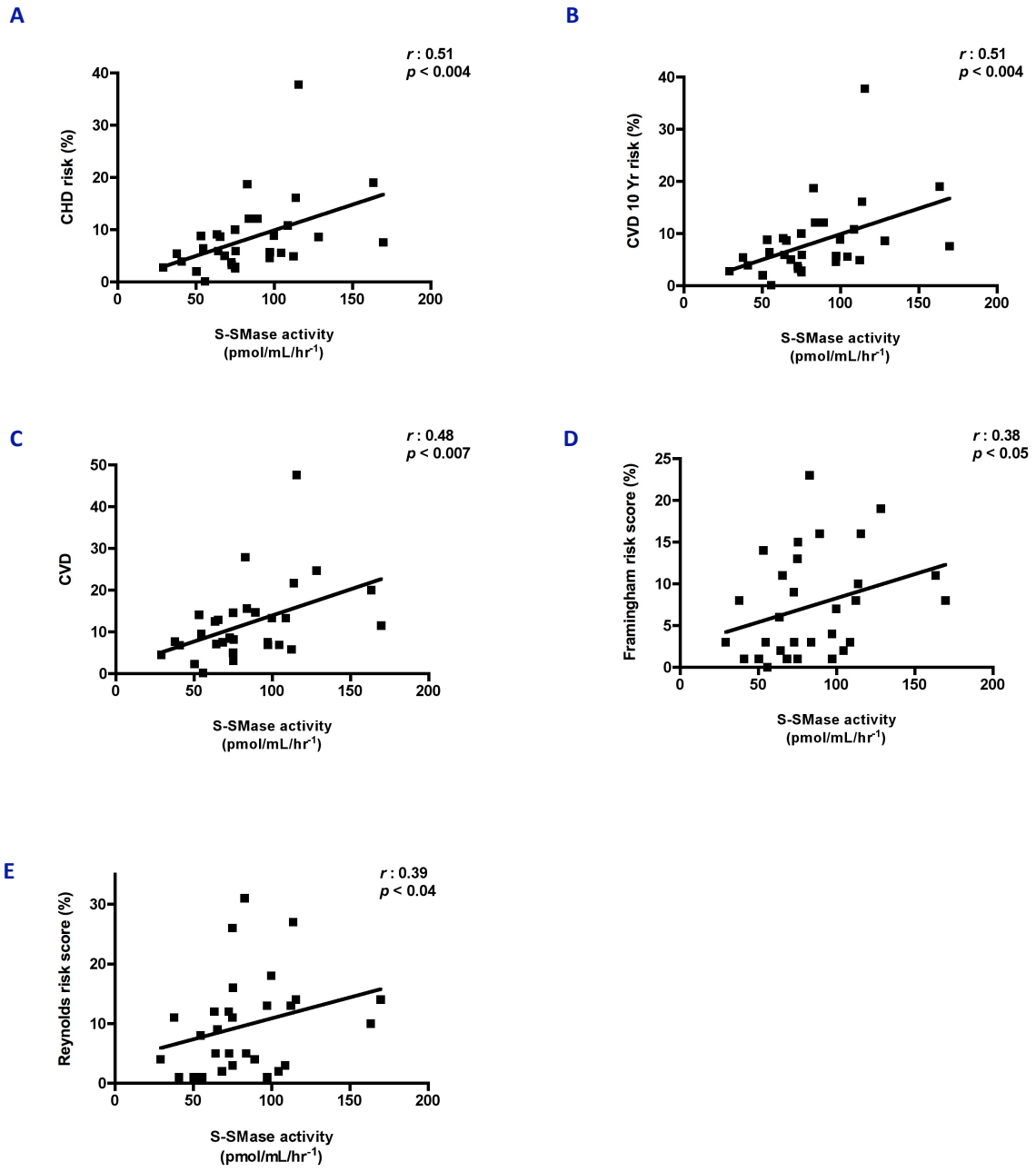


**Figure 3.12 S-SMase activity compared to CV endpoints in RA patient sera**

S-SMase activity positively correlated with **(A)** coronary heart disease risk, **(B)** absolute 10 year CVD risk, **(C)** CVD, **(D)** Framingham score and the Reynold's score **(E)**. Statistical significance was determined using the Spearman rank correlation test

| Univariate correlation analysis of S-SMase | | | |
|---|---|---|---|
| **S-SMase Vs** | | ***R-value*** | ***P-value*** |
| **Age** | **(yrs)** | 0.073 | 0.69 |
| **BMI** | **(kg/m$^2$)** | - 0.117 | 0.54 |
| **Height** | **(cm)** | - 0.016 | 0.93 |
| **Weight** | **(kg)** | - 0.061 | 0.74 |
| **Waist** | **(cm)** | 0.101 | 0.60 |

BMI – Body mass index

## Table 3.2 Univariate correlation analysis of S-SMase with anthropometric parameters in RA patients

| Univariate correlation analysis of S-SMase against blood profile markers | | | |
|---|---|---|---|
| **S-SMase Vs** | | ***R-value*** | ***P-value*** |
| **VEGF** | **(pg/mL)** | 0.28 | 0.56 |
| **Homocysteine** | **(μmol/L)** | ***- 0.93*** | ***< 0.007*** |
| **VCAM1** | **(pg/mL)** | 0.15 | 0.43 |
| **Wcc** | **(x10$^9$/L)** | ***0.39*** | ***0.03*** |
| **Hb** | **(g/dL)** | 0.07 | 0.67 |
| **Creatinine** | **(μmol/L)** | - 0.12 | 0.49 |
| **Uric acid** | **(μmol/L)** | - 0.08 | 0.64 |
| **Total cholesterol** | **(mmol/L)** | 0.29 | 0.11 |
| **HDL** | **(mmol/L)** | - 0.07 | 0.68 |
| **LDL** | **(mmol/L)** | ***0.59*** | ***< 0.0006*** |
| **LDL:HDL ratio** | **(LDL/HDL)** | ***0.57*** | ***< 0.002*** |
| **ApoA** | **(g/L)** | 0.15 | 0.42 |
| **ApoB** | **(g/L)** | ***0.36*** | ***< 0.05*** |
| **ApoB:ApoA ratio** | **(ApoB/ApoA)** | 0.24 | 0.19 |
| **Triglycerides** | **(mmol/L)** | ***0.44*** | ***< 0.02*** |
| **ESR** | **(mm/hr$^{-1}$)** | 0.02 | 0.88 |
| **CRP** | **(mg/mL)** | 0.13 | 0.48 |
| **TNFa** | **(pg/mL)** | - 0.10 | 0.84 |
| **sTNF-R** | **(pg/mL)** | 0.08 | 0.66 |
| **IL-1b** | **(pg/mL)** | 0.68 | 0.11 |
| **IFNg** | **(pg/mL)** | 0.74 | 0.06 |
| **IL-6** | **(pg/mL)** | ***0.86*** | ***< 0.03*** |

Wcc – white cell count
Hb – Haemoglobin

## Table 3.3 Univariate correlation analysis of S-SMase with laboratory parameters in RA patients

**Univariate correlation analysis of S-SMase against disease and CV endpoints**

| S-SMase Vs | | *R-value* | *P-value* |
|---|---|---|---|
| Smoking | (pack years) | ***0.46*** | ***< 0.009*** |
| Pulse pressure | (mmHg) | 0.35 | 0.052 |
| Pulse pressure X HR* | ($mmHg/min^{-1}$) | ***0.48*** | ***< 0.009*** |
| SCORE high risk | (%) | 0.20 | 0.27 |
| CVD | (%) | ***0.48*** | ***< 0.007*** |
| CVD 10 year risk | (%) | ***0.51*** | ***< 0.004*** |
| CHD risk | (%) | ***0.51*** | ***< 0.004*** |
| Reynolds risk score | (%) | ***0.36*** | ***< 0.04*** |
| Framingham risk score | (%) | ***0.38*** | ***< 0.04*** |
| HAQ score | | - 0.13 | 0.48 |
| RA disease duration | (yrs) | 0.22 | 0.23 |
| DAS | | - 0.09 | 0.65 |
| Systolic BP | (mmHg) | 0.29 | 0.11 |
| Diastolic BP | (mmHg) | 0.05 | 0.78 |

*Heart rate

**Table 3.4 Univariate correlation analysis of S-SMase disease and cardiovascular endpoints in RA**

**Comparison of S-SMase activity**

| S-SMase levels | *P-value* | |
|---|---|---|
| Hyperchol. Hist. | ***< 0.02*** | * |
| Hypertension | 0.44 | {} |
| CVD death | 0.17 | § |
| CVD-RA | 0.17 | [] |
| CXR | 0.11 | $ |
| Extraarticular disease | 0.27 | € |
| Smoker status | ***< 0.05*** | @ |

* Presence Vs absence of hyperchol. hist. $p < 0.02$ (Mann-Whitney U test)
{} Hypertension, presence Vs absence
$ CXR, abnormalities Vs no abnormalities
€ Extraarticular disease, Presence Vs Absence (Mann-Whitney U test)
§ CVD death, Yes Vs No
[] CVD-RA, Yes Vs NO (Mann-Whitney U test)
@ Smoking status, Current smoker Vs Never smoked (one-way ANOVA)

**Table 3.5 Intra-group comparison of S-SMase in disease parameters in RA**

### 3.2.7 Confirmation of S-SMase activity using the Amplex Red SMase assay

Our data on the levels of S-SMase in inflammatory conditions suggest it might be a useful biomarker of disease. However, the assay we used is not well suited to high throughput assessment and so we thought it worthwhile to compare two other assays for S-SMase, which may be more suitable to the routine clinical laboratory.

S-SMase activity in clinical samples was calculated using non-linear regression analysis from standard curves **(Figures 2.2, 2.11)** and compared **(Figure 3.13a-c).** The TLC assay appeared to be more sensitive at detecting higher S-SMase levels **(Figure 3.13a)**. This purposefully composed cohort included healthy individuals and diseased patients with varying degrees of S-SMase activity. Both methods detected similarities in S-SMase activity in these patients. **Figure 3.13b** clearly shows the same trend of S-SMase activity in both assays used. Non-parametric correlation analysis using the Spearman rank coefficient suggested a positive relationship of S-SMase activity between the two methods ($r^2$=0.91, $p < 0.0001$) **(Figure 3.13c).** This confirmed the relationship trend seen in **figure 3.13b.** However, the TLC method has detected higher S-SMase levels in 70% of the patients examined. Clearly shown in **figure 3.13a-b**, the two methods appear to differ in their sensitivity. This may not be surprising since the simpler 1-step TLC method only relies on interaction of the enzyme with its substrate whereas the multi-step Amplex Red method depends on multiple enzymes and does not measure the cleaved substrate directly. In summary, this altered novel method of S-SMase detection was developed upon an existing commercially available kit (Molecular probes). We have shown that this is a sensitive, high throughput method that can accurately determine S-SMase activity in human plasma and is comparable to existing methods.

### 3.2.8 Confirming S-SMase activity by HPLC detection of fluorescent NBD-SM

Detecting ASM activity by high-performance liquid chromatography (HPLC) using radiolabelled SM substrates is established (He et al., 2003). We utilised this method to detect ASM activity using the NBD-SM previously utilised for the TLC method. Selected plasma from healthy controls, ANCA positive and ANCA negative inflammatory disease patients was used here. HPLC analysis was the third independent assay used to determine S-SMase activity in these selected patients **(Figure 3.13)**. As with the Amplex Red method, analyses of the same patient samples by HPLC produced the same trend of S-Smase activity similar to the previous two methodologies employed (TLC & Amplex Red) **(Figure 3.13d)** with healthy controls exhibiting low activity whilst diseased patients had raised S-SMase plasma levels. Both TLC and HPLC methods incorporate a fluorescent NBD-SM substrate and followed the same reaction procedure but the two assays differ in terms of the detection method used. The data here suggest that the HPLC method lacks the sensitivity of its TLC counterpart **(Figure 3.13e)** in similar fashion to the Amplex Red assay. The TLC assay was able to detect higher S-SMase levels in almost all (13 of 14) patients and in some cases this was > 2-fold higher **(Figure 3.13e).** Non-parametric correlation analysis revealed a positive relationship ($r^2 = 0.87$, $p < 0.002$) between the TLC and HPLC methods **(Figure 3.13f)** however; low activity samples may be prone to inadequate separation during this assay at least in comparison to the TLC method. In conclusion, the HPLC based assay is a fast and accurate method for the detection of S-SMase activity in clinical samples. It is less labour intensive than the TLC and Amplex red methods and is also semi-automated adding to its qualities as a routine laboratory technique.

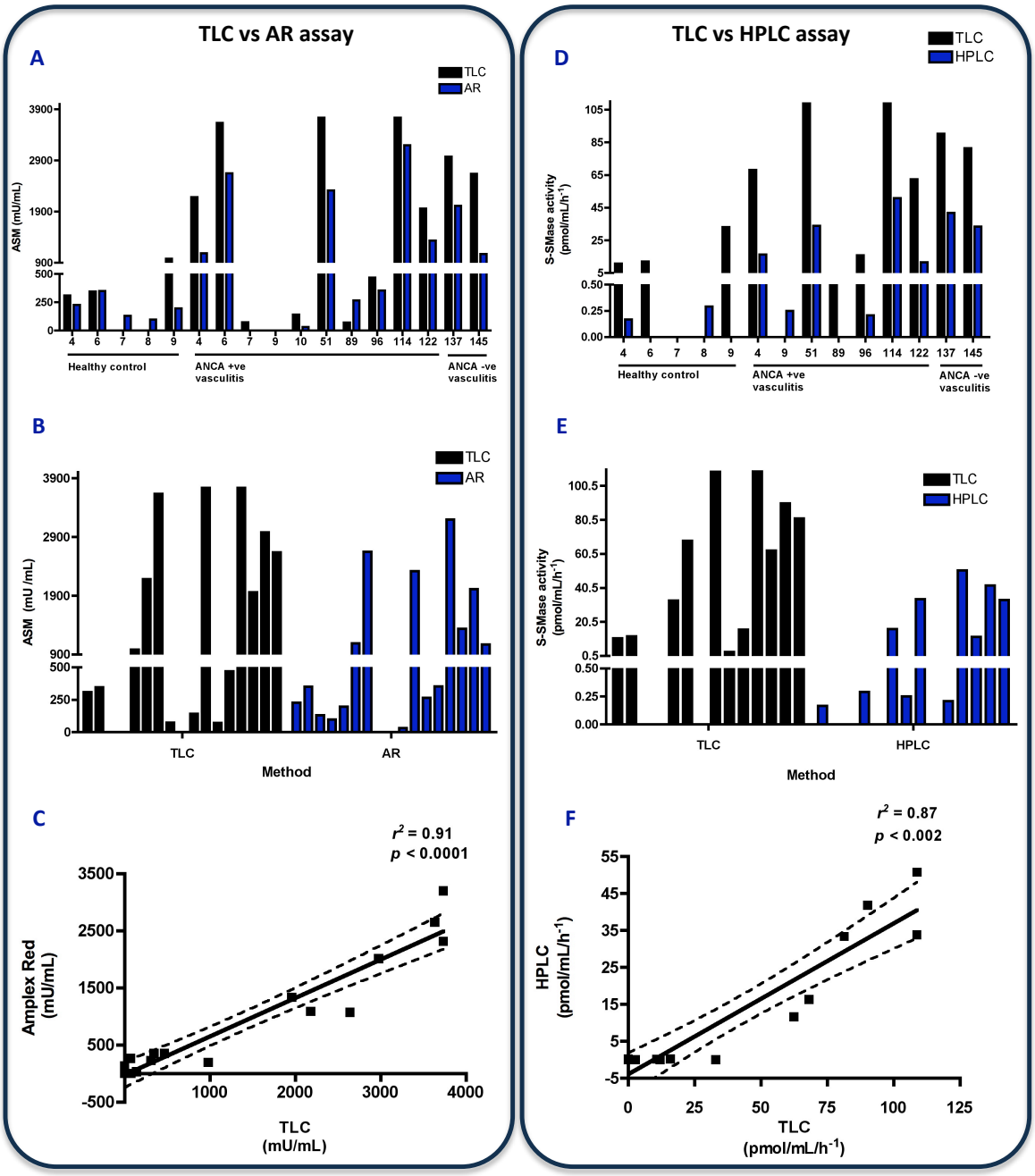


**Figure 3.13 Confirmation and comparison of patient S-SMase activity using two independent methods**

S-SMase activity in ANCA negative and positive patients, and healthy controls was assessed using the Amplex Red SMase activity assay **(Left panel).** Confirmation of S-SMase activity using NBD-SM substrate and fluorescence detected by HPLC **(Right panel)**. Both were compared against values estimated by the TLC activity assay for the same patients. The TLC assay is more sensitive than the Amplex Red assay and HPLC detection **(A+D)**. Both assays indicate the same trend of activity amongst the same panel of patient samples **(B+E).** The Amplex red assay and HPLC detection positively relate to the TLC assay **(C+F)**.

## 3.3 Summary of results

Our data concurs with other publications showing that active S-SMase is also found in healthy individuals (Doehner et al., 2007, Takahashi et al., 2002). However, we are the first to observe that increased S-SMase levels are present in chronic inflammatory immune diseases. This was first shown in plasma from renal vasculitis patients undergoing plasmapheresis **(3.2.1-2)** and then validated by assessing serum from two further independent AASV cohorts **(3.2.3-5).**

We also found that treatment in AASV led to a concurrent decrease in S-SMase activity in these patients when observing paired samples before and after treatment. This was then confirmed in an independent group of AASV patients that were at least 6 months in remission. To further characterise the role of S-SMase in rheumatic disease, a cohort of established RA patients was employed, analysis of which demonstrated that elevated S-SMase activity also extends to patients with RA. Three independent methods accurately confirmed S-SMase activity in a select group of disease patients and active controls.

## 3.4 Discussion

Chronic inflammatory diseases such as PSV and RA are associated with increased CVD, which drives higher mortality rates and decreased life expectancy compared to the healthy population (Gonzalez-Gay and Garcia-Porrua, 2002, Jacobsson et al., 1993, Jacobsson et al., 2005, Kremers et al., 2008). These diseases have been conclusively demonstrated to show a long-standing association with accelerated atherosclerosis and the initiating mechanisms that drive this process are not fully understood (Gonzalez-Gay et al., 2005a, Gonzalez-Gay et al., 2008, Mukhtyar et al., 2009, Ross, 1999, Shoenfeld et al., 2005, van Leuven et al., 2006). In this retrospective study, we investigated the presence and activity of S-SMase in two different diseases that feature primary (AASV) and secondary vascular inflammation (RA). The patient cohorts used here were from a hospital setting, the majority reflecting highly active clinical disease.

In recent years S-SMase has been linked with clinical disease (Gorska et al., 2003, Tilg and Moschen, 2008, Claus et al., 2005, Doehner et al., 2007, Takahashi et al., 2002, Sathishkumar et al., 2005), however, data herein provides a novel insight into S-SMase presence in autoimmune inflammatory diseases. It has been suggested that increasing age is associated with raised S-SMase activity levels (Doehner et al., 2007). Due to the small healthy control population it was not possible to age-match nor sex-match these patients rather, the cohorts were matched as a group, similar to that from other studies looking at CVD in RA (Kremers et al., 2008, Jacobsson et al., 2005) and observing S-SMase in disease (Doehner et al., 2007). Risk ratio for CVD in women with RA is higher compared to that of men (Gabriel et al., 2003), raising the need for individual sex-matching in our

study. Furthermore, endothelial function also differs between the sexes as women may have higher basal FMD (%) than men (Gonzalez-Gay et al., 2008) suggesting that women may respond differently to endothelial stress. The patients used in our study were collected retrospectively not allowing sex-matching. The healthy controls in our study were all of white ethnic background and the patients were of a demographic unknown to us, thus ethnic bias was not accounted for. Ethnic sub-grouping is also important in endothelial responses which may differ by race with Caucasians having larger FMD (%) values compared to African Americans (Campia et al., 2002) while also exhibiting higher prevalence of CV risk factors (Burt et al., 1995).

The AASV cohorts were composed of patients with WG, MPA and renal-limited vasculitis, however due to sample size we were not able to subgroup our analyses as was the case with the early RA patient cohort. To control for this using the AASV patients, a small longitudinal study using the same population of patients would allow more clear conclusions to be drawn on the involvement between disease subtypes. In addition to the above, several traditional risk factors predispose to CVD development including smoking status, diabetes mellitus, dyslipidemia and hypertension (Gonzalez-Gay et al., 2005a) while diabetes has already been linked with raised S-SMase levels (Gorska et al., 2003). We did not account for these backgrounds above nor were obesity and cardiac health considered.

Our data confirmed previous reports (Doehner et al., 2007, He et al., 2003, Takahashi et al., 2002) that even healthy individuals have active S-SMase in their circulation (20-300 pmol/mL/$h^{-1}$) (Doehner et al., 2007, Gorska et al., 2003). PSV patients

undergoing PEX exhibited raised S-SMase levels compared to healthy controls **(Figure 3.1)**. It therefore may be the case that PEX patients have higher levels of S-SMase than those stated in this study due to diluted plasma **(Figure 3.1).** Plasmapheresis is a stressful procedure that may lead to psychological and physiological stress. Accordingly, we examined serum from AASV patients. Patients with inactive disease and those in remission appeared to have lower S-SMase activity than those with active disease confirmed following induction of treatment (Week 14) and in early remission patients (>6 months) **(Figure 3.5).** This data suggests that the ongoing inflammatory process may indeed drive S-SMase activity levels.

EDV has been shown to improve following treatment in AASV (Raza et al., 2000) and we hypothesise that vascular inflammation induces endothelial S-SMase secretion to cause diffuse ECD. ANCA status does not appear to discriminate ECD in PSV (Filer et al., 2003). Thus, another systemic inflammatory mediator, not specific to vasculitis, may drive ECD. TNF$\alpha$ has been linked with ECD (Wang et al., 1994), and inhibition of TNF$\alpha$ has been shown to alleviate the inflammatory process improving vascular function in PSV and RA (Booth et al., 2004b, Raza et al., 2006, Hurlimann et al., 2002).

ECD in PSV can be seen in stable disease and during acute flares indicating a process not directly related to overt disease activity (Raza et al., 2000). Filer *et al.* (2003) demonstrated that EDV lacked any correlation with BVAS, CRP, VWf, VDI and disease duration in AASV, whilst there was no difference between active and remission patients' EDV ability according to BVAS. The lack of relationship between ECD and ANCA status may suggest that diffuse ECD is a transient process, not governed directly by inflammatory mediators rather, supporting a role for S-SMase. The lack of relationship between S-

SMase and disease parameters in the second serum AASV cohort **(Figure 3.6, Table 3.1)** is therefore not without reason. BVAS, ESR and CRP were decreased in these patients by week 14 indicating successful improvement of clinical disease and early remission **(Figure 3.7).** However, neither IL-1β, IFNγ or TNFα, all of which induce S-SMase release, fell significantly in these patients **(Figure 3.7)**. One of the caveats of small heterogeneous patient populations is the variation of treatment regimens**.** Not all patients were receiving Infliximab while in those who did, TNFα levels had not declined significantly by week 14 reasoning for the significant, yet modest decrease of S-SMase levels by week 14 **(Figure 3.7)**.

In PSV, CRP has been shown not to correlate with ECD (Filer et al., 2003) which is closely linked with TNFα levels (Wang et al., 1994) and may explain the lack of relationship between CRP and S-SMase in our AASV cohort **(Figure 3.6)**. As expected, anti-inflammatory cytokine IL-10 showed no relationship with S-SMase supporting the role of S-SMase as a possible specific inflammatory biomarker. Interestingly pro-inflammatory cytokines IL-6 and IL-8 also did not relate to S-SMase suggesting that only certain cytokines mediate its secretion. However, S-SMase related to IL-1ra levels in AASV which is present in inflammatory conditions regulating IL-1β. This lone correlation is intriguing without any support from other disease markers and may be an anomaly. To date there has been no evidence of a link between S-SMase and IL-1ra. BVAS did not correlate with S-SMase in AASV **(Figure 3.3, 3.6).** This was surprising since TNFα closely associates with disease activity (DAS 28) in RA at least (Petrovic-Rackov and Pejnovic, 2006). A decrease in TNFα is at least partially responsible for the induction of clinical remission (Booth et al., 2004a), an observation in our cohort reflected in the BVAS at week 14 in the AASV

patients **(Figure 3.7a)**. It could be argued that a correlation between S-SMase and BVAS arose through a decrease of TNFα that has been shown stimulate S-SMase secretion *in vivo* (Wong et al., 2000). However, secretion of S-SMase may be transient, not necessarily reflecting current disease activity.

The independence of S-SMase from established disease markers in AASV and RA is supported by the lack of relationship with blood lipids previously reported in CHF and diabetes patients (Doehner et al., 2007, Gorska et al., 2003). This is not surprising given the lack of dispersion of BVAS in PEX cohort 3 **(Figure 3.3a)**. The VDI scores accumulated vascular scarring measured at an inception point in time not reflecting active disease at presentation. Increased S-SMase activity may therefore relate to sub-clinical manifestations not evident following early remission. This may account for the differential correlations between S-SMase, VDI and the duration of follow-up.

The RA patients used in this chapter formed part of an extensive well-characterised cohort with documented vascular and CV parameters. Age is a CV risk factor in RA and non-RA individuals (Kremers et al., 2008). Despite a recent observation that S-SMase correlates with age, weight and BMI in CHF patients, this was not evident in our AASV or RA patient cohorts (Doehner et al., 2007). S-SMase is considered to play a role in atherogenesis through increased sub-endothelial LDL retention and MΦ foam cell formation and therefore may be an important CV risk factor (Tabas et al., 2007, Devlin et al., 2008). We found a strong correlation of S-SMase activity with plasma LDL in these patients in contrast to Gorska et al., (2003) in diabetes. This finding is supported by the

association of S-SMase with a constituent of LDL, ApoB and with triglyceride levels which are carried in LDL **(Figure 3.9).** To reduce this occurring by chance, there was no association found between S-SMase and HDL and ApoA **(Figure 3.9).** Homocysteine is an independent CV risk factor known to propagate LDL oxidation (Clarke et al., 1991) whilst raised levels of homocysteine are found in patients with RA (Hernanz et al., 1999). We found a positive relationship between S-SMase and homocysteine levels in RA patients **(Figure 3.10),** however, this analysis was performed using only 7 patients with data. Small sample size was also a problem when comparing cytokine levels in these patients **(Table 3.3)**. IL-6 is elevated in RA and atherosclerosis (Pasceri and Yeh, 1999), however the lack of patient IL-6 data (8 of 31) also did not allow us to accurately comment on the significance of its relationship with S-SMase ($p < 0.03$). Interestingly there was a positive correlation between S-SMase and Wcc in RA patients **(Figure 3.10),** which have long been associated with increased CV risk. This contrasts earlier observations of Wcc and leukocytes in AASV **(Table 3.1)** and the lack of S-SMase correlation with cytokine profiles does not lend much support to a cytokine-mediated association of Wcc with S-SMase. S-SMase activity did not correlate with disease duration or disease activity (DAS-28) in RA. This is not surprising given the lack of association between S-SMase and TNF$\alpha$ or CRP in AASV and RA as the secretion of S-SMase may be transient not reflecting clinical observations.

We hypothesise that the S-SMase product Cer may interfere with EC signalling. In line with this idea we found a positive association between S-SMase and pulse pressure (PP), a measure of arterial stiffness and vascular function. In addition, there was a strong correlation with PP x HR used to describe pulsatile stress**.** To support the above we found

a strong association of S-SMase levels with smoking in RA. These observations suggest a specific relationship of S-SMase with vessel stiffness and ECD. The lack of association with extraarticular disease may not be surprising as it uses a variety of vascular-specific parameters. Including in these calculations is the presence of lung fibrosis examined by chest X-ray in these patients, which also showed no association with S-SMase.

RA patients are at increased risk of CVD. We hypothesise that S-SMase is linked to the initiating stages of atherosclerosis. To this end, our data revealed strong associations of S-SMase with CV and cardiac risk parameters. Specifically S-SMase showed a positive correlation with CHD risk supporting data from Doehner et al., (2007). RA patients have an increased absolute 10-year risk of developing CVD (Kremers et al., 2008). The Framingham risk score takes into account the age, sex, total cholesterol level, HDL, diabetes, systemic BP and smoking status of an individual and predicts a variety of CV endpoints including generalised 10-year CVD risk predicted here. We also found a significant association of S-SMase with 10-year CVD risk ($p < 0.004$) (**Figure 3.12)**, which was calculated using the Framingham risk score and the Joint British Societies criteria from the guidelines on prevention of CVD. This was also confirmed using the Framingham risk score alone **(Figure 3.12).** The Reynolds risk score is a novel algorithm and recent alteration to the Framingham score that also takes into account CRP levels and parental CV history. The Reynolds score, which was first developed due to the lack of specific CVD risk algorithms for women, is considered more accurate than the Framingham risk score as the latter is believed to be more effective in the elderly (Ridker et al., 2008). Importantly we found a higher correlation between S-SMase and the Reynolds risk score than with using the Framingham algorithm **(Figure 3.12)**.

These data generated significant S-SMase correlations with four different CV parameters and a number of methods used in cardiology to calculate risk of cardiac events, which further decreases the chances of the above correlation occurring by chance. This study has revealed a possible link of S-SMase with increased CV risk and other traditional risk factors including blood lipids, smoking status, Wcc and aortic stiffness. Interestingly however we failed to find a correlation with any inducers of S-SMase secretion (CRP, TNF$\alpha$, IL-1$\beta$, IFN$\gamma$) in AASV and RA. Recent observations revealing a prolonged half-life of S-SMase, following blockade of transcriptional activation of *SMPD1* (Jenkins et al., 2010a), suggest that S-SMase activity may 'out-live' its inducers.

Probability assumes that in 20 statistical tests, if the null hypothesis is true at a level of significance of $p < 0.05$, we should expect to gain at least 1 significant outcome. Put simply the more tests one performs, the greater the chance of generating statistical significance in one of these tests by chance. This observation is a type I error and Bonferroni's correction (BC) aims to help prevent this occurring; it provides stringent and just control over the generation of false positives thus avoiding misinterpreting data as significant when in fact it is not. BC however, is a fairly conservative and contentious method and there are no criteria for its use even among statisticians (Perneger, 1998). In BC, adjustment of the p value depends on the total number of parameters or statistical tests performed. For example, where the level of significance ($\alpha$) is $p < 0.05$ and 10 univariate analyses are performed, the adjusted level of significance becomes $\alpha$ 0.05/10 = 0.005. When performed post-hoc, the level of significance is multiplied by the number of tests i.e. where the resulting $\alpha$ is 0.03, then 0.03 x 10 = 0.3 after BC (non-significant).

Bonferroni's correction is used often when large cohorts of parameters are compared (100's), for example in microarray analysis (Smith and Schuchman, 2008b).

Using BC may be considered by some to make data even more significant due to its stringent handling of $\alpha$, whereas this may not actually the case. In fact in reality it is thought to lead to publication bias with researchers not revealing non-significant results (Perneger, 1998, Nakagawa, 2004). Indeed BC is a good method of preventing type I errors but it also leaves a study open to type II errors (over-looking a statistical significance when it is true). Researchers may often appear to test as many parameters as possible. Subsequently statistical significance would be achieved by chance in one or more of those tests, without the parameters used necessarily forming part of the original hypothesis (Nakagawa, 2004). It is therefore important to select the parameters carefully.

In a set of 20 tests and at a level of significance $p < 0.05$, at least a single type I error (false positive) can be theoretically generated by virtue of probability. Table 3.3, composed largely of independent variables shows correlations in 7 out of 22 tests performed which suggests that BC is potentially inappropriate. Undoubtedly, corrections performed on this data set would lead to more of the correlations becoming non-significant. However, it then would not be possible to know which tests were truly significant in the first place. In this table (3.3), S-SMase strongly associates with LDL and the LDL:HDL ratio even after post-hoc BC ($p < 0.02$; $p < 0.05$ respectively; data not shown in results). Table 3.5 shows several measures of RA disease activity and CV risk algorithms. Although some of these parameters are related by sharing similar endpoints

(e.g. Framingham & Reynolds scores), others are independent from each other. In 14 comparisons, less than 1 false positive is expected while in reality 7 parameters correlated with S-SMase levels (**table 3.5)**. BC may have been beneficial when assessing the correlation between S-SMase and the various CV risk categories in table 3.5, however, such statistical adjustment could legitimately give rise to increased type II errors masking any true association of S-SMase with these algorithms. A particular example is the relationship of S-SMase with the CVD 10-year risk and CHD risk algorithms ($p = 0.056$ after BC, significant with 15% variation). Thus, although S-SMase appeared to significantly correlate with various CV risk algorithms without adjustment, these data must be interpreted with caution in light of the multiple parameters considered, at least in table 3.5.

The above underline the need for well-designed prospective studies with a breadth of clinical backgrounds and a causative link of S-SMase as a marker in ECD. Additional considerations for appropriate disease controls include the use of osteoarthritis (OA) patients and Behcet's disease patients, the latter exhibiting impaired vascular functions (Schmitz-Huebner and Knop, 1984, Chambers et al., 2001). Furthermore, given that ECD is considered an early event in atherosclerosis (Gonzalez-Gay et al., 2008) it would be interesting to distinguish S-SMase profiles in patients with early (<18 mo) versus established RA. Most CVD events involve large vessels such as the common carotid artery (CCA) (Shoenfeld et al., 2005, Del Rincon et al., 2003, Van Doornum et al., 2002). Although subclinical atherosclerosis has been recently reported in small vessel vasculitis (Chironi et al., 2007), this pathology is increasingly prevalent in large vessel vasculitides such as TAK

with characteristic common carotid. aortic and subclavian atherosclerotic plaques (Seyahi et al., 2006).

Understanding the role of SMases in disease offers considerable advantages in many pathophysiological conditions. Currently there is no routine test for measuring S-SMase activity from human blood. In the quest to develop a robust, easy-to-handle method to measure S-SMase in plasma or serum we altered a commercially available kit from Molecular Probes that relies on Amplex red oxidation. Data from patients used in the development of this assay was confirmed in another two independent assays (TLC, HPLC). Due to its multistep methodology it may lack the sensitivity of other assays while it is slightly more expensive. However, this method has a low requirement for biological material (10 μL/sample) and is safer than those involving radioisotope labeled substrates. The assay is reproducible, high-throughput, less labour intensive and can be performed in a routine clinical laboratory making it suitable for as a test for a novel biomarker in clinical disease.

In summary, chronic ECD in PSV and RA may share similar characteristics with the vascular endothelium becoming more susceptible to CV risk factors. We envisage a mechanism where the prevalent systemic inflammation in RA independently drives SMase and RA related processes which synergise alongside traditional risk factors. The lack of relationship between S-SMase and markers of disease in PSV may indicate that S-SMase is an independent marker of ECD and accelerated atherosclerosis. The findings in this pilot study provide ground to warrant further research behind the role of S-SMase in chronic inflammatory diseases.

# Chapter 4

# The regulation of ASM activation and secretion

# 4 Regulation of ASM activation and secretion

## 4.1 Introduction

The previous chapter described studies on the levels of active S-SMase in the blood in primary vasculitis and RA. S-SMase was raised in patients compared to healthy controls but the level decreased following treatment in AASV. In this chapter the regulation of S-SMase secretion and activation were investigated.

TNFα plays a critical role in the inflammatory response and has been shown to contribute to disease progression and severity in a wide range of conditions including RA, AASV and heart failure (Listing et al., 2008, Booth et al., 2004a, Booth et al., 2004b, Feldmann and Pusey, 2006). Inflammation has profound effects on the vascular system and is thought to be a major contributor to vascular damage in processes such as atherosclerosis (Hansson and Libby, 2006). Pro-inflammatory cytokines such as IL-1β and IFNγ have been shown to promote S-SMase release from isolated EC (Marathe et al., 1998). Whether TNFα induces the secretion of S-SMase remains unclear but evidence suggested a link *in vivo* (Wong et al., 2000). TNFα is thought to play a prominent role in regulating the production of other pro-inflammatory cytokines in clinical disease (Brennan et al., 1989). Given this primary role for TNFα we therefore wanted to ask whether TNFα directly regulates S-SMase release from human EC. This would be of particular significance to diseases that feature raised TNFα such as RA and PSV.

The regulation of SMase activation is complex. The SMase/Cer pathway is a complex web enzymatically governed by 4 genes (*SMPD1-4*) and 5 distinct phenotypes all of which have different localizations from the PM (Tani et al., 2007), ER and Golgi (nSMase) (Stoffel et al., 2007, Krut et al., 2006, Hofmann et al., 2000), endo-lysosomes (L-SMase) (Marathe et al., 1998) and a secretory fraction (S-SMase) (Schissel et al., 1996a, Tabas, 1999). All SMases are ubiquitously expressed at cellular level, however, much more S-SMase is found in MΦ and stromal cells with EC being by far the most abundant source (Marathe et al., 1998). SMase activity is differentially regulated between cell types. nSMase can be inhibited by GSH (Hofmann et al., 2000, Liu and Hannun, 1997, Krut et al., 2006) while several biological activators have been described in cardiac myocytes (CM), vascular smooth muscle cells (VSMC) and EC reviewed in Pavoine and Pecker (2009). Apart from pro-inflammatory cytokines, reactive oxygen species (ROS) are also increasingly considered to have a central role in ASMase regulation (Dumitru and Gulbins, 2006).

The presence of inflammation is accompanied by increases in oxidative stress with detrimental effects on the endothelium (Harrison, 1997) which, leads to decreased anti-oxidant capacity. ROS have been linked with regulating ASM activity (Scheel-Toellner et al., 2004, Grammatikos et al., 2007, Charruyer et al., 2005, Claus et al., 2005), possibly by molecular modification of the ASM carboxy-terminal (Qiu et al., 2003).

Glutathione (GSH) forms part of one of the most important antioxidant systems in mammalian cells and so it would be reasonable to hypothesise that increased oxidative

stress, may affect S-SMase activity in a process augmented by depleted GSH levels during inflammation. However, a direct effect of GSH cannot be excluded given its ability to interact with, and regulate the oxidation state of -SH groups like those found in ASMase. Given this, we sought to manipulate GSH levels and examine the differential activation of S-SMase from human EC.

In this chapter we developed a model to study native human EC-derived S-SMase. Here we tried to elucidate the importance of TNF$\alpha$ in S-SMase secretion from EC and examine a possible mechanism for S-SMase activation when exposed to *in situ* oxidative stress in EC.

## 4.2 Results

### 4.2.1 Development of the model

A model was developed to facilitate the detection of active S-SMase in cultured HUVEC media supernates and using this, one of the aims of this chapter was to establish whether TNFα could directly induce S-SMase release from human EC. The standard culture medium used for routine HUVEC growth is medium 199 (M199) (+FCS, 15% v/v) (2.2.1.1). Early experiments revealed high background levels of S-SMase in the culture medium (data not shown) and no significant difference between TNFα-treated (100 ng/mL) and un-treated control cells, confirmed by immunoblotting **(Appendices; Figure A1.1).** Thus components of M199 culture medium were examined for possible S-SMase activity. Human pooled serum did not demonstrate significant levels of S-SMase and neither did standard M199 alone and thus were not considered major sources of contamination (data not shown). However, FCS was found to be a rich source of the enzyme, in line with previous literature (Spence et al., 1989). Fully supplemented M199 showed high S-SMase levels while FCS (100%) appeared to have even greater S-SMase activity **(Figure 4.1a).** This linked to the level of activity seen in earlier experiments **(Appendices; figure A1)** as a 15% (v/v) solution of FCS diluted in M199 gave similar S-SMase activity to that found in untreated cells cultured in 15% FCS that could be titrated **(Appendix, Figure A1a-c)**. This activity was severely diminished in heat-inactivated FCS (HIFCS, 100%), whereas adjusting the HIFCS to the volume found in our culture medium (15% v/v) did not reveal any detectable S-SMase activity **(Figure 4.1b),** suggesting that heat-inactivating the serum abrogates enzymatic activity as expected.

#### *4.2.1.1 The role of HIFCS and medium 199 in the model*

Using HIFCS, HUVEC proliferation and viability was maintained. Experiments described here were designed to detect S-SMase in HUVEC media utilised HIFCS (15% v/v). HUVEC were seeded into 24-well plates and cultured in fully supplemented M199/HIFCS until confluent. Previous experiments from our group using T lymphocytes suggested that 10 and 100 ng/mL TNFα led to similar levels of ASM activation, thus to prevent TNFα being a rate limiting factor, 100ng/mL was chosen to provoke a significant HUVEC response which were incubated for 18 hours as per Marathe et al., (1998) and Schissel et al., (1998a).

Despite inactivating the S-SMase in FCS, no effect on HUVEC S-SMase secretion was observed following TNFα treatment **(Figure 4.1c)**. This contradicts earlier findings showing that pure HIFCS (100% v/v) had minimal activity and complete absence in diluted HIFCS (15% v/v) **(Figure 4.1b),** however the presence of this serum may induce S-SMase secretion. A high dose of TNFα (100 ng/mL) did not seem to induce greater S-SMase secretion from HUVEC compared to untreated cells while S-SMase in the medium appears to increase with time regardless of TNFα presence. This suggested that HUVEC secreted basal levels of S-SMase at least up to 24 hours in culture confirming a previous publication and agreeing with data in chapter 3 where healthy control individuals showed some S-SMase activity in their blood (Marathe et al., 1998).

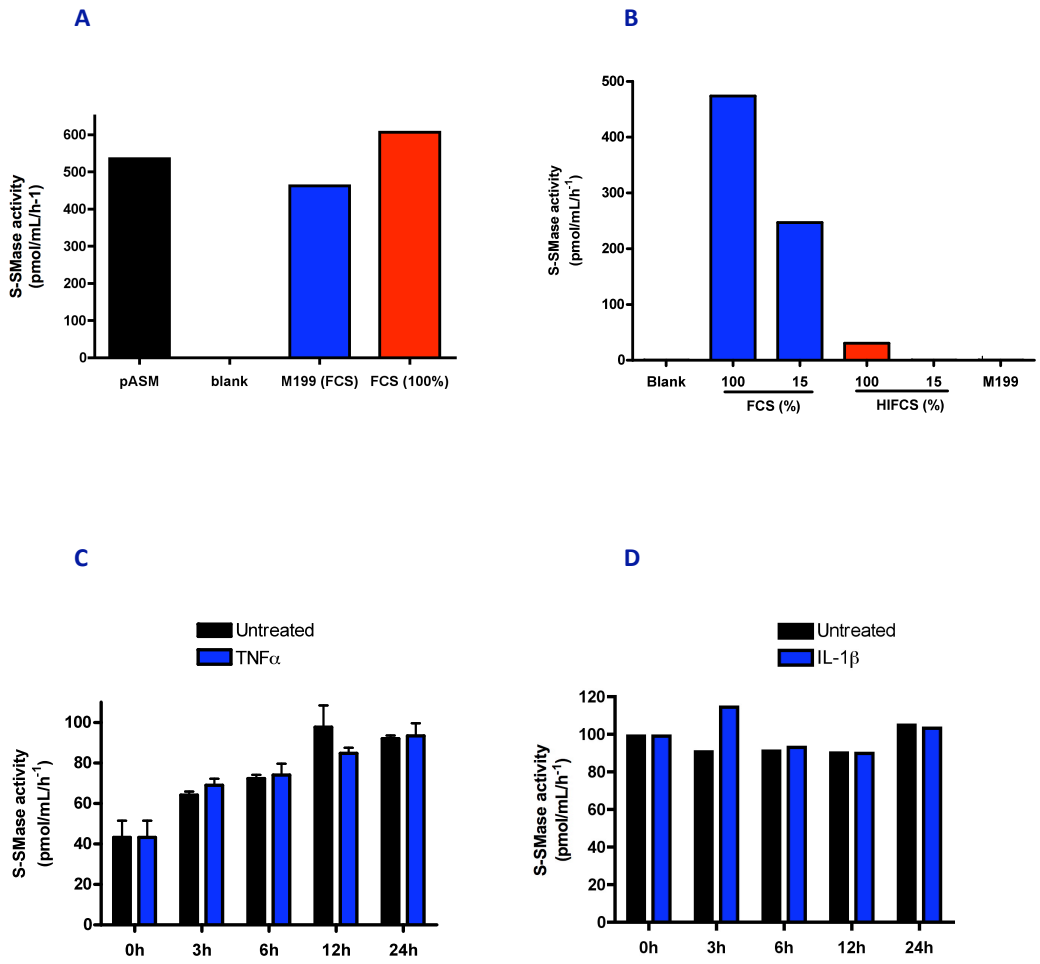


## Figure 4.1 Presence of serum obscures detection of HUVEC S-SMase in media supernates

S-SMase activity was measured in **(A)** fully supplemented M199 with FCS, 100% FCS. **(B)** S-SMase activity in FCS and HIFCS and serum-free M199. FCS and HIFCS (15% v/v) represents culture medium volume. **(C)** HUVEC were brought to confluence in 24-well plates and incubated with TNFα (100 ng/mL) and **(D)** IL-1β (5 ng/mL) for 18 hours in M199 supplemented with HIFCS (15% v/v). S-SMase activity was determined by the TLC activity assay. **(C)** represents means of two experiments ± SD. **(D)** represents values from one experiment.

#### *4.2.1.2 The role of serum-free Dulbecco's modified Eagle's Medium*

Earlier publications on secretion of SMase from EC *in vitro* utilised serum-free Dulbecco's Modified Eagle's Medium (DMEM) supplemented with 0.2% BSA (Marathe et al., 1998, Schissel et al., 1998a, Schissel et al., 1996a). The use of such medium posed a particular problem with regard to cell viability during prolonged incubations. We were not able to maintain HUVEC viability beyond 6 hours compared to that of 18 to 48 hours reported above. In our laboratory, the majority of HUVEC were not adherent by 6 hours, and so media were harvested between 0-6 hours in the first instance. We found that TNFα (100 ng/mL) here did not induce significant S-SMase release from HUVEC into the medium compared to untreated cells **(Figure 4.2a).** However, the excess cell death or stress due to starvation may have led to non-specific S-SMase release. Since IL-1β has been shown previously to induce S-SMase secretion (Marathe et al., 1998), it was employed as a positive control in further experiments. The culture times and conditions were also altered in an attempt to increase cell viability. HUVEC were treated in serum-free DMEM with TNFα (10 ng/mL), IL-1β (5 ng/mL) or PBS (v/v) for 0-180 minutes **(Figure 4.2b-c)**. Within this timeframe cell death was minimal according to morphology. We found highly variable responses to the cytokines, and non-significant differences between cytokine treated and untreated cells. This was likely to be due to the short exposure time to cytokines. Monitoring cell death was important since TNFα and L-SMase are associated with apoptosis. The experiments were not continued due to a change in experimental protocol and more were carried out using the finalised model (fig. 4.7 onwards). Accordingly, we looked to optimise culture conditions to further improve HUVEC viability in serum-free conditions using human endothelial serum-free medium (HESFM) (Gibco).

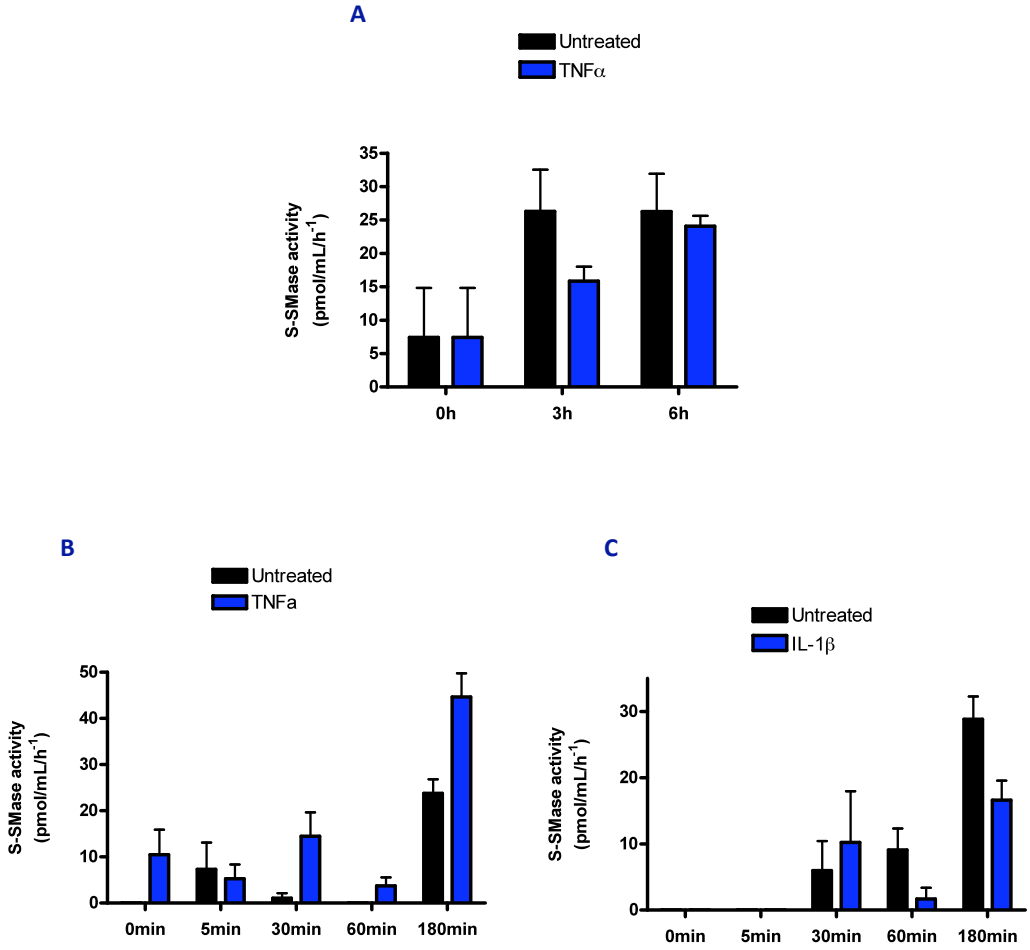


**Figure 4.2 The effect of serum-free DMEM on S-SMase secretion from HUVEC**

**(A)** HUVEC were brought to confluence in 24-well tissue culture plates using M199 with HIFCS. HUVEC were then treated with TNFα (100 ng/mL) for 3 or 6 hours in serum-free DMEM containing 0.2% BSA. Data represent mean values of two independent experiments ± SD. HUVEC were treated with **(B)** TNFα (10 ng/mL) and **(C)** IL-1β (5 ng/mL) in serum free DMEM containing 0.2% BSA. S-SMase activity was detected by the TLC activity assay. Data represent means and technical triplicates ± SD from one experiment.

#### *4.2.1.3 Optimising the model in serum-free culture conditions*

As mentioned above, DMEM alongside Roswell Park Memorial Institute (RPMI) have been the media of choice for the study of S-SMase secretion *in vitro* to date (Marathe et al., 1998, Schissel et al., 1998a, Schissel et al., 1996a, McCollister et al., 2007). We found limited cell growth and viability using serum-free M199 and DMEM media. Human endothelial serum-free medium (HESFM) was developed for long-term cultures and was recommended for sustained proliferation of HUVEC up to 15 passages. It was suggested to be as beneficial as using fully supplemented M199 with 20% FCS, bFGF and heparin.

Cell viability was therefore assessed by the MTS assay (Promega) (abbreviations list) over 18 hours. HUVEC were incubated with different media formulations for 18 hours in 96-well plates. DMEM with 0.2% BSA led to higher dead cell numbers while the addition of heat-inactivated foetal calf serum (HIFCS), endothelial cell growth factor (EGF) and heparin ameliorated this effect. HESFM, which included basal fibroblast growth factor (bFGF), was the best performing medium with the least dead cells **(Figure 4.3).** Serum-free conditions generally led to some decrease in HUVEC viability, however, the cells retained their natural morphology and hallmark cobblestone appearance. Although more than 3 experiments would allow for safer conclusions, the experiments in **figure 4.3** clarified that using DMEM used in these conditions led to increased cell death. **Figure 4.3** also confirmed that HESFM was suitable for use in this model due to the increased HUVEC viability and their ability to retain their natural morphology in HEFM when observed under light microscopy. HESFM was also chosen because it was purposefully developed for these culture conditions.

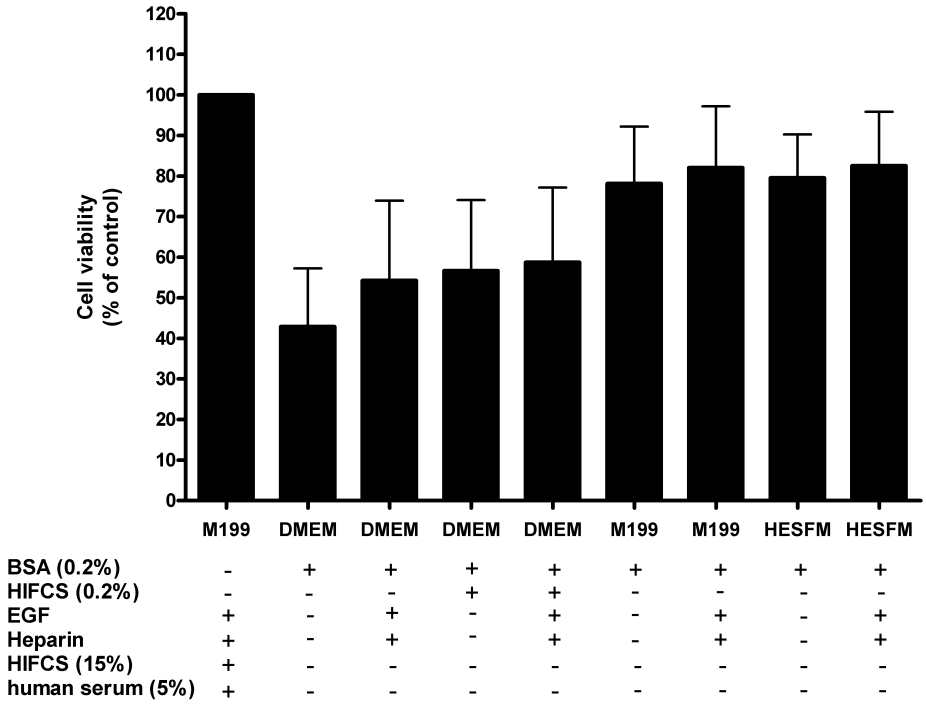


**Figure 4.3 Effect of different low serum media on HUVEC viability**

HUVEC were brought to confluence in 96-well tissue culture plates using fully supplemented M199. M199 was removed and replaced with the combinations above for 24 hours. Cell viability was determined by the MTS assay. Data are expressed as a percentage of control fully supplemented M199 treated cells. Data are mean ± SD from three independent experiments (n=3).

#### *4.2.1.4 The effect of TNFα on HUVEC viability in serum free conditions*

Serum deprivation and TNFα have been shown to induce EC apoptosis *in vitro* (Kwon et al., 2001, Zoellner et al., 1996). Thus HUVEC cytotoxic responses to TNFα were measured by the MTS assay.

##### 4.2.1.4.1 HUVEC morphology and viability is not affected by TNFα

Healthy viable HUVEC exhibit a smooth spindle-shaped outline under rigorous proliferation and a cobblestone appearance with larger nuclei upon confluence. HUVEC under distress or committed to apoptosis, however, are characterised as highly vesiculating cells, that undergo fragmentation and begin to shrink while at the same time lose physical contact with neighboring cells and underlying matrices. We found that HUVEC could usually remain adhered for up to 6 hours with M199 whilst this was not possible in DMEM, both without serum. Since loss of adhesion is an early event in EC apoptosis (Zoellner et al., 1996), viability should have been easily distinguishable by 18 hours. For comparison, **figure 4.4 (upper panel a-c)** illustrates HUVEC viability in serum-deprived conditions using M199, where in **(A)** HUVEC are healthy upon removal of serum, in **(B)** increasing detachment of cells (3 hours) leads to overt cell death in **(C)** by 12 hours. We found that increasing concentrations of TNFα (0-100 ng/mL) did not induce any morphological changes in HUVEC incubated in serum-free HESFM for 24 hours whilst $H_2O_2$ confirmed overall necrosis **(Figure 4.4, lower panel 1-6)**. Although serum-free conditions appeared to reduce HUVEC viability compared to cultures in fully supplemented M199, TNFα did not induce cell death in our system assessed by the MTS assay **(Figure 4.5)** contradicting previous findings (Xia et al., 2006).

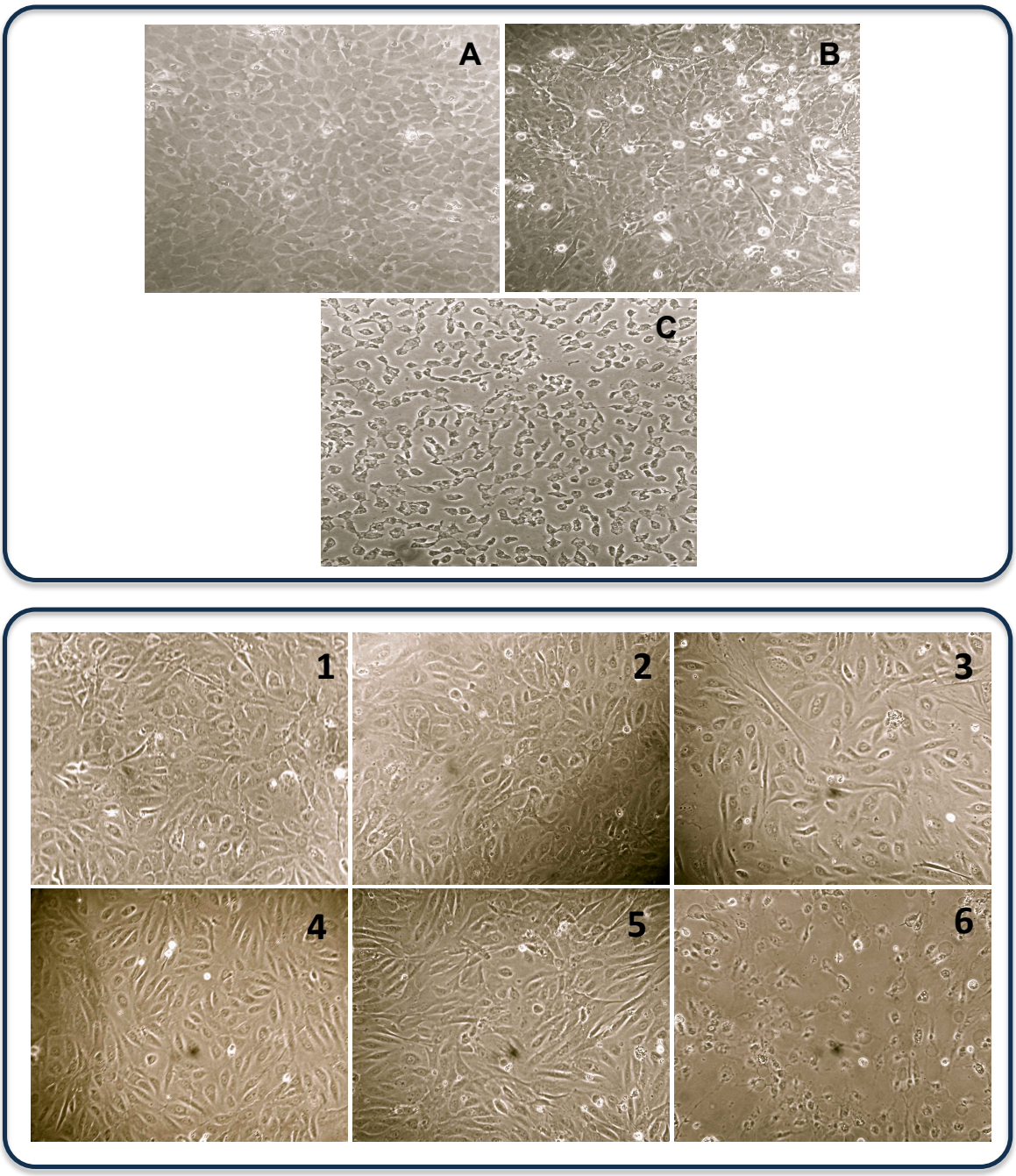


**Figure 4.4 TNFα does not affect HUVEC morphology**

**Upper panel,** HUVEC in 24-well tissue culture plates were grown to confluence in fully supplemented M199. Medium was replaced with serum-free M199 (A). Cells begin to detach by 3 hours (B) and continue by 12 hours (C). **Lower panel,** HUVEC were cultured in M199 until confluent, the medium replaced with serum-free HESFM for 24 hours containing **(1)** HESFM alone, **(2)** TNFα (0.1 ng/mL,) **(3)** TNFα (1 ng/mL), **(4)** TNFα (10 ng/mL), **(5)** TNFα (100 ng/mL), **(6)** $H_2O_2$ (1 mmol/L). Visualised at 10x magnification using a Carl Zeiss Tessar 2.8/5.6 lens.

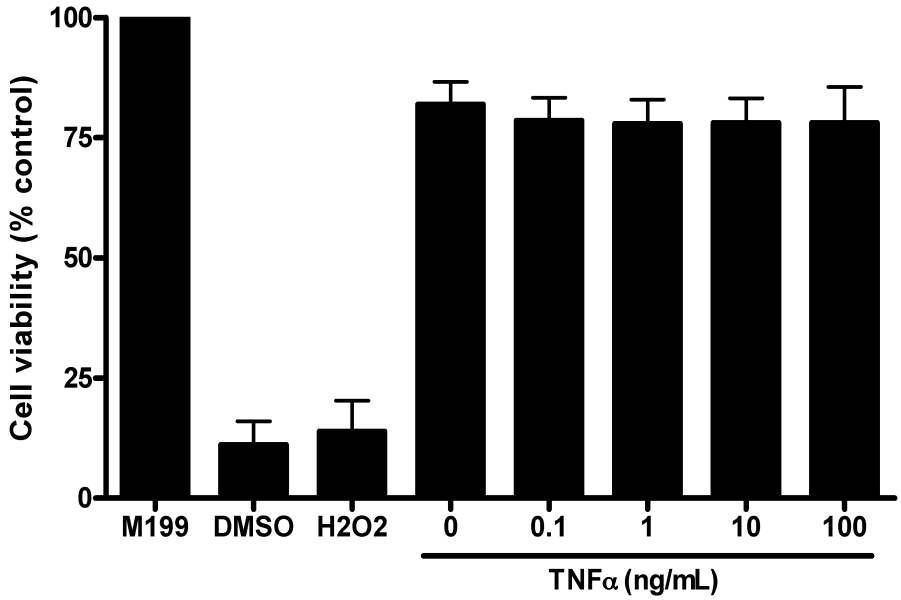


**Figure 4.5 TNFα does not affect HUVEC viability**

HUVEC were brought to confluence in 96-well tissue culture plates using fully supplemented M199. M199 was removed and replaced serum-free HESFM supplemented with either DMSO (10% v/v), $H_2O_2$ (1 mmol/L) or varying concentrations of TNFα for 18 hours. Cell viability was determined by the MTS assay. Data are expressed as a percentage of control fully supplemented M199 cultured cells. Data are mean ± SD from five independent experiments (n=5).

#### 4.2.1.4.2 The effect of TNFα on HUVEC apoptosis determined by $DiOC_6$ retention

TNFα-induced apoptosis has been associated with the SM/Cer pathway (Krown et al., 1996, Haimovitz-Friedman et al., 1997). Our data so far illustrate that TNFα did not lead to morphological changes or decrease cell viability. A hallmark of apoptosis is mitochondrial membrane depolarization. To ensure there was no effect of TNFα in prolonged culture, we observed the mitochondrial membrane potential of HUVEC treated with TNFα. Viable cells uptake 3,3'-dihexyloxacarbocyanine iodide ($DiOC_6$) dye and are able to retain it in intact mitochondria called $DiOC_6^{high}$. In apoptotic cells the dye is bleached from the mitochondria and are thus called $DiOC_6^{low}$. This is a method positively comparable to Annexin-V staining of externalised phosphatidylserine residues on apoptotic mitochondria (Ozgen et al., 2000). To minimise the effect of handling adherent cells on the assay outcome we found that trypsinisation could interfere with dye loading (9-19% $DiOC_6^{low}$) thus harvesting the cells prior to $DiOC_6$ loading ensured greater dye retention (95%) **(Appendix Figure A2a).** HUVEC were therefore treated as in 2.2.7, page 84. Approximately 13.6% of untreated cells were $DiOC_6^{low}$ while both DMSO (10%) and CHX/TNFα (10 μM/100 ng/mL) led to a 2-fold increase in apoptosis compared to untreated/solvent control. Furthermore, cycloheximide (CHX) and TNFα co-treatment showed a 1.7-2.1-fold increase in apoptosis compared to TNFα alone treated HUVEC **(Figure 4.6; (Appendix Figure A2b).** CHX pre-treatment may have enhanced apoptosis in CHX/TNFα treatments. The percentage of TNFα–alone treated HUVEC apoptosis did not significantly vary compared to untreated cells suggesting that TNFα did not induce significant apoptosis in HUVEC based on our model.

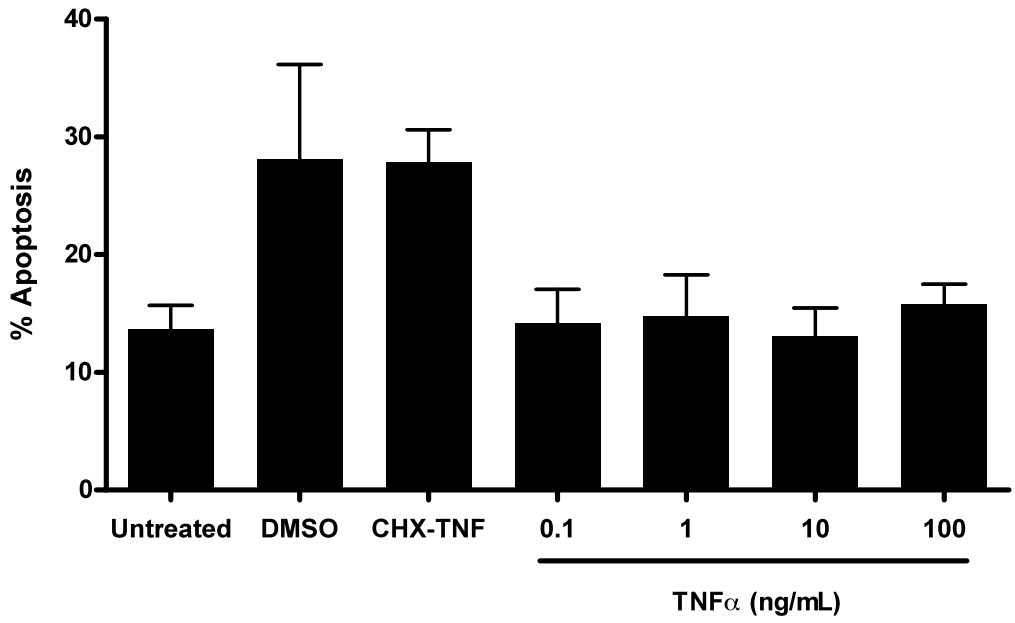


**Figure 4.6 TNFα does not induce HUVEC apoptosis**

HUVEC were brought to confluence in 24-well tissue culture plates in M199. The media were removed, the cells washed twice with HBSS-$Ca^{2+}$ and incubated with untreated serum-free HESFM (0 ng/mL TNFα), HESFM containing DMSO (10% v/v), HESFM containing CHX/TNFα (10 μM/100 ng/mL) or varying concentrations of TNFα alone. Apoptosis was assessed by $DiOC_6$ retention. Data represents the mean values ± SD of five independent experiments (n=5).

### 4.2.2 Using the model to observe cytokine regulation of S-SMase secretion

#### *4.2.2.1 Detecting S-SMase in human endothelial serum free medium*

HUVEC responded well in culture to HESFM and their viability did not appear to be affected even by 36 hours (data not shown). With this in mind HUVEC cultured in 24-well plates were treated with TNFα (10 ng/mL), IL-1β (5 ng/mL) or solvent control (PBS) for 18 hours in serum-free HESFM (2.2.1.1a) as performed in (Marathe et al., 1998). We found a non-significant increase of S-SMase levels in HUVEC treated with TNFα (20.96 ± 18.52 pmol/mL/$h^{-1}$) and IL-1β compared with untreated control HUVEC (5.76 ± 8.38 pmol/mL/$h^{-1}$) **(Figure 4.7).** These data indicated that TNFα and IL-1β either provoked a weak HUVEC response or only a small fraction of S-SMase was captured and assayed from each sample of medium because it was too dilute. Sampling could be improved by using smaller volumes of media or concentrating the media itself.

#### *4.2.2.2 TNFα directly induces S-SMase secretion from human endothelial cells*

To improve the sensitivity of the assay we increased the cell material and concentrated the media supernates and thus the S-SMase. Rather than using 24-well plates with 1-1.5x$10^5$ HUVEC when confluent, 75$cm^2$ tissue culture flasks were used (6-8x$10^6$ HUVEC). The supernates were then concentrated 20-fold from a 10 mL/sample to a final 0.5 mL/sample; an overall 25-fold concentration factor between samples from 75$cm^2$ culture flasks compared to those from 24-well plates (2.2.8.4; Tables 2.4-5). This enhanced the sensitivity of the assay and allowed greater differentiation between samples **(Figure 4.8a)**. Comparatively, concentrating the supernates increased S-SMase activity in untreated, TNFα and IL-1β treated samples by 4.5, 5.1 and 4.6-fold respectively **(Figure**

**4.8c)** and **figure 4.8b** depicts this. Importantly, concentrating supernates led to decreased variation ratio due to the improved sampling **(Figure 4.8c)**. Each sample was then normalised for protein content **(Figure 4.8d).** This confirmed that TNFα directly (10 ng/mL) could lead to an increase in S-SMase activity compared to un-treated HUVEC ($p < 0.01$) **(Figure 4.8a-d).** Similarly, IL-1β also induced significantly higher S-SMase secretion compared to untreated controls ($p < 0.05$). The data in **figure 4.8d** also hints that TNFα may be a more potent inducer of S-SMase than IL-1β in HUVEC, although this was not significant. To our knowledge, these data were the first to suggest that TNFα could directly induce S-SMase secretion from human primary EC.

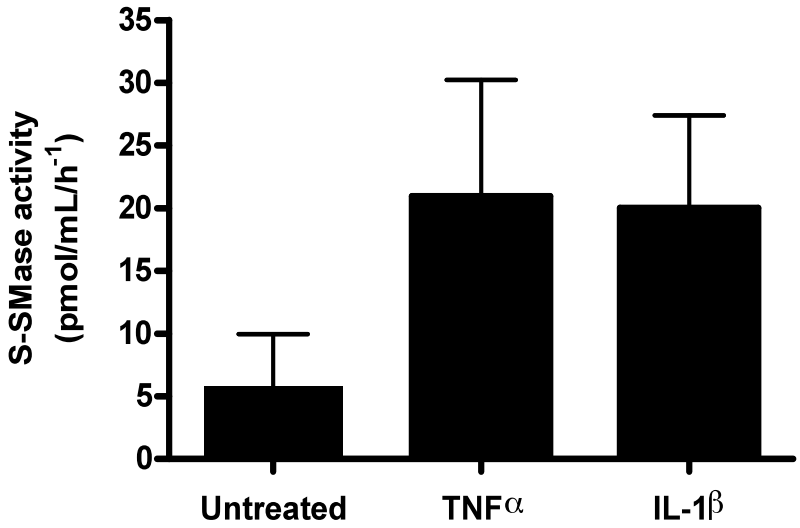


**Figure 4.7 TNFα and IL-1β induce S-SMase secretion from HUVEC *in vitro***

HUVEC were brought to confluence in 24-well tissue culture plates in fully supplemented M199. The medium was removed and the cells washed twice with HBSS-$Ca^{2+}$. Medium was replaced with fresh serum-free HESFM supplemented with TNFα (10 ng/mL) or IL-1β (5 ng/mL) for 18 hours. S-SMase activity from un-concentrated media was assessed by the TLC activity assay. Data represent mean values of four independent experiments ± SD (n=4).

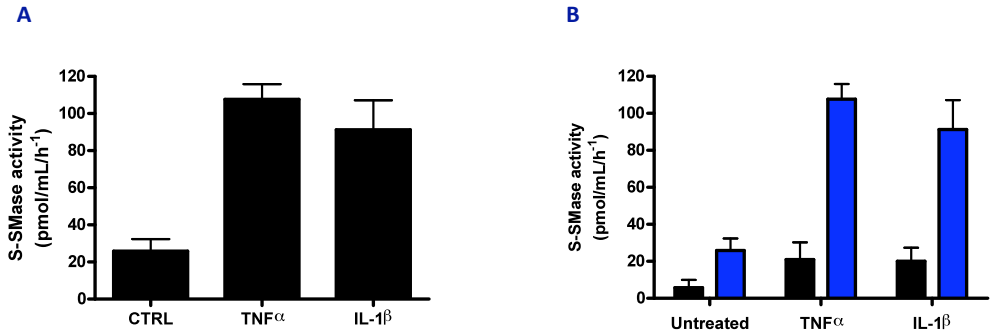


C

| | S-SMase activity (pmol/mL/h$^{-1}$) | | | | | |
|---|---|---|---|---|---|---|
| | Untreated UC | TNFα UC | IL-1β UC | Untreated C | TNFα C | IL-1β C |
| Mean | 5.8 | 21.0 | 20.0 | 25.9 | 107.7 | 91.3 |
| Std. Deviation | 8.4 | 18.5 | 12.8 | 11.3 | 14.2 | 27.5 |
| Std. Error | 4.2 | 9.3 | 7.4 | 6.5 | 8.2 | 15.9 |

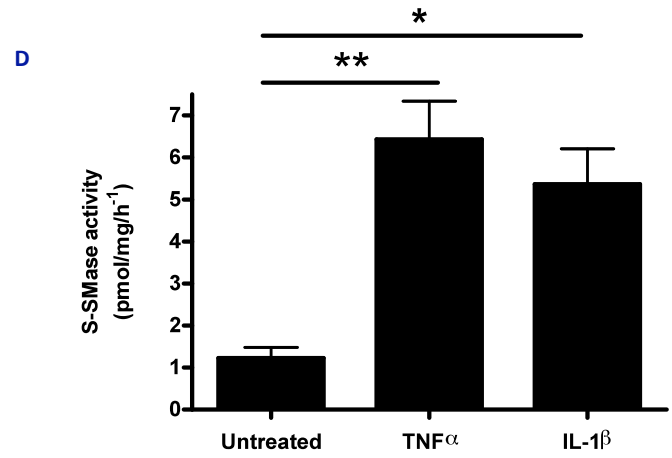


**Figure 4.8 S-SMase levels in concentrated HUVEC media supernates**

Concentrated serum-free HESFM from 18 hour TNFα (10 ng/mL) or IL-1β (5 ng/mL) treated HUVEC in 75 cm$^2$ tissue culture flasks. S-SMase activity was assessed by the TLC assay. **(A)** S-SMase activity from concentrated HUVEC media not normalised to protein and compared to S-SMase activity from un-concentrated media **(B). (A)** represents values from 3 independent experiments, **(B)** represents values from 4 independent experiments. **(C)** Tabular comparison of S-SMase activity variation between S-SMase activity from concentrated (C) and un-concentrated (UC) media supernates. **(D)** Data represent mean values of three independents experiments (n=5) ± S.D.* $P < 0.05$; ** $p < 0.01$ determined by Kruskal Wallis ANOVA.

#### *4.2.2.3 Chronic TNFα treatment leads to S-SMase secretion from HUVEC*

The *SMPD1* products L-SMase and S-SMase can be differentiated according to their cellular trafficking. L-SMase is mannose-6-phosphorylated (M6P) and shuttled within lysosomes whereas conversely S-SMase is believed to follow the Golgi secretory pathway. Interestingly the two products appear to be simultaneously regulated by pro-inflammatory cytokines (Marathe et al., 1998). To date, the precise mechanism and timing of S-SMase trafficking remain unclear, although *in vivo* evidence has shown this to occur within 3 hours (Haimovitz-Friedman et al., 1997, Wong et al., 2000).

Due to the increased requirement for cell material, HUVEC were brought to confluence in 25 $cm^2$ rather than 75 $cm^2$ culture flasks and treated as described previously in HESFM (2.2.1.1), and media supernatants were concentrated 20-fold (2.2.8.4; Tables 2.4-5). HUVEC TNFα-induced (10 ng/mL) S-SMase secretion was assessed at 0.5, 3, 6, 12 and 24 hours. As shown in **figure 4.9,** spontaneous secretion of S-SMase occurs within 0.5 hours, however, this basal secretion clearly varies. TNFα led to a sharp rise in S-SMase secretion between 12-24 hours **(Figure 4.9)**. This raises the question as to whether the excess S-SMase originates from intracellular pools, transcriptional activation of *SMPD1* or release of plasma membrane-associated ASM. To eliminate this observation as an *in vitro* artifact employment of LPS and other cytokine cocktails would support a synergistic effect for S-SMase regulation by pro-inflammatory mediators. S-SMase is Zn-dependent thus removal of Zn from the assay would help ascertain its identity compared to L-SMase.

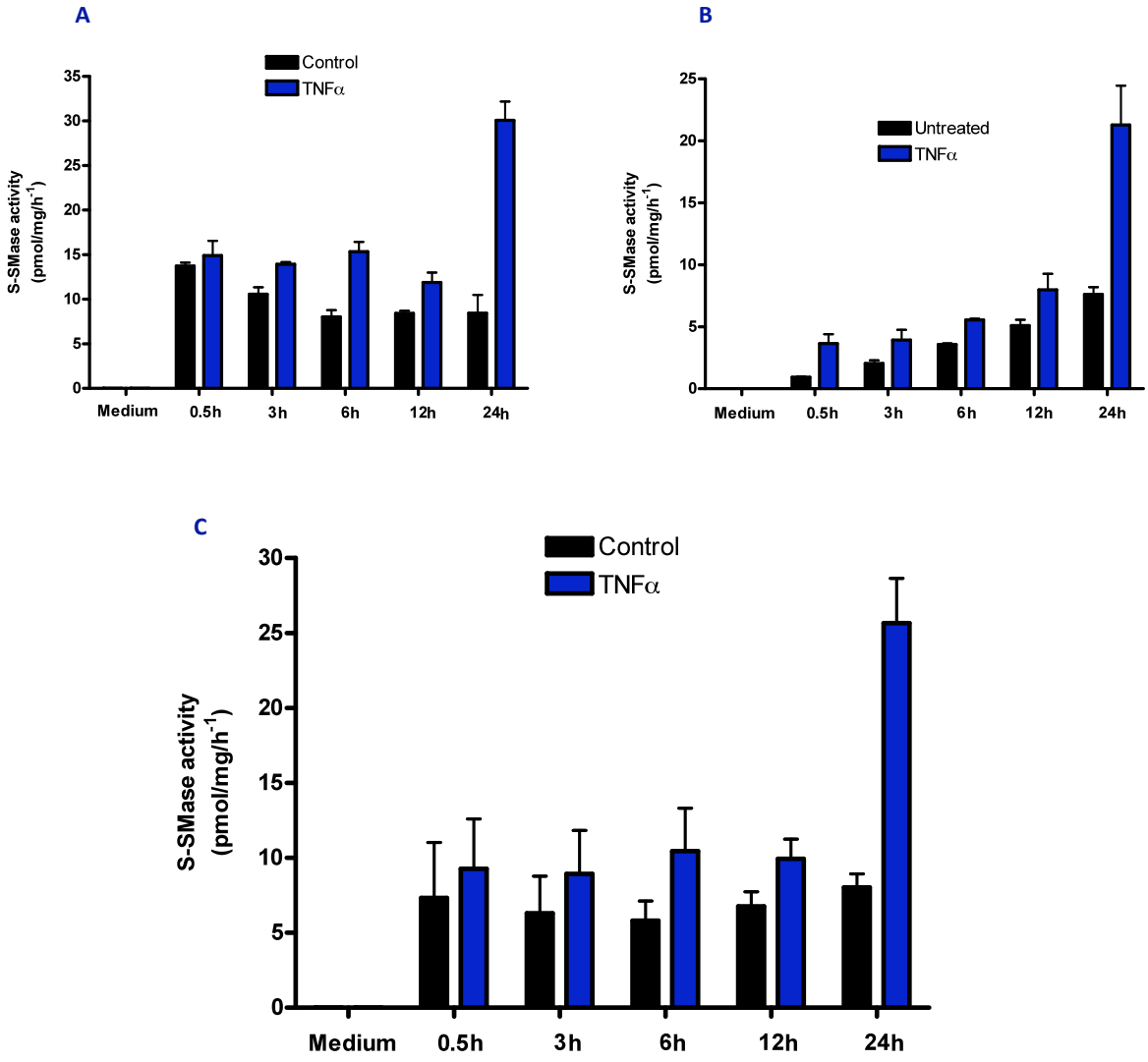


**Figure 4.9 Chronic and not acute exposure to TNFα induces secretion of active S-SMase**

HUVEC were grown to confluence in 25 $cm^2$ tissue culture flasks in M199, the medium removed, the cells washed with HBSS-$Ca^{2+}$ and replaced with serum-free HESFM supplemented with TNFα (10 ng/mL) for the 0.5, 3, 6, 12, and 24 hours. TNFα treated HUVEC medium (Blue bars) was compared to control (black bars). HUVEC media were concentrated and S-SMase activity was assessed by the TLC assay. Data in **(A)** represents experiment 1, data in **(B)** represents experiment 2, data in **(C)** represent mean values from the two independent experiments in **(A)** and **(B)** ± S.D.

#### *4.2.2.4 The action of TNFα can be blocked through antibody-mediated inhibition*

In order to further establish the regulatory role of TNFα mediated S-SMase secretion we examined the effect of TNFα-blockade using the chimeric monoclonal anti-TNFα antibody infliximab (Remicade). Infliximab is now an established treatment regime for a variety of diseases including RA (Feldmann and Pusey, 2006) and a promising avenue for vasculitis (Booth et al., 2004a). Infliximab is able to neutralise TNFα by binding to the soluble form of the cytokine and preventing it from interacting with its target receptors TNFR1 and TNFR2 on EC.

As shown in **figure 4.10,** infliximab was able to completely block the effect of TNFα on HUVEC S-SMase release. Furthermore, infliximab appears to decrease basal levels of S-SMase secretion however, the mechanism by which this might occur is unknown. This suggests that TNFα does indeed directly induce the secretion of S-SMase from human primary EC. These data would benefit from the observation of infliximab incubation with other known inducers of S-SMase secretion such as IL-1β to clarify the specificity of TNFα inhibition on S-SMase secretion.

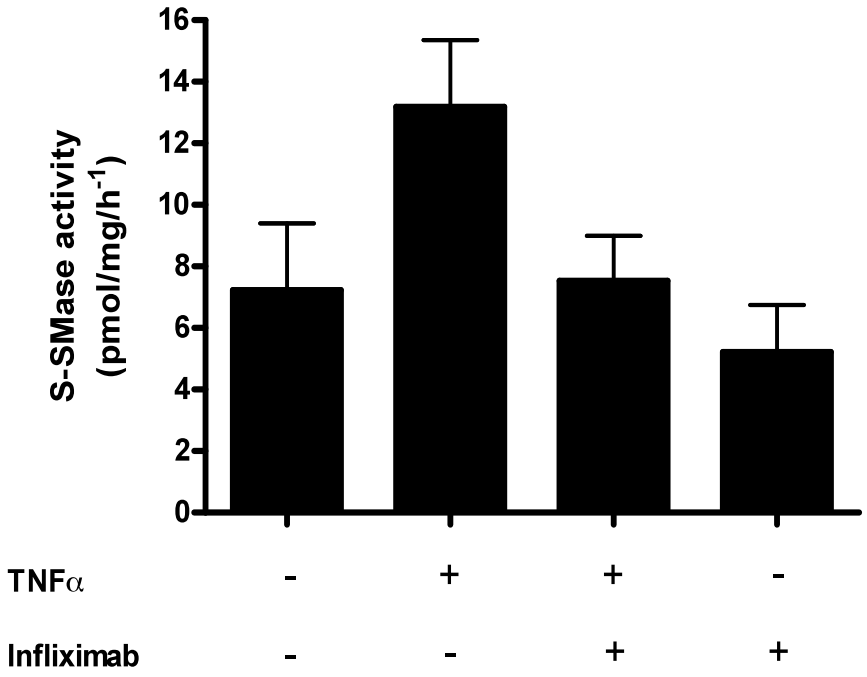


**Figure 4.10 Anti-TNFα antibody infliximab blocks TNFα-induced S-SMase secretion**

HUVEC were grown to confluence in 75 $cm^2$ tissue culture flasks in M199, the medium removed, the cells washed with HBSS-$Ca^{2+}$ and replaced with serum-free HESFM supplemented with TNFα (10 ng/mL), TNFα and 2 μg infliximab antibody or 2 μg infliximab antibody alone and incubated for 18 hours. HUVEC media were concentrated and S-SMase activity was assessed by the TLC activity assay. Data represent mean values from two independent experiments ± SD (n=2).

#### *4.2.2.5 IL-6 does not lead to S-SMase secretion*

LPS and pro-inflammatory cytokines have been shown to induce S-SMase secretion *in vitro* and *in vivo* (Marathe et al., 1998, Wong et al., 2000). IL-6 is a pro-inflammatory cytokine with an important role in RA pathogenesis propagating acute phase responses and T and B cell proliferation. Recently the IL-6 receptor antagonist, Tocilizumab, a humanised monoclonal antibody was licensed for use in the treatment of RA. LPS has been shown to increase TNF$\alpha$ levels while LPS-induced S-SMase secretion is suggested to be mediated by IL-1 production *in vivo* (Wong et al., 2000). This underlines the importance of cytokine involvement in S-SMase secretion. **Figure 4.11** clearly shows that IL-6 does not induce S-SMase secretion from HUVEC suggesting that regulation of S-SMase is confined only to certain pro-inflammatory mediators.

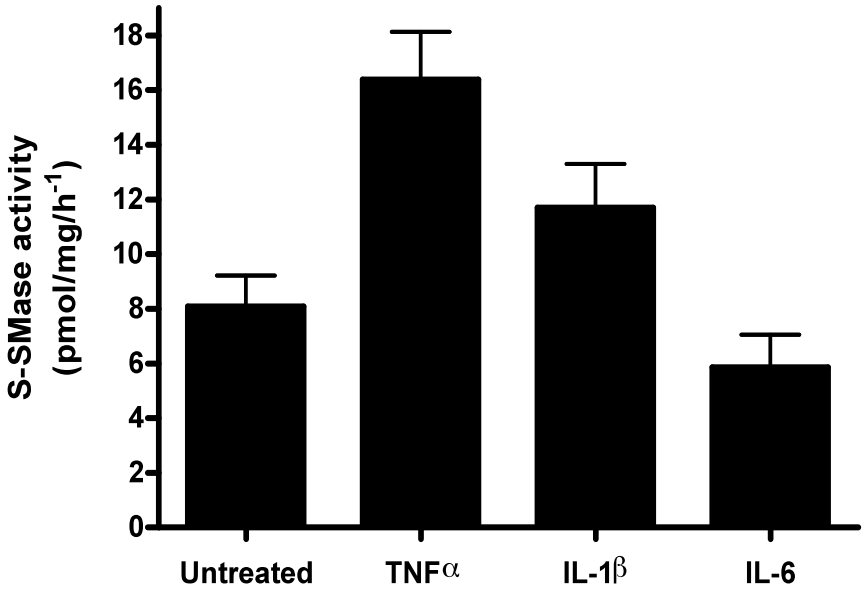


**Figure 4.11 IL-6 does not induce secretion of active S-SMase from HUVEC**

HUVEC were grown to confluence in 75 $cm^2$ tissue culture flasks in M199, the medium removed, the cells washed with HBSS-$Ca^{2+}$ and replaced with serum-free HESFM supplemented with TNFα (10 ng/mL), IL-1β (5 ng/mL) or IL-6 (5 ng/mL) for 18 hours. HUVEC media were concentrated and S-SMase activity was assessed by the TLC assay. Data represent mean values from two independent experiments ± SD (n=2).

### 4.2.3 Using the model to predict redox manipulation of S-SMase activity

ROS were first proposed to alter ASM activity by oxidative switching of C-terminal cysteine residues, specifically $Cys^{629}$ (Qiu et al., 2003) later shown using UV-C light-induced ROS in U937 cells (Charruyer et al., 2005) and TNF-related apoptosis-inducing ligand (TRAIL) stimulation which could be inhibited by GSH precursor *N*-acetylcysteine (NAC) (Dumitru and Gulbins, 2006). Oxidative stress is evident during inflammation in diseases such as CHF and RA (Kamanli et al., 2004, Sarban et al., 2005, Anker et al., 1998, Castro et al., 2002). Previous research from our laboratory found glutathione (GSH) to be decreased in RA synovial fluid, serum and peripheral $CD4^+$ T cells compared to healthy controls. Thus elevated ROS due to depleted antioxidant capacity may affect the redox-sensitive S-SMase. The studies detailed above concentrated on L-SMase and to our knowledge, no one had examined the effects of redox manipulation on native, EC-derived S-SMase enzyme activity.

#### *4.2.3.1 Manipulating redox-sensitive amino acid residues regulates S-SMase activity*

We have obtained the most physiologically relevant S-SMase and placed it under a redox environment to examine its susceptibility to chemical changes *in vitro* (4.2.3.1-2). Stock S-SMase activity was confirmed using the TLC-based assay. A 10-fold lower concentration of dithiothreitol (DTT) than previously published (Qiu et al., 2003) was used to study the reduction potential S-SMase. As shown with recombinant human ASM (rhASM), treatment of isolated EC-derived S-SMase with DTT (10 mmol/L) completely abolishes any detectable enzymatic activity **(Figure 4.12)** suggesting that the enzyme is directly susceptible to chemical reduction. Due to limited S-SMase sample, this proof of

concept experiment was carried out once and was designed to see whether S-SMase activity could be suppressed by chemical reduction. More experiments were subsequently carried out using a range of DTT and hydrogen peroxide ($H_2O_2$) **(figure 4.13).**

Accordingly, to see whether S-SMase activity could be rescued, S-SMase was incubated with DTT followed by hydrogen peroxide $H_2O_2$ (2.2.9). DTT was titrated (0.1-10 mmol/L) and $H_2O_2$ (1 mmol/L) was used to re-oxidise the enzyme **(Figure 4.13a)**. We confirmed that DTT could decrease S-SMase activity in a dose-dependent manner while $H_2O_2$ was able to re-oxidise S-SMase increasing its activity, albeit modestly **(Figure 4.13a)**. This data suggests that S-SMase could be partially rescued following excess chemical reduction (DTT, >1 mmol/L) despite using a strong free radical generator. Catalase, added to each reaction to neutralise the $H_2O_2$ was itself not found to affect S-SMase activity.

To induce a partial reduction of S-SMase, a constant concentration of DTT (0.5 mmol/L) was added to a reaction, allowing scope for re-oxidation with reasonable levels of $H_2O_2$ (0.1, 1 mmol/L), preventing enzyme damage **(Figure 4.13b)**. We found that increasing concentrations of $H_2O_2$ may partially re-oxidise the previously reduced S-SMase. These data suggest the enzyme is secreted in an activated form, can be chemically reduced using DTT and may regain its activity through re-oxidation using $H_2O_2$. Due to the lack of protein availability (S-SMase from media culture supernates) for further experiments, more work would be required to supplement this data and better characterise S-SMase here. This was followed by experiments that assessed S-SMase activity in response to intracellular redox changes (section 4.2.3.2).

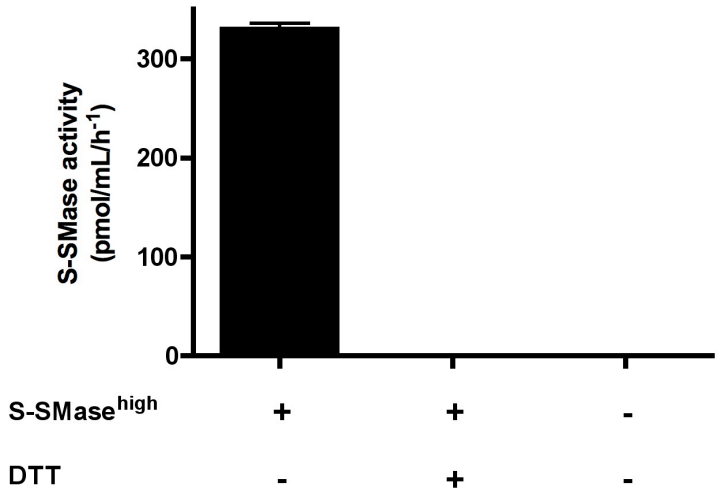


**Figure 4.12 Chemical reduction with DTT decreases S-SMase activity**

HUVEC were grown to confluence in 175 $cm^2$ tissue culture flasks in fully supplemented M199, the medium removed, cells washed with HBSS-$Ca^{2+}$ and replaced with serum-free HESFM supplemented with TNF$\alpha$ (10 ng/mL) for 18 hours. The medium was removed and concentrated. The S-$SMase^{high}$ medium was subjected to DTT (10 mmol/L) for 15 minutes at $37^0$C followed. Each aliquot was assessed for S-SMase activity by the TLC activity assay. Values are representative of one experiment (n=1).

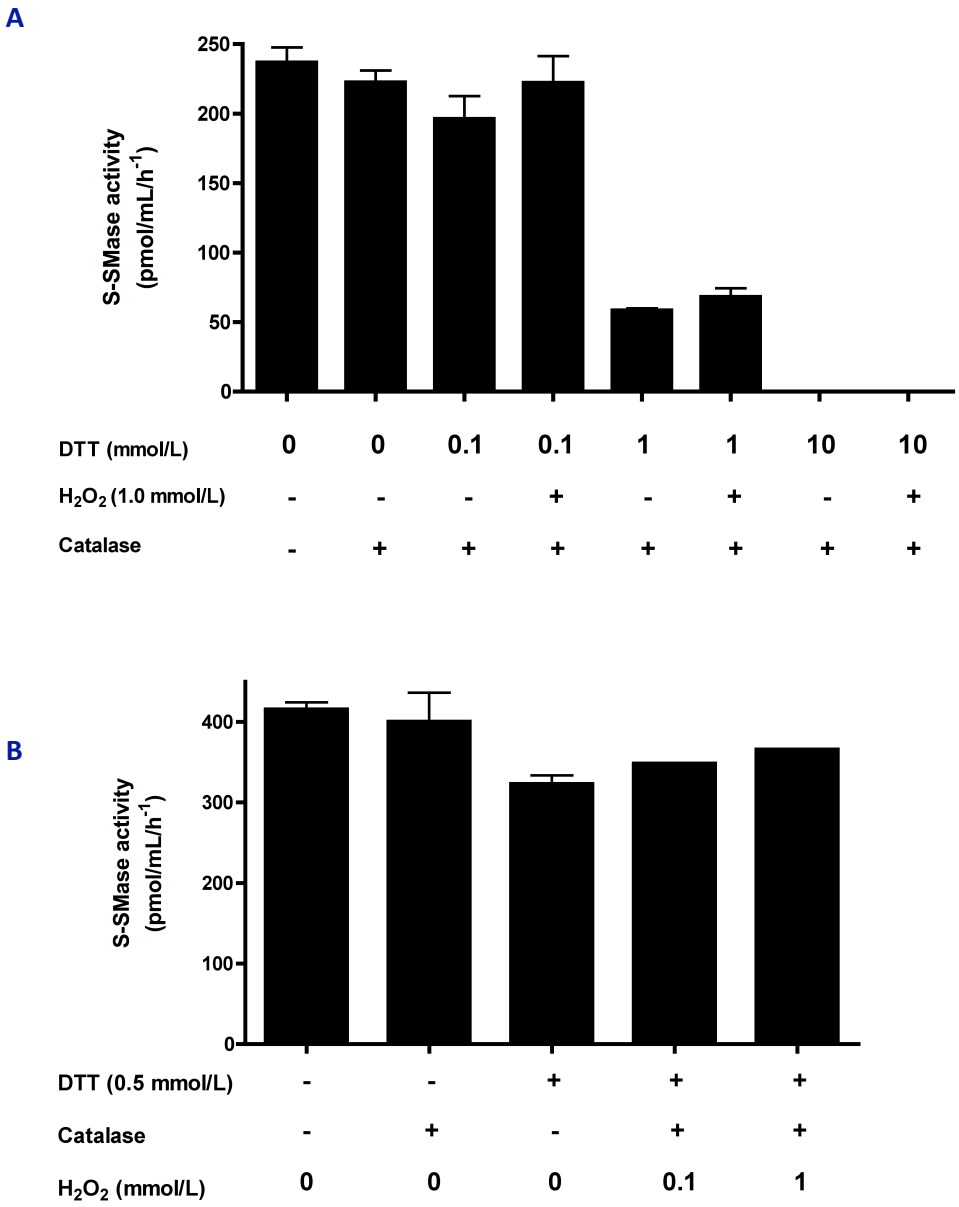


**Figure 4.13 Oxidation may rescue enzymatic activity of chemically reduced S-SMase**

HUVEC in HESFM were treated with TNFα (10 ng/mL) for 18 hours, the medium was removed and concentrated. **(A)** The S-SMase$^{high}$ medium was subjected to varying concentrations of DTT for 15 minutes at 37$^0$C followed by incubation with $H_2O_2$ (1 mmol/L) for 15 minutes at 37$^0$C. All aliquots were exposed to catalase (10 U/mL) for 30 minutes at 37$^0$C. Values are representative of one experiment (n=1). **(B)** The S-SMase$^{high}$ medium was subjected to DTT (0.5 mmol/L) for 15 minutes at 37$^0$C followed by incubation with $H_2O_2$ (0.1; 1 mmol/L) for 15 minutes at 37$^0$C. All aliquots were exposed to catalase (10 U/mL) for 30 minutes at 37$^0$C. Each aliquot was assessed for S-SMase activity by TLC activity assay. Values are representative of one experiment (n=1) in **A** and **B** ± S.D. from technical triplicates.

#### *4.2.3.2 Manipulating intracellular redox environments alters activity of native S-SMase*

GSH and the enzymes associated with the GSH system are depleted in RA (Hassan et al., 2001). Although GSH does not have a direct effect on ASM activity (Liu and Hannun, 1997), increased ROS as a result of depleted anti-oxidant systems may have a significant effect of ASM redox status and activity. To address this, we employed buthionine sulfoximine (BSO), an inhibitor of GSH synthesis and NAC, a GSH precursor and cysteine residue donor. The experiments focused on exposure of HUVEC to BSO (100 μmol/L) and NAC (1 mmol/L).

We first observed the effect of acute BSO/NAC exposure through a co-culture assay of these compounds with TNFα (10 ng/mL). This allowed minimal exposure of GSH regulating agents. Accordingly, **figure 4.14a** demonstrated that co-treatment of BSO or NAC with TNFα for 18 hours did not alter S-SMase activity. This may suggest that GSH levels have not been adequately depleted despite previous indications (Jornot and Junod, 1993, Toborek et al., 1995). With this in mind, HUVEC were pre-treated with BSO and NAC for 16 hours, and then treated with TNFα alone for a further 18 hours **(Figure 4.14b).** Interestingly, this lead to slightly depressed S-SMase activity from HUVEC treated with BSO compared to those treated with TNFα alone. NAC was able to cause a non-significant decrease in S-SMase activity as predicted. This surprising finding using BSO led to us to try and augment these observations by increasing HUVEC exposure to BSO and NAC. Accordingly, HUVEC were pre-treated with BSO or NAC for 16 hours followed by co-treatment with TNFα for a further 18 hours increasing the total exposure time with BSO or NAC 34 to hours. This timeframe is similar to a published method where however a 32-fold higher concentration of BSO (3.2 mmol/L; 48 hours) had minimal effect on HUVEC

death (Tsou et al., 2007). In line with data from **figure 4.14b,** these treatments led to a significant decrease in S-SMase activity from medium of HUVEC treated with BSO and TNFα compared to TNFα alone ($p < 0.04$) **(Figure 4.14c)**. Furthermore, S-SMase activity was lower in medium from NAC and TNFα treated HUVEC compared to TNFα only treated cells **(Figure 4.14c)**.

Accordingly, the above would benefit from the observation of cell death in these cultures, albeit not evident by light microscopy at the time. To support the effect of BSO and NAC on GSH levels, estimation of GSH, GSSG and ROS following treatments would allow for robust conclusions. Whether the S-SMase measured is less active or there is less S-SMase secreted is also unclear as protein estimation was not possible because the yield of secreted protein (S-SMase) was not large enough for protein estimation using the BCA assay (2.2.14)

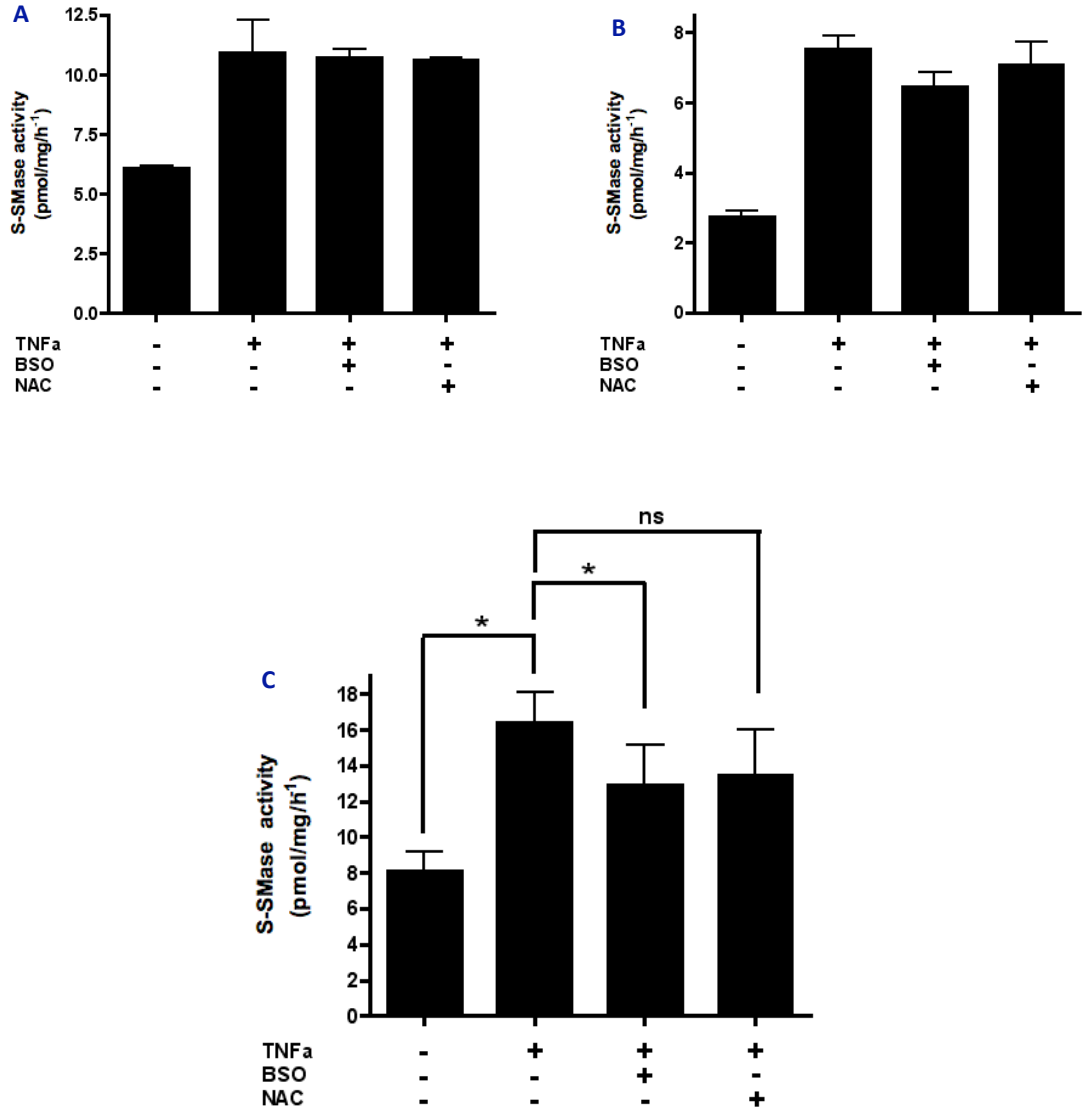


**Figure 4.14 Intracellular redox imbalance may affect TNFα-induced S-SMase activity**

HUVEC in HESFM were incubated with **(A)** BSO (100 μmol/L) or NAC (1 mmol/L) alongside TNFα (10 ng/mL) for 18 hours. **(B)** HUVEC in serum-free HESFM were pre-treated with BSO (100 μmol/L) or NAC (1 mmol/L) for 16 hours. The media were then replaced with serum-free HESFM containing TNFα alone for 18 hours**. (C)** HUVEC in HESFM were pre-treated BSO (100 μmol/L) or NAC (1 mmol/L) for 16 hours. The media were replaced with fresh serum-free HESFM containing BSO (100 μmol/L) or NAC (1 mmol/L) alongside TNFα (10 ng/mL) for 18 hours. Media were concentrated and S-SMase activity was assessed by the TLC activity assay. Data represents mean values (A-B; one experiment) ± SD from technical variation and (C) shows values from three independent experiments ± SEM.

## 4.3 Discussion

In the current chapter we show that S-SMase secretion is induced by only certain pro-inflammatory cytokines in human EC and also characterized the possible redox sensitivity of an EC-derived S-SMase. This now adds to the schema of cytokine mediators in the SM:Cer pathway and its regulation.

Anti-TNFα treatment successfully leads to improved clinical and biochemical outcomes including CRP, swollen joint count, DAS-28 and BVAS in RA and AASV (Elliott et al., 1993, Hurlimann et al., 2002, Booth et al., 2004a, Booth et al., 2004b). Inflammatory mediators have been shown to directly regulate S-SMase secretion *in vitro* including IL-1β, IFNγ, IFNβ (Marathe et al., 1998) and TNFα indirectly *in vivo* (Wong et al., 2000). Accordingly, TNFα can reach a maximal plasma concentration before IL-1β and IL-6. Anti-TNFα infusions were shown to significantly decrease IL-1β and IL-6 in lethal bacteraemia (Tracey et al., 1987, Fong et al., 1989). We found that TNFα directly induces S-SMase from human EC *in vitro* and that this could be blocked with the anti-TNFα antibody (Infliximab). However, there appears to be specificity to S-SMase regulation by cytokines. IL-4, a pro-inflammatory cytokine notably involved in $T_h0$ to $T_h2$ differentiation, did not affect S-SMase levels and neither did IL-6 (Fig. 4.17) (Marathe et al., 1998). This is supported by IL-4-induced inhibition of ASM mRNA upregulated by TNFα (Hatano et al., 2005, Hatano et al., 2007). This is not surprising since IL-4 can itself inhibit IL-1β and TNFα production (Miossec et al., 1992). This highlights the importance of TNFα in the process as a possible Th1-type inflammatory response since it can stimulate MΦ to release S-SMase (Schissel et al., 1996a). Furthermore, TNFα is considered central to ECD

development where in combination with IL-1β decreased EDV in response to bradykinin in humans, whilst IL-6 alone had no effect (Bhagat and Vallance, 1997). These data increase the focus of TNFα as the primary mediator of S-SMase secretion as it appears to be a more potent inducer of S-SMase than IL-1β **(Figures 4.8)** (Wong et al., 2000, Jenkins et al., 2010a).

Rapid activation of ASM by TNFα (2 min. and 3 hr.) has been previously described (Wong et al., 2000, Zhang et al., 2002). We found that un-stimulated human EC secrete basal levels of S-SMase. However, significant activation and secretion of S-SMase occurred between 12-18 hours and remained high up to 24 hours later confirming a recent report in MCF7 cells (Jenkins et al., 2010a). Our data suggest that EC may have pools of S-SMase that when depleted upon stimulation require transcriptional activation to ensure continued enzyme secretion. Like SMase, soluble inflammatory mediators are trafficked and secreted in different spatial and temporal patterns (Manderson et al., 2007). Constitutive secretion of S-SMase occurs through the Golgi secretory pathway as blockade of ER-Golgi transport abolished release of V5-tagged S-SMase (Jenkins et al., 2010a).

Proteins are transported from the ER and trans-Golgi network (TGN) to the PM for secretion generally via the constitutive or regulated secretory pathways (CSP; RSP). Constitutive secretion occurs in small secretory Golgi-vesicles from the TGN to the PM reviewed in Bard and Malhotra, (2006). The RSP often relies on stored proteins in lysososmes, where the external signalling mechanisms remain unclear (Stow et al., 2009,

Stanley and Lacy, 2010). In EC, Weibel-Palade bodies (WPB) are specialised storage granules that can be activated by IL-4, TNFα, SMase and exogenous Cer (Inomata et al., 2009, Bhatia et al., 2004). Secretion pathways vary between molecules and cell type (Reefman et al., 2010, Huse et al., 2006, Murray et al., 2005a). A specific example is IL-1β with multiple release mechanisms (Eder, 2009) while TNFα itself is trafficked via recycling endosomes in addition to the CSP and exocytosed by vesicle fusion (Murray et al., 2005b, Pagan et al., 2003). S-SMase however may be trafficked via the CSP and RSP as observed in this chapter and reported previously (Marathe et al., 1998, Wong et al., 2000, Jenkins et al., 2010a).

Mannose-6-phosphate (M6P) or sortilin tagged ASM pre-cursors are trafficked to lysosomes. Thus ASM pre-cursors not M6P tagged are shuttled to the Golgi secretory pathway (Schissel et al., 1998a, Jenkins et al., 2010b, Schissel et al., 1998b, Marathe et al., 1998, Ni and Morales, 2006). Evidence for this lies in I-cell fibroblasts which have mutations of M6P machinery proteins such as NAGTP, where most of ASM precursor is secreted (Takahashi et al., 2005). While the M6P theory remains under debate (Quintern et al., 1989b), the alternative sortilin pathway has received yet less attention and both pathways might be involved in regulating ASM secretion (Jin et al., 2008).

TNFα itself binds to TNFR1 and TNFR2 directly and mediates signals through adapter proteins (Bradley et al., 1995, Jones et al., 1999). It has been postulated that ASM/Cer form part of a complex TNFα/NF-κB signalling cascade (Schutze et al., 1992, Wiegmann et al., 1994). The ASM (*SMPD1*) promoter region has putative binding sites for transcription

factors Sp1, TATA and AP-1 (Schuchman et al., 1992). It was suggested that phosphatidylcholine phospholipase C (PC-PLC) could lead to sequential diacyglycerol (DAG) and NF-κB translocation via TNFR1 using ASM activation (Schutze et al., 1992, Kolesnick, 1987, Wiegmann et al., 1994). However, this involvement of ASM in TNFα/NF-κB signalling has also been disputed (Zumbansen and Stoffel, 1997, Kuno et al., 1994, Modur et al., 1996, Manthey and Schuchman, 1998). Similarly, TNFR1 stimulation leading to ASM activation was shown to occur via Fas associated death domain (FADD) and TNF Receptor type-1 Associated Death Domain (TRADD) (Wiegmann et al., 1999, Schwandner et al., 1998), the authors proposing fusion of internalized TNFR1 with ASM-carrying Golgi endosomes (Schneider-Brachert et al., 2004, Schutze et al., 1999). These processes however were observed during apoptosis involving lysosomal L-SMase rather than S-SMase.

TNFα leads to the secretion of cytokines (IL-1, IL-6, IL-8, GM-CSF), matrix metalloproteinases (MMP), prostaglandins, chemokines, complement factors, lysosomal enzymes and protease inhibitors (Brennan et al., 1989, Haworth et al., 1991, Butler et al., 1995, Dayer et al., 1985, Brennan and McInnes, 2008, Lee et al., 2010). TNFR1 stimulation by TNFα was shown to be linked to MMP-9 release in a PKC-dependent manner (Chakrabarti et al., 2006, Li et al., 2010). Interestingly this may share similar mechanisms to ASM activation, involving PKCδ-mediated phosphorylation of ASM $Ser^{508}$ (Zeidan and Hannun, 2007). Pro-inflammatory cytokine regulation of lysosomal enzymes like ASM was previously established (Huet et al., 1993). Cathepsins, are cystine proteinases found active in the RA synovium, regulated by TNFα and IFNγ (Maciewicz et al., 1990, Huet et

al., 1992, Zerimech et al., 1993, Lemaire et al., 1997). Importantly, the mechanisms of cytokine-induced cathepsin secretion are not yet fully understood (Krueger et al., 2009, Lemaire et al., 1997). In addition to ASM, TNFα and IL-1β can also activate other lipases such as pro-inflammatory type IIA secreted phospholipase A2 (sPLA2) and endothelial lipase (EL) (Andreani et al., 2000). In HUVEC, EL secretion was also shown within 12-24 hours using similar TNFα concentrations (10 ng/mL; Fig. 4.9) (Jin et al., 2003, Hirata et al., 2000). This was at least partially due to regulation at mRNA level in HUVEC (Jin et al., 2003) similar to the effect of IL-1β on ASM in breast carcinoma cells MCF7 (Jenkins et al., 2010a).

Recently, TNFα, IL-1β and phorbol myristate acetate (PMA) (PKC activator, structural homologue of DAG) were shown to increase S-SMase release from MCF7 cells while IL-1β was able to increase *SMPD1* transcripts in contrast to PMA. This suggested an alternative mechanism to account for the enhanced protein secreted. As such, it was shown that S-SMase could retain its activity following CHX treatment implying little protein turnover (Jenkins et al., 2010a), thus supporting a role for S-SMase in chronic inflammatory disease. The above observations suggest that S-SMase release may occur through the CSP, however the precise mechanisms of TNFα-induced S-SMase secretion remain unclear. $Ser^{508}$ on ASM, situated in the C-terminal end of the protein, has been associated with its release as secretion-incompetent $Ser^{508}$ mutants failed to generate PM-specific $C_{16}$-Cer and retained their lysosomal targeting (Jenkins et al., 2010a, Lee et al., 2007). Perhaps the best evidence to date of an S-SMase pathway in MCF7 cells describes an IL-1β/TNFα-induced, $Ser^{508}$-dependent increase in S-SMase release. This also included selective generation of $C_{16}$-Cer on the outer plasma membrane leaflet without L-

SMase activation (Jenkins et al., 2010a). In contrast to L-SMase, which undergoes complete carboxy-terminal removal, S-SMase retains the entire C-terminal and is a regulator of its activity by terminal cysteine ($Cys^{629}$) switching of rhASM (Jenkins et al., 2010b, Qiu et al., 2003).

TNF$\alpha$–mediated ROS production has been linked with ASM activation (Gao et al., 2007, Dumitru and Gulbins, 2006). This redox sensitivity of ASM was also confirmed in neutrophils, glioma and U937 cells (Scheel-Toellner et al., 2004, Grammatikos et al., 2007). We investigated the redox regulation of human endothelial-derived S-SMase by applying non-specific oxidative stress using $H_2O_2$. Our data showing that DTT could abrogate S-SMase activity (**figure 4.12-13**) confirmed previous observations that S-SMase is secreted in an activated state (Claus et al., 2005, Wong et al., 2000, Marathe et al., 1998). Subsequent application of $H_2O_2$ (1 mmol/L) then suggested a partial rescue of S-SMase activity as shown in **figure 4.13.** This contrasts with Claus et al., (2005) who used a 10-fold higher concentration of oxidising agent 2,2'azobis-2-amidinopropane (AAPH). The authors showed that addition of ascorbic acid to plasma of septic shock patients led to a minimal decrease in activity compared to a significant rise using AAPH (Claus et al., 2005). This suggested that S-SMase might not be secreted fully activated. Further experiments using a range of oxidant concentrations would clarify the oxidative plasticity of S-SMase. Thus inflammatory conditions *in vivo* might also regulate S-SMase activation. Inflammation and increased oxidative stress diminish GSH levels. Accordingly, GSH can directly inhibit nSMase but not ASM *in vitro* in contrast to DTT (Liu and Hannun, 1997).

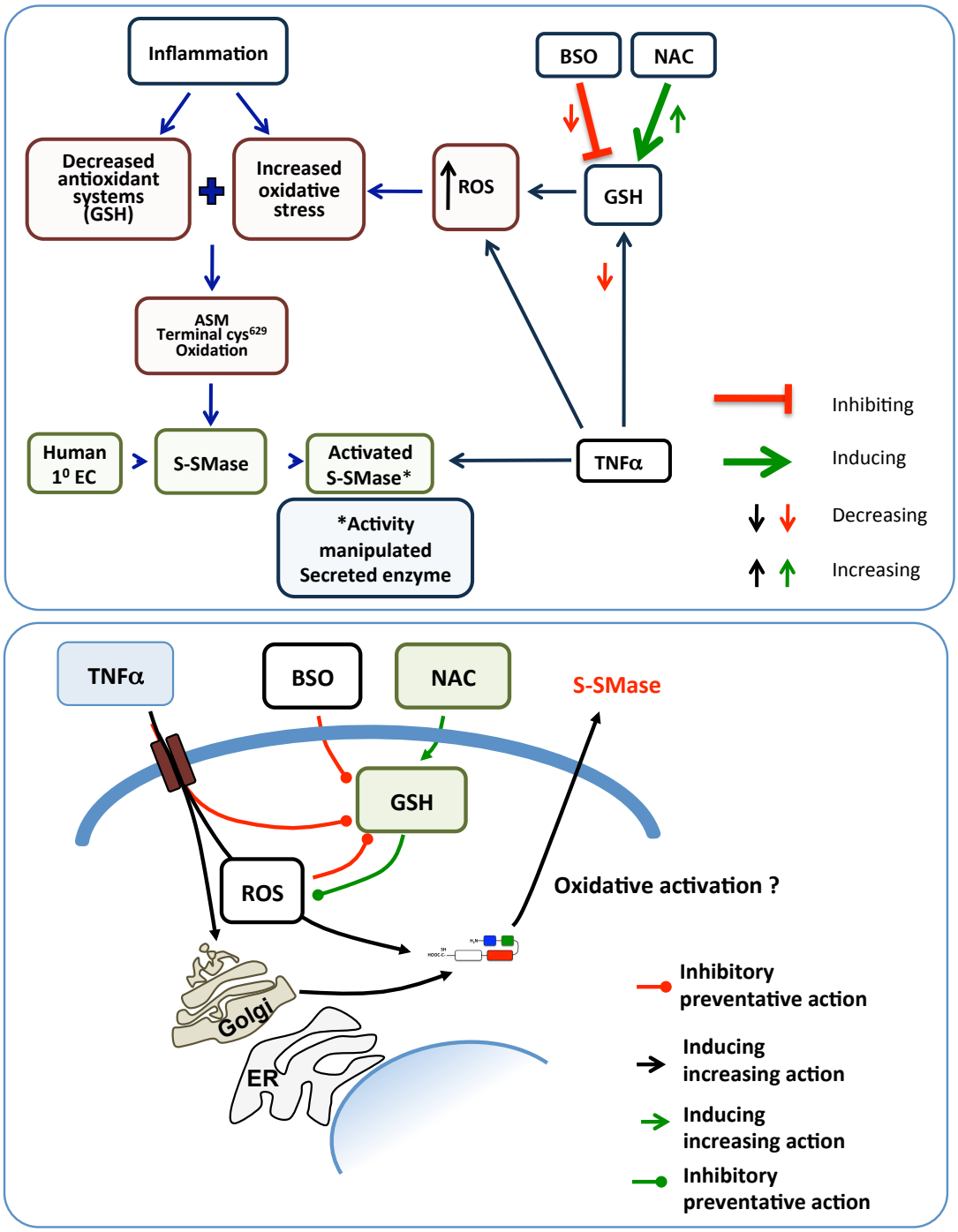


**Figure 4.15 Hypothetical redox regulation of S-SMase activation in EC**

Inflammatory conditions and increased reactive oxygen species (ROS) lead to oxidative activation of S-SMase by terminal $Cys^{629}$ switching. Increased levels of ROS diminish anti-oxidant systems such as glutathione (GSH). *In vitro* this is described using buthionine sulfoximine (BSO) and *N*-acetylcysteine (NAC) which decrease and augment GSH respectively. TNFα coupled with increased ROS may synergise to induce enhanced secretion and activity of endothelial S-SMase.

Recently, NAC was shown to inhibit ASM suggesting that GSH regulates ASM activation by maintaining an intracellular redox balance (Charruyer et al., 2005, Dumitru and Gulbins, 2006). To further clarify the role of oxidative switching on S-SMase activity we decided to manipulate intracellular (GSH) EC redox environments. Even modest concentrations of BSO (2 to 200 μmol/L) can deplete HUVEC of GSH up to 95% even after 27 hours (Jornot and Junod, 1993, Heng-Long Hu et al., 2000, Toborek et al., 1995). A decrease in GSH renders cells in a pro-oxidant state and since ASM is activated by oxidation of $Cys^{629}$, this should lead to increased S-SMase activity. S-SMase activity in medium from NAC & TNFα treated cells appeared to be decreased compared to TNFα alone treated cells suggesting that raised GSH, due to NAC, maintained physiological ROS levels preventing ASM cysteine switching. However, this was also the case for S-SMase in medium from BSO & TNFα treated cells. Interestingly, TNFα itself has been shown to increase GSH levels in EC and hepatocytes by 24 hours (Toborek et al., 1995, Morales et al., 1997). This supports our observations that showed both BSO and NAC treatments independently decreasing S-SMase activation. It remains unclear whether the effect of BSO/TNFα was an *in vitro* artefact since the effect was consistent.

In summary, IL-1β and TNFα directly induced the secretion of a redox-sensitive enzyme from human EC *in vitro.* This was not seen with IL-6 suggesting specificity in the regulation of S-SMase by inflammatory cytokines. Our model is arguably the most physiologically relevant for characterising native S-SMase as a redox-sensitive enzyme. More work is needed to characterise this SMase, clarify the extent of intracellular oxidative stress on its activation and translate this to *in vivo* models of inflammation.

# Chapter 5

# Effects of ASM on endothelial cell function

# 5 Effects of ASM on endothelial cell function

## 5.1 Introduction

Although many studies have investigated the regulation and cellular effects of ASM and nSMase following stimulation of cell surface receptors, none have looked directly at the effect of exogenous ASM on the outer PM leaflet and the consequences on intracellular responses. Given that in the previous chapter we showed that TNFα could directly mediate the secretion of S-SMase from EC, this chapter set out to investigate a role for extracellular ASM in altering EC signalling.

The current literature paints an extensive and complex picture in which downstream lipid messengers of SM catabolism have contrasting effects. ASM has been linked to apoptosis and the strongest link came from the protection offered to cells in its absence (Santana et al., 1996, Separovic et al., 1999, Llacuna et al., 2006). There are conflicting reports concerning the roles of SMase and Cer in eNOS regulation. Cer has been shown to mediate EDV in rat aorta, a process blocked in eNOS-inactivated tissue (Johns et al., 1998). TNFα was reported to increase eNOS activation in EC through Cer generation independent of $Ca^{2+}$ (Bulotta et al., 2001). However, in bovine coronary artery EC, Cer could activate eNOS in a $Ca^{2+}$-dependent manner (Igarashi et al., 1999). These events are likely to be mediated through the Cer messenger, sphingosine-1-phosphate (S1P) that has been linked with eNOS activation, however, the precise mechanisms remain unclear (Igarashi and Michel, 2001, Igarashi and Michel, 2008).

The plasticity of the sphingomyelin pathway was highlighted in a series of studies where Cer-induced eNOS uncoupling led to decreased NO output through ROS production and subsequent peroxynitrite formation (Zhang et al., 2002, Zhang et al., 2001, Zhang et al., 2003). This suggested an auto-regulatory mechanism where Cer and S1P may increase eNOS activation but decrease NO output through $O_2^-$ generation and $ONOO^-$ formation. However, S1P formation is a downstream event of Cer catabolism. Closer to the cell surface, formation of Cer in lipid rafts (LR) at the PM is believed to have detrimental effects on membrane dynamics (van Blitterswijk et al., 2003). Cer is highly hydrophobic and tends to associate in lipid rich compartments, such as the PM itself. Previous work in our laboratory showed that TNF$\alpha$ can decrease $Ca^{2+}$ signals in T cells and that this was mediated by ASM blocking $Ca^{2+}$ through $I_{CRAC}$ (Church et al., 2005). Capacitative calcium entry (CCE) describes the influx of $Ca^{2+}$ through membrane SOC in response and parallel to, depletion of ER $Ca^{2+}$ stores (Putney, 1986). $Ca^{2+}$ influx in response to ER store emptying occurs through $Ca^{2+}$ release-activated $Ca^{2+}$ channels ($I_{CRAC}$) (Parekh, 2008b), found in close vicinity to caveolae, which are rich in SM and considered a target for exogenous, secreted SMase (Isshiki et al., 1998, Isshiki et al., 2002). SMases were indeed first suggested as modulators of $_i Ca^{2+}$ mobilisation in T lymphocytes (Breittmayer et al., 1994). Furthermore, TNF$\alpha$ was shown to inhibit store-operated $Ca^{2+}$ entry (SOCE) into thyroid FRTL-5 cells, as did brain-derived SMase and Cer (Tornquist et al., 1999). Subsequently, blockade of $I_{CRAC}$ and inhibition of $Ca^{2+}$ influx following stimulation of CD95 (FAS) also occurred through L-SMase (Lepple-Wienhues et al., 1999).

Endothelial dysfunction as a result of eNOS dysregulation, a process tightly coupled to $_i Ca^{2+}$ signalling, manifests as defective endothelium-dependent vasodilation and leads to

CV complications (Vanhoutte et al., 2009). Store operated $Ca^{2+}$ influx leads to eNOS activation, found to co-localise in a PM domain probably within caveolae (Lin et al., 2000), specifically caveolin-1, which blocks eNOS activation through protein-protein interaction (Feron et al., 1998). Influx of $Ca^{2+}$ breaks the caveolin-1/eNOS association while calmodulin (CaM) binding to eNOS, necessary for its activation, facilitates the transfer of electrons from the eNOS reductase domain to the oxidase domain (Ghosh et al., 1998, Dudzinski and Michel, 2007, Michel and Vanhoutte, 2010).

Impaired EDV is depicted as ECD, considered an early step in atherosclerosis. ECD features decreased NO production that can come as a result of decreased eNOS expression, depleted substrate (L-arginine) or co-factors, altered eNOS signalling and inactivation (Shimokawa et al., 1991, Schmidt and Alp, 2007). eNOS dysregulation can manifest as dysfunctional phosphorylation status on multiple residues. The two most studied eNOS phosphorylation sites include $Ser^{1177}$ which has been shown to activate eNOS and $Thr^{495}$ that keeps eNOS in an inactive state (Mount et al., 2007). To date, the effect of exogenous ASM on agonist-evoked $_{i}Ca^{2+}$ signalling and eNOS activation and NO production has not been addressed. The aims of this chapter were to examine the effect of exogenous ASM on $_{i}Ca^{2+}$ mobilisation and eNOS activation in EC. Thus we asked whether ASM could cause ECD through decreasing $_{i}Ca^{2+}$ signalling and inhibiting eNOS activation and NO production.

## 5.2 Results

### 5.2.1 Effect of ASM on HUVEC viability

#### *5.2.1.1 Exogenous ASM does not induce HUVEC cytotoxicity*

To ensure that exogenous ASM does not affect cell viability we examined the effect of exogenous ASM on HUVEC cytotoxicity. HUVEC cultured in 96-well plates were treated with ASM in M199 supplemented with HIFCS, the medium to be used when assessing $Ca^{2+}$ responses in HUVEC. **Figure 5.1** indicates that 60-minute exposure to ASM is not cytotoxic to HUVEC. Observation of HUVEC under light microscopy also suggested that ASM did not induce alteration in their morphology (not shown).

#### *5.2.1.2 Exogenous ASM does not induce HUVEC apoptosis*

L-SMase has been implicated in apoptosis pathways induced by death ligands such as TNF$\alpha$ and FAS (Haimovitz-Friedman et al., 1997, Sawada et al., 2002, Garcia-Ruiz et al., 2003). This work involved activation of intracellular ASM. We therefore wanted to examine the effect of prolonged incubation with exogenous ASM on HUVEC apoptosis. This was performed in fully supplemented M199 to also mimic future $Ca^{2+}$ assays. HUVEC in 24-well plates were treated with ASM (0-1250 mU/mL) for 18 hours and assessed for the ability to retain the mitochondrial semi-permeable dye $DiOC_6$ (as shown in chapter 4). We found that ASM did not affect HUVEC viability and the percentage of apoptotic cells did not differ compared to untreated control cells **(Figure 5.2).**

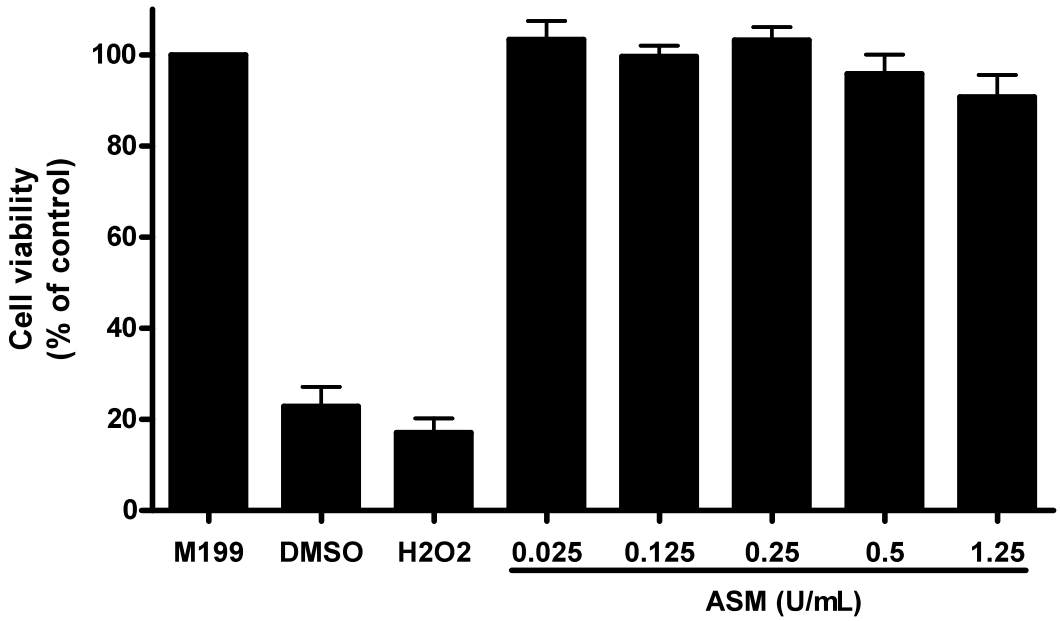


**Figure 5.1 ASM does not affect HUVEC viability**

HUVEC were brought to confluence in 96-well tissue culture plates and treated with exogenous ASM (Sigma-Aldrich) in fully supplemented M199 for 60 minutes. HUVEC were also treated with DMSO (10% v/v) and $H_2O_2$ (1 mmol/L) for 60 minutes. Cell viability was determined by the MTS assay. Data are expressed as a percentage of control fully supplemented M199 untreated cells. Data are mean ± SD from five independent experiments (n=5).

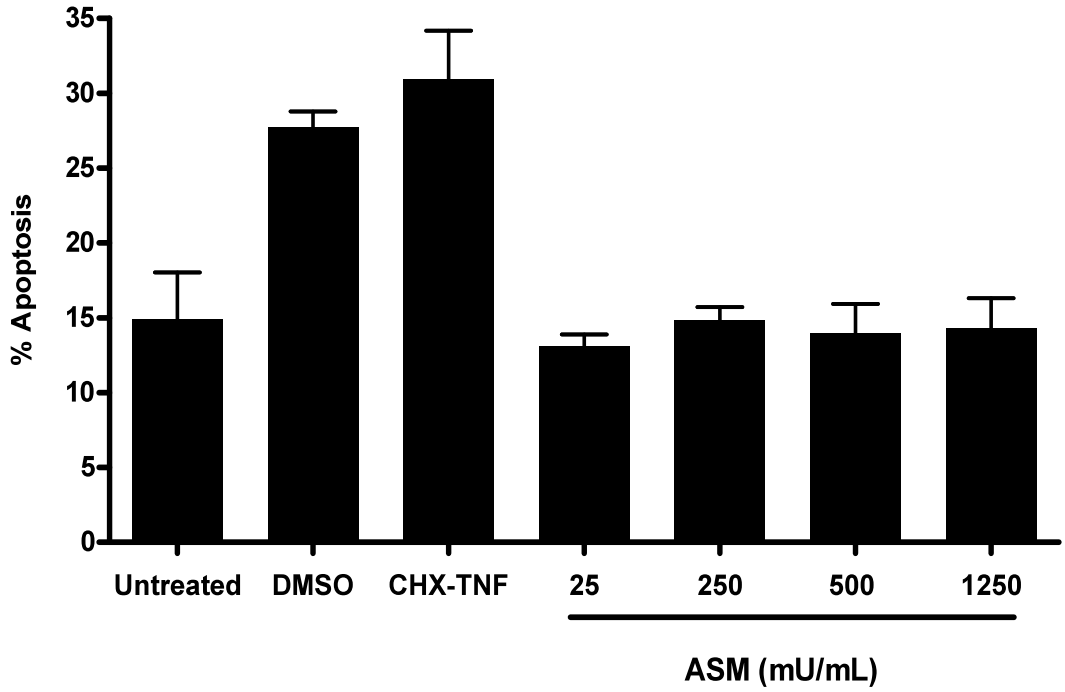


**Figure 5.2 ASM does not induce HUVEC apoptosis**

HUVEC were brought to confluence in 24-well tissue culture plates in M199. The media were removed, the cells washed twice with HBSS-$Ca^{2+}$ and incubated with fully supplemented M199 containing solvent control, DMSO (10% v/v), CHX/TNFα (10 μM/100 ng/mL) or varying concentrations of ASM alone. Apoptosis was assessed by $DiOC_6$ retention. Data represents the mean values of five independent experiments (n=4) ± SD.

### 5.2.2 Effect of exogenous ASM on HUVEC intracellular calcium ($_{i}Ca^{2+}$) responses

The assays featuring $_{i}Ca^{2+}$ signalling in EC *in vitro* were carried out at neutral pH to mimic the near-vascular microenvironment. Thus, Hank's Buffered Saline Solution (HBSS) (Table 2.2, p61) was used to visualise EC under fluorescence microscopy because of its neutral pH and suitability for sustained HUVEC viability. ASM can hydrolyse SM on LDL at neutral pH (Schissel et al., 1998a). Furthermore, we found that ASM, if anything, was more potent at neutral pH in HBSS compared to its activity in a buffered aqueous acid solution **(Appendix figure A3).**

Given the previous work showing that SMase could depress $_{i}Ca^{2+}$ signals in lymphocytes and the importance of the $Ca^{2+}$ signal in EC function, we next went on to study the effects of ASM on $_{i}Ca^{2+}$ responses in HUVEC. Application of exogenous ASM should lead to generation of Cer on the extracellular PM leaflet. It was hypothesised that Cer would interfere with PM raft organisation proximal to $I_{CRAC}$ thus regulating $Ca^{2+}$ influx.

Measurement of $_{i}Ca^{2+}$ responses in HUVEC evoked by vasoactive agonists was performed using the $_{i}Ca^{2+}$ specific chelator type dye Fura-2 AM (Invitrogen, UK). HUVEC were stimulated with bradykinin (Bk) and thrombin (Thr) to elicit a $Ca^{2+}$ flux. Typical responses to Bk and Thr are shown in **figure 5.3.** A baseline was measured for 30 seconds prior to addition of agonist. In this false colour representation of the ratiometric Fura images, cells with low cytoplasmic $Ca^{2+}$ appear green (Fura emission, 340) while those in which the $Ca^{2+}$ is raised appear red/orange (Fura emission, 380). Mean values of the red/green ratio for each cell in the field were calculated over time and mean ratios deduced to allow comparison of the groups treated under different conditions.

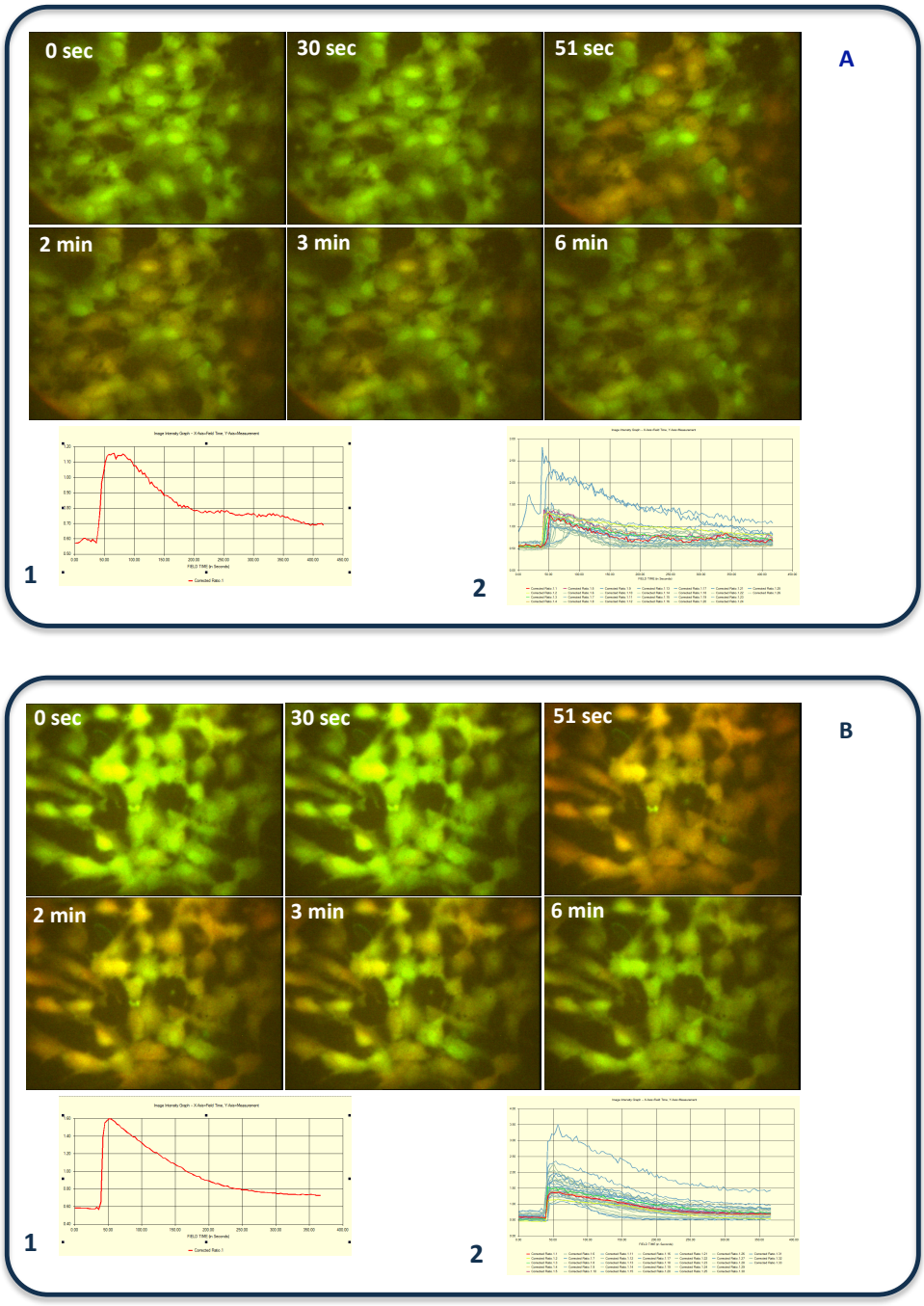


**Figure 5.3 Typical HUVEC $_{i}Ca^{2+}$ responses to bradykinin and thrombin**

HUVEC between 2-4 passages were re-seeded into 8-well glass coverslides for 24-48 hours in fully supplemented M199. HUVEC were loaded with FURA-2 and stimulated with **(A)** bradykinin (1 μmol/L) and **(B)** thrombin (1 U/mL) to evoke $_{i}Ca^{2+}$ responses detected by fluorescence microscopy. Field average (total cell average) **(1)** and single cell responses **(2)** recorded over time in graphical representation for each agonist. Panels **(1)** and **(2)** are for illustration purposes only.

### *5.2.2.1 Exogenous ASM decreases $_{i}Ca^{2+}$ responses to bradykinin in HUVEC*

Application of exogenous ASM onto HUVEC reduces $_{i}Ca^{2+}$ responses to Bk. Previous experiments in our laboratory showed that 10 mU of bacterial nSMase could decrease $_{i}Ca^{2+}$ signals in jurkat T lymphocytes (L.D. Church). HUVEC were pre-incubated with ASM or vehicle for 30 or 60 minutes in fully supplemented M199. To decide on an appropriate concentration range for ASM we calculated the activity of S-SMase in plasma from patients. This was expressed as international units (I.U.) of activity estimated using a standard curve (**Figure 2.2)**. In the AASV PEX cohorts, mean ASM activity corresponded to 900 mU/mL. Patients with higher ASM activity hydrolysed between 5% and 10% of 1 nmol NBD-SM equal to 2 and 4.4 U/mL respectively. A treatment range below these levels was decided which included 25, 250 and 500 mU/mL, thus reflecting concentrations utilised previously *in vitro* (above) and extended to lower *in vivo* levels found in diseased patients.

Treatment of HUVEC to ASM alone did not affect baseline $_{i}Ca^{2+}$ levels nor did it cause a $_{i}Ca^{2+}$ response in the absence of agonist (data not shown). Even at low concentrations (25 mU/mL), ASM decreased HUVEC $_{i}Ca^{2+}$ signals in response to 1 μmol/L Bk compared to control un-treated HUVEC **(Figure 5.4)**. Incubation of HUVEC with ASM for 30 minutes inhibited Bk-induced $_{i}Ca^{2+}$ responses with the most profound effect observed in HUVEC treated with 250 mU/mL ($p < 0.05$) whereas 500 mU/mL ASM induced a significantly depressed ($p < 0.05$ vs control) but slightly elevated response compared to 250 mU/mL ASM **(Figure 5.4a).** Application of ASM for 60 minutes enhanced the depression in $_{i}Ca^{2+}$ responses ($p < 0.02$) with an effect even with 25 mU/mL ASM **(Figure 5.4b)**.

To understand whether the effects of ASM are transient, occurring only in the presence of ASM in the medium, we decided to examine the persistence of the effect of ASM on $_{i}Ca^{2+}$ responses. Here, HUVEC were pre-treated with ASM for 30 minutes, the ASM was removed and the cells incubated for a further 60 minutes with fresh medium 199 (recovered cells, **R)**. In parallel, separate cultures were latently pre-treated with ASM for 30 minutes but not allowed to rest in fresh medium (unrecovered cells, **UR**). ASM inhibited Bk-induced $_{i}Ca^{2+}$ responses in a dose-dependent manner **(Figure 5.5)**.

In recovered (R) HUVEC, intra-group comparison (e.g. control Vs ASM-treated recovered HUVEC) confirmed that ASM caused decreased $_{i}Ca^{2+}$ responses to Bk compared to control HUVEC. In recovered HUVEC, $_{i}Ca^{2+}$ responses remained the same between control (untreated) and ASM-treated (25 mU/mL) cells **(Figure 5.5)**. This was expected as no effect was seen previously using 25 mU/mL of ASM **(Figure 5.4a)**. Furthermore, $_{i}Ca^{2+}$ responses in recovered HUVEC appear to initially respond to ASM quenching however, did not return to baseline levels in cells treated with 250 and 500 mU/mL of ASM and were significantly lower than control untreated HUVEC ($p < 0.05$, $p < 0.01$) (**Figure 5.5)**.

Unrecovered (UR) HUVEC treated with ASM also showed decreased $_{i}Ca^{2+}$ flux (250 mU/mL, $p < 0.05$) which did not return to baseline levels of untreated control cells. Inter-group comparison (e.g. UR Vs R) by one-way analysis of variance (ANOVA, Kruskal-Wallis) showed no significant difference between unrecovered and recovered (UR vs R) HUVEC in all ASM concentrations (25-500 mU/mL). In conclusion, the effects of ASM persist following its removal from culture medium suggesting that a second messenger, such as Cer, may indeed mediate the inhibition of $_{i}Ca^{2+}$ responses. More experiments are required to clarify the effects of ASM during different time-points and concentrations.

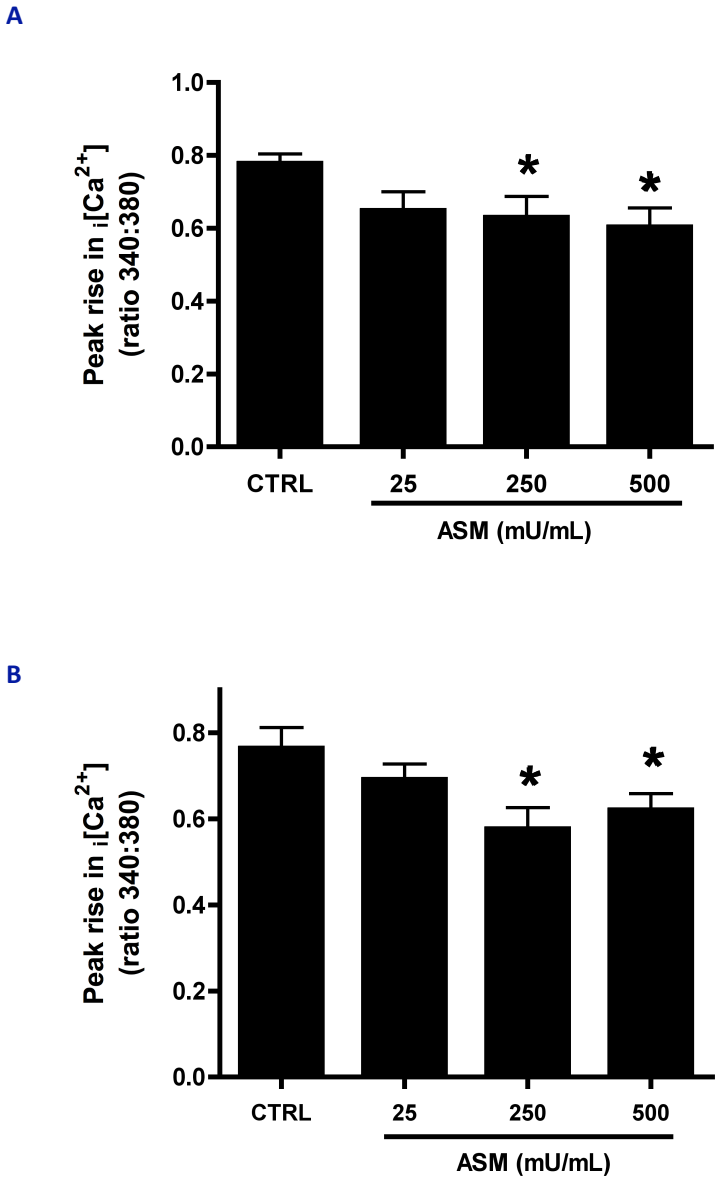


**Figure 5.4 Dose-response effect of ASM treatment on HUVEC $_{i}Ca^{2+}$ signalling**

HUVEC were seeded in 8-well glass coverslides for 24-48 hours in M199. HUVEC were incubated with solvent control or ASM (25-500 mU/mL) for **(A)** 30 minutes, **(B)** 60 minutes. In ASM treated HUVEC, intracellular $Ca^{2+}$ responses evoked by bradykinin (1 μmol/L) were compared to control, untreated HUVEC (CTRL). Intracellular $Ca^{2+}$ signalling is expressed as the peak rise ratio of 340:380 nm. Statistical significance was determined by the Mann-Whitney U test. * indicates $p < 0.05$. Data represent means ± SEM of five independent experiments (n=5).

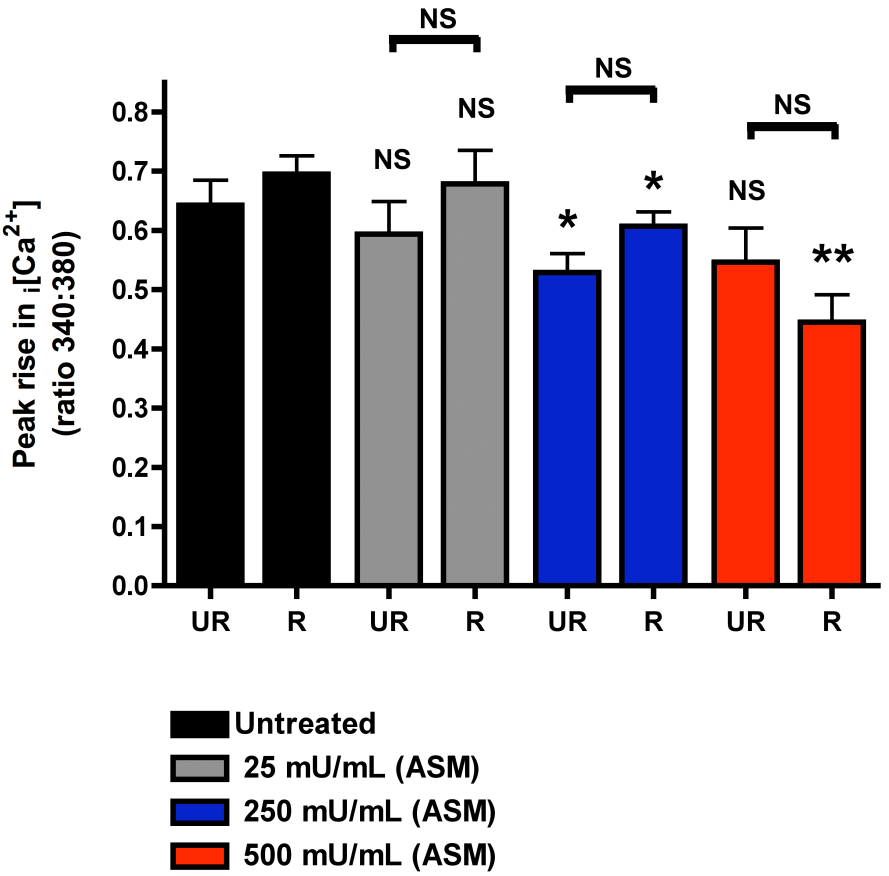


**Figure 5.5 Depleted HUVEC $_{i}Ca^{2+}$ signals do not fully recover after removal of ASM**

HUVEC were seeded in 8-well glass coverslides for 24-48 hours in M199. HUVEC were incubated with solvent control or ASM (25-500 mU/mL) for 30 minutes. Following ASM treatment, half of the cells were allowed to rest for 60 minutes in fresh ASM-free medium (recovered group, **R**). The other half of the cells was not allowed to rest in fresh ASM-free medium (unrecovered group, **UR**). All HUVEC (including untreated and ASM-treated cells) were stimulated with bradykinin (1 μmol/L) to evoke intracellular $Ca^{2+}$ responses. For intra-group comparisons, intracellular $Ca^{2+}$ responses to bradykinin were compared between untreated and ASM-treated HUVEC in both recovered and unrecovered groups. For example, comparisons were made in unrecovered cells (untreated vs ASM) and in recovered cells (untreated vs ASM). ASM-treated recovered (R) HUVEC were also compared to ASM-treated unrecovered (UR) HUVEC. Statistical significance was determined by one-way ANOVA for multiple comparison of all inter-group sample differences (e.g. 500 mU/mL ASM, UR Vs R), and the Mann-Whitney U test all for intra-group sample differences (e.g untreated Vs ASM treated; R Vs R). * indicates $p < 0.05$, ** indicates $p < 0.01$. Data are means ± SEM of three independent experiments (n=3).

### *5.2.2.2 The effect of vasculitis patient plasma on HUVEC $_{i}Ca^{2+}$ responses*

Given the high *in vivo* levels of S-SMase, we examined the effect of a high dose of exogenous ASM on HUVEC $_{i}Ca^{2+}$ responses that resembled levels in disease. ASM does not affect cell viability when applied up to 1.25 U/mL, thus this concentration was chosen **(Figures 5.1-2).** Pre-treatment of HUVEC with exogenous purified ASM (Sigma-Aldrich) for 30 minutes led to a significant decrease in the magnitude of $_{i}Ca^{2+}$ response compared to untreated cells ($p < 0.02$) **(Figure 5.6a).** As a result we used *ex vivo* S-SMase from patient plasma and examined its effects on HUVEC $_{i}Ca^{2+}$ signalling. Plasma from a patient who had undergone PEX was diluted in M199 for HUVEC incubation and termed 'Vasc'. In order to maintain HUVEC viability, a compromise on medium plasma concentration volume over volume (v/v) and thus plasma S-SMase activity, had to be made. This plasma was compared to an equivalent sample that was heat-inactivated to neutralise S-SMase activity, termed 'Vasc-HI'. Patient plasma was also compared to pooled plasma (PP) from healthy controls and M199 alone as a negative control. Vasculitis patient plasma S-SMase activity was assessed using the SMase TLC assay and found to be 3.73 U/mL. Serial dilutions of human plasma up to 60% (v/v) in M199 did not affect HUVEC viability. Thus, a final solution of 1:1 (v/v) plasma and M199 was prepared (1.86 U/mL). A similar solution was prepared using pooled plasma (PP) and both fractions were heat-inactivated. **Figure 5.6b** shows that PP had no effect on HUVEC $_{i}Ca^{2+}$ responses to Bk. This was also the case for heat-inactivated PP (PP-HI*)* pre-treated HUVEC. By contrast, HUVEC pre-treated with 'Vasc' plasma showed non-significant inhibition of $_{i}Ca^{2+}$ responses to Bk brought back to baseline levels when the plasma was heat-inactivated (Vasc-HI). Further investigations are required to clarify the role of S-SMase from diseased patients on HUVEC $_{i}Ca^{2+}$ signalling.

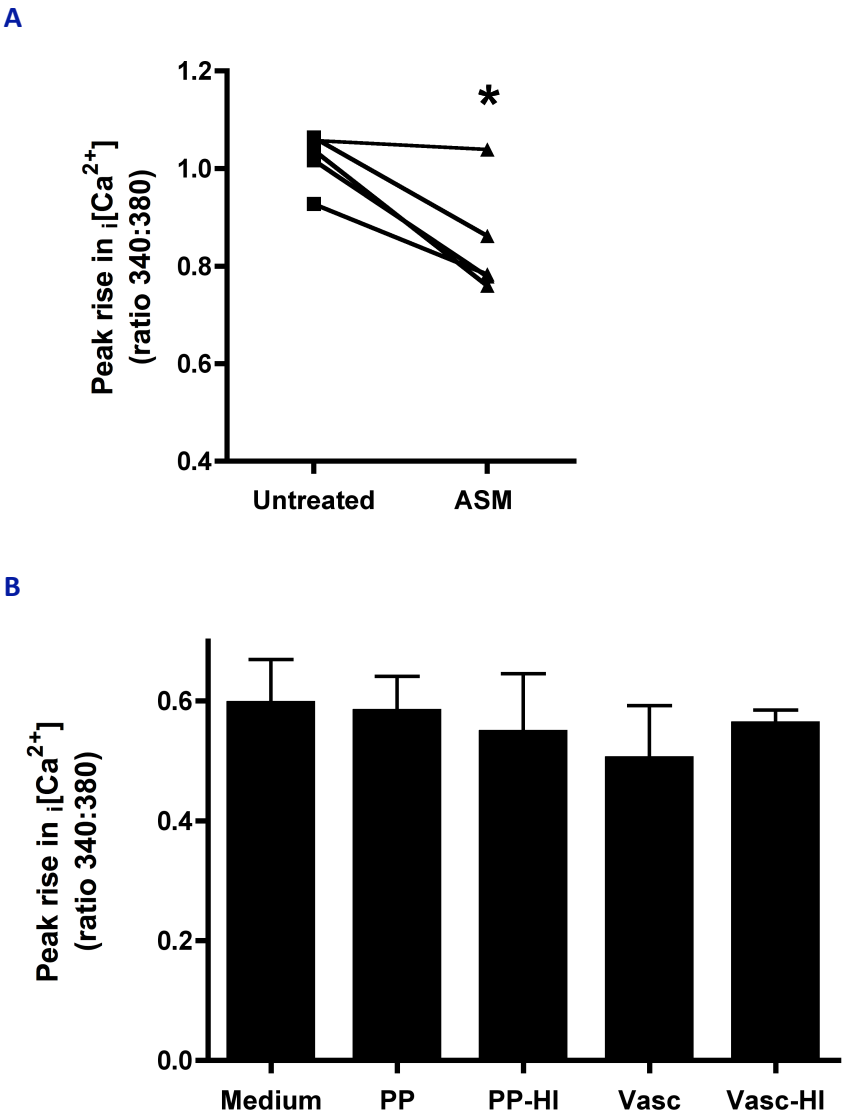


**Figure 5.6 The effect of ASM$^{high}$ vasculitis patient plasma on HUVEC $_iCa^{2+}$ signalling**

**(A)** HUVEC were seeded in 8-well glass coverslides for 24-48 hours in M199. The cells were incubated with ASM (1.25 U/mL) for 30 minutes. Intracellular $Ca^{2+}$ responses evoked by bradykinin (1 μmol/L) were compared to un-treated HUVEC. Statistical significance was determined by the Mann-Whitney U test. * indicates $p < 0.02$ Data represent means of five independent experiments (n=5). **(B)** HUVEC were seeded as in (A) and incubated with either M199 **(medium)** or human plasma for 30 minutes. HUVEC were then stimulated with bradykinin (1 μmol/L) and $_iCa^{2+}$ responses were recorded. **(Medium)** unconditioned culture medium, **(PP)** healthy control pooled plasma, **(PP-HI)** heat-inactivated healthy control pooled plasma, **(Vasc)** AASV patient plasma, **(Vasc-HI)** heat-inactivated AASV patient plasma. Data are means ± SEM of two independent experiment (n=2).

### *5.2.2.3 ASM$^{high}$ media supernate transfer inhibits HUVEC $_{i}Ca^{2+}$ responses*

Following on from experiments in 5.2.2.2 and in an attempt to avoid the complications of high plasma cell culture, we applied concentrated S-SMase supernate. This is because non-physiological high levels of culture plasma may affect assay validity. To do this, HUVEC were stimulated with TNFα (10 ng/mL) for 18 hours, the medium harvested and concentrated as described in chapter 2. Prior to use, the excess TNFα that may have been concentrated in the medium was removed by immunoprecipitation using the anti-TNFα antibody infliximab. The media supernates were assayed for S-SMase activity and frozen in small aliquots at -80$^{0}$C until use. Aliquots used showed an estimated S-SMase activity of 10.7 U/mL. The advantage of these experiments was that the vehicle used to carry the S-SMase was culture medium instead of human plasma. Furthermore, a considerably lower volume of supernate was required to reach the desired high final S-SMase activity. HUVEC were pre-treated with S-SMase$^{high}$ medium (10% v/v; 1.07 U/mL), whilst untreated HUVEC were loaded with medium conditioned with 10% (v/v) concentrated supernate from previously un-stimulated HUVEC. These were compared to heat-inactivated-S-SMase$^{high}$ pre-treated HUVEC. **Figure 5.7** shows that S-SMase$^{high}$ treated HUVEC demonstrated decreased $_{i}Ca^{2+}$ responses to Bk, whilst this effect was abrogated in cells pre-treated with heat-inactivated-S-SMase$^{high}$ supernates similar to baseline, untreated controls. Although 2 experiments are not enough and more are required, these data suggest that EC-derived secreted S-SMase, when transferred onto fresh HUVEC, can decrease $_{i}Ca^{2+}$ responses. This model predicts that pro-inflammatory induced secretion of EC-derived S-SMase can have diffuse autocrine or paracrine effects on local or distal endothelial beds. Thus, we decided to look at downstream signalling events that govern NO production in EC.

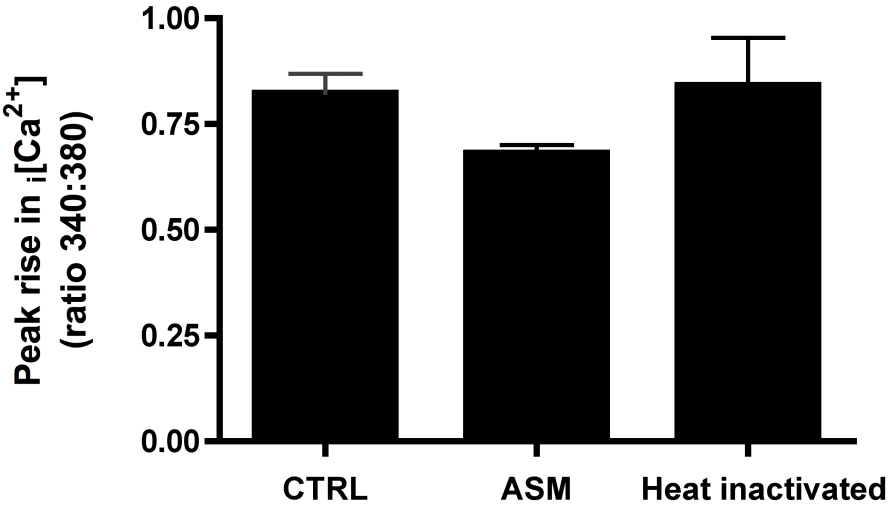


**Figure 5.7 The effect of S-SMase$^{high}$ culture medium supernatates on HUVEC $Ca^{2+}$ signalling**

HUVEC were seeded in 8-well glass coverslides for 24-48 hours in M199. HUVEC were incubated with either M199 or S-SMase$^{high}$ media supernate. HUVEC concentrated medium was derived from HUVEC treated with TNFα (10 ng/mL) for 18 hours. **(CTRL)** untreated HUVEC in M199; **(heat-inactivated)** heat-inactivated S-SMase$^{high}$ concentrated media supernate; **(ASM)** normal S-SMase$^{high}$ concentrated media supernate. Data are means ± SEM of two independent experiments (n=2).

### 5.2.3 The effect of ASM on eNOS activation

In a quiescent state, eNOS is localised to caveolae on the intracellular leaflet of the plasma membrane (PM). When EC are stimulated by agonist, eNOS is activated and translocates to the cytosol where it converts L-arginine to L-citrulline and nitric oxide. Phosphorylation at $Ser^{1177}$ and de-phosphorylation of $Thr^{495}$ are associated with eNOS activation, leading to caveolar dissociation and cytosolic translocation. A mechanism for decreased NO availability may involve disruption of $_{i}Ca^{2+}$ signalling. eNOS activation, which precedes NO generation is a $Ca^{2+}$-dependent process. This decreased $_{i}Ca^{2+}$ influx may inhibit eNOS activation through decreased $Ca^{2+}$-dependent phosphorylation leading to diminished NO production. We therefore examined phosphorylation status as a marker of eNOS activation. Both Bk and thrombin induce $Ca^{2+}$-dependent activation of eNOS. So far, Bk was used to induce $_{i}Ca^{2+}$ responses in HUVEC following ASM treatment. However, Bk has been shown to activate eNOS by dephosphorylating eNOS at $Thr^{495}$ and weakly phosphorylating $Ser^{1177}$ residues whereas thrombin activates eNOS by strongly phosphorylating $Ser^{1177}$ alone **(Figure 1.4)**.

#### *5.2.3.1 eNOS activation through dephosphorylation of $Thr^{495}$*

To study the eNOS protein HUVEC were seeded from primary cells in 6-well tissue culture plates. HUVEC were serum starved for one hour and lysed on ice in Radio-Immunoprecipitation Assay (RIPA) buffer supplemented with protease and phosphatase inhibitors as indicated in chapter 2. Protein was estimated by the BCA assay (Pierce) and typically between 20-70 μg of protein per lane per SDS-PAGE gel was loaded for electrophoresis. As shown in **figure 5.8a** an amount of protein as low as 2.5 μg could be

captured by the anti-eNOS antibody and easily visualised by immunoblotting. In **figure 5.8a**, 5x concentrated loading buffer could be used (10 μg samples) without affecting migration in the acrylamide gel as indicated relative to samples loaded in 2x loading buffer (titration 20 – 0 μg).

Bk is known to activate eNOS by differential phosphorylation changes on $Thr^{495}$ and $Ser^{1177}$ whilst there is no evidence that thrombin induces changes at the threonine residue, rather it only phosphorylates $Ser^{1177}$ alone. Accordingly we examined the ability to detect changes in $Thr^{495}$ phosphorylation by Bk and thrombin **(Figure 5.8b)**. Capture time for optimal phosphorylation of eNOS is between 1-3 minutes when EC are stimulated with either Bk or thrombin. Therefore, HUVEC were stimulated with 1 or 2 μmol/L Bk for 1 and 2 minutes ($BK_1$, $BK_2$ respectively; **figure 5.8b**) (Harris et al., 2001) and 1 U/mL thrombin for the same time periods (Stahmann et al., 2006). We found no change in total eNOS protein following either stimulation. However in this model, we were unable to detect Bk-induced $Thr^{495}$ dephosphorylation. As expected, thrombin also did not alter the $Thr^{495}$ phosphorylation status. This suggests that our model was not sensitive enough to detect such changes, possibly requiring increased cell material. Thus, in line with previous studies, we decided to monitor $Ser^{1177}$ phosphorylation as a marker of eNOS activation.

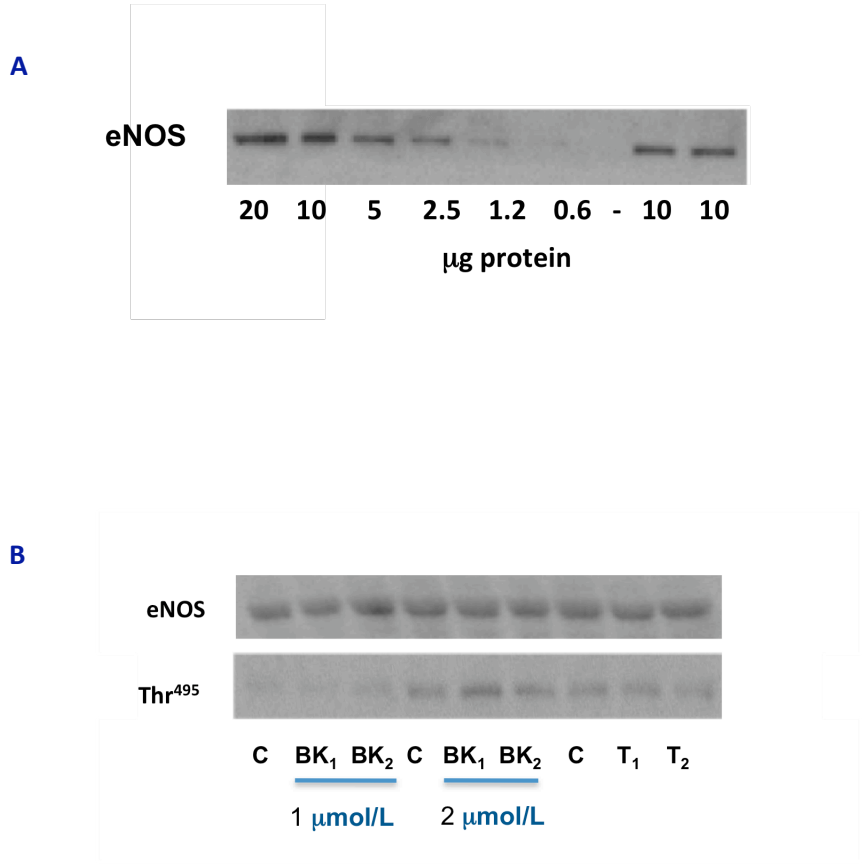


**Figure 5.8 Monitoring eNOS Thr$^{495}$ dephosphorylation from HUVEC**

HUVEC were brought to confluence in 6-well tissue culture plates in M199. HUVEC were serum-starved for 60 minutes and stimulated with solvent control or bradykinin and thrombin. **(A)** Capture of native eNOS using an anti-eNOS antibody raised against residues in the vicinity of Ser$^{600}$ in animals immunised with a keyhole limpet haemocyanin (KLH)-coupled synthetic peptide. eNOS protein was loaded onto the SDS-PAGE gel from 20-0.6 µg in 2x concentrated loading buffer or in two 10 µg aliquots in 5x concentrated loading buffer. **(B)** Detection of eNOS and phosphorylated eNOS at Thr$^{495}$. Where: bradykinin (BK), thrombin (T) (1 U/mL), control/untreated (C), ($BK_1$) 1 minute exposure to bradykinin, ($BK_2$) 2 minutes exposure to bradykinin, ($T_1$) 1 minute exposure to thrombin, ($T_2$) 2 minutes exposure to thrombin.

### *5.2.3.2 eNOS activation through phosphorylation of Ser$^{1177}$*

eNOS phosphorylation at Ser$^{1177}$ is arguably the most studied eNOS residue that affects its activation. Both Bk and thrombin stimulate phosphorylation of eNOS at Ser$^{1177}$ in a $Ca^{2+}$-dependent manner through $Ca^{2+}$/Calmodulin-dependent protein kinase II (CaMKII). Accordingly, we examined the effect of both agonists on their suitability to induce Ser$^{1177}$ phosphorylation in our HUVEC model. ASM can lead to decreased HUVEC $_{i}Ca^{2+}$ responses to thrombin **(Figure 5.9a).** To test the suitability of thrombin on eNOS Ser$^{1177}$ phosphorylation, HUVEC were again stimulated with both agonists for 2 minutes and the lysates were probed by immunoblotting for native eNOS and phosphorylated eNOS (peNOS) at Ser$^{1177}$. Bk is known to only weakly phosphorylate eNOS at Ser$^{1177}$ an observation witnessed in our experiments **(Figure 5.9b).** By contrast, thrombin stimulation led to more evident protein bands stained for peNOS-Ser$^{1177}$ compared to control un-stimulated cells. Due to greater eNOS responses, thrombin was chosen to study eNOS phosphorylation. HUVEC were then serum-starved in M199 and subsequently stimulated with thrombin in either M199 or HBSS suggesting that peNOS responses did not differ in HBSS allowing experiments to be undertaken in culture medium **(Figure 5.9c)**. During initial experiments Ser$^{1177}$ phosphorylated protein was evident by a double band as previously described in Bk stimulated cells (Fleming et al., 2001). The model was then tested for its suitability by observing background basal phosphorylation of eNOS at Ser$^{1177}$, the application of exogenous pASM (Sigma) on Ser$^{1177}$ phosphorylation, and eNOS responses to thrombin and the $Ca^{2+}$ ionophore ionomycin. Previous reports have shown that eNOS was only weakly phosphorylated at Ser$^{1177}$ during resting conditions (Motley et

al., 2007), confirmed in **figure 5.9d** making it distinguishable from agonist-stimulated protein. We then went on to explore the effect of exogenous ASM on eNOS activation.

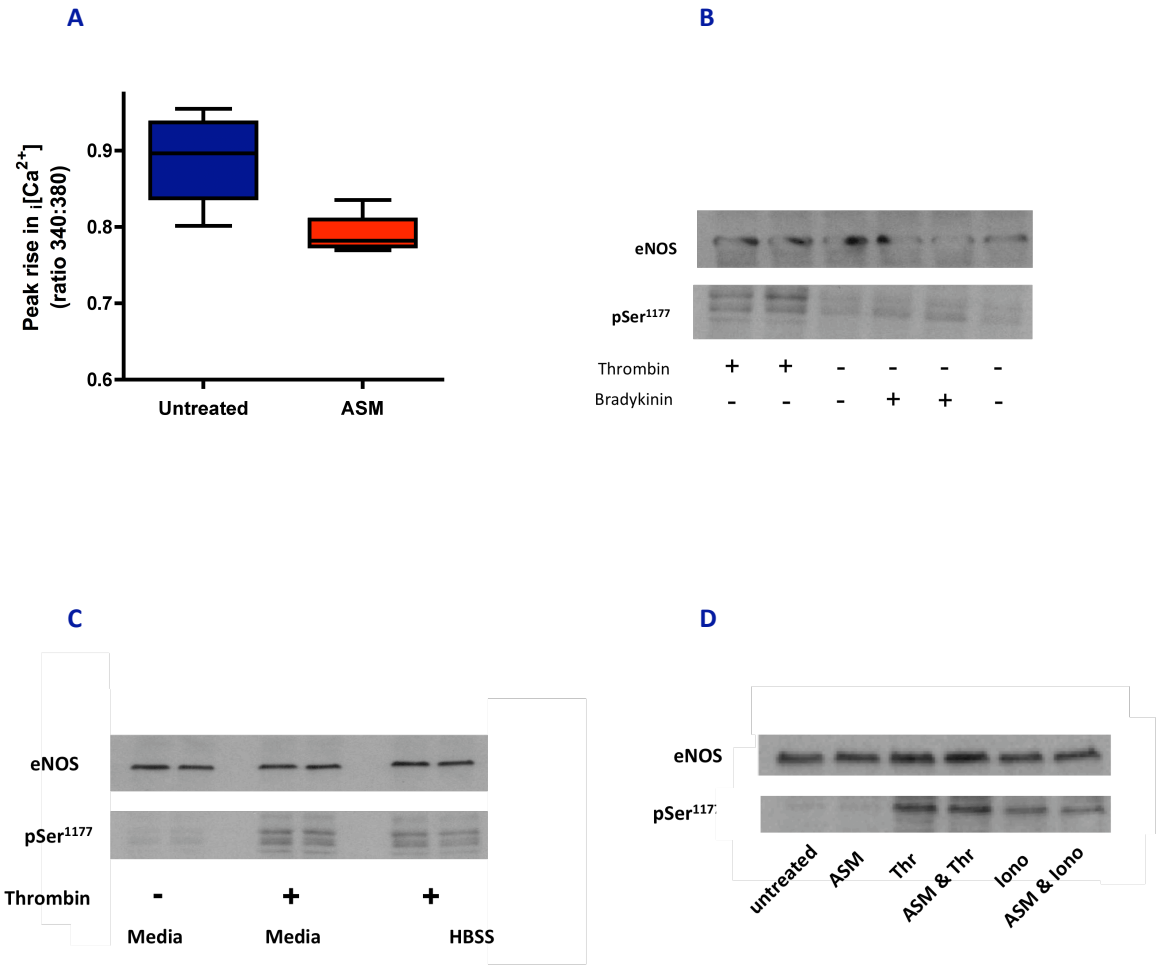


**Figure 5.9 Bradykinin and thrombin-induced phosphorylation of eNOS Ser$^{1177}$**

**(A)** HUVEC were seeded on glass coverslides for 24-48 hours. HUVEC were treated with exogenous ASM (1.25 U/mL) for 60 minutes and stimulated with thrombin (1 U/mL) to provoke $_{i}Ca^{2+}$ responses. Data represent four independent experiments (n=4). Panels **(B-D)** show the capture of eNOS in the region of Ser$^{600}$ and phosphorylated eNOS at Ser$^{1177}$. HUVEC were brought to confluence in 6-well tissue culture plates in M199, serum-starved for 60 minutes and stimulated with bradykinin or thrombin for 2 minutes. **(B)** HUVEC were stimulated with bradykinin (1 μmol/L) and thrombin (1 U/mL) for 2 minutes and the lysates probed for eNOS and phosphorylated eNOS. **(C)** HUVEC were stimulated with thrombin (1 U/mL) in culture medium and in HBSS buffer and the lysates probed for eNOS and phosphorylated eNOS. **(D)** HUVEC were treated with ASM (1.25 U/mL) for 30 minutes in serum-free M199 and stimulated with thrombin (1 U/mL) and ionomycin (Iono) (5.60 μmol/L) for 2 minutes.

### *5.2.3.3 The effect of ASM on phosphorylation of eNOS Ser$^{1177}$*

HUVEC were stimulated with a high dose of exogenous ASM (1.25 U/mL) to prevent the enzyme being a limiting factor**.** This closely reflected the mean activity of diseased patients. eNOS activation was described as increases in Ser$^{1177}$ phosphorylation, calculated as a ratio of β-actin-normalised, peNOS/eNOS **(Figures 5.10)**. Total eNOS levels did not differ between pASM pre-treated and untreated cells. ASM alone appeared to slightly increase Ser$^{1177}$ phosphorylation following 30 and 60 minute treatments. Pre-treatment with pASM for 30 minutes caused a 15.8% decrease in Ser$^{1177}$ phosphorylation compared to untreated cells thrombin stimulated cells **(Figure 5.10a)**. After 60 minutes however, ASM pre-treated HUVEC stimulated with thrombin exhibited an 18% increase in Ser$^{1177}$ phosphorylation compared to untreated, thrombin stimulated cells **(Figure 5.10b)**. This differs in comparison to 30 minute treatments where pASM appeared to decrease Ser$^{1177}$ phosphorylation but could be as a result of the lower magnitude of thrombin-induced phosphorylation. Ionomycin caused a 75% increase in Ser$^{1177}$ phosphorylation compared to unstimulated cells, however, this was 37% lower than thrombin stimulated cells (3-fold increase vs unstimulated cells) **(Figure 5.10a)**. Ionomycin provoked decreased eNOS responses compared to thrombin which could suggest an alternate signalling mechanism for thrombin. Interestingly, in some cases ionomycin led to decreased eNOS phosphorylation in ASM-treated cells compared to ionomycin alone, evident by the protein band intensity (phosphorylated Ser$^{1177}$)**.** This may indeed suggest a direct effect of ASM on HUVEC $Ca^{2+}$ regulation in EC. Taken together, ASM may differentially influence eNOS phosphorylation depending on the length of treatment.

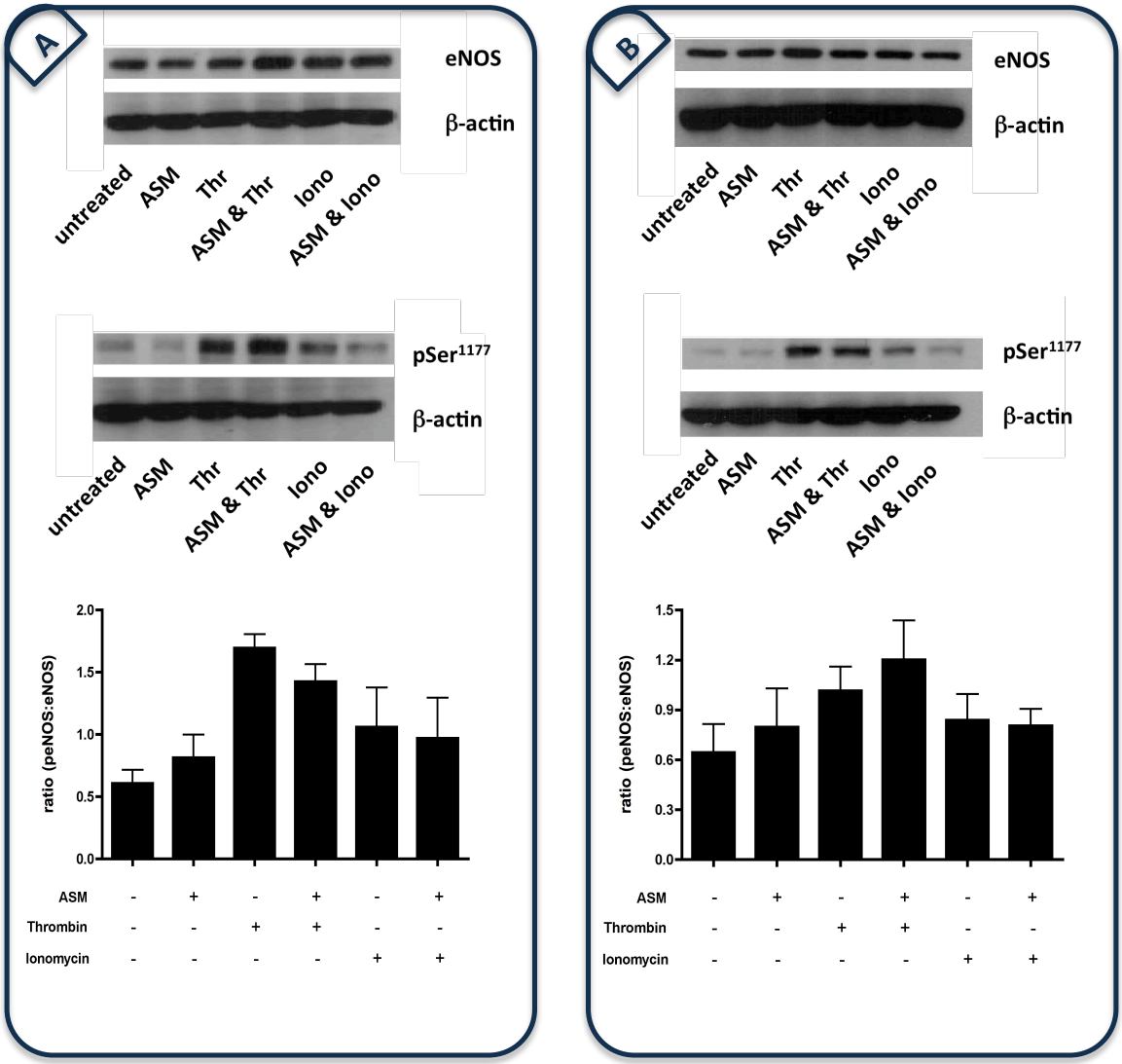


**Figure 5.10 ASM potentially regulates thrombin-induced phosphorylation of Ser$^{1177}$**

HUVEC were brought to confluence in 6-well tissue culture plates in M199 and serum-starved for 60 minutes. The cells were treated with exogenous ASM for **(A)** 30 and **(B)** 60 minutes and then stimulated with thrombin (1 U/mL) for 2 minutes. Capture of eNOS was performed using an antibody against eNOS in the region of Ser$^{600}$ and a separate antibody against phosphorylated eNOS at Ser$^{1177}$. The top panels of (A) and (B) show representative immunoblots of total eNOS, phosphorylated eNOS and β-actin. All lysates were normalised to β-actin showing levels of total eNOS (eNOS) and phosphorylated eNOS (pSer$^{1177}$). The column graphs represent the ratio of peNOS:eNOS. Data are means ± SEM of three independent experiments (n=3).

### *5.2.4 The effect of ASM on NO production in HUVEC*

More experiments are needed to clarify the observations in 5.2.3.3 including experiments performed in $Ca^{2+}$-free media to question the involvement of Cer in $Ca^{2+}$ influx inhibition. eNOS activation leads to the production of freely diffusible NO from EC. Bk and thrombin both activate eNOS leading to NO production in a $Ca^{2+}$-dependent fashion. Exogenous ASM previously inhibited Bk-induced $Ca^{2+}$ signals in our HUVEC model. Bk has been extensively studied in receptor-mediated eNOS activation and was used here to study the effect of exogenous ASM on NO production. HUVEC in 24-well tissue culture plates were serum starved for 1 hour in serum-free HESFM and treated with vehicle, pASM (1.25 U/mL), $C_2$-Cer (500 μmol/L) or nSMase (25 mU/mL) for 30 minutes. Nitric oxide in the media supernates was analysed in the gas phase using a Sievers NO chemiluminescence analyzer (Analytix, Sunderland, UK). Samples containing nitrates and nitrites alongside any NO, if present, are injected into a reflux chamber containing vanadium (III) chloride ($VaCl_3$) at $95^0$C. In the gas phase this reacts with ozone to form nitrogen dioxide ($NO_2^*$). In an excited state, the decay of $NO_2^*$ back to $NO_2^-$ (nitrite) emits a signal at 600 nm directly proportional to NO concentration (Kleinhenz et al., 2003). Pre-treatment with pASM and nSMase inhibited NO production by HUVEC stimulated with Bk compared to un-treated controls whereas HUVEC pre-treated with $C_2$-Cer were not affected **(Figure 5.11)**. This data may be in agreement with that in **figure 5.10a** indicating a decrease in eNOS activation by inhibition of $Ser^{1177}$ phosphorylation. More experiments are required to clarify this observation using $Ca^{2+}$-free media but also intracellular antioxidants such as PEG-superoxide dismutase to eliminate the possibility of ROS-induced NO uncoupling as the source of decrease NO production.

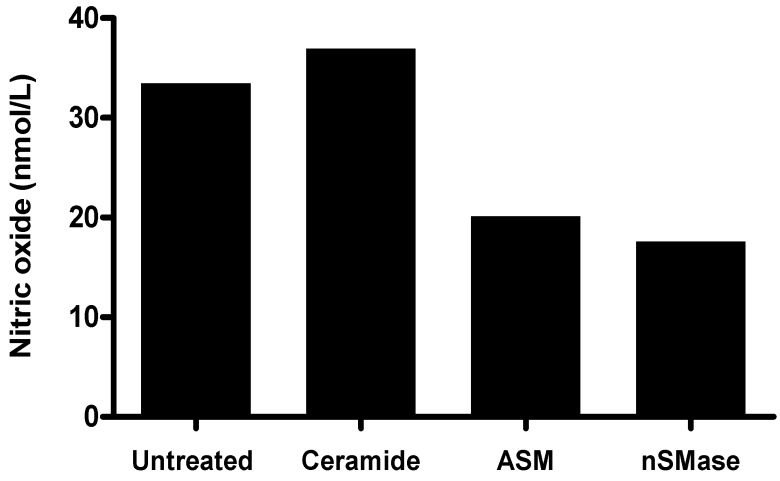


**Figure 5.11 ASM may decrease nitric oxide production from HUVEC**

HUVEC were brought to confluence in 24-well tissue culture plates, serum starved for 60 minutes and treated in HESFM containing with Cer (500 μmol/L), ASM (1.25 U/mL) and nSMase (25 mU/mL) or left untreated in fresh HESFM for 30 minutes. HUVEC were stimulated with bradykinin (1 μmol/L). Data are normalised to recordings of basal NO production from unstimulated solvent control HUVEC. Data are representative of one experiment (n=1) and show mean values of triplicate readings from technical triplicate wells in a 24-well culture plate.

## 5.3 Discussion

EC are a particularly rich source of ASM where both L-SMase and S-SMase can gain access to SM pools on the PM generating Cer, a bioactive lipid messenger that has diverse actions depending on the locus of stimulation (Gulbins and Li, 2006, Jenkins et al., 2010a). The aim of this chapter was to investigate the effect of exogenous ASM on EC signalling by looking at $_{i}Ca^{2+}$ signalling, eNOS activation and NO production.

SM metabolites are involved in housekeeping reactions but many of the pathways remain poorly understood. This is highlighted here due to their increasing pluripotency in downstream cell signalling. ASM has been shown to have a prominent role in apoptosis as $ASM^{-/-}$ mice showed defective apoptotic responses to TNFα signalling (Haimovitz-Friedman et al., 1997, Garcia-Ruiz et al., 2003). Interestingly, application of exogenous ASM led to melanoma cells becoming sensitised to irradiation in a dose-dependent manner, however, *in vitro*, this was evident only at low pH (Smith and Schuchman, 2008a). Due to these observations we investigated the effect of exogenous human ASM on HUVEC cytotoxicity and apoptosis. Our data showed that exogenous ASM does not cause necrotic cell death nor did it contribute to HUVEC apoptosis. One explanation is that intracellular stress responses to ASM come from stimulation of death ligands (FAS) (Sawada et al., 2002), or require co-stimulation with TNFα. Both these events however give rise L-SMase or nSMase activation, which differ in cellular location, generating different cellular responses compared to cell surface Cer.

Bk and thrombin were used to stimulate EC, acting through $\beta_2$ adrenergic receptors and Proteinase-Activated Receptors (PAR) respectively (Hirano et al., 2007, Mount et al., 2007). Their signalling pathways are complex but have similar endpoints. Bk (1 μmol/L) and thrombin (1 U/mL) both led to elevated $_{i}Ca^{2+}$ responses in HUVEC at concentrations deemed sufficient to elicit significant $Ca^{2+}$-dependent eNOS responses in HUVEC (Stahmann et al., 2006, Fleming et al., 2001, Harris et al., 2001), although lower concentrations of agonist have been previously used (David-Dufilho et al., 2005, Bao et al., 2010, Fleming et al., 2001). Pre-treatment of HUVEC with ASM resulted in decreased receptor-mediated agonist $_{i}Ca^{2+}$ responses. The effect of ASM on EC may be long lasting as shown by the maintained inhibition of $_{i}Ca^{2+}$ signals in EC following its removal. These data also suggest that the secreted fraction could provoke long lasting effects in its absence, supported recently by Jenkins et al., (2010a). The observation that $_{i}Ca^{2+}$ signals potentially affected by S-SMase$^{high}$ supernate transfer implies that secreted SMases could alter membrane properties on distal EC *in vivo*, supporting the concept for S-SMase-mediated diffuse ECD.

Distinguishing Cer species (C16, C24) and their region of aggregation (e.g. caveolae) would help to confirm the role of exogenous ASM. The precise mechanism of decreased $_{i}Ca^{2+}$ signalling was not addressed in this chapter but It is likely that ASM cleaves SM on the extracellular leaflet of the PM thereby generating Cer (Jenkins et al., 2010a). Three possible mechanisms exist for S-SMase access to SM pools including 1) secretion of S-SMase in a soluble form and access to outer leaflet plasmalemmal SM, 2) ASM translocation and incorporation into the PM outer leaflet or 3) association and transport

with LDL where it could access LDL-SM or is again released in a soluble form. SM is one of the most abundant lipids in the PM. The topology of Cer generation following SM cleavage by ASM has been co-localised with caveolae where it could alter membrane architecture in lipid rafts (LR) (Jin et al., 2008). Cer in LR has been associated with raft fusion creating large platforms found in close proximity to SOC channels such as $I_{CRAC}$ (Li and Gulbins, 2007). The depressed agonist-induced $_{i}Ca^{2+}$ responses observed here may indeed occur due to Cer interference with $I_{CRAC}$. SMases have been previously associated with inhibiting $_{i}Ca^{2+}$ signalling in T cells required for T cell activation. ASM has been shown to block $Ca^{2+}$ influx provoked by thapsigargin, ionomycin, FAS antibody binding, and TNFR1 activation by TNF$\alpha$ (Lepple-Wienhues et al., 1999, Breittmayer et al., 1994, Church et al., 2005). The first of such observations showed that TNF$\alpha$, SMase and Cer could block $Ca^{2+}$ influx into thyroid FRTL-5 cells. However, no evidence of increased Cer was seen and these experiments utilised a short-chain, water-soluble analogue of native Cer, $C_2$-Cer (*N*-acetylsphingosine), which can easily cross membranes (Tornquist et al., 1999). Most definite evidence for ASM/Cer blockade of $Ca^{2+}$ influx came from the use of $ASM^{-/-}$ cells (Lepple-Wienhues et al., 1999, Church et al., 2005), a mechanism supported by the emptying of ER $Ca^{2+}$ stores using the sarco/endoplasmic $Ca^{2+}$ pump (SERCA) inhibitor thapsigargin and chelating extracellular $Ca^{2+}$ with ethylene glycol tetraacetic acid (EGTA), to show that blockade of $Ca^{2+}$ influx was abrogated in the absence of ASM (Church et al., 2005). Similar experiments are required in order to address this in EC, however the requirement of $Ca^{2+}$ for EC adherence onto glass slides makes this problematic. This can be overcome by using EC in suspension questioning its physiological relevance due to EC being adherent cells.

To study the downstream effects of decreased $_{i}Ca^{2+}$ responses, eNOS $Ser^{1177}$ phosphorylation was used as a marker of its activation. Different stimuli provoke varied eNOS responses ($Ca^{2+}$-dependent/independent) and can lead to activation of the enzyme by translocation or phosphorylation (Park et al., 2009b, Chan et al., 2010, Pott et al., 2006, Dimmeler et al., 1999). eNOS activation is inhibited by anchorage to the PM at the intracellular catalytic domain of the plasma membrane $Ca^{2+}$ ATPase (PMCA). PMCA was thought to negatively regulate eNOS activity in HUVEC by increasing $Thr^{495}$ phosphorylation and slightly decreasing $Ser^{1177}$ phosphorylation, inhibiting NO production and keeping eNOS in low $Ca^{2+}$ microenvironments. This could then be reversed by CCE from $I_{CRAC}$, a process that could be inhibited by Cer (Holton et al., 2010).

Bk and thrombin were chosen as agonists because they have similar mechanisms of EC stimulation, activating eNOS in a $Ca^{2+}$/CaM, CaMKII and AMPK-dependent manner, independent of Akt activation, depicted in **figure 1.4** (Fleming et al., 2001, Motley et al., 2007, Thors et al., 2004, Michel and Vanhoutte, 2010). Bk-induced NO production, unaffected by PI3K inhibition, suggests that agonists of G-protein coupled receptors (GPCR) evoke eNOS responses independent of the PI3K/Akt/PKB pathway; whereas CaMKII inhibition which, abolished $Ser^{1177}$ phosphorylation and decreased cGMP accumulation suggested that CaMKII phosphorylates eNOS at $Ser^{1177}$ in Bk-stimulated EC (Fleming et al., 2001). Similarly, thrombin is also believed to work through a $Ca^{2+}$/CaM, CaMKII pathway that is PKCδ-sensitive, but is PI3K/Akt independent (Motley et al., 2007, Thors et al., 2004, Stahmann et al., 2006, David-Dufilho et al., 2005). Two pathways may therefore exist in *thrombin-mediated* eNOS activation including a) $Ca^{2+}$/CaMKII and b)

AMPK through AMP/LKB1 (LKB1 phosphorylates AMPK) **(Figure 1.4)**. Thus, thrombin-mediated eNOS activation may be either $Ca^{2+}$-dependent or energy-dependent, while there may also be two separate energy-dependent pathways involving an adenosine monophosphate/adenosine triphosphate (AMP/ATP) ratio (Stahmann et al., 2006, Thors et al., 2008). This could be a matter for consideration in subsequent assays.

Thrombin receptor-mediated eNOS activation requires both ER store and SOCE for $Ser^{1177}$ phosphorylation (Motley et al., 2007). $Thr^{495}$ dephosphorylation, another marker of eNOS activation, was not detected with the required sensitivity in our experiments confirming observations of greater $Thr^{495}$ responses in human dermal microvascular EC (HDMEC) compared to HUVEC (Holton et al., 2010). To a lesser extent than with Bk previously, ASM pre-treatment inhibited $_{i}Ca^{2+}$ responses stimulated by thrombin **(Figure 5.9a)**. This was accompanied by a small decrease in eNOS $Ser^{1177}$ phosphorylation after 30 minutes of ASM pre-treatment **(Figure 5.10a)**, which appeared to increase after 60 minutes **(Figure 5.10b)**. One possible explanation for this is offered by Cer, which was shown to activate eNOS in a $Ca^{2+}$-independent manner by inducing eNOS dissociation from the PM (Igarashi et al., 1999). Similarly, Cer metabolite sphingosine-1-phosphate (S-1-P), was also proposed to activate eNOS ($Ser^{1177}$) in an AMPK/PI3K/Akt manner (Igarashi et al., 2007, Igarashi and Michel, 2008). The studies by Igarashi et al. and Tornquist et al. however, again used exogenous *$C_2$-ceramide* that could easily diffuse across the PM whereas native, long-chain Cer is more hydrophobic and would not readily incorporate into bio-membranes (Chatelut et al., 1998, Venkataraman and Futerman, 2000). These approaches differ to ours, which used exogenous ASM, producing a theoretically PM-

incorporated long chain Cer, associated with caveolar-rich regions not bound to the same fate as $C_2$-Cer. However, Mogami et al., showed that application of nSMase (50 mU/mL) also led to increased eNOS translocation and phosphorylation at $Ser^{1179}$ also in a $Ca^{2+}$-independent manner (Mogami et al., 2005), suggesting that Cer generation by exogenous SMases could indeed increase eNOS phosphorylation through S-1-P (Barsacchi et al., 2003, Bulotta et al., 2001).

The precise mechanisms of Bk/thrombin-induced NO regulation are still being unraveled. A recent publication suggested that transient $Ser^{1177}$ phosphorylation by thrombin was not sufficient for significant NO production (Watts and Motley, 2009). $Thr^{495}$ phosphorylation is known to decrease eNOS activity and NO production. This, however, was shown to occur after $Ser^{1177}$ phosphorylation suggesting an auto-inhibitory mechanism. Importantly, these measurements were performed using a low sensitivity assay (Greiss) employing high concentrations of agonist (20 μM Bk, 10 U/mL thrombin). The authors also did not clarify why PAR-1 activation was shown to increase the inhibitory $Thr^{495}$ site not the stimulatory $Ser^{1177}$ site whereas the opposite occurred through PAR-2 activation (Watts and Motley, 2009), begging the question as to why thrombin as a PAR-1 agonist leads to increased $Ser^{1177}$ activation. Furthermore Bk, which usually acts through the $\beta_2$ receptor increasing NO production, has been suggested to increase $Thr^{495}$ activation through the $\beta_1$ receptor suggesting another auto-inhibitory function.

In this chapter, treatment of HUVEC with ASM and nSMase appeared to reduce NO production in response to Bk. More experiments are required to clarify the role of ASM

on NO mediated signalling in EC. Chemiluminescence detection of nitrites is considered the most sensitive method available with a lower detection limit of 1 pmol/L (Kleinhenz et al., 2003) and has been used successfully with EC (Al-Ani et al., 2006, Ahmad et al., 2006, Cudmore et al., 2006, Brien et al., 1996). In this chapter, however, the method was not without its shortfalls and repeated attempts to replicate our findings were thwarted by technical issues with temperature regulation as the assay depends on low working temperatures (>-12$^0$C).

Diaminofluorescein (DAF-2) is a highly specific and sensitive NO probe (2-5 nmol/L) (Chapter 2; 2.2.12.1) (Nakatsubo et al., 1998). It directly binds NO, which in the presence of $O_2$ forms the fluorescent triazolofluorescein compound DAF-2T. Due to the high autofluorescence of DAF, it had been proposed that the final concentration was kept low (<1 μmol/L) (Rathel et al., 2003). This was examined using NO donor NOC-9 with varying concentrations of DAF-2 (0.01-1 μmol/L) **(Appendices, figure A4, upper panel).** However, subsequent experiments using Bk to stimulate NO production suggested the assay lacked the required sensitivity to distinguish between background and agonist-stimulated NO production (**Appendices, figure A4 lower panel).**

Another method used for the direct detection of NO, incorporated an NO-specific electrode/sensor (World Precision Instruments, WPI, Stevenage, UK) with a reported sensitivity as low as 1 nmol/L (WPI). Nitric oxide rapidly diffuses and reacts with oxygen. It is believed that cell monolayers do not provide enough NO output to measure NO directly (Personal communication, Julian Williams, WPI). Several other caveats affect this method such as temperature-sensitivity and positioning of the electrode over an area where NO

*will* be produced in the cell monolayer. Thus, application of agonist must be in close proximity to the electrode. Agonist dilution across the monolayer can be done using a magnetic flea, however, this led to cell death. These factors create unstable background readings making it difficult to decipher NO responses from *in vitro* artefacts. Alternatively vascular tissue sections, commonly aortic patches or employing EC in suspension can be used in an attempt to increase cell yield the latter having questionable physiological relevance.

NO production by eNOS is a process tightly coupled to $_{i}Ca^{2+}$ mobilization (Nilius and Droogmans, 2001). SMase and Cer can both decrease $Ca^{2+}$ influx in Jurkat T cells (Church et al., 2005) suggesting that a similar mechanism in EC would decrease GPCR agonist-mediated NO production by inhibiting SOCE. Experiments that would benefit the studies in this chapter include looking at the effect of purified ASM and *ex vivo* S-SMase on $_{i}Ca^{2+}$ signalling in $Ca^{2+}$-free conditions to observe direct $Ca^{2+}$ influx, eNOS activation and NO production. Since Cer has been shown to increase $ONOO^{-}$ production through increased ROS, polyethylene glycol (PEG)-superoxide dismutase would allow one to assess the effect of Cer on ROS production (Zhang et al., 2002), delineating its role in $Ca^{2+}$ signalling. These experiments would provide a real insight into the role of EC-derived S-SMase.

Taken together, these data suggest that ASM does lead to decreased agonist-induced $_{i}Ca^{2+}$ responses, may affect eNOS activation and also downstream NO production. These results provide a novel insight into the effects of ASM on EC and where its extracellular activity may generate locus-specific Cer in the PM altering membrane dynamics.

# Chapter 6

# General Discussion

# 6 General discussion

Chronic autoimmune inflammatory diseases such as PSV and RA are associated with an increased incidence of CVD often manifesting as accelerated atherosclerosis. The initiating mechanisms underlying the development of atherosclerosis remain unclear. Vascular inflammation in PSV and RA has been shown to induce ECD and loss of NO production. Ceramide (Cer) produced by sphingomyelinase activated during vascular inflammation is a potent regulator of membrane dynamics altering biophysical properties of the PM, interfering with $Ca^{2+}$ influx channels and downstream EC signalling. Thus we hypothesised that vascular inflammation induced the secretion of SMase, which could cause diffuse ECD through Cer generation inhibiting $Ca^{2+}$-dependent NO production.

This thesis investigated the presence and activity of peripheral blood S-SMase from patients with AASV and RA against healthy controls. We subsequently attempted to elucidate the effects of exogenous ASM on endothelial function *in vitro* by concentrating on sequential HUVEC intracellular $Ca^{2+}$ mobilization, eNOS activation and NO production, signalling pathways that contribute to endothelial dependent vasorelaxation.

To our knowledge this study is the first to document raised S-SMase activity in rheumatic disease detected in 4 independent AASV cohorts and an established RA cohort. In a cross-sectional AASV cohort, S-SMase correlated with accumulated organ/tissue damage whilst in serial samples S-SMase levels fell by 14 weeks following treatment and continued to fall by at least 6 months in patients with established remission. In the RA cohort, S-SMase levels were raised compared to controls and correlated with various CVD risk factors including raised lipid profiles, smoking and several CV risk algorithms. These

results suggest a link for circulating active S-SMase in the process of vascular dysfunction. *In vitro*, key inflammatory mediators such as IL-1β and TNFα but not IL-6 induced the secretion of active S-SMase while application of exogenous ASM was able to decrease $_{i}Ca^{2+}$ signalling in EC, alter eNOS activation and NO production.

**The TNFα/S-SMase axis in chronic inflammation.** TNFα is a pivotal inflammatory marker that has also been shown to drive the disease process in chronic rheumatic diseases. Models of acute systemic inflammation using LPS have been shown to activate S-SMase *in vivo* through TNFα, while other inflammatory mediators including IL-1β and IFNγ are capable of directly inducing S-SMase release *in vitro* (Wong et al., 2000). IFNγ, IL-1β and TNFα are present in atheromatous disease. We found that TNFα could directly induce S-SMase release from EC while its effect was blocked using anti-TNFα antibody infliximab; suggesting that in areas of acute and chronic inflammation, TNFα-induced S-SMase release from EC could act as a secondary messenger and potential marker of endothelial activation.

The specificity of the induction of S-SMase release from EC is intriguing. LPS causes TNFα but also IL-1β production via the IL-1 converting enzyme (ICE; caspase-1), which in turn can induce the release of other inflammatory cytokines such as IL-1β and IL-6. LPS also leads to IL-6 production however, only TNFα, IL-1β, IFNγ but not IL-4 or IL-6 can mediate S-SMase release from EC (Kishimoto, 2005, Marathe et al., 1998, Wong et al., 2000, Feldmann and Pusey, 2006). Data from chapter 4 reveal that TNFα is a potent direct inducer of S-SMase secretion from EC, a process that may readily occur in inflammatory diseases. The precise mechanism of TNFα-mediated activation and

secretion of S-SMase is not known. ASM mRNA induction was observed in non-quiescent cell states such as monocyte to MΦ, and drug-induced leukemic cell differentiation mediated by transcription factors Sp1 and AP-2 (Langmann et al., 1999, Murate et al., 2002). Increased ASM transcripts were also observed following long-term incubation of DU145 prostate cells with the chicken anaemia virus apoptin (Liu et al., 2006) and in murine models of obesity (Samad et al., 2006, Shah et al., 2008). To date there is limited evidence for transcriptional up-regulation of ASM mRNA by IL-1β which was recently confirmed in MCF-7 cells (Marathe et al., 1998, Jenkins et al., 2010a). However, similar findings with TNFα are lacking. This is due to the other adverse signalling events leading from TNFα stimulation including apoptosis. Given that TNFα induces a latent significant surge of ASM secretion after 10 hours, it is logical to assume that this may involve induction of transcription while evidence exists for a positive feedback loop as Cer, sphingosine and S1P can upregulate TNFα mRNA contributing to the inflammatory process, possibly promoting further ASM activation (Samad et al., 2006).

**Site of action of S-SMase & physiological significance.** How can S-SMase gain access to SM pools? One option is that S-SMase is secreted and internalized in non-host cells (not secreting) where it meets internal leaflet SM on the PM. Another option is that S-SMase is secreted and hydrolyses outer leaflet SM. As SM is mostly found on the outer plasmalemmal leaflet, S-SMase would gain access to an abundant source of SM explaining its active secretion (Schuchman, 2010). Downstream metabolites of SM hydrolysis such as S1P were shown to have pro-survival effects (Spiegel and Milstien, 2003). Similarly S-SMase may also contribute to cell remodeling by facilitating endocytosis of wounded

PMs. Here ASM in vesicles of new membrane can fuse with the PM, releasing ASM into the extracellular space (Tam et al., 2010). The precise physiological role of the S-SMase variant remains unclear. Although present in the arterial trees, venous predominance could provide a role by stunning EC, preventing overt vasodilation and diminishing venous flow restricting return; thus preventing blood from leaving the inflammatory site facilitating local hypertension, altering local barrier function and adhesion molecule expression.

**The importance of Cer in orchestrated cell signalling.** SMase may hold a critical position in cell governance whereby different variants exist in different cells executing highly varied tasks. A prime example is cell death where Cer generation is required for signalling efficiency. Cer alters membrane fluidics causing death receptor clustering which provides a significant concentrated response rather than diffuse signals across the PM, the resulting signals culminating within the same spatial topology (Grassme et al., 2001, Gulbins and Grassme, 2002, Dumitru and Gulbins, 2006). Plasma membrane platform formation is an intriguing mechanism to explain the efficiency of upstream PM receptor signalling. Despite great efforts however, uncertainty remains over how, when and how much ASM is required for Cer-rich raft and platform formation.

**Contribution of S-SMase/Cer to ECD.** ECD is not an 'all-or-nothing' phenomenon thus no single event contributes to vascular dysfunction. The mechanisms behind the initial step in atherosclerosis are supported on a variety of platforms including abnormal lipid profiles (LDL/HDL), increased oxidative stress, enhanced EC apoptosis, thrombophilia, presence of immune complexes, and increased mononuclear cell infiltration into the sub-

endothelium causing local generation of cytokines and ECD (Haskard, 2004, Gonzalez-Gay et al., 2008). However to date the initiating mechanism, if one predominates, has not been elucidated. S-SMase has been incorporated in an elaborate model shaped by Tabas and Williams to describe a process to support the early steps of atherogenesis. This was coined the 'response-to-retention' (RTR) model (Williams and Tabas, 1995) where increased sub-endothelial LDL retention could be mediated at least in part by S-SMase (Tabas, 1999, Tabas et al., 2007).

Sphingolipids were first associated with atherosclerosis 40 years ago (Portman and Alexander, 1970). Sub-endothelial lipid aggregation is a major contributing factor in atheroma formation. In the RTR model, the role of S-SMase lies within facilitation of LDL retention in the intimal layers of vessels (Xu and Tabas, 1991). S-SMase alongside lipoprotein lipase (LpL) and secretory phospholipase $A_2$ ($sPLA_2$) are among the studied non-matrix proteins involved in atheroma formation with LpL and S-SMase thought to work in a synergistic manner in LDL retention (Tabas et al., 1993). Treatment of LDL with SMase was shown to increase LDL aggregation due to hydrolysis of LDL-SM, facilitating uptake by MΦ (Xu and Tabas, 1991, Schissel et al., 1996b). S-SMase can hydrolyse native plasma LDL at acid pH only, but can hydrolyse lesional LDL efficiently at neutral pH, providing a physiological means behind this theory (Schissel et al., 1998a). A causal link for S-SMase was provided in a recent paper by Devlin et al., (2008) whereby *Ldlr*$^{-/-}$ and *ASM*$^{-/-}$ mice showed decreased arterial lesional areas, lower total cholesterol (unchanged HDL-cholesterol), and decreased LDL retention (Devlin et al., 2008). This S-SMase involvement is believed to arise through cytokine-mediated secretion, which can occur basolaterally in EC towards the intimal layer (Marathe et al., 1998). The SM-Cer pathway

is tightly involved in oxidized-LDL (oxLDL) induced SMC proliferation (Auge et al., 1996), which may sustain the latent stages of atherosclerosis. A caveat however, comes from Niemann-Pick disease (NPD) patients who exhibit altered lipoprotein profiles even though they lack ASM, lending support for an alternative mechanism behind accelerated atherogenesis involving ECD.

Although S-SMase was convincingly associated with sub-endothelial lipid retention it does not adequately explain early physiological changes in endothelial responses such as decreased blood flow. We proposed a mechanism that may precede these lipid abnormalities. A process potentially induced and propagated by inflammation and immune dysregulation. TNF$\alpha$ is of particular interest as it has been shown to decrease eNOS mRNA degradation (Yoshizumi et al., 1993). Wang et al. first showed that TNF$\alpha$ impairs endothelial responses to ACh (Wang et al., 1994). Soon after, early studies linked the presence of infection and acute inflammatory responses to endotoxin with EC stunning (Bhagat et al., 1996). TNF$\alpha$ is also associated with ECD through impairment of EDV responses to Bk and vasodilator prostanoid arachidonic acid (Bhagat and Vallance, 1997), and though a follow-up study from this group using typhoid vaccination failed to show a link with a particular cytokine, it revealed 'diffuse ECD' in the brachial artery distal to the gluteal muscle vaccination (Hingorani et al., 2000).

The SM:Cer pathway is particularly regulated by TNF$\alpha$, a signaling cascade that is characterised by its pleiotropism and upstream ubiquity in cell signalling. Governed through the SMase family of enzymes, cells elicit different responses depending on the stimulus and topology of SMase activation. Our increasing understanding of this pathway places it central to many pathophysiological conditions including atherosclerosis

(Alewijnse and Peters, 2008, Smith and Schuchman, 2008b). Cer generation in the PM results in the reorganisation of PM architecture. SM hydrolysis creates Cer-rich LR that can aggregate forming larger membrane platforms (Holopainen et al., 1998, Zhang et al., 2009b) resulting in the clustering and concentration of membrane signaling receptors and proteins involved in cell death, proliferation and differentiation (Gulbins and Grassme, 2002, Zhang et al., 2009b, Zhang et al., 2008). Our *in vitro* data also suggests that Cer, once generated in the PM, may decrease $Ca^{2+}$ signals for at least 3 hours, consistent with previous reports that Cer has long-lasting effects on PM architecture (Gulbins and Li, 2006, Li and Gulbins, 2007). Various stimulatory signals have been shown to inhibit SOCE including FcgRII cross-linking in B cells (Choquet et al., 1993) and PKC activation (Parekh and Penner, 1995). SMases have also been reported to inhibit $Ca^{2+}$ signals in response to CD3 stimulation in Jurkat T cells and TNF$\alpha$ in thyroid cells (Tornquist et al., 1999, Breittmayer et al., 1994) whereas, CD95 stimulation in T cells was shown to block $I_{CRAC}$ in an ASM-dependent manner (Lepple-Wienhues et al., 1999). Importantly, the Cer metabolite sphingosine could also directly inhibit voltage operated $Ca^{2+}$ channels in pituitary cells and $I_{CRAC}$ in basophils (Titievsky et al., 1998, Mathes et al., 1998). Similarly, $C_2$-Cer also inhibited $Ca^{2+}$ influx possibly due to its ability to readily cross the PM, suggesting an important requirement for *in situ* hydrolysis of SM within the PM (Mathes et al., 1998). In a recent study from our group, TNF$\alpha$-mediated depression of $Ca^{2+}$ signals occured through ASM activation and generation of Cer, events abrogated in *ASM*$^{-/-}$ T lymphocytes. Furthermore, Cer was able to inhibit $Ca^{2+}$ influx following ER store $Ca^{2+}$ emptying using thapsigargin (Church et al., 2005). This event may plausibly occur in other non-excitable cells such as EC that share similarities in $Ca^{2+}$ influx, proposed in **figure 6.1**.

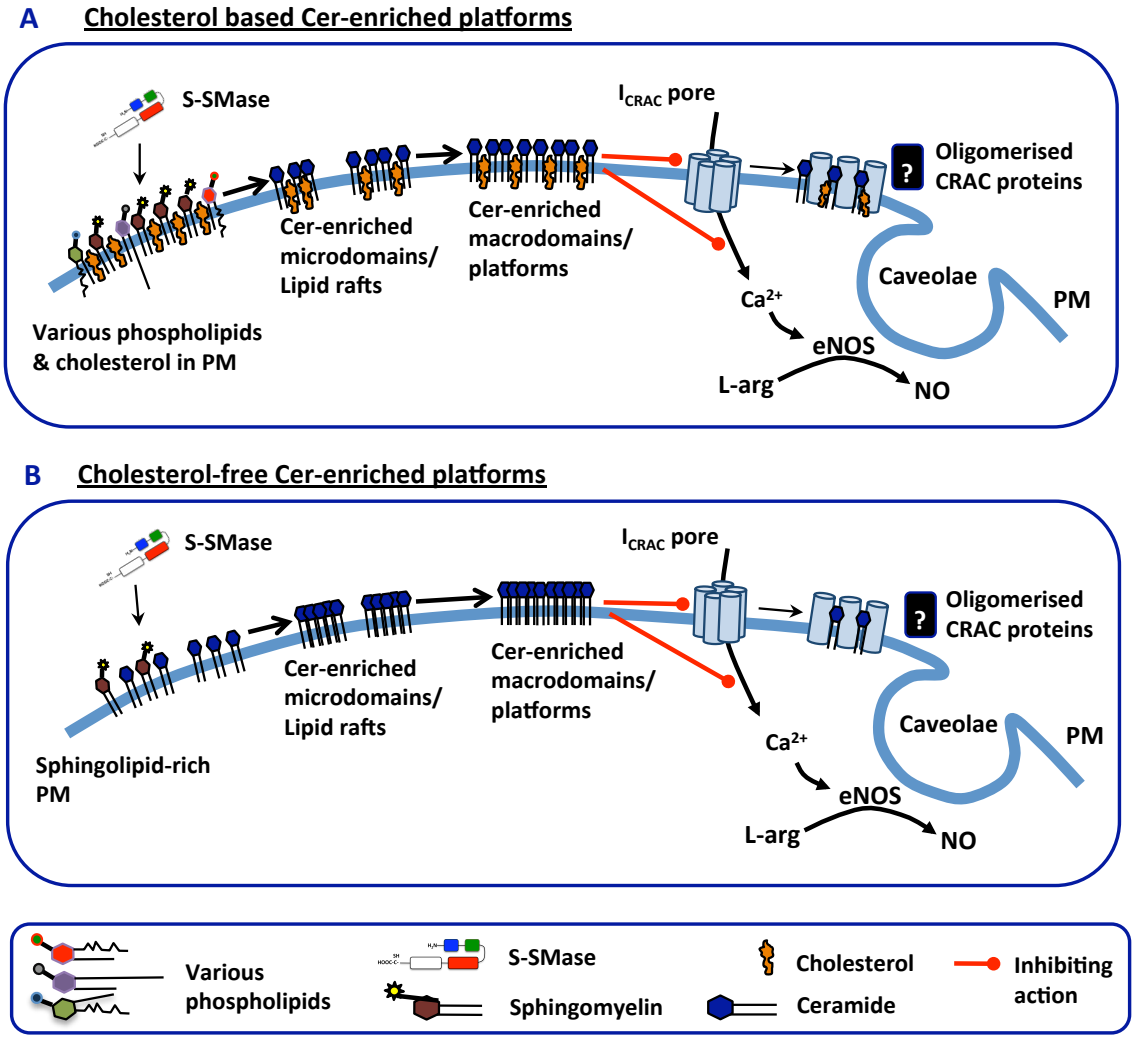


**Figure 6.1 Hypothetical role of S-SMase and ceramide in the disruption of $_{i}Ca^{2+}$ signalling in endothelial cells**

Secretory sphingomyelinase (S-SMase) may hydrolyse sphingomyelin (SM) on endothelial cell outer membranes giving rise to ceramide (Cer). Due their biophysical characteristics Cer oligomers pack tightly together forming lipid rafts (LR). **(A)** Cer-enriched LR can arise in cholesterol and sphingolipid rich areas of the plasma membrane. The hydrophobic Cer species in SM closely interact with cholesterol rings creating tightly packed structures (microdomains, LR) that exist in a more rigid state than normal plasma membrane fluidics. Due to the behaviour of Cer, these LR can fuse with other Cer-enriched LR yielding larger Cer-enriched macrodomains or platforms. **(B)** Cer-enriched LR can also be cholesterol-free, arising from SM molecules not within traditional sphingolipid/cholesterol-rich LR or even from *de novo* ceramide synthesis thus also excluding cholesterol**.** Cer-enriched LR are distinct from caveolar-based LR however, Cer-enriched platform formation may occur close to caveolae **(A,B)**. Calcium channels such as $I_{CRAC}$ are found in close proximity to caveolae thus S-SMase-induced Cer-enriched platform formation adjacent to caveolae may affect $Ca^{2+}$ influx by interfering with $Ca^{2+}$ channel integrity.

Signalling units relying on $Ca^{2+}$ influx such as eNOS, are associated with caveolae. Thus altering $Ca^{2+}$ influx may have downstream effects on eNOS regulation and NO synthesis (Fleming and Busse, 2003, Fleming, 2010). SOCE generates local $Ca^{2+}$ microdomains, areas of high $Ca^{2+}$ concentration, often occurring in close vicinity to caveolae and PM-anchored eNOS, facilitating enhanced intracellular signalling of this $Ca^{2+}$-dependent protein (Lin et al., 2000). Cer was previously reported to mediate vasodilation as $C_2$-Cer, however the authors did not rule out the role of S1P (Johns et al., 1998). The precise effect of Cer on eNOS itself remains controversial and has been suggested to activate the enzyme in a $Ca^{2+}$-independent manner (Bulotta et al., 2001) possibly through TNF$\alpha$-mediated nSMase activation (Barsacchi et al., 2003), however since Cer inhibits Akt kinase it may also significantly impair eNOS phosphorylation and therefore inhibit its activation (Schubert et al., 2000, Bourbon et al., 2002, Zhou et al., 1998). Since eNOS activation in response to G-protein coupled receptors (GPCR) agonists is largely dependent on $Ca^{2+}$ one could convincingly argue a role for Cer in NO regulation here.

My thesis reveals for the first time that exogenous ASM can directly decrease $Ca^{2+}$ mobilisation in EC and provides a hint for altered NO signalling, a classical feature of ECD. As a system however, these findings are likely to complement others indicating that Cer generation and ROS production indirectly diminish NO production (Zhang et al., 2001, Zhang et al., 2002, Zhang et al., 2003, Li et al., 2002). Importantly, $ONOO^-$ formation is favored as $O_2^-$ will readily react with NO rather than SOD (Cai and Harrison, 2000); thus asking does $Ca^{2+}$ inhibition or $ONOO^-$ formation lead to greater NO diminution? Given the susceptibility of ASM to oxidation, one may envisage ASM being activated by ROS producing Cer to create LR. This would activate NADPH oxidases increasing ROS

generation thus further enhancing ASM activation (Jin and Zhou, 2009). The most important remark however is that Cer is a versatile molecule that exerts very specific actions depending on its topology, the SMase that produced it and importantly the upstream stimulant of that SMase activity.

Much like $Ca^{2+}$, information about the effects of Cer might be contained in the frequency and amplitude of the intracellular signal itself (Parekh, 2008a). These events depend on the intracellular topology of Cer generation (PM, nuclear membrane, cytosolic cleavage), which may give rise to intracellular messengers or proteins (S1P, sphingosine) or remain as Cer and translated into specific responses. Such responses vary from Cer-derived apoptosis to S1P-derived proliferative signals (Igarashi and Michel, 2008, Ogretmen and Hannun, 2004). Thus the actions of Cer may resemble the pluripotency of intracellular $Ca^{2+}$ signals and their effects depending on cellular topology (Clapham, 2007).

The contribution of S-SMase may also lie beyond LDL retention and NO dysregulation. $Ca^{2+}$ signalling in EC is important for adhesion molecule expression, but also cell viability as $Ca^{2+}$ is vital for mitochondrial function. Inhibition of NO yields a pro-retentive endothelium, opening a place for S-SMase in atherogenesis thus inhibition of $Ca^{2+}$ signalling from S-SMase may have wide-ranging effects. A further clue supporting an alternative mechanism comes from the increased IMT seen in GPA patients, independent of traditional risk factors including LDL (de Leeuw et al., 2005). However, this may not account for retained LDL. It is likely LDL retention contributes to ECD alongside NO dysregulation and both may share an S-SMase link. Thus it is feasible that S-SMase may

play a role in part of the initiating mechanism of ECD and propagates atherogenesis by interfering with sub-endothelial lipid deposition.

**Beyond $Ca^{2+}$ dependence: low anti-oxidant capacity in chronic inflammation, S-SMase and ECD**. There is strong evidence for the involvement of oxidative stress in chronic inflammatory disease and CVD. Both nSMase and ASM isoforms have been previously associated with an element of redox-mediated amplification of enzymatic activity (Liu and Hannun, 1997, Liu et al., 1998, Claus et al., 2005, Qiu et al., 2003). GSH was first associated as a biological inhibitor of nSMase (Liu and Hannun, 1997), however this was not the case with L-SMase specifically, in which chemical reducing agent dithiothreitol (DTT) was favorable (Liu and Hannun, 1997). However a pivotal paper by Qiu et al. showed that recombinant ASM could be activated by oxidation or mutation of its terminal cysteine (Qiu et al., 2003). To our knowledge this thesis outlines the first example of examining the redox manipulation of native EC-derived S-SMase *ex vivo* and *in situ*.

Our investigations although not achieving the desired clarity, described an upward shift in S-SMase activity in the presence of $H_2O_2$ suggesting it may also be susceptible to regulation by oxidative stress. This finding may be of significance for ECD during inflammatory conditions with low antioxidant capacity. Previous unpublished material from our group found decreased GSH levels in peripheral blood and synovial fluid T cells of RA patients. EC, a rich source of ROS (Cai and Harrison, 2000), are likely to also exhibit decreased anti-oxidant capacity and therefore loss of vascular function (Landmesser et al., 2002). Increased ROS production by MΦ and neutrophils, raised peroxidation

products and decreased plasma GSH are found in RA and heart failure (Karatas et al., 2003, Seven et al., 2008, Tang et al., 2007, McMurray et al., 1993, Keith et al., 1998). The increased ROS/GSH ratio could predispose to increase S-SMase activation through terminal $Cys^{629}$ oxidation. Cer itself has been shown to increase eNOS expression but also lead to ROS generation reducing NO bioavailability in EC (Li et al., 2002). SM hydrolysis leading to Cer-derived ROS generation may further contribute to ECD by $ONOO^-$ formation, decreased eNOS-$BH_4$ availability and increased eNOS uncoupling. Critical to GSH cycling is ascorbic acid, which can also maintain the downstream eNOS-$BH_4$ stoichiometry (Heller et al., 2001, Huang et al., 2000) whereas vascular function has been shown to improve following vitamin C infusion in CHF and Behcet's disease (Chambers et al., 2001, Landmesser et al., 2002).

Given the susceptibility of S-SMase to redox-imbalance, oxidative stress could be expected to contribute to ECD by directly diminishing NO levels; an elaborate feedback loop is formed that involves TNF$\alpha$, S-SMase, and Cer production inducing ROS generation and/or upstream inhibition of $Ca^{2+}$ influx through Cer-mediated blockade of PM $i_{CRAC}$ channels leading to decreased $Ca^{2+}$-dependent NO production. Thus an imbalance of cytokine expression and redox dysregulation may contribute to ECD.

**Vascular inflammation, S-SMase and accelerated atherosclerosis**. The key question asks why there is increased cardiovascular mortality in PSV and RA that cannot be fully explained by traditional cardiovascular risk factors (Del Rincon et al., 2001, Solomon et al., 2003)? Synovitis in RA is a primary site of inflammation from which TNF$\alpha$, IL-1$\beta$, IFN$\gamma$ and IL-6 can enter the circulation. One of the caveats of using RA patients is

that the primary synovitis may obscure the vascular inflammation often found in RA. Rheumatoid vasculitis may be driven by activation of synovial fibroblasts, T cells and MΦ in RA all of which secrete TNFα. To date there are no surrogate markers for active vascular damage and the effects of S-SMase and Cer on vascular function have not been explored in relation to disease activity in chronic inflammation. This study set out to investigate the presence and activity of S-SMase in PSV and RA in relation to rheumatic and cardiovascular disease parameters. As a model, primary vasculitis, the archetypal form of idiopathic vascular inflammation has been shown to feature enhanced atherogenesis.

S-SMase previously correlated with disease severity in CHF when compared to the New York Heart Associated functional class. However this was not the case in our cohorts using the BVAS or DAS-28 in AASV and RA respectively. In the CHF patients, serum S-SMase levels correlated with impairment of vasodilator responses measured by forearm post-ischaemic blood flow (Doehner et al., 2007). Interestingly, local vascular inflammation has been shown to also target distant unaffected vessels. ECD in PSV was shown to be widespread and diffusely present in different vascular beds. Filer et al., (2003) revealed that ECD occurred independently of ANCA status and renal involvement, essentially regardless of the site of involvement of the primary vasculitis, suggesting that it could be brought about as a result of overt vascular inflammation. Although anti-TNFα and anti-IL-1 treatment was shown to significantly improve vascular function regressing ECD (Booth et al., 2004b, Ikonomidis et al., 2008), this thesis did not reveal an association between TNFα levels and S-SMase in AASV patients before and after treatment. This is probably owed to the transient nature of anti-TNFα regimens, the small

group of patients on infliximab and the presence of other inflammatory markers (IL-1β, IFNγ).

Suppression of disease activity (BVAS) in our AASV cohorts was not associated with S-SMase activity. However cross sectional sampling was performed early in the clinical response (w14) where It is known that prolonged treatment is required to prevent early relapse even after 1 year. Thus S-SMase levels may be a marker of endothelial damage as supported by its correlation with the VDI rather than of active inflammation. The RA studies in this thesis suggest that S-SMase correlates with established damage and CV risk factors in RA. S-SMase levels might be best compared in relation to CVD complications that affect PSV. A clue for the lack of relationship between S-SMase, disease activity and pro-inflammatory cytokine levels is the apparent prolonged half-life of S-SMase *in vitro* (Jenkins et al., 2010a). As its transience *in vivo* and the kinetics have not been described in relation to inflammatory disease, the question arises, what is the half-life of S-SMase in the circulation? If S-SMase is secreted during disease flares, and persists even after disease activity has clinically regressed it remains difficult to retrospectively translate enzymatic to disease activity.

These data do not provide a causative link of S-SMase with the disease process but provide clues for S-SMase in clinical disease and EC dysregulation. Thus S-SMase may be a novel biomarker directly relating to vascular damage and given its source may prove a unique indicator of endothelial dysfunction. The above suggest that S-SMase is worth examining in detail, in longitudinal prospective studies as the link with ECD and therefore predictive value of CV complications is intriguing.

## 6.1 Future directions arising from this thesis

**Prospective clinical approach.** The study of ASM blood levels in patients warrants further work, and would benefit from a prospective study of the presence and temporal changes of S-SMase in clinical disease. This should include well-characterised cohorts inclusive of PSV patients with small, medium and large vessel involvement. RA cohorts with early and established disease would be of particular interest while it would be valuable to look at patients with other systemic inflammatory involvement such as Behcet's disease and SLE. S-SMase data would benefit from vascular function analyses in patients to help validate it as a novel and useful marker of vascular disease activity and damage.

**The effect of TNFα on ASM mRNA expression**. From the work here it is not certain how TNFα regulates ASM secretion. If it is through induction of transcription, a study of mRNA expression of ASM in EC in relation to the timing of its secretion will help clarify its association with disease activity in clinical disease. While inflammation is present in chronic active disease, remission and acute flares may affect S-SMase activity. Assessment of the relationship between TNF, disease activity and ASM will allow more clarity of S-SMase biology and further validate its use as a diagnostic/prognostic marker.

**The effect of S-SMase on spatial and temporal molecule association in the PM**. It remains unknown how S-SMase accesses pools of SM in the PM. Immunohistochemical studies of ASM translocation and secretion would enable us to understand the topology of ASM action on the EC surface. To elucidate the role of Cer formation in rafts and its association with $Ca^{2+}$ channels, co-localisation of ASM at caveolae and Cer generation in

LR would be made possible through immunoblotting for ASM with raft markers (ganglioside GM1 & CTXB) and caveolin preparations. Fluorescence resonance energy transfer (FRET) analysis would provide an insight into disruptions of protein interactions e.g. $I_{CRAC}$ components, Orai proteins.

**Does ASM inhibit $_{i}Ca^{2+}$ signalling specifically through blockade of SOCE?** In lymphocytes it has been shown that SMase and Cer block $Ca^{2+}$ entry. That this process occurs in EC needs to be confirmed to address whether Cer can inhibit NO production by decreasing $Ca^{2+}$ availability or through generation of $O_2^-$ and subsequent $ONOO^-$ formation, or both? Studies would focus on depleting intracellular stores of $Ca^{2+}$ using thapsigargin in an extracellular $Ca^{2+}$-free medium. Upon addition of $Ca^{2+}$ into the medium, SOCE would be compared between treated and untreated cells with those affected by channel blockade exhibiting decreased $Ca^{2+}$ influx. Similar studies should be performed for NO assays. Employment of PEG-SOD (intracellular $O_2^-$ scavenger) would help differentiate between eNOS uncoupling due to ROS and decreased eNOS activity due to $Ca^{2+}$ inhibition. These studies could use a cGMP assay as a surrogate marker for NO production, measure GSH levels as a marker of antioxidant capacity and ROS as a marker of oxidative stress.

**Effect of ASM on adhesion molecule expression**. Given the importance of $Ca^{2+}$ in membrane dynamics and adhesion molecule expression, ECD can also be expressed as altered adhesion molecule expression e.g. E-selectin. This would impact on leukocyte migration and affect the immune response in atherosclerosis. Redistribution of these and other membrane proteins between the SM-rich caveolae and plasma membrane would also be relevant, perhaps highlighting other receptor-mediated pathways affected in EC.

# Publications arising from thesis

## Abstracts

Kiprianos, A., Little, M., Morgan, M., Harper, L., Savage, C., Bacon, P., Young, S., (2011) 'Elevated active secretory acid sphingomyelinase activity in ANCA associated vasculitis' *Clinical & Experimental Immunology,* (*expected May, 2011*).

Kiprianos, A., Church, L., Little, M., Savage, C., Bacon, P., Young, S., (2010) 'Serum acid sphingomyelinase as a marker and mediator of vascular damage', *Rheumatology*, 49 (S1) i122-i124, 233

Kiprianos, A., Church, L., Ahmad, S., Little, M., Savage, C., Bacon, P., Young, S., (2009) 'Acid sphingomyelinase as a marker of vascular damage in vasculitis' *APMIS*, 117 (S127): 130–133

## Research articles

Kiprianos, A., Little, M., Morgan, M., Harper, L., Savage, C., Bacon, P., Young, S., (2011) 'Active secretory acid sphingomyelinase in ANCA-associated primary vasculitis' *(Awaiting submission, Arthritis & Rheumatism)*

Kiprianos, A., Kitas, G., Bacon, P., Young, S., (2011) 'Raised active secretory acid sphingomyelinase in rheumatoid arthritis' *(In preparation)*

Kiprianos, A., Bacon, P., Young, S., (2011) 'TNF$\alpha$ directly induces secretion of secretory acid sphingomyelinase from human primary endothelial cells *(In preparation, short communication, FEBS Lett.*).

## Methodological articles

Kiprianos, A., Young, S., (2011) 'Detection of secretory acid sphingomyelinase in clinical samples using an altered commercially available method' *(In preparation)*

## Review articles

Kiprianos, A., Church, L., Young, S., (2011) 'Sphingomyelinases and their products as regulators of inflammatory processes' *(In preparation)*

# Appendices

## Appendix, Chapter 4

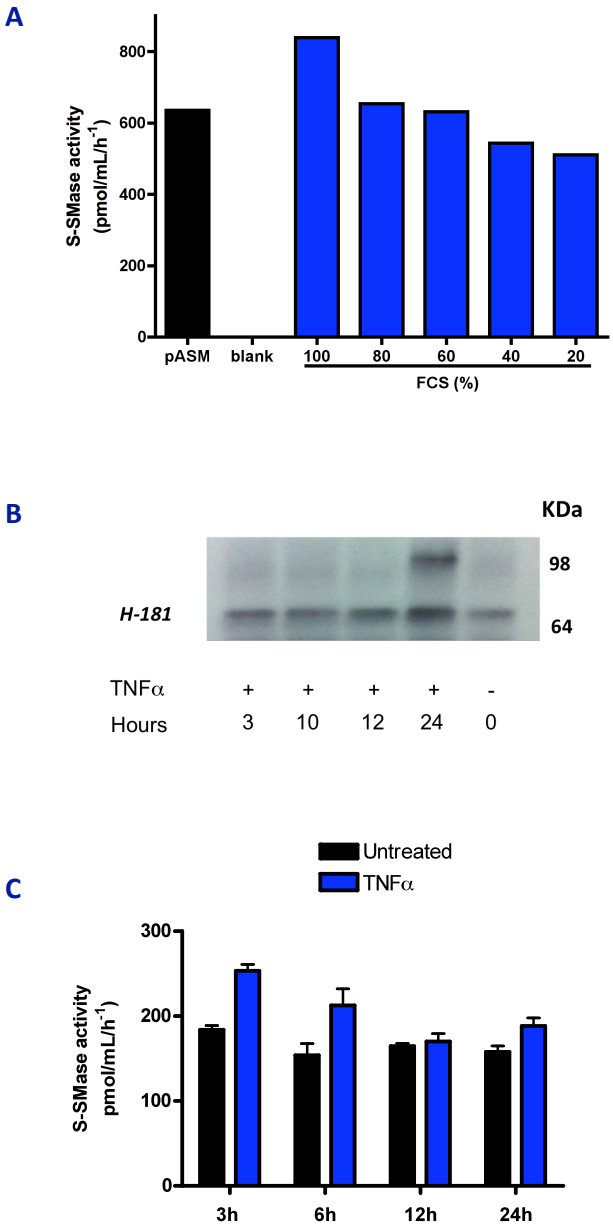


**Figure A.1 FCS masks HUVEC-derived S-SMase activity culture supernates**

Foetal calf serum (FCS) is a rich source of active soluble S-SMase **(A).** S-SMase activity in media supernates from TNFα treatment (100 ng/mL) HUVEC. **(B)** S-SMase detected by immunoblotting in media supernates and **(C)** S-SMase activity detected by the thin layer chromatography SMase activity assay **.** Significant differences in S-SMase activity between untreated and TNFa treated cells is not evident due to high presence of S-SMase activity in M199 (15% v/v) used for culture of HUVEC **(B-C).**

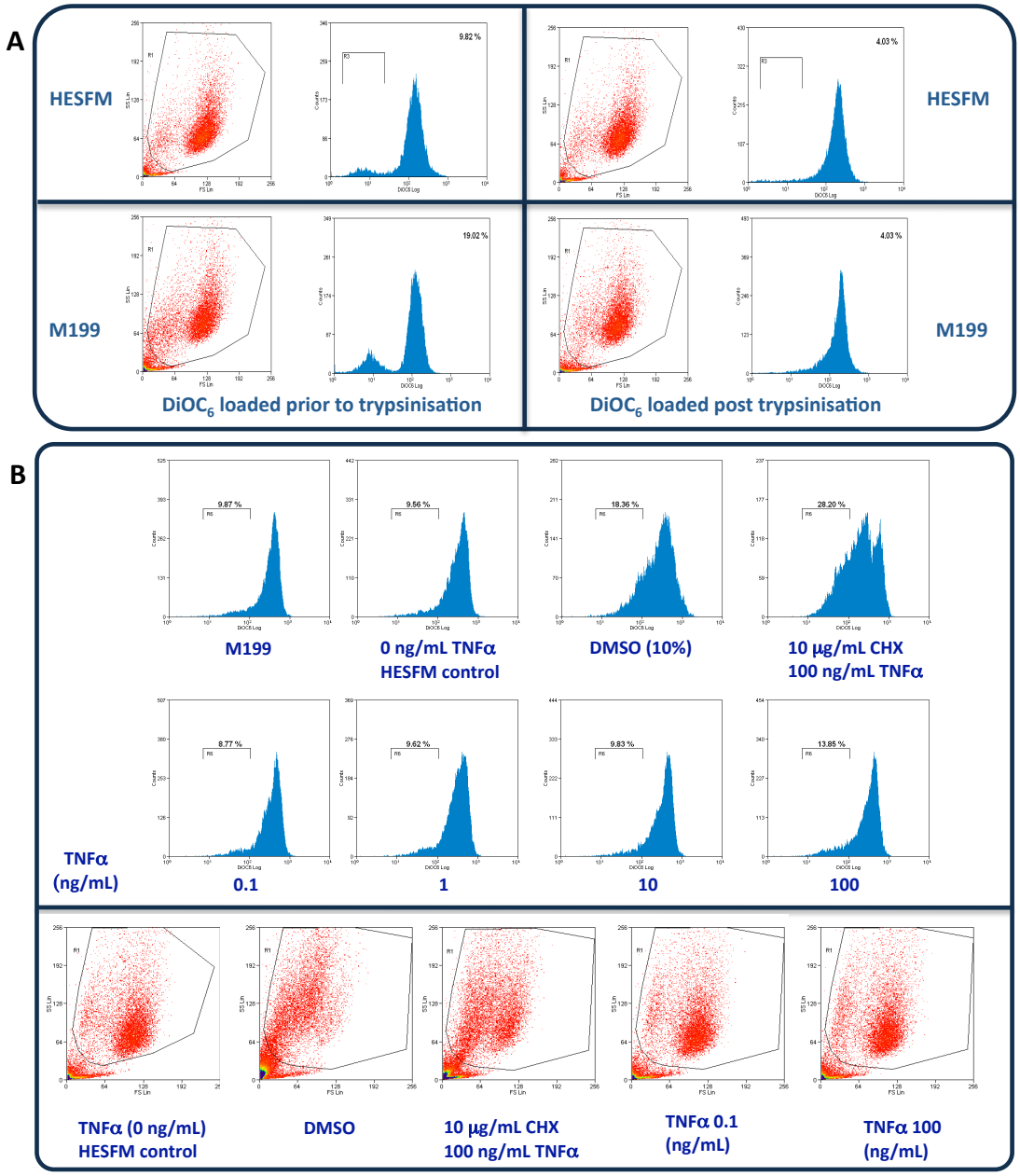


**Figure A.2 Optimising $DiOC_6$ loading conditions to ensure maximal absorbance**

**(A)** HUVEC were brought to 90% confluence in M199, the cells washed twice in HBSS-$Ca^{2+}$ and the medium replaced with fresh fully supplemented M199 or serum-free HESFM for 18 hours. $DiOC_6$ dye was loaded prior to trypsinisation **(A, left panels)** or following trypsinisation **(A, right panels)**. Cells cultured with HESFM **(A, top panels)**, and M199 **(A, bottom panels)** for dye loading. **(B)** Figures representative of a typical experiment of HUVEC counts by flow cytometry.HUVEC were cultured and treated with serum-free HESFM containing DMSO, CHX/TNFα or varying concentrations of TNFα alone. (CHX – cycloheximide).

## Appendix, Chapter 5

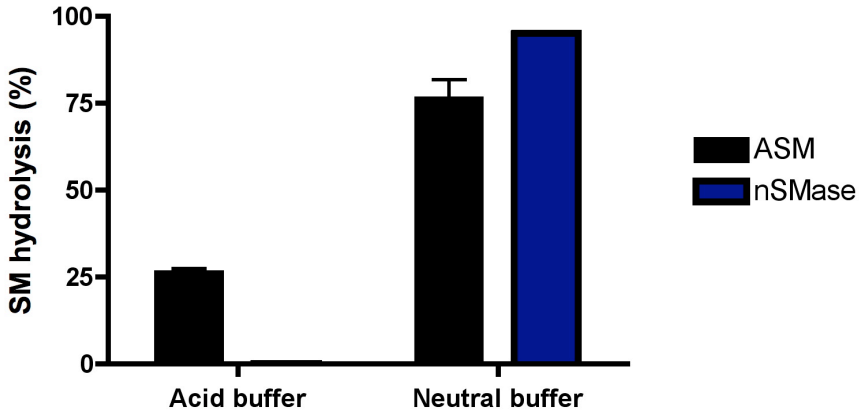


**Figure A.3 ASM retains its activity at neutral pH**

Exogenous ASM (Sigma-Aldrich) or nSMase (Sigma-Aldrich) were added to a reaction mixture including 62 mmol/L sodium acetate, 0.1% Igepal (NP-40) supplemented with 2 mmol/L $ZnSO_4$ (5% v/v) at pH 7.1 in HBSS. The enzymes were incubated for 2 hours at $37^0$C and assayed as described in 2.2.3.

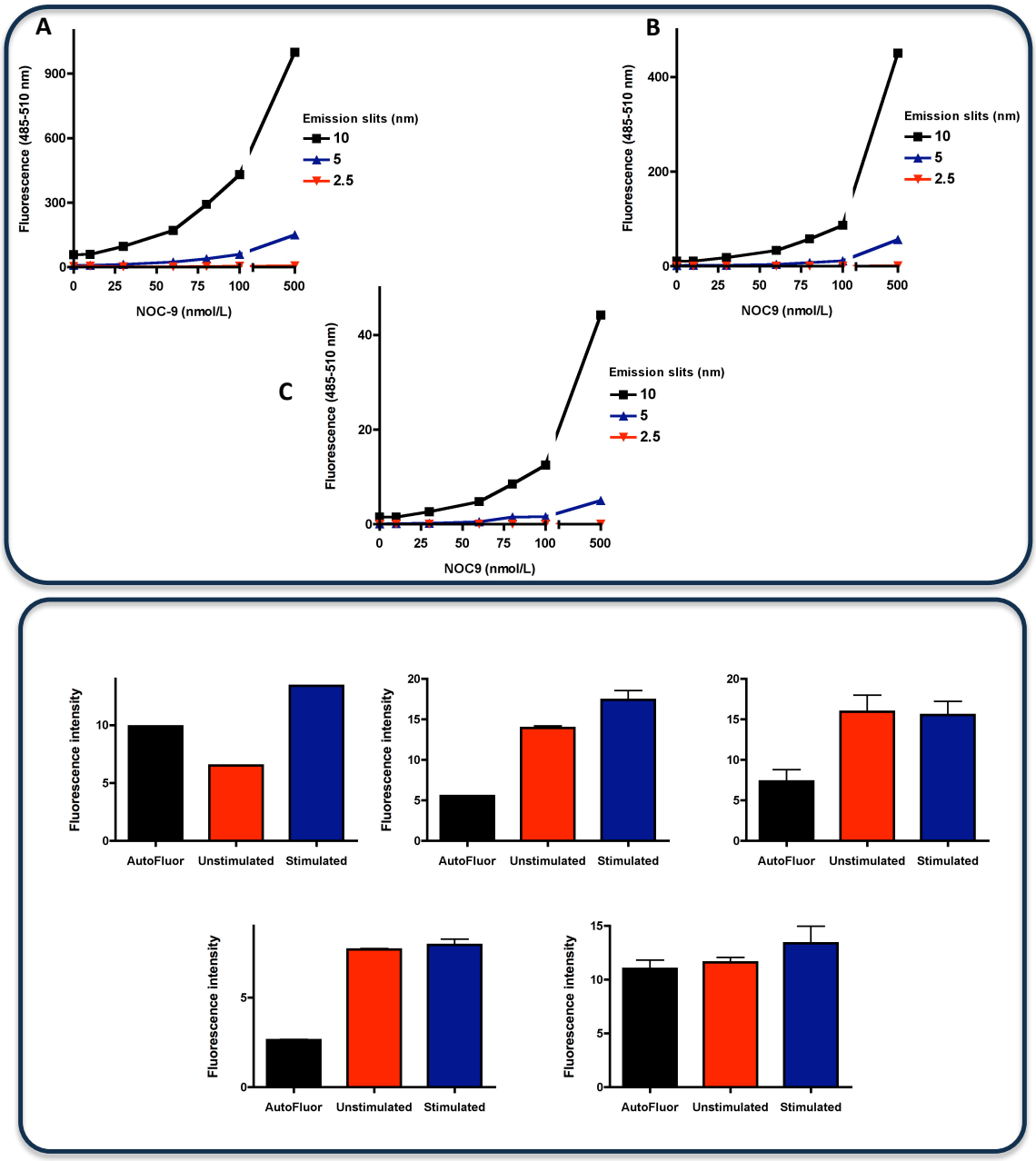


## Figure A.4 Using DAF-2 to detect NO production from HUVEC

**Upper panel**, NOC-9 titration. DAF-2 was incubated with varying concentrations of the NO donor NOC-9. Fluorescence was detected using different emission slits. **(A)** 0.01 μmol/L DAF-2, **(B)** 0.1 μmol/L DAF-2, **(C)** 1 μmol/L DAF-2. **Lower panel**, Selected experiments measuring NO production from HUVEC stimulated with bradykinin (1 μmol/L) compared to solvent control (PBS) treated cells and DAF-2 auto-fluorescence using 0.1 μmol/L DAF-2. For method see 2.2.13.1

.

## Reference List

ABU-SOUD, H. M., FELDMAN, P. L., CLARK, P. & STUEHR, D. J. 1994. Electron transfer in the nitric-oxide synthases. Characterization of L-arginine analogs that block heme iron reduction. *J Biol Chem,* 269**,** 32318-26.

ADAMS, M. R. & CELERMAJER, D. S. 1999. Detection of presymptomatic atherosclerosis: a current perspective. *Clin Sci (Lond),* 97**,** 615-24.

ADAMY, C., MULDER, P., KHOUZAMI, L., ANDRIEU-ABADIE, N., DEFER, N., CANDIANI, G., PAVOINE, C., CARAMELLE, P., SOUKTANI, R., LE CORVOISIER, P., PERIER, M., KIRSCH, M., DAMY, T., BERDEAUX, A., LEVADE, T., THUILLEZ, C., HITTINGER, L. & PECKER, F. 2007. Neutral sphingomyelinase inhibition participates to the benefits of N-acetylcysteine treatment in post-myocardial infarction failing heart rats. *J Mol Cell Cardiol,* 43**,** 344-53.

AHMAD, S., HEWETT, P. W., WANG, P., AL-ANI, B., CUDMORE, M., FUJISAWA, T., HAIGH, J. J., LE NOBLE, F., WANG, L., MUKHOPADHYAY, D. & AHMED, A. 2006. Direct evidence for endothelial vascular endothelial growth factor receptor-1 function in nitric oxide-mediated angiogenesis. *Circ Res,* 99**,** 715-22.

AL-ANI, B., HEWETT, P. W., AHMED, S., CUDMORE, M., FUJISAWA, T., AHMAD, S. & AHMED, A. 2006. The release of nitric oxide from S-nitrosothiols promotes angiogenesis. *PLoS One,* 1**,** e25.

ALETAHA, D., NEOGI, T., SILMAN, A. J., FUNOVITS, J., FELSON, D. T., BINGHAM, C. O., 3RD, BIRNBAUM, N. S., BURMESTER, G. R., BYKERK, V. P., COHEN, M. D., COMBE, B., COSTENBADER, K. H., DOUGADOS, M., EMERY, P., FERRACCIOLI, G., HAZES, J. M., HOBBS, K., HUIZINGA, T. W., KAVANAUGH, A., KAY, J., KVIEN, T. K., LAING, T., MEASE, P., MENARD, H. A., MORELAND, L. W., NADEN, R. L., PINCUS, T., SMOLEN, J. S., STANISLAWSKA-BIERNAT, E., SYMMONS, D., TAK, P. P., UPCHURCH, K. S., VENCOVSKY, J., WOLFE, F. & HAWKER, G. 2010. 2010 Rheumatoid arthritis classification criteria: an American College of Rheumatology/European League Against Rheumatism collaborative initiative. *Arthritis Rheum,* 62**,** 2569-81.

ALEWIJNSE, A. E. & PETERS, S. L. 2008. Sphingolipid signalling in the cardiovascular system: good, bad or both? *Eur J Pharmacol,* 585**,** 292-302.

AMERICAN COLLEGE OF RHEUMATOLOGY SUBCOMMITTEE ON RHEUMATOID ARTHRITIS 2002. Guidelines for the management of rheumatoid arthritis: 2002 Update. *Arthritis Rheum,* 46**,** 328-46.

ANDERSON, H. D., RAHMUTULA, D. & GARDNER, D. G. 2004. Tumor necrosis factor-alpha inhibits endothelial nitric-oxide synthase gene promoter activity in bovine aortic endothelial cells. *J Biol Chem,* 279**,** 963-9.

ANDREANI, M., OLIVIER, J. L., BERENBAUM, F., RAYMONDJEAN, M. & BEREZIAT, G. 2000. Transcriptional regulation of inflammatory secreted phospholipases A(2). *Biochim Biophys Acta,* 1488**,** 149-58.

ANKER, S. D., VOLTERRANI, M., EGERER, K. R., FELTON, C. V., KOX, W. J., POOLE-WILSON, P. A. & COATS, A. J. 1998. Tumour necrosis factor alpha as a predictor of impaired peak leg blood flow in patients with chronic heart failure. *QJM,* 91**,** 199-203.

ARNETT, F. C., EDWORTHY, S. M., BLOCH, D. A., MCSHANE, D. J., FRIES, J. F., COOPER, N. S., HEALEY, L. A., KAPLAN, S. R., LIANG, M. H., LUTHRA, H. S. & ET AL. 1988. The American Rheumatism Association 1987 revised criteria for the classification of rheumatoid arthritis. *Arthritis Rheum,* 31**,** 315-24.

AUGE, N., ANDRIEU, N., NEGRE-SALVAYRE, A., THIERS, J. C., LEVADE, T. & SALVAYRE, R. 1996. The sphingomyelin-ceramide signaling pathway is involved in oxidized low density lipoprotein-induced cell proliferation. *J Biol Chem,* 271**,** 19251-5.

AVOUAC, J., GOSSEC, L. & DOUGADOS, M. 2006. Diagnostic and predictive value of anti-cyclic citrullinated protein antibodies in rheumatoid arthritis: a systematic literature review. *Ann Rheum Dis,* 65**,** 845-51.

BACON, P. A. 2005. Endothelial cell dysfunction in systemic vasculitis: new developments and therapeutic prospects. *Curr Opin Rheumatol,* 17**,** 49-55.

BACON, P. A. & KITAS, G. D. 1994. The significance of vascular inflammation in rheumatoid arthritis. *Ann Rheum Dis,* 53**,** 621-3.

BACON, P. A., STEVENS, R. J., CARRUTHERS, D. M., YOUNG, S. P. & KITAS, G. D. 2002. Accelerated atherogenesis in autoimmune rheumatic diseases. *Autoimmun Rev,* 1**,** 338-47.

BACON, P. A. & TOWNEND, J. N. 2001. Nails in the coffin: increasing evidence for the role of rheumatic disease in the cardiovascular mortality of rheumatoid arthritis. *Arthritis Rheum,* 44**,** 2707-10.

BALLIGAND, J. L., FERON, O. & DESSY, C. 2009. eNOS activation by physical forces: from short-term regulation of contraction to chronic remodeling of cardiovascular tissues. *Physiol Rev,* 89**,** 481-534.

BAO, J. X., XIA, M., POKLIS, J. L., HAN, W. Q., BRIMSON, C. & LI, P. L. 2010. Triggering role of acid sphingomyelinase in endothelial lysosome-membrane fusion and dysfunction in coronary arteries. *Am J Physiol Heart Circ Physiol,* 298**,** H992-H1002.

BARD, F. & MALHOTRA, V. 2006. The formation of TGN-to-plasma-membrane transport carriers. *Annu Rev Cell Dev Biol,* 22**,** 439-55.

BARSACCHI, R., PERROTTA, C., BULOTTA, S., MONCADA, S., BORGESE, N. & CLEMENTI, E. 2003. Activation of endothelial nitric-oxide synthase by tumor necrosis factor-alpha: a novel pathway involving sequential activation of neutral sphingomyelinase, phosphatidylinositol-3' kinase, and Akt. *Mol Pharmacol,* 63**,** 886-95.

BASU, N., WATTS, R., BAJEMA, I., BASLUND, B., BLEY, T., BOERS, M., BROGAN, P., CALABRESE, L., CID, M. C., COHEN-TERVAERT, J. W., FLORES-SUAREZ, L. F., FUJIMOTO, S., DE GROOT, K., GUILLEVIN, L., HATEMI, G., HAUSER, T., JAYNE, D., JENNETTE, C., KALLENBERG, C. G., KOBAYASHI, S., LITTLE, M. A., MAHR, A., MCLAREN, J., MERKEL, P. A., OZEN, S., PUECHAL, X., RASMUSSEN, N., SALAMA, A., SALVARANI, C., SAVAGE, C., SCOTT, D. G., SEGELMARK, M., SPECKS, U., SUNDERKOETTER, C., SUZUKI, K., TESAR, V., WIIK, A., YAZICI, H. &

LUQMANI, R. 2010. EULAR points to consider in the development of classification and diagnostic criteria in systemic vasculitis. *Ann Rheum Dis*.

BAUER, P. M., FULTON, D., BOO, Y. C., SORESCU, G. P., KEMP, B. E., JO, H. & SESSA, W. C. 2003. Compensatory phosphorylation and protein-protein interactions revealed by loss of function and gain of function mutants of multiple serine phosphorylation sites in endothelial nitric-oxide synthase. *J Biol Chem,* 278**,** 14841-9.

BERGHOLM, R., LEIRISALO-REPO, M., VEHKAVAARA, S., MAKIMATTILA, S., TASKINEN, M. R. & YKI-JARVINEN, H. 2002. Impaired responsiveness to NO in newly diagnosed patients with rheumatoid arthritis. *Arterioscler Thromb Vasc Biol,* 22**,** 1637-41.

BERKA, V., WU, G., YEH, H. C., PALMER, G. & TSAI, A. L. 2004a. Three different oxygen-induced radical species in endothelial nitric-oxide synthase oxygenase domain under regulation by L-arginine and tetrahydrobiopterin. *J Biol Chem,* 279**,** 32243-51.

BERKA, V., YEH, H. C., GAO, D., KIRAN, F. & TSAI, A. L. 2004b. Redox function of tetrahydrobiopterin and effect of L-arginine on oxygen binding in endothelial nitric oxide synthase. *Biochemistry,* 43**,** 13137-48.

BERTOLINI, D. R., NEDWIN, G. E., BRINGMAN, T. S., SMITH, D. D. & MUNDY, G. R. 1986. Stimulation of bone resorption and inhibition of bone formation in vitro by human tumour necrosis factors. *Nature,* 319**,** 516-8.

BHAGAT, K., MOSS, R., COLLIER, J. & VALLANCE, P. 1996. Endothelial "stunning" following a brief exposure to endotoxin: a mechanism to link infection and infarction? *Cardiovasc Res,* 32**,** 822-9.

BHAGAT, K. & VALLANCE, P. 1997. Inflammatory cytokines impair endothelium-dependent dilatation in human veins in vivo. *Circulation,* 96**,** 3042-7.

BHATIA, R., MATSUSHITA, K., YAMAKUCHI, M., MORRELL, C. N., CAO, W. & LOWENSTEIN, C. J. 2004. Ceramide triggers Weibel-Palade body exocytosis. *Circ Res,* 95**,** 319-24.

BIRD, G. S., HWANG, S. Y., SMYTH, J. T., FUKUSHIMA, M., BOYLES, R. R. & PUTNEY, J. W., JR. 2009. STIM1 is a calcium sensor specialized for digital signaling. *Curr Biol,* 19**,** 1724-9.

BOESTERLI, J. A. 2003. *Mechanistic Toxicology: The molecular basis of how chemicals disrupt biological agents,* London, Taylor & Francis.

BOLOTINA, V. M. 2008. Orai, STIM1 and iPLA2beta: a view from a different perspective. *J Physiol,* 586**,** 3035-42.

BONETTI, P. O., LERMAN, L. O. & LERMAN, A. 2003. Endothelial dysfunction: a marker of atherosclerotic risk. *Arterioscler Thromb Vasc Biol,* 23**,** 168-75.

BOO, Y. C., HWANG, J., SYKES, M., MICHELL, B. J., KEMP, B. E., LUM, H. & JO, H. 2002a. Shear stress stimulates phosphorylation of eNOS at Ser(635) by a protein kinase A-dependent mechanism. *Am J Physiol Heart Circ Physiol,* 283**,** H1819-28.

BOO, Y. C., SORESCU, G., BOYD, N., SHIOJIMA, I., WALSH, K., DU, J. & JO, H. 2002b. Shear stress stimulates phosphorylation of endothelial nitric-oxide synthase at Ser1179 by Akt-independent mechanisms: role of protein kinase A. *J Biol Chem,* 277**,** 3388-96.

BOOTH, A., HARPER, L., HAMMAD, T., BACON, P., GRIFFITH, M., LEVY, J., SAVAGE, C., PUSEY, C. & JAYNE, D. 2004a. Prospective study of TNFalpha blockade with infliximab in anti-neutrophil cytoplasmic antibody-associated systemic vasculitis. *J Am Soc Nephrol,* 15**,** 717-21.

BOOTH, A. D., JAYNE, D. R., KHARBANDA, R. K., MCENIERY, C. M., MACKENZIE, I. S., BROWN, J. & WILKINSON, I. B. 2004b. Infliximab improves endothelial dysfunction in systemic vasculitis: a model of vascular inflammation. *Circulation,* 109**,** 1718-23.

BOOTH, A. D., WALLACE, S., MCENIERY, C. M., YASMIN, BROWN, J., JAYNE, D. R. & WILKINSON, I. B. 2004c. Inflammation and arterial stiffness in systemic vasculitis: a model of vascular inflammation. *Arthritis Rheum,* 50**,** 581-8.

BORBIEV, T., VERIN, A. D., SHI, S., LIU, F. & GARCIA, J. G. 2001. Regulation of endothelial cell barrier function by calcium/calmodulin-dependent protein kinase II. *Am J Physiol Lung Cell Mol Physiol,* 280**,** L983-90.

BOSCH, X., GUILABERT, A. & FONT, J. 2006. Antineutrophil cytoplasmic antibodies. *Lancet,* 368**,** 404-18.

BOSELLO, S., SANTOLIQUIDO, A., ZOLI, A., DI CAMPLI, C., FLORE, R., TONDI, P. & FERRACCIOLI, G. 2008. TNF-alpha blockade induces a reversible but transient effect on endothelial dysfunction in patients with long-standing severe rheumatoid arthritis. *Clin Rheumatol,* 27**,** 833-9.

BOURBON, N. A., SANDIRASEGARANE, L. & KESTER, M. 2002. Ceramide-induced inhibition of Akt is mediated through protein kinase Czeta: implications for growth arrest. *J Biol Chem,* 277**,** 3286-92.

BRADLEY, J. R., THIRU, S. & POBER, J. S. 1995. Disparate localization of 55-kd and 75-kd tumor necrosis factor receptors in human endothelial cells. *Am J Pathol,* 146**,** 27-32.

BRADY, R. O., KANFER, J. N., MOCK, M. B. & FREDRICKSON, D. S. 1966. The metabolism of sphingomyelin. II. Evidence of an enzymatic deficiency in Niemann-Pick diseae. *Proc Natl Acad Sci U S A,* 55**,** 366-9.

BREITTMAYER, J. P., BERNARD, A. & AUSSEL, C. 1994. Regulation by sphingomyelinase and sphingosine of Ca2+ signals elicited by CD3 monoclonal antibody, thapsigargin, or ionomycin in the Jurkat T cell line. *J Biol Chem,* 269**,** 5054-8.

BRENNAN, F. M., CHANTRY, D., JACKSON, A., MAINI, R. & FELDMANN, M. 1989. Inhibitory effect of TNF alpha antibodies on synovial cell interleukin-1 production in rheumatoid arthritis. *Lancet,* 2**,** 244-7.

BRENNAN, F. M. & MCINNES, I. B. 2008. Evidence that cytokines play a role in rheumatoid arthritis. *J Clin Invest,* 118**,** 3537-45.

BRIEN, J. F., MCLAUGHLIN, B. E., NAKATSU, K. & MARKS, G. S. 1996. Chemiluminescence headspace-gas analysis for determination of nitric oxide formation in biological systems. *Methods Enzymol,* 268**,** 83-92.

BUCCI, M., GRATTON, J. P., RUDIC, R. D., ACEVEDO, L., ROVIEZZO, F., CIRINO, G. & SESSA, W. C. 2000. In vivo delivery of the caveolin-1 scaffolding domain inhibits nitric oxide synthesis and reduces inflammation. *Nat Med,* 6**,** 1362-7.

BUGATTI, S., CODULLO, V., CAPORALI, R. & MONTECUCCO, C. 2007. B cells in rheumatoid arthritis. *Autoimmun Rev,* 6**,** 482-7.

BUJAK, M. & FRANGOGIANNIS, N. G. 2009. The role of IL-1 in the pathogenesis of heart disease. *Arch Immunol Ther Exp (Warsz),* 57**,** 165-76.

BULOTTA, S., BARSACCHI, R., ROTIROTI, D., BORGESE, N. & CLEMENTI, E. 2001. Activation of the endothelial nitric-oxide synthase by tumor necrosis factor-alpha. A novel feedback mechanism regulating cell death. *J Biol Chem,* 276**,** 6529-36.

BURT, V. L., WHELTON, P., ROCCELLA, E. J., BROWN, C., CUTLER, J. A., HIGGINS, M., HORAN, M. J. & LABARTHE, D. 1995. Prevalence of hypertension in the US adult population. Results from the Third National Health and Nutrition Examination Survey, 1988-1991. *Hypertension,* 25**,** 305-13.

BUTLER, D. M., MAINI, R. N., FELDMANN, M. & BRENNAN, F. M. 1995. Modulation of proinflammatory cytokine release in rheumatoid synovial membrane cell cultures. Comparison of monoclonal anti TNF-alpha antibody with the interleukin-1 receptor antagonist. *Eur Cytokine Netw,* 6**,** 225-30.

CAI, H. & HARRISON, D. G. 2000. Endothelial dysfunction in cardiovascular diseases: the role of oxidant stress. *Circ Res,* 87**,** 840-4.

CAI, H., LIU, D. & GARCIA, J. G. 2008. CaM Kinase II-dependent pathophysiological signalling in endothelial cells. *Cardiovasc Res,* 77**,** 30-4.

CAILLERET, M., AMADOU, A., ANDRIEU-ABADIE, N., NAWROCKI, A., ADAMY, C., AIT-MAMAR, B., ROCARIES, F., BEST-BELPOMME, M., LEVADE, T., PAVOINE, C. & PECKER, F. 2004. N-acetylcysteine prevents the deleterious effect of tumor necrosis factor-(alpha) on calcium transients and contraction in adult rat cardiomyocytes. *Circulation,* 109**,** 406-11.

CAMPIA, U., CHOUCAIR, W. K., BRYANT, M. B., WACLAWIW, M. A., CARDILLO, C. & PANZA, J. A. 2002. Reduced endothelium-dependent and -independent dilation of conductance arteries in African Americans. *J Am Coll Cardiol,* 40**,** 754-60.

CAPECE, L., ESTRIN, D. A. & MARTI, M. A. 2008. Dynamical characterization of the heme NO oxygen binding (HNOX) domain. Insight into soluble guanylate cyclase allosteric transition. *Biochemistry,* 47**,** 9416-27.

CARSWELL, E. A., OLD, L. J., KASSEL, R. L., GREEN, S., FIORE, N. & WILLIAMSON, B. 1975. An endotoxin-induced serum factor that causes necrosis of tumors. *Proc Natl Acad Sci U S A,* 72**,** 3666-70.

CASCAO, R., ROSARIO, H. S., SOUTO-CARNEIRO, M. M. & FONSECA, J. E. 2010. Neutrophils in rheumatoid arthritis: More than simple final effectors. *Autoimmun Rev,* 9**,** 531-5.

CASSATELLA, M. A., PEREIRA-DA-SILVA, G., TINAZZI, I., FACCHETTI, F., SCAPINI, P., CALZETTI, F., TAMASSIA, N., WEI, P., NARDELLI, B., ROSCHKE, V., VECCHI, A., MANTOVANI, A., BAMBARA, L. M., EDWARDS, S. W. & CARLETTO, A. 2007. Soluble TNF-like cytokine (TL1A) production by immune complexes stimulated monocytes in rheumatoid arthritis. *J Immunol,* 178**,** 7325-33.

CASTRO, P. F., DIAZ-ARAYA, G., NETTLE, D., CORBALAN, R., PEREZ, O., NAZZAL, C., LARRAIN, G. & LAVANDERO, S. 2002. Effects of early decrease in oxidative stress after medical therapy in patients with class IV congestive heart failure. *Am J Cardiol,* 89**,** 236-9.

CHAKRABARTI, S., ZEE, J. M. & PATEL, K. D. 2006. Regulation of matrix metalloproteinase-9 (MMP-9) in TNF-stimulated neutrophils: novel pathways for tertiary granule release. *J Leukoc Biol,* 79**,** 214-22.

CHAMBERS, J. C., HASKARD, D. O. & KOONER, J. S. 2001. Vascular endothelial function and oxidative stress mechanisms in patients with Behcet's syndrome. *J Am Coll Cardiol,* 37**,** 517-20.

CHAN, Y. C., LEUNG, F. P., WONG, W. T., TIAN, X. Y., YUNG, L. M., LAU, C. W., TSANG, S. Y., YAO, X., CHEN, Z. Y. & HUANG, Y. 2010. Therapeutically Relevant Concentrations of Raloxifene Dilate Pressurized Rat Resistance Arteries via Calcium-Dependent Endothelial Nitric Oxide Synthase Activation. *Arterioscler Thromb Vasc Biol,* 30.

CHARRUYER, A., GRAZIDE, S., BEZOMBES, C., MULLER, S., LAURENT, G. & JAFFREZOU, J. P. 2005. UV-C light induces raft-associated acid sphingomyelinase and JNK activation and translocation independently on a nuclear signal. *J Biol Chem,* 280**,** 19196-204.

CHATELUT, M., LERUTH, M., HARZER, K., DAGAN, A., MARCHESINI, S., GATT, S., SALVAYRE, R., COURTOY, P. & LEVADE, T. 1998. Natural ceramide is unable to escape the lysosome, in contrast to a fluorescent analogue. *FEBS Lett,* 426**,** 102-6.

CHEN, Z. P., MITCHELHILL, K. I., MICHELL, B. J., STAPLETON, D., RODRIGUEZ-CRESPO, I., WITTERS, L. A., POWER, D. A., ORTIZ DE MONTELLANO, P. R. & KEMP, B. E. 1999. AMP-activated protein kinase phosphorylation of endothelial NO synthase. *FEBS Lett,* 443**,** 285-9.

CHIA, S., QADAN, M., NEWTON, R., LUDLAM, C. A., FOX, K. A. & NEWBY, D. E. 2003. Intra-arterial tumor necrosis factor-alpha impairs endothelium-dependent vasodilatation and stimulates local tissue plasminogen activator release in humans. *Arterioscler Thromb Vasc Biol,* 23**,** 695-701.

CHIRONI, G., PAGNOUX, C., SIMON, A., PASQUINELLI-BALICE, M., DEL-PINO, M., GARIEPY, J. & GUILLEVIN, L. 2007. Increased prevalence of subclinical atherosclerosis in patients with small-vessel vasculitis. *Heart,* 93**,** 96-9.

CHOQUET, D., PARTISETI, M., AMIGORENA, S., BONNEROT, C., FRIDMAN, W. H. & KORN, H. 1993. Cross-linking of IgG receptors inhibits membrane immunoglobulin-stimulated calcium influx in B lymphocytes. *J Cell Biol,* 121**,** 355-63.

CHURCH, L. D., HESSLER, G., GOODALL, J. E., RIDER, D. A., WORKMAN, C. J., VIGNALI, D. A., BACON, P. A., GULBINS, E. & YOUNG, S. P. 2005. TNFR1-induced sphingomyelinase activation modulates TCR signaling by impairing store-operated Ca2+ influx. *J Leukoc Biol,* 78**,** 266-78.

CLAPHAM, D. E. 2007. Calcium signaling. *Cell,* 131**,** 1047-58.

CLARKE, R., DALY, L., ROBINSON, K., NAUGHTEN, E., CAHALANE, S., FOWLER, B. & GRAHAM, I. 1991. Hyperhomocysteinemia: an independent risk factor for vascular disease. *N Engl J Med,* 324**,** 1149-55.

CLAUS, R. A., BUNCK, A. C., BOCKMEYER, C. L., BRUNKHORST, F. M., LOSCHE, W., KINSCHERF, R. & DEIGNER, H. P. 2005. Role of increased sphingomyelinase activity in apoptosis and organ failure of patients with severe sepsis. *FASEB J,* 19**,** 1719-21.

COHEN, P., GUILLEVIN, L., BARIL, L., LHOTE, F., NOEL, L. H. & LESAVRE, P. 1995. Persistence of antineutrophil cytoplasmic antibodies (ANCA) in asymptomatic patients with systemic polyarteritis nodosa or Churg-Strauss syndrome: follow-up of 53 patients. *Clin Exp Rheumatol,* 13**,** 193-8.

COLELL, A., MORALES, A., FERNANDEZ-CHECA, J. C. & GARCIA-RUIZ, C. 2002. Ceramide generated by acidic sphingomyelinase contributes to tumor necrosis factor-alpha-mediated apoptosis in human colon HT-29 cells through glycosphingolipids formation. Possible role of ganglioside GD3. *FEBS Lett,* 526**,** 135-41.

CONDRESCU, M. & REEVES, J. P. 2001. Inhibition of sodium-calcium exchange by ceramide and sphingosine. *J Biol Chem,* 276**,** 4046-54.

COPE, A. P. 2008. T cells in rheumatoid arthritis. *Arthritis Res Ther,* 10 Suppl 1**,** S1.

CORDA, S., LAPLACE, C., VICAUT, E. & DURANTEAU, J. 2001. Rapid reactive oxygen species production by mitochondria in endothelial cells exposed to tumor necrosis factor-alpha is mediated by ceramide. *Am J Respir Cell Mol Biol,* 24**,** 762-8.

CORRETTI, M. C., ANDERSON, T. J., BENJAMIN, E. J., CELERMAJER, D., CHARBONNEAU, F., CREAGER, M. A., DEANFIELD, J., DREXLER, H., GERHARD-HERMAN, M., HERRINGTON, D., VALLANCE, P., VITA, J. & VOGEL, R. 2002. Guidelines for the ultrasound assessment of endothelial-dependent flow-mediated vasodilation of the brachial artery: a report of the International Brachial Artery Reactivity Task Force. *J Am Coll Cardiol,* 39**,** 257-65.

COUGHLIN, S. R. 2000. Thrombin signalling and protease-activated receptors. *Nature,* 407**,** 258-64.

CRANE, B. R., ARVAI, A. S., GHOSH, D. K., WU, C., GETZOFF, E. D., STUEHR, D. J. & TAINER, J. A. 1998. Structure of nitric oxide synthase oxygenase dimer with pterin and substrate. *Science,* 279**,** 2121-6.

CROWSON, C. S., NICOLA, P. J., KREMERS, H. M., O'FALLON, W. M., THERNEAU, T. M., JACOBSEN, S. J., ROGER, V. L., BALLMAN, K. V. & GABRIEL, S. E. 2005. How much of the increased incidence of heart failure in rheumatoid arthritis is attributable to traditional cardiovascular risk factors and ischemic heart disease? *Arthritis Rheum,* 52**,** 3039-44.

CSUTORA, P., PETER, K., KILIC, H., PARK, K. M., ZARAYSKIY, V., GWOZDZ, T. & BOLOTINA, V. M. 2008. Novel role for STIM1 as a trigger for calcium influx factor production. *J Biol Chem,* 283**,** 14524-31.

CUDMORE, M., AHMAD, S., AL-ANI, B., HEWETT, P., AHMED, S. & AHMED, A. 2006. VEGF-E activates endothelial nitric oxide synthase to induce angiogenesis via cGMP and PKG-independent pathways. *Biochem Biophys Res Commun,* 345**,** 1275-82.

DAVID-DUFILHO, M., MILLANVOYE-VAN BRUSSEL, E., TOPAL, G., WALCH, L., BRUNET, A. & RENDU, F. 2005. Endothelial thrombomodulin induces Ca2+ signals and nitric oxide synthesis through epidermal growth factor receptor kinase and calmodulin kinase II. *J Biol Chem,* 280**,** 35999-6006.

DAYER, J. M. 2003. The pivotal role of interleukin-1 in the clinical manifestations of rheumatoid arthritis. *Rheumatology (Oxford),* 42 Suppl 2**,** ii3-10.

DAYER, J. M., BEUTLER, B. & CERAMI, A. 1985. Cachectin/tumor necrosis factor stimulates collagenase and prostaglandin E2 production by human synovial cells and dermal fibroblasts. *J Exp Med,* 162**,** 2163-8.

DE GROOT, K., RASMUSSEN, N., BACON, P. A., TERVAERT, J. W., FEIGHERY, C., GREGORINI, G., GROSS, W. L., LUQMANI, R. & JAYNE, D. R. 2005. Randomized trial of cyclophosphamide versus methotrexate for induction of remission in early systemic antineutrophil cytoplasmic antibody-associated vasculitis. *Arthritis Rheum,* 52**,** 2461-9.

DE LEEUW, K., SANDERS, J. S., STEGEMAN, C., SMIT, A., KALLENBERG, C. G. & BIJL, M. 2005. Accelerated atherosclerosis in patients with Wegener's granulomatosis. *Ann Rheum Dis,* 64**,** 753-9.

DE PALMA, C., MEACCI, E., PERROTTA, C., BRUNI, P. & CLEMENTI, E. 2006. Endothelial nitric oxide synthase activation by tumor necrosis factor alpha through neutral sphingomyelinase 2, sphingosine kinase 1, and sphingosine 1 phosphate receptors: a novel pathway relevant to the pathophysiology of endothelium. *Arterioscler Thromb Vasc Biol,* 26**,** 99-105.

DEAGLIO, S., VAISITTI, T., BILLINGTON, R., BERGUI, L., OMEDE, P., GENAZZANI, A. A. & MALAVASI, F. 2007. CD38/CD19: a lipid raft-dependent signaling complex in human B cells. *Blood,* 109**,** 5390-8.

DEJANA, E. 1996. Endothelial adherens junctions: implications in the control of vascular permeability and angiogenesis. *J Clin Invest,* 98**,** 1949-53.

DEL RINCON, I. 2009. Atherothrombotic comorbidity in the rheumatic diseases. The evidence becomes clearer. What should clinicians do? *Arthritis Rheum,* 61**,** 1284-6.

DEL RINCON, I., WILLIAMS, K., STERN, M. P., FREEMAN, G. L., O'LEARY, D. H. & ESCALANTE, A. 2003. Association between carotid atherosclerosis and markers of inflammation in rheumatoid arthritis patients and healthy subjects. *Arthritis Rheum,* 48**,** 1833-40.

DEL RINCON, I. D., WILLIAMS, K., STERN, M. P., FREEMAN, G. L. & ESCALANTE, A. 2001. High incidence of cardiovascular events in a rheumatoid arthritis cohort not explained by traditional cardiac risk factors. *Arthritis Rheum,* 44**,** 2737-45.

DELEURAN, B. W., CHU, C. Q., FIELD, M., BRENNAN, F. M., MITCHELL, T., FELDMANN, M. & MAINI, R. N. 1992. Localization of tumor necrosis factor receptors in the synovial tissue and cartilage-pannus junction in patients with rheumatoid arthritis. Implications for local actions of tumor necrosis factor alpha. *Arthritis Rheum,* 35**,** 1170-8.

DENG, Y. B., LI, T. L., XIANG, H. J., CHANG, Q. & LI, C. L. 2003. Impaired endothelial function in the brachial artery after Kawasaki disease and the effects of intravenous administration of vitamin C. *Pediatr Infect Dis J,* 22**,** 34-9.

DER, P., CUI, J. & DAS, D. K. 2006. Role of lipid rafts in ceramide and nitric oxide signaling in the ischemic and preconditioned hearts. *J Mol Cell Cardiol,* 40**,** 313-20.

DESSEIN, P. H., JOFFE, B. I. & SINGH, S. 2005. Biomarkers of endothelial dysfunction, cardiovascular risk factors and atherosclerosis in rheumatoid arthritis. *Arthritis Res Ther,* 7**,** R634-43.

DEVLIN, C. M., LEVENTHAL, A. R., KURIAKOSE, G., SCHUCHMAN, E. H., WILLIAMS, K. J. & TABAS, I. 2008. Acid sphingomyelinase promotes lipoprotein retention within early atheromata and accelerates lesion progression. *Arterioscler Thromb Vasc Biol,* 28**,** 1723-30.

DHILLON, R., CLARKSON, P., DONALD, A. E., POWE, A. J., NASH, M., NOVELLI, V., DILLON, M. J. & DEANFIELD, J. E. 1996. Endothelial dysfunction late after Kawasaki disease. *Circulation,* 94**,** 2103-6.

DIMMELER, S., FLEMING, I., FISSLTHALER, B., HERMANN, C., BUSSE, R. & ZEIHER, A. M. 1999. Activation of nitric oxide synthase in endothelial cells by Akt-dependent phosphorylation. *Nature,* 399**,** 601-5.

DINARELLO, C. A. 1996. Biologic basis for interleukin-1 in disease. *Blood,* 87**,** 2095-147.

DIXON, W. G., WATSON, K. D., LUNT, M., HYRICH, K. L., SILMAN, A. J. & SYMMONS, D. P. 2007. Reduction in the incidence of myocardial infarction in patients with rheumatoid arthritis who respond to anti-tumor necrosis factor alpha therapy: results from the British Society for Rheumatology Biologics Register. *Arthritis Rheum,* 56**,** 2905-12.

DOEHNER, W., BUNCK, A. C., RAUCHHAUS, M., VON HAEHLING, S., BRUNKHORST, F. M., CICOIRA, M., TSCHOPE, C., PONIKOWSKI, P., CLAUS, R. A. & ANKER, S. D. 2007. Secretory sphingomyelinase is upregulated in chronic heart failure: a second messenger system of immune activation relates to body composition, muscular functional capacity, and peripheral blood flow. *Eur Heart J,* 28**,** 821-8.

DREW, B. G., FIDGE, N. H., GALLON-BEAUMIER, G., KEMP, B. E. & KINGWELL, B. A. 2004. High-density lipoprotein and apolipoprotein AI increase endothelial NO synthase activity by protein association and multisite phosphorylation. *Proc Natl Acad Sci U S A,* 101**,** 6999-7004.

DUAN, R. D. 2006. Alkaline sphingomyelinase: an old enzyme with novel implications. *Biochim Biophys Acta,* 1761**,** 281-91.

DUDZINSKI, D. M., IGARASHI, J., GREIF, D. & MICHEL, T. 2006. The regulation and pharmacology of endothelial nitric oxide synthase. *Annu Rev Pharmacol Toxicol,* 46**,** 235-76.

DUDZINSKI, D. M. & MICHEL, T. 2007. Life history of eNOS: partners and pathways. *Cardiovasc Res,* 75**,** 247-60.

DUMITRU, C. A. & GULBINS, E. 2006. TRAIL activates acid sphingomyelinase via a redox mechanism and releases ceramide to trigger apoptosis. *Oncogene,* 25**,** 5612-25.

DUMITRU, C. A., ZHANG, Y., LI, X. & GULBINS, E. 2007. Ceramide: a novel player in reactive oxygen species-induced signaling? *Antioxid Redox Signal,* 9**,** 1535-40.

EDER, C. 2009. Mechanisms of interleukin-1beta release. *Immunobiology,* 214**,** 543-53.

ELLIOTT, M. J., MAINI, R. N., FELDMANN, M., LONG-FOX, A., CHARLES, P., KATSIKIS, P., BRENNAN, F. M., WALKER, J., BIJL, H., GHRAYEB, J. & ET AL. 1993. Treatment of rheumatoid arthritis

with chimeric monoclonal antibodies to tumor necrosis factor alpha. *Arthritis Rheum,* 36**,** 1681-90.

ERWIN, P. A., MITCHELL, D. A., SARTORETTO, J., MARLETTA, M. A. & MICHEL, T. 2006. Subcellular targeting and differential S-nitrosylation of endothelial nitric-oxide synthase. *J Biol Chem,* 281**,** 151-7.

EXLEY, A. R., BACON, P. A., LUQMANI, R. A., KITAS, G. D., CARRUTHERS, D. M. & MOOTS, R. 1998. Examination of disease severity in systemic vasculitis from the novel perspective of damage using the vasculitis damage index (VDI). *Br J Rheumatol,* 37**,** 57-63.

EXLEY, A. R., BACON, P. A., LUQMANI, R. A., KITAS, G. D., GORDON, C., SAVAGE, C. O. & ADU, D. 1997. Development and initial validation of the Vasculitis Damage Index for the standardized clinical assessment of damage in the systemic vasculitides. *Arthritis Rheum,* 40**,** 371-80.

FELDMANN, M., BRENNAN, F. M. & MAINI, R. N. 1996. Role of cytokines in rheumatoid arthritis. *Annu Rev Immunol,* 14**,** 397-440.

FELDMANN, M. & PUSEY, C. D. 2006. Is there a role for TNF-alpha in anti-neutrophil cytoplasmic antibody-associated vasculitis? Lessons from other chronic inflammatory diseases. *J Am Soc Nephrol,* 17**,** 1243-52.

FERLINZ, K., HURWITZ, R., VIELHABER, G., SUZUKI, K. & SANDHOFF, K. 1994. Occurrence of two molecular forms of human acid sphingomyelinase. *Biochem J,* 301 ( Pt 3)**,** 855-62.

FERON, O. & BALLIGAND, J. L. 2006. Caveolins and the regulation of endothelial nitric oxide synthase in the heart. *Cardiovasc Res,* 69**,** 788-97.

FERON, O., BELHASSEN, L., KOBZIK, L., SMITH, T. W., KELLY, R. A. & MICHEL, T. 1996. Endothelial nitric oxide synthase targeting to caveolae. Specific interactions with caveolin isoforms in cardiac myocytes and endothelial cells. *J Biol Chem,* 271**,** 22810-4.

FERON, O., SALDANA, F., MICHEL, J. B. & MICHEL, T. 1998. The endothelial nitric-oxide synthase-caveolin regulatory cycle. *J Biol Chem,* 273**,** 3125-8.

FERRERO, E., ZOCCHI, M. R., MAGNI, E., PANZERI, M. C., CURNIS, F., RUGARLI, C., FERRERO, M. E. & CORTI, A. 2001. Roles of tumor necrosis factor p55 and p75 receptors in TNF-alpha-induced vascular permeability. *Am J Physiol Cell Physiol,* 281**,** C1173-9.

FILER, A. D., GARDNER-MEDWIN, J. M., THAMBYRAJAH, J., RAZA, K., CARRUTHERS, D. M., STEVENS, R. J., LIU, L., LOWE, S. E., TOWNEND, J. N. & BACON, P. A. 2003. Diffuse endothelial dysfunction is common to ANCA associated systemic vasculitis and polyarteritis nodosa. *Ann Rheum Dis,* 62**,** 162-7.

FISSLTHALER, B., DIMMELER, S., HERMANN, C., BUSSE, R. & FLEMING, I. 2000. Phosphorylation and activation of the endothelial nitric oxide synthase by fluid shear stress. *Acta Physiol Scand,* 168**,** 81-8.

FLEMING, I. 2010. Molecular mechanisms underlying the activation of eNOS. *Pflugers Arch,* 459**,** 793-806.

FLEMING, I. & BUSSE, R. 1999. Signal transduction of eNOS activation. *Cardiovasc Res,* 43**,** 532-41.

FLEMING, I. & BUSSE, R. 2003. Molecular mechanisms involved in the regulation of the endothelial nitric oxide synthase. *Am J Physiol Regul Integr Comp Physiol,* 284**,** R1-12.

FLEMING, I., FISSLTHALER, B., DIMMELER, S., KEMP, B. E. & BUSSE, R. 2001. Phosphorylation of Thr(495) regulates Ca(2+)/calmodulin-dependent endothelial nitric oxide synthase activity. *Circ Res,* 88**,** E68-75.

FONG, Y., TRACEY, K. J., MOLDAWER, L. L., HESSE, D. G., MANOGUE, K. B., KENNEY, J. S., LEE, A. T., KUO, G. C., ALLISON, A. C., LOWRY, S. F. & ET AL. 1989. Antibodies to cachectin/tumor necrosis factor reduce interleukin 1 beta and interleukin 6 appearance during lethal bacteremia. *J Exp Med,* 170**,** 1627-33.

FOSTER, W., CARRUTHERS, D., LIP, G. Y. & BLANN, A. D. 2010. Inflammation and microvascular and macrovascular endothelial dysfunction in rheumatoid arthritis: effect of treatment. *J Rheumatol,* 37**,** 711-6.

FULTON, D., RUAN, L., SOOD, S. G., LI, C., ZHANG, Q. & VENEMA, R. C. 2008. Agonist-stimulated endothelial nitric oxide synthase activation and vascular relaxation. Role of eNOS phosphorylation at Tyr83. *Circ Res,* 102**,** 497-504.

FURUYAMA, H., ODAGAWA, Y., KATOH, C., IWADO, Y., ITO, Y., NORIYASU, K., MABUCHI, M., YOSHINAGA, K., KUGE, Y., KOBAYASHI, K. & TAMAKI, N. 2003. Altered myocardial flow reserve and endothelial function late after Kawasaki disease. *J Pediatr,* 142**,** 149-54.

GABRIEL, S. E., CROWSON, C. S., KREMERS, H. M., DORAN, M. F., TURESSON, C., O'FALLON, W. M. & MATTESON, E. L. 2003. Survival in rheumatoid arthritis: a population-based analysis of trends over 40 years. *Arthritis Rheum,* 48**,** 54-8.

GAO, X., BELMADANI, S., PICCHI, A., XU, X., POTTER, B. J., TEWARI-SINGH, N., CAPOBIANCO, S., CHILIAN, W. M. & ZHANG, C. 2007. Tumor necrosis factor-alpha induces endothelial dysfunction in Lepr(db) mice. *Circulation,* 115**,** 245-54.

GAO, Y. 2010. The multiple actions of NO. *Pflugers Arch,* 459**,** 829-39.

GARCIA-RUIZ, C., COLELL, A., MARI, M., MORALES, A., CALVO, M., ENRICH, C. & FERNANDEZ-CHECA, J. C. 2003. Defective TNF-alpha-mediated hepatocellular apoptosis and liver damage in acidic sphingomyelinase knockout mice. *J Clin Invest,* 111**,** 197-208.

GENTA, M. S., GENTA, R. M. & GABAY, C. 2006. Systemic rheumatoid vasculitis: a review. *Semin Arthritis Rheum,* 36**,** 88-98.

GERLI, R., SCHILLACI, G., GIORDANO, A., BOCCI, E. B., BISTONI, O., VAUDO, G., MARCHESI, S., PIRRO, M., RAGNI, F., SHOENFELD, Y. & MANNARINO, E. 2004. CD4+CD28- T lymphocytes contribute to early atherosclerotic damage in rheumatoid arthritis patients. *Circulation,* 109**,** 2744-8.

GHOSH, S., GACHHUI, R., CROOKS, C., WU, C., LISANTI, M. P. & STUEHR, D. J. 1998. Interaction between caveolin-1 and the reductase domain of endothelial nitric-oxide synthase. Consequences for catalysis. *J Biol Chem,* 273**,** 22267-71.

GIBSON, L. E. 2001. Cutaneous vasculitis update. *Dermatol Clin,* 19**,** 603-15, vii.

GLADMAN, D. D., ANG, M., SU, L., TOM, B. D., SCHENTAG, C. T. & FAREWELL, V. T. 2009. Cardiovascular morbidity in psoriatic arthritis. *Ann Rheum Dis,* 68**,** 1131-5.

GONI, F. M. & ALONSO, A. 2002. Sphingomyelinases: enzymology and membrane activity. *FEBS Lett,* 531**,** 38-46.

GONZALEZ-GAY, M. A. & GARCIA-PORRUA, C. 2002. Systemic vasculitides. *Best Pract Res Clin Rheumatol,* 16**,** 833-45.

GONZALEZ-GAY, M. A., GONZALEZ-JUANATEY, C. & MARTIN, J. 2005a. Rheumatoid arthritis: a disease associated with accelerated atherogenesis. *Semin Arthritis Rheum,* 35**,** 8-17.

GONZALEZ-GAY, M. A., GONZALEZ-JUANATEY, C., PINEIRO, A., GARCIA-PORRUA, C., TESTA, A. & LLORCA, J. 2005b. High-grade C-reactive protein elevation correlates with accelerated atherogenesis in patients with rheumatoid arthritis. *J Rheumatol,* 32**,** 1219-23.

GONZALEZ-GAY, M. A., GONZALEZ-JUANATEY, C., VAZQUEZ-RODRIGUEZ, T. R., MARTIN, J. & LLORCA, J. 2008. Endothelial dysfunction, carotid intima-media thickness, and accelerated atherosclerosis in rheumatoid arthritis. *Semin Arthritis Rheum,* 38**,** 67-70.

GONZALEZ-JUANATEY, C., LLORCA, J., GARCIA-PORRUA, C., MARTIN, J. & GONZALEZ-GAY, M. A. 2006. Effect of anti-tumor necrosis factor alpha therapy on the progression of subclinical atherosclerosis in severe rheumatoid arthritis. *Arthritis Rheum,* 55**,** 150-3.

GONZALEZ-JUANATEY, C., LOPEZ-DIAZ, M. J., MARTIN, J., LLORCA, J. & GONZALEZ-GAY, M. A. 2007. Atherosclerosis in patients with biopsy-proven giant cell arteritis. *Arthritis Rheum,* 57**,** 1481-6.

GONZALEZ-JUANATEY, C., TESTA, A., GARCIA-CASTELO, A., GARCIA-PORRUA, C., LLORCA, J. & GONZALEZ-GAY, M. A. 2004. Active but transient improvement of endothelial function in rheumatoid arthritis patients undergoing long-term treatment with anti-tumor necrosis factor alpha antibody. *Arthritis Rheum,* 51**,** 447-50.

GOODSON, N., MARKS, J., LUNT, M. & SYMMONS, D. 2005. Cardiovascular admissions and mortality in an inception cohort of patients with rheumatoid arthritis with onset in the 1980s and 1990s. *Ann Rheum Dis,* 64**,** 1595-601.

GORSKA, M., BARANCZUK, E. & DOBRZYN, A. 2003. Secretory Zn2+-dependent sphingomyelinase activity in the serum of patients with type 2 diabetes is elevated. *Horm Metab Res,* 35**,** 506-7.

GRAMMATIKOS, G., TEICHGRABER, V., CARPINTEIRO, A., TRARBACH, T., WELLER, M., HENGGE, U. R. & GULBINS, E. 2007. Overexpression of acid sphingomyelinase sensitizes glioma cells to chemotherapy. *Antioxid Redox Signal,* 9**,** 1449-56.

GRASSME, H., CREMESTI, A., KOLESNICK, R. & GULBINS, E. 2003. Ceramide-mediated clustering is required for CD95-DISC formation. *Oncogene,* 22**,** 5457-70.

GRASSME, H., JEKLE, A., RIEHLE, A., SCHWARZ, H., BERGER, J., SANDHOFF, K., KOLESNICK, R. & GULBINS, E. 2001. CD95 signaling via ceramide-rich membrane rafts. *J Biol Chem,* 276**,** 20589-96.

GRASSME, H., JENDROSSEK, V., BOCK, J., RIEHLE, A. & GULBINS, E. 2002. Ceramide-rich membrane rafts mediate CD40 clustering. *J Immunol,* 168**,** 298-307.

GREIF, D. M., KOU, R. & MICHEL, T. 2002. Site-specific dephosphorylation of endothelial nitric oxide synthase by protein phosphatase 2A: evidence for crosstalk between phosphorylation sites. *Biochemistry,* 41**,** 15845-53.

GRISAR, J., ALETAHA, D., STEINER, C. W., KAPRAL, T., STEINER, S., SEIDINGER, D., WEIGEL, G., SCHWARZINGER, I., WOLOZCSZUK, W., STEINER, G. & SMOLEN, J. S. 2005. Depletion of endothelial progenitor cells in the peripheral blood of patients with rheumatoid arthritis. *Circulation,* 111**,** 204-11.

GUILLEVIN, L., COHEN, P., GAYRAUD, M., LHOTE, F., JARROUSSE, B. & CASASSUS, P. 1999a. Churg-Strauss syndrome. Clinical study and long-term follow-up of 96 patients. *Medicine (Baltimore),* 78**,** 26-37.

GUILLEVIN, L., DURAND-GASSELIN, B., CEVALLOS, R., GAYRAUD, M., LHOTE, F., CALLARD, P., AMOUROUX, J., CASASSUS, P. & JARROUSSE, B. 1999b. Microscopic polyangiitis: clinical and laboratory findings in eighty-five patients. *Arthritis Rheum,* 42**,** 421-30.

GUILLEVIN, L., MAHR, A., CALLARD, P., GODMER, P., PAGNOUX, C., LERAY, E. & COHEN, P. 2005. Hepatitis B virus-associated polyarteritis nodosa: clinical characteristics, outcome, and impact of treatment in 115 patients. *Medicine (Baltimore),* 84**,** 313-22.

GULBINS, E. 2003. Regulation of death receptor signaling and apoptosis by ceramide. *Pharmacol Res,* 47**,** 393-9.

GULBINS, E. & GRASSME, H. 2002. Ceramide and cell death receptor clustering. *Biochim Biophys Acta,* 1585**,** 139-45.

GULBINS, E. & LI, P. L. 2006. Physiological and pathophysiological aspects of ceramide. *Am J Physiol Regul Integr Comp Physiol,* 290**,** R11-26.

HAIMOVITZ-FRIEDMAN, A., CORDON-CARDO, C., BAYOUMY, S., GARZOTTO, M., MCLOUGHLIN, M., GALLILY, R., EDWARDS, C. K., 3RD, SCHUCHMAN, E. H., FUKS, Z. & KOLESNICK, R. 1997. Lipopolysaccharide induces disseminated endothelial apoptosis requiring ceramide generation. *J Exp Med,* 186**,** 1831-41.

HALL, S., BARR, W., LIE, J. T., STANSON, A. W., KAZMIER, F. J. & HUNDER, G. G. 1985. Takayasu arteritis. A study of 32 North American patients. *Medicine (Baltimore),* 64**,** 89-99.

HAN, C., ROBINSON, D. W., JR., HACKETT, M. V., PARAMORE, L. C., FRAEMAN, K. H. & BALA, M. V. 2006. Cardiovascular disease and risk factors in patients with rheumatoid arthritis, psoriatic arthritis, and ankylosing spondylitis. *J Rheumatol,* 33**,** 2167-72.

HANNUN, Y. A. & OBEID, L. M. 2008. Principles of bioactive lipid signalling: lessons from sphingolipids. *Nat Rev Mol Cell Biol,* 9**,** 139-50.

HANSSON, G. K. & LIBBY, P. 2006. The immune response in atherosclerosis: a double-edged sword. *Nat Rev Immunol,* 6**,** 508-19.

HARPER, L., COCKWELL, P., ADU, D. & SAVAGE, C. O. 2001. Neutrophil priming and apoptosis in anti-neutrophil cytoplasmic autoantibody-associated vasculitis. *Kidney Int,* 59**,** 1729-38.

HARPER, L., REN, Y., SAVILL, J., ADU, D. & SAVAGE, C. O. 2000. Antineutrophil cytoplasmic antibodies induce reactive oxygen-dependent dysregulation of primed neutrophil apoptosis and clearance by macrophages. *Am J Pathol,* 157**,** 211-20.

HARRIS, E. D., JR. 1990. Rheumatoid arthritis. Pathophysiology and implications for therapy. *N Engl J Med,* 322**,** 1277-89.

HARRIS, M. B., BLACKSTONE, M. A., SOOD, S. G., LI, C., GOOLSBY, J. M., VENEMA, V. J., KEMP, B. E. & VENEMA, R. C. 2004. Acute activation and phosphorylation of endothelial nitric oxide synthase by HMG-CoA reductase inhibitors. *Am J Physiol Heart Circ Physiol,* 287**,** H560-6.

HARRIS, M. B., JU, H., VENEMA, V. J., LIANG, H., ZOU, R., MICHELL, B. J., CHEN, Z. P., KEMP, B. E. & VENEMA, R. C. 2001. Reciprocal phosphorylation and regulation of endothelial nitric-oxide synthase in response to bradykinin stimulation. *J Biol Chem,* 276**,** 16587-91.

HARRISON, D. G. 1997. Endothelial function and oxidant stress. *Clin Cardiol,* 20**,** II-11-7.

HASKARD, D. O. 2004. Accelerated atherosclerosis in inflammatory rheumatic diseases. *Scand J Rheumatol,* 33**,** 281-92.

HASSAN, M. Q., HADI, R. A., AL-RAWI, Z. S., PADRON, V. A. & STOHS, S. J. 2001. The glutathione defense system in the pathogenesis of rheumatoid arthritis. *J Appl Toxicol,* 21**,** 69-73.

HATANO, Y., KATAGIRI, K., ARAKAWA, S. & FUJIWARA, S. 2007. Interleukin-4 depresses levels of transcripts for acid sphingomyelinase and glucocerebroside and the amount of ceramide in acetone-wounded epidermis, as demonstrated in a living skin equivalent. *Journal of dermatological science,* 47**,** 45-47.

HATANO, Y., TERASHI, H., ARAKAWA, S. & KATAGIRI, K. 2005. Interleukin-4 suppresses the enhancement of ceramide synthesis and cutaneous permeability barrier functions induced by tumor necrosis factor-alpha and interferon-gamma in human epidermis. *J Invest Dermatol,* 124**,** 786-92.

HAWORTH, C., BRENNAN, F. M., CHANTRY, D., TURNER, M., MAINI, R. N. & FELDMANN, M. 1991. Expression of granulocyte-macrophage colony-stimulating factor in rheumatoid arthritis: regulation by tumor necrosis factor-alpha. *Eur J Immunol,* 21**,** 2575-9.

HE, X., CHEN, F., DAGAN, A., GATT, S. & SCHUCHMAN, E. H. 2003. A fluorescence-based, high-performance liquid chromatographic assay to determine acid sphingomyelinase activity and diagnose types A and B Niemann-Pick disease. *Anal Biochem,* 314**,** 116-20.

HELLER, R., UNBEHAUN, A., SCHELLENBERG, B., MAYER, B., WERNER-FELMAYER, G. & WERNER, E. R. 2001. L-ascorbic acid potentiates endothelial nitric oxide synthesis via a chemical stabilization of tetrahydrobiopterin. *J Biol Chem,* 276**,** 40-7.

HENG-LONG HU, R.J. FORSEY, T. J. BLADES, M. E.J. BARRATT, P, P. & J, R., POWELL 2000. Antioxidants may contribute in the fight against ageing: an in vitro model. *Mechanisms of Ageing and Development,* 121**,** 217-230.

HERNANDEZ, O. M., DISCHER, D. J., BISHOPRIC, N. H. & WEBSTER, K. A. 2000. Rapid activation of neutral sphingomyelinase by hypoxia-reoxygenation of cardiac myocytes. *Circ Res,* 86**,** 198-204.

HERNANZ, A., PLAZA, A., MARTIN-MOLA, E. & DE MIGUEL, E. 1999. Increased plasma levels of homocysteine and other thiol compounds in rheumatoid arthritis women. *Clin Biochem,* 32**,** 65-70.

HIDAKA, H., YAMAUCHI, K., OHTA, H., AKAMATSU, T., HONDA, T. & KATSUYAMA, T. 2008. Specific, rapid, and sensitive enzymatic measurement of sphingomyelin, phosphatidylcholine and lysophosphatidylcholine in serum and lipid extracts. *Clin Biochem,* 41**,** 1211-7.

HINGORANI, A. D., CROSS, J., KHARBANDA, R. K., MULLEN, M. J., BHAGAT, K., TAYLOR, M., DONALD, A. E., PALACIOS, M., GRIFFIN, G. E., DEANFIELD, J. E., MACALLISTER, R. J. & VALLANCE, P. 2000. Acute systemic inflammation impairs endothelium-dependent dilatation in humans. *Circulation,* 102**,** 994-9.

HIRANO, K., NOMOTO, N., HIRANO, M., MOMOTA, F., HANADA, A. & KANAIDE, H. 2007. Distinct Ca2+ requirement for NO production between proteinase-activated receptor 1 and 4 (PAR1 and PAR4) in vascular endothelial cells. *J Pharmacol Exp Ther,* 322**,** 668-77.

HIRATA, K., ISHIDA, T., MATSUSHITA, H., TSAO, P. S. & QUERTERMOUS, T. 2000. Regulated expression of endothelial cell-derived lipase. *Biochem Biophys Res Commun,* 272**,** 90-3.

HOCHBERG, M. C. 1981. Adult and juvenile rheumatoid arthritis: current epidemiologic concepts. *Epidemiol Rev,* 3**,** 27-44.

HOFER, A. M., FASOLATO, C. & POZZAN, T. 1998. Capacitative Ca2+ entry is closely linked to the filling state of internal Ca2+ stores: a study using simultaneous measurements of ICRAC and intraluminal [Ca2+]. *J Cell Biol,* 140**,** 325-34.

HOFMANN, K., TOMIUK, S., WOLFF, G. & STOFFEL, W. 2000. Cloning and characterization of the mammalian brain-specific, Mg2+-dependent neutral sphingomyelinase. *Proc Natl Acad Sci U S A,* 97**,** 5895-900.

HOJJATI, M. R., LI, Z., ZHOU, H., TANG, S., HUAN, C., OOI, E., LU, S. & JIANG, X. C. 2005. Effect of myriocin on plasma sphingolipid metabolism and atherosclerosis in apoE-deficient mice. *J Biol Chem,* 280**,** 10284-9.

HOLOPAINEN, J. M., SUBRAMANIAN, M. & KINNUNEN, P. K. 1998. Sphingomyelinase induces lipid microdomain formation in a fluid phosphatidylcholine/sphingomyelin membrane. *Biochemistry,* 37**,** 17562-70.

HOLTON, M., MOHAMED, T. M., OCEANDY, D., WANG, W., LAMAS, S., EMERSON, M., NEYSES, L. & ARMESILLA, A. L. 2010. Endothelial Nitric Oxide Synthase Activity Is Inhibited by the Plasma Membrane Calcium Atpase in Human Endothelial Cells. *Cardiovasc Res*.

HOTH, M. & PENNER, R. 1992. Depletion of intracellular calcium stores activates a calcium current in mast cells. *Nature,* 355**,** 353-6.

HUANG, A., VITA, J. A., VENEMA, R. C. & KEANEY, J. F., JR. 2000. Ascorbic acid enhances endothelial nitric-oxide synthase activity by increasing intracellular tetrahydrobiopterin. *J Biol Chem,* 275**,** 17399-406.

HUET, G., FLIPO, R. M., COLIN, C., JANIN, A., HEMON, B., COLLYN-D'HOOGHE, M., LAFYATIS, R., DUQUESNOY, B. & DEGAND, P. 1993. Stimulation of the secretion of latent cysteine proteinase activity by tumor necrosis factor alpha and interleukin-1. *Arthritis Rheum,* 36**,** 772-80.

HUET, G., FLIPO, R. M., RICHET, C., THIEBAUT, C., DEMEYER, D., BALDUYCK, M., DUQUESNOY, B. & DEGAND, P. 1992. Measurement of elastase and cysteine proteinases in synovial fluid

of patients with rheumatoid arthritis, sero-negative spondylarthropathies, and osteoarthritis. *Clin Chem,* 38**,** 1694-7.

HURLIMANN, D., FORSTER, A., NOLL, G., ENSELEIT, F., CHENEVARD, R., DISTLER, O., BECHIR, M., SPIEKER, L. E., NEIDHART, M., MICHEL, B. A., GAY, R. E., LUSCHER, T. F., GAY, S. & RUSCHITZKA, F. 2002. Anti-tumor necrosis factor-alpha treatment improves endothelial function in patients with rheumatoid arthritis. *Circulation,* 106**,** 2184-7.

HURWITZ, R., FERLINZ, K. & SANDHOFF, K. 1994a. The tricyclic antidepressant desipramine causes proteolytic degradation of lysosomal sphingomyelinase in human fibroblasts. *Biol Chem Hoppe Seyler,* 375**,** 447-50.

HURWITZ, R., FERLINZ, K., VIELHABER, G., MOCZALL, H. & SANDHOFF, K. 1994b. Processing of human acid sphingomyelinase in normal and I-cell fibroblasts. *J Biol Chem,* 269**,** 5440-5.

HUSE, M., LILLEMEIER, B. F., KUHNS, M. S., CHEN, D. S. & DAVIS, M. M. 2006. T cells use two directionally distinct pathways for cytokine secretion. *Nat Immunol,* 7**,** 247-55.

HUSSEIN, M. R., FATHI, N. A., EL-DIN, A. M., HASSAN, H. I., ABDULLAH, F., AL-HAKEEM, E. & BACKER, E. A. 2008. Alterations of the CD4(+), CD8 (+) T cell subsets, interleukins-1beta, IL-10, IL-17, tumor necrosis factor-alpha and soluble intercellular adhesion molecule-1 in rheumatoid arthritis and osteoarthritis: preliminary observations. *Pathol Oncol Res,* 14**,** 321-8.

HUWILER, A., KOLTER, T., PFEILSCHIFTER, J. & SANDHOFF, K. 2000. Physiology and pathophysiology of sphingolipid metabolism and signaling. *Biochim Biophys Acta,* 1485**,** 63-99.

IGARASHI, J. & MICHEL, T. 2001. Sphingosine 1-phosphate and isoform-specific activation of phosphoinositide 3-kinase beta. Evidence for divergence and convergence of receptor-regulated endothelial nitric-oxide synthase signaling pathways. *J Biol Chem,* 276**,** 36281-8.

IGARASHI, J. & MICHEL, T. 2008. S1P and eNOS regulation. *Biochim Biophys Acta,* 1781**,** 489-95.

IGARASHI, J., MIYOSHI, M., HASHIMOTO, T., KUBOTA, Y. & KOSAKA, H. 2007. Statins induce S1P1 receptors and enhance endothelial nitric oxide production in response to high-density lipoproteins. *Br J Pharmacol,* 150**,** 470-9.

IGARASHI, J., THATTE, H. S., PRABHAKAR, P., GOLAN, D. E. & MICHEL, T. 1999. Calcium-independent activation of endothelial nitric oxide synthase by ceramide. *Proc Natl Acad Sci U S A,* 96**,** 12583-8.

IKONOMIDIS, I., LEKAKIS, J. P., NIKOLAOU, M., PARASKEVAIDIS, I., ANDREADOU, I., KAPLANOGLOU, T., KATSIMBRI, P., SKARANTAVOS, G., SOUCACOS, P. N. & KREMASTINOS, D. T. 2008. Inhibition of interleukin-1 by anakinra improves vascular and left ventricular function in patients with rheumatoid arthritis. *Circulation,* 117**,** 2662-9.

ILCOL, Y. O., UNCU, G., GOREN, S., SAYAN, E. & ULUS, I. H. 2004. Declines in serum free and bound choline concentrations in humans after three different types of major surgery. *Clin Chem Lab Med,* 42**,** 1390-5.

INOMATA, M., INTO, T., NAKASHIMA, M., NOGUCHI, T. & MATSUSHITA, K. 2009. IL-4 alters expression patterns of storage components of vascular endothelial cell-specific granules through STAT6- and SOCS-1-dependent mechanisms. *Mol Immunol,* 46**,** 2080-9.

ISSHIKI, M., ANDO, J., KORENAGA, R., KOGO, H., FUJIMOTO, T., FUJITA, T. & KAMIYA, A. 1998. Endothelial Ca2+ waves preferentially originate at specific loci in caveolin-rich cell edges. *Proc Natl Acad Sci U S A,* 95**,** 5009-14.

ISSHIKI, M., ANDO, J., YAMAMOTO, K., FUJITA, T., YING, Y. & ANDERSON, R. G. 2002. Sites of Ca(2+) wave initiation move with caveolae to the trailing edge of migrating cells. *J Cell Sci,* 115**,** 475-84.

ITO, M., NAKANO, T., ERDODI, F. & HARTSHORNE, D. J. 2004. Myosin phosphatase: structure, regulation and function. *Mol Cell Biochem,* 259**,** 197-209.

JACOBSSON, L. T., KNOWLER, W. C., PILLEMER, S., HANSON, R. L., PETTITT, D. J., NELSON, R. G., DEL PUENTE, A., MCCANCE, D. R., CHARLES, M. A. & BENNETT, P. H. 1993. Rheumatoid arthritis and mortality. A longitudinal study in Pima Indians. *Arthritis Rheum,* 36**,** 1045-53.

JACOBSSON, L. T., TURESSON, C., GULFE, A., KAPETANOVIC, M. C., PETERSSON, I. F., SAXNE, T. & GEBOREK, P. 2005. Treatment with tumor necrosis factor blockers is associated with a lower incidence of first cardiovascular events in patients with rheumatoid arthritis. *J Rheumatol,* 32**,** 1213-8.

JAYNE, D. 2009. The diagnosis of vasculitis. *Best Pract Res Clin Rheumatol,* 23**,** 445-53.

JAYNE, D. R., GASKIN, G., RASMUSSEN, N., ABRAMOWICZ, D., FERRARIO, F., GUILLEVIN, L., MIRAPEIX, E., SAVAGE, C. O., SINICO, R. A., STEGEMAN, C. A., WESTMAN, K. W., VAN DER WOUDE, F. J., DE LIND VAN WIJNGAARDEN, R. A. & PUSEY, C. D. 2007. Randomized trial of plasma exchange or high-dosage methylprednisolone as adjunctive therapy for severe renal vasculitis. *J Am Soc Nephrol,* 18**,** 2180-8.

JENKINS, R. W., CANALS, D. & HANNUN, Y. A. 2009. Roles and regulation of secretory and lysosomal acid sphingomyelinase. *Cell Signal,* 21**,** 836-46.

JENKINS, R. W., CANALS, D., IDKOWIAK-BALDYS, J., SIMBARI, F., RODDY, P., PERRY, D. M., KITATANI, K., LUBERTO, C. & HANNUN, Y. A. 2010a. Regulated secretion of acid sphingomyelinase: implications for selectivity of ceramide formation. *J Biol Chem,* 285**,** 35706-18.

JENKINS, R. W., IDKOWIAK-BALDYS, J., SIMBARI, F., CANALS, D., RODDY, P., RINER, C. D., CLARKE, C. J. & HANNUN, Y. A. 2010b. A novel mechanism of lysosomal acid sphingomyelinase maturation - requirement for carboxy-terminal proteolytic processing. *J Biol Chem*.

JENNETTE, J. C., FALK, R. J., ANDRASSY, K., BACON, P. A., CHURG, J., GROSS, W. L., HAGEN, E. C., HOFFMAN, G. S., HUNDER, G. G., KALLENBERG, C. G. & ET AL. 1994. Nomenclature of systemic vasculitides. Proposal of an international consensus conference. *Arthritis Rheum,* 37**,** 187-92.

JESSOP, C. E. & BULLEID, N. J. 2004. Glutathione directly reduces an oxidoreductase in the endoplasmic reticulum of mammalian cells. *J Biol Chem,* 279**,** 55341-7.

JIN, S., YI, F., ZHANG, F., POKLIS, J. L. & LI, P. L. 2008. Lysosomal targeting and trafficking of acid sphingomyelinase to lipid raft platforms in coronary endothelial cells. *Arterioscler Thromb Vasc Biol,* 28**,** 2056-62.

JIN, S. & ZHOU, F. 2009. Lipid raft redox signaling platforms in vascular dysfunction: features and mechanisms. *Curr Atheroscler Rep,* 11**,** 220-6.

JIN, W., SUN, G. S., MARCHADIER, D., OCTTAVIANI, E., GLICK, J. M. & RADER, D. J. 2003. Endothelial cells secrete triglyceride lipase and phospholipase activities in response to cytokines as a result of endothelial lipase. *Circ Res,* 92**,** 644-50.

JODON DE VILLEROCHE, V., AVOUAC, J., PONCEAU, A., RUIZ, B., KAHAN, A., BOILEAU, C., UZAN, G. & ALLANORE, Y. 2010. Enhanced late-outgrowth circulating endothelial progenitor cell levels in rheumatoid arthritis and correlation with disease activity. *Arthritis Res Ther,* 12**,** R27.

JOHNS, D. G., JIN, J. S. & WEBB, R. C. 1998. The role of the endothelium in ceramide-induced vasodilation. *Eur J Pharmacol,* 349**,** R9-10.

JONASSON, L., HOLM, J., SKALLI, O., BONDJERS, G. & HANSSON, G. K. 1986. Regional accumulations of T cells, macrophages, and smooth muscle cells in the human atherosclerotic plaque. *Arteriosclerosis,* 6**,** 131-8.

JONES, S. J., LEDGERWOOD, E. C., PRINS, J. B., GALBRAITH, J., JOHNSON, D. R., POBER, J. S. & BRADLEY, J. R. 1999. TNF recruits TRADD to the plasma membrane but not the trans-Golgi network, the principal subcellular location of TNF-R1. *J Immunol,* 162**,** 1042-8.

JOOSTEN, L. A., HELSEN, M. M., SAXNE, T., VAN DE LOO, F. A., HEINEGARD, D. & VAN DEN BERG, W. B. 1999. IL-1 alpha beta blockade prevents cartilage and bone destruction in murine type II collagen-induced arthritis, whereas TNF-alpha blockade only ameliorates joint inflammation. *J Immunol,* 163**,** 5049-55.

JORNOT, L. & JUNOD, A. F. 1993. Variable glutathione levels and expression of antioxidant enzymes in human endothelial cells. *Am J Physiol,* 264**,** L482-9.

KAMANLI, A., NAZIROGLU, M., AYDILEK, N. & HACIEVLIYAGIL, C. 2004. Plasma lipid peroxidation and antioxidant levels in patients with rheumatoid arthritis. *Cell Biochem Funct,* 22**,** 53-7.

KANFER, J. N., YOUNG, O. M., SHAPIRO, D. & BRADY, R. O. 1966. The metabolism of sphingomyelin. I. Purification and properties of a sphingomyelin-cleaving enzyme from rat liver tissue. *J Biol Chem,* 241**,** 1081-4.

KAPLAN, D. 1986. The age of death of the parents of patients with rheumatoid arthritis: a preliminary study. *J Rheumatol,* 13**,** 903-6.

KAPLAN, D. & FELDMAN, J. 1991. A preliminary study of excess risk of cardiovascular disease in the mothers of patients with rheumatoid arthritis. *Am J Epidemiol,* 133**,** 715-20.

KARATAS, F., OZATES, I., CANATAN, H., HALIFEOGLU, I., KARATEPE, M. & COLAKT, R. 2003. Antioxidant status & lipid peroxidation in patients with rheumatoid arthritis. *Indian J Med Res,* 118**,** 178-81.

KEFFER, J., PROBERT, L., CAZLARIS, H., GEORGOPOULOS, S., KASLARIS, E., KIOUSSIS, D. & KOLLIAS, G. 1991. Transgenic mice expressing human tumour necrosis factor: a predictive genetic model of arthritis. *EMBO J,* 10**,** 4025-31.

KEITH, M., GERANMAYEGAN, A., SOLE, M. J., KURIAN, R., ROBINSON, A., OMRAN, A. S. & JEEJEEBHOY, K. N. 1998. Increased oxidative stress in patients with congestive heart failure. *J Am Coll Cardiol,* 31**,** 1352-6.

KEMP, M., GO, Y. M. & JONES, D. P. 2008. Nonequilibrium thermodynamics of thiol/disulfide redox systems: a perspective on redox systems biology. *Free Radic Biol Med,* 44**,** 921-37.

KEOGH, K. A. & SPECKS, U. 2006. Churg-Strauss syndrome. *Semin Respir Crit Care Med,* 27**,** 148-57.

KEREKES, G., SZEKANECZ, Z., DER, H., SANDOR, Z., LAKOS, G., MUSZBEK, L., CSIPO, I., SIPKA, S., SERES, I., PARAGH, G., KAPPELMAYER, J., SZOMJAK, E., VERES, K., SZEGEDI, G., SHOENFELD, Y. & SOLTESZ, P. 2008. Endothelial dysfunction and atherosclerosis in rheumatoid arthritis: a multiparametric analysis using imaging techniques and laboratory markers of inflammation and autoimmunity. *J Rheumatol,* 35**,** 398-406.

KEVIL, C. G. 2003. Endothelial cell activation in inflammation: lessons from mutant mouse models. *Pathophysiology,* 9**,** 63-74.

KHAN, F., GALARRAGA, B. & BELCH, J. J. 2010. The role of endothelial function and its assessment in rheumatoid arthritis. *Nat Rev Rheumatol,* 6**,** 253-61.

KIM, F., GALLIS, B. & CORSON, M. A. 2001. TNF-alpha inhibits flow and insulin signaling leading to NO production in aortic endothelial cells. *Am J Physiol Cell Physiol,* 280**,** C1057-65.

KISHIMOTO, T. 2005. Interleukin-6: from basic science to medicine--40 years in immunology. *Annu Rev Immunol,* 23**,** 1-21.

KITAS, G., BANKS, M. J. & BACON, P. A. 2001. Cardiac involvement in rheumatoid disease. *Clin Med,* 1**,** 18-21.

KITATANI, K., IDKOWIAK-BALDYS, J. & HANNUN, Y. A. 2008. The sphingolipid salvage pathway in ceramide metabolism and signaling. *Cell Signal,* 20**,** 1010-8.

KLEINHENZ, D. J., FAN, X., RUBIN, J. & HART, C. M. 2003. Detection of endothelial nitric oxide release with the 2,3-diaminonapthalene assay. *Free Radic Biol Med,* 34**,** 856-61.

KOCH, A. E. 2003. Angiogenesis as a target in rheumatoid arthritis. *Ann Rheum Dis,* 62 Suppl 2**,** ii60-7.

KOHEN, R. & NYSKA, A. 2002. Oxidation of biological systems: oxidative stress phenomena, antioxidants, redox reactions, and methods for their quantification. *Toxicol Pathol,* 30**,** 620-50.

KOLB, W. P. & GRANGER, G. A. 1968. Lymphocyte in vitro cytotoxicity: characterization of human lymphotoxin. *Proc Natl Acad Sci U S A,* 61**,** 1250-5.

KOLESNICK, R. & FUKS, Z. 2003. Radiation and ceramide-induced apoptosis. *Oncogene,* 22**,** 5897-906.

KOLESNICK, R. N. 1987. 1,2-Diacylglycerols but not phorbol esters stimulate sphingomyelin hydrolysis in GH3 pituitary cells. *J Biol Chem,* 262**,** 16759-62.

KOLESNICK, R. N., GONI, F. M. & ALONSO, A. 2000. Compartmentalization of ceramide signaling: physical foundations and biological effects. *J Cell Physiol,* 184**,** 285-300.

KOLMAKOVA, A., KWITEROVICH, P., VIRGIL, D., ALAUPOVIC, P., KNIGHT-GIBSON, C., MARTIN, S. F. & CHATTERJEE, S. 2004. Apolipoprotein C-I induces apoptosis in human aortic smooth muscle cells via recruiting neutral sphingomyelinase. *Arterioscler Thromb Vasc Biol,* 24**,** 264-9.

KOLTER, T. & SANDHOFF, K. 2005. Principles of lysosomal membrane digestion: stimulation of sphingolipid degradation by sphingolipid activator proteins and anionic lysosomal lipids. *Annu Rev Cell Dev Biol,* 21**,** 81-103.

KORNFELD, S. 1987. Trafficking of lysosomal enzymes. *FASEB J,* 1**,** 462-8.

KOU, R., GREIF, D. & MICHEL, T. 2002. Dephosphorylation of endothelial nitric-oxide synthase by vascular endothelial growth factor. Implications for the vascular responses to cyclosporin A. *J Biol Chem,* 277**,** 29669-73.

KRADIN, R. L. & MARK, E. J. 2002. Case records of the Massachusetts General Hospital. Weekly clinicopathological exercises. Case 18-2002. A 48-year-old man with a cough and bloody sputum. *N Engl J Med,* 346**,** 1892-9.

KREMERS, H. M., CROWSON, C. S., THERNEAU, T. M., ROGER, V. L. & GABRIEL, S. E. 2008. High ten-year risk of cardiovascular disease in newly diagnosed rheumatoid arthritis patients: a population-based cohort study. *Arthritis Rheum,* 58**,** 2268-74.

KROWN, K. A., PAGE, M. T., NGUYEN, C., ZECHNER, D., GUTIERREZ, V., COMSTOCK, K. L., GLEMBOTSKI, C. C., QUINTANA, P. J. & SABBADINI, R. A. 1996. Tumor necrosis factor alpha-induced apoptosis in cardiac myocytes. Involvement of the sphingolipid signaling cascade in cardiac cell death. *J Clin Invest,* 98**,** 2854-65.

KRUEGER, S., KUESTER, D., BERNHARDT, A., WEX, T. & ROESSNER, A. 2009. Regulation of cathepsin X overexpression in H. pylori-infected gastric epithelial cells and macrophages. *J Pathol,* 217**,** 581-8.

KRUT, O., WIEGMANN, K., KASHKAR, H., YAZDANPANAH, B. & KRONKE, M. 2006. Novel tumor necrosis factor-responsive mammalian neutral sphingomyelinase-3 is a C-tail-anchored protein. *J Biol Chem,* 281**,** 13784-93.

KUNO, K., SUKEGAWA, K., ISHIKAWA, Y., ORII, T. & MATSUSHIMA, K. 1994. Acid sphingomyelinase is not essential for the IL-1 and tumor necrosis factor receptor signaling pathway leading to NFkB activation. *Int Immunol,* 6**,** 1269-72.

KUSSMAUL, A. & MAIER, R. 1866. Ueber eine bisher nicht beschriebene eigenthumliche Arterienerkrankung (Periarteritis nodosa), die mit Morbus Brightii und rapid fortschreitender allgemeiner Muskellahmung einhergeht. *Dtsch Arch Klin Med,* 1**,** 484 – 518.

KWON, Y. G., MIN, J. K., KIM, K. M., LEE, D. J., BILLIAR, T. R. & KIM, Y. M. 2001. Sphingosine 1-phosphate protects human umbilical vein endothelial cells from serum-deprived apoptosis by nitric oxide production. *J Biol Chem,* 276**,** 10627-33.

LANDMESSER, U., SPIEKERMANN, S., DIKALOV, S., TATGE, H., WILKE, R., KOHLER, C., HARRISON, D. G., HORNIG, B. & DREXLER, H. 2002. Vascular oxidative stress and endothelial dysfunction in patients with chronic heart failure: role of xanthine-oxidase and extracellular superoxide dismutase. *Circulation,* 106**,** 3073-8.

LANGMANN, T., BUECHLER, C., RIES, S., SCHAEFFLER, A., ASLANIDIS, C., SCHUIERER, M., WEILER, M., SANDHOFF, K., DE JONG, P. J. & SCHMITZ, G. 1999. Transcription factors Sp1 and AP-2 mediate induction of acid sphingomyelinase during monocytic differentiation. *J Lipid Res,* 40**,** 870-80.

LANSMANN, S., SCHUETTE, C. G., BARTELSEN, O., HOERNSCHEMEYER, J., LINKE, T., WEISGERBER, J. & SANDHOFF, K. 2003. Human acid sphingomyelinase. *Eur J Biochem,* 270**,** 1076-88.

LEE, C. Y., TAMURA, T., RABAH, N., LEE, D. Y., RUEL, I., HAFIANE, A., IATAN, I., NYHOLT, D., LAPORTE, F., LAZURE, C., WADA, I., KRIMBOU, L. & GENEST, J. 2007. Carboxyl-terminal disulfide bond of acid sphingomyelinase is critical for its secretion and enzymatic function. *Biochemistry,* 46**,** 14969-78.

LEE, D. M. & WEINBLATT, M. E. 2001. Rheumatoid arthritis. *Lancet,* 358**,** 903-11.

LEE, M. J., KIM, J., KIM, M. Y., BAE, Y. S., RYU, S. H., LEE, T. G. & KIM, J. H. 2010. Proteomic analysis of tumor necrosis factor-alpha-induced secretome of human adipose tissue-derived mesenchymal stem cells. *J Proteome Res,* 9**,** 1754-62.

LEMAIRE, R., HUET, G., ZERIMECH, F., GRARD, G., FONTAINE, C., DUQUESNOY, B. & FLIPO, R. M. 1997. Selective induction of the secretion of cathepsins B and L by cytokines in synovial fibroblast-like cells. *Br J Rheumatol,* 36**,** 735-43.

LEPPLE-WIENHUES, A., BELKA, C., LAUN, T., JEKLE, A., WALTER, B., WIELAND, U., WELZ, M., HEIL, L., KUN, J., BUSCH, G., WELLER, M., BAMBERG, M., GULBINS, E. & LANG, F. 1999. Stimulation of CD95 (Fas) blocks T lymphocyte calcium channels through sphingomyelinase and sphingolipids. *Proc Natl Acad Sci U S A,* 96**,** 13795-800.

LEVADE, T., AUGE, N., VELDMAN, R. J., CUVILLIER, O., NEGRE-SALVAYRE, A. & SALVAYRE, R. 2001. Sphingolipid mediators in cardiovascular cell biology and pathology. *Circ Res,* 89**,** 957-68.

LEVADE, T., GATT, S., MARET, A. & SALVAYRE, R. 1991. Different pathways of uptake and degradation of sphingomyelin by lymphoblastoid cells and the potential participation of the neutral sphingomyelinase. *J Biol Chem,* 266**,** 13519-29.

LEWIS, R. S. 2007. The molecular choreography of a store-operated calcium channel. *Nature,* 446**,** 284-7.

LI, H., JUNK, P., HUWILER, A., BURKHARDT, C., WALLERATH, T., PFEILSCHIFTER, J. & FORSTERMANN, U. 2002. Dual effect of ceramide on human endothelial cells: induction of oxidative stress and transcriptional upregulation of endothelial nitric oxide synthase. *Circulation,* 106**,** 2250-6.

LI, P. L. & GULBINS, E. 2007. Lipid rafts and redox signaling. *Antioxid Redox Signal,* 9**,** 1411-5.

LI, W., LI, H., BOCKING, A. D. & CHALLIS, J. R. 2010. Tumor necrosis factor stimulates matrix metalloproteinase 9 secretion from cultured human chorionic trophoblast cells through TNF receptor 1 signaling to IKBKB-NFKB and MAPK1/3 pathway. *Biol Reprod,* 83**,** 481-7.

LIMA, D. S., SATO, E. I., LIMA, V. C., MIRANDA, F., JR. & HATTA, F. H. 2002. Brachial endothelial function is impaired in patients with systemic lupus erythematosus. *J Rheumatol,* 29**,** 292-7.

LIN, S., FAGAN, K. A., LI, K. X., SHAUL, P. W., COOPER, D. M. & RODMAN, D. M. 2000. Sustained endothelial nitric-oxide synthase activation requires capacitative Ca2+ entry. *J Biol Chem,* 275**,** 17979-85.

LIOU, J., FIVAZ, M., INOUE, T. & MEYER, T. 2007. Live-cell imaging reveals sequential oligomerization and local plasma membrane targeting of stromal interaction molecule 1 after Ca2+ store depletion. *Proc Natl Acad Sci U S A,* 104**,** 9301-6.

LIOU, J., KIM, M. L., HEO, W. D., JONES, J. T., MYERS, J. W., FERRELL, J. E., JR. & MEYER, T. 2005. STIM is a Ca2+ sensor essential for Ca2+-store-depletion-triggered Ca2+ influx. *Curr Biol,* 15**,** 1235-41.

LISTING, J., STRANGFELD, A., KEKOW, J., SCHNEIDER, M., KAPELLE, A., WASSENBERG, S. & ZINK, A. 2008. Does tumor necrosis factor alpha inhibition promote or prevent heart failure in patients with rheumatoid arthritis? *Arthritis Rheum,* 58**,** 667-77.

LIU, B., ANDRIEU-ABADIE, N., LEVADE, T., ZHANG, P., OBEID, L. M. & HANNUN, Y. A. 1998. Glutathione regulation of neutral sphingomyelinase in tumor necrosis factor-alpha-induced cell death. *J Biol Chem,* 273**,** 11313-20.

LIU, B. & HANNUN, Y. A. 1997. Inhibition of the neutral magnesium-dependent sphingomyelinase by glutathione. *J Biol Chem,* 272**,** 16281-7.

LIU, X., ZEIDAN, Y. H., ELOJEIMY, S., HOLMAN, D. H., EL-ZAWAHRY, A. M., GUO, G. W., BIELAWSKA, A., BIELAWSKI, J., SZULC, Z., RUBINCHIK, S., DONG, J. Y., KEANE, T. E., TAVASSOLI, M., HANNUN, Y. A. & NORRIS, J. S. 2006. Involvement of sphingolipids in apoptin-induced cell killing. *Mol Ther,* 14**,** 627-36.

LIUZZO, G., GORONZY, J. J., YANG, H., KOPECKY, S. L., HOLMES, D. R., FRYE, R. L. & WEYAND, C. M. 2000. Monoclonal T-cell proliferation and plaque instability in acute coronary syndromes. *Circulation,* 101**,** 2883-8.

LLACUNA, L., MARI, M., GARCIA-RUIZ, C., FERNANDEZ-CHECA, J. C. & MORALES, A. 2006. Critical role of acidic sphingomyelinase in murine hepatic ischemia-reperfusion injury. *Hepatology,* 44**,** 561-72.

LOIDL, A., CLAUS, R., DEIGNER, H. P. & HERMETTER, A. 2002. High-precision fluorescence assay for sphingomyelinase activity of isolated enzymes and cell lysates. *J Lipid Res,* 43**,** 815-23.

LU, S. C. 1999. Regulation of hepatic glutathione synthesis: current concepts and controversies. *FASEB J,* 13**,** 1169-83.

LUQMANI, R. A., BACON, P. A., MOOTS, R. J., JANSSEN, B. A., PALL, A., EMERY, P., SAVAGE, C. & ADU, D. 1994. Birmingham Vasculitis Activity Score (BVAS) in systemic necrotizing vasculitis. *QJM,* 87**,** 671-8.

LYTWYN, M., WALKER, J., KIRKPATRICK, I. D., DUCAS, J. & JASSAL, D. S. 2010. Giant coronary artery aneurysms in Kawasaki's disease. *Echocardiography,* 27**,** E53-4.

MACIEWICZ, R. A., WOTTON, S. F., ETHERINGTON, D. J. & DUANCE, V. C. 1990. Susceptibility of the cartilage collagens types II, IX and XI to degradation by the cysteine proteinases, cathepsins B and L. *FEBS Lett,* 269**,** 189-93.

MAKSIMOWICZ-MCKINNON, K., CLARK, T. M. & HOFFMAN, G. S. 2007. Limitations of therapy and a guarded prognosis in an American cohort of Takayasu arteritis patients. *Arthritis Rheum,* 56**,** 1000-9.

MANDERSON, A. P., KAY, J. G., HAMMOND, L. A., BROWN, D. L. & STOW, J. L. 2007. Subcompartments of the macrophage recycling endosome direct the differential secretion of IL-6 and TNFalpha. *J Cell Biol,* 178**,** 57-69.

MANTHEY, C. L. & SCHUCHMAN, E. H. 1998. Acid sphingomyelinase-derived ceramide is not required for inflammatory cytokine signalling in murine macrophages. *Cytokine,* 10**,** 654-61.

MANZI, S., MEILAHN, E. N., RAIRIE, J. E., CONTE, C. G., MEDSGER, T. A., JR., JANSEN-MCWILLIAMS, L., D'AGOSTINO, R. B. & KULLER, L. H. 1997. Age-specific incidence rates of myocardial infarction and angina in women with systemic lupus erythematosus: comparison with the Framingham Study. *Am J Epidemiol,* 145**,** 408-15.

MARADIT-KREMERS, H., CROWSON, C. S., NICOLA, P. J., BALLMAN, K. V., ROGER, V. L., JACOBSEN, S. J. & GABRIEL, S. E. 2005a. Increased unrecognized coronary heart disease and sudden deaths in rheumatoid arthritis: a population-based cohort study. *Arthritis Rheum,* 52**,** 402-11.

MARADIT-KREMERS, H., NICOLA, P. J., CROWSON, C. S., BALLMAN, K. V. & GABRIEL, S. E. 2005b. Cardiovascular death in rheumatoid arthritis: a population-based study. *Arthritis Rheum,* 52**,** 722-32.

MARATHE, S., CHOI, Y., LEVENTHAL, A. R. & TABAS, I. 2000. Sphingomyelinase converts lipoproteins from apolipoprotein E knockout mice into potent inducers of macrophage foam cell formation. *Arterioscler Thromb Vasc Biol,* 20**,** 2607-13.

MARATHE, S., KURIAKOSE, G., WILLIAMS, K. J. & TABAS, I. 1999. Sphingomyelinase, an enzyme implicated in atherogenesis, is present in atherosclerotic lesions and binds to specific components of the subendothelial extracellular matrix. *Arterioscler Thromb Vasc Biol,* 19**,** 2648-58.

MARATHE, S., SCHISSEL, S. L., YELLIN, M. J., BEATINI, N., MINTZER, R., WILLIAMS, K. J. & TABAS, I. 1998. Human vascular endothelial cells are a rich and regulatable source of secretory sphingomyelinase. Implications for early atherogenesis and ceramide-mediated cell signaling. *J Biol Chem,* 273**,** 4081-8.

MARKOVIC, J., BORRAS, C., ORTEGA, A., SASTRE, J., VINA, J. & PALLARDO, F. V. 2007. Glutathione is recruited into the nucleus in early phases of cell proliferation. *J Biol Chem,* 282**,** 20416-24.

MATHES, C., FLEIG, A. & PENNER, R. 1998. Calcium release-activated calcium current (ICRAC) is a direct target for sphingosine. *J Biol Chem,* 273**,** 25020-30.

MCCOLLISTER, B. D., MYERS, J. T., JONES-CARSON, J., VOELKER, D. R. & VAZQUEZ-TORRES, A. 2007. Constitutive acid sphingomyelinase enhances early and late macrophage killing of Salmonella enterica serovar Typhimurium. *Infect Immun,* 75**,** 5346-52.

MCINNES, I. B. & SCHETT, G. 2007. Cytokines in the pathogenesis of rheumatoid arthritis. *Nat Rev Immunol,* 7**,** 429-42.

MCMURRAY, J., CHOPRA, M., ABDULLAH, I., SMITH, W. E. & DARGIE, H. J. 1993. Evidence of oxidative stress in chronic heart failure in humans. *Eur Heart J,* 14**,** 1493-8.

MEGHA & LONDON, E. 2004. Ceramide selectively displaces cholesterol from ordered lipid domains (rafts): implications for lipid raft structure and function. *J Biol Chem,* 279**,** 9997-10004.

MEISTER, A. & ANDERSON, M. E. 1983. Glutathione. *Annu Rev Biochem,* 52**,** 711-60.

MERRILL, A. H., JR. & JONES, D. D. 1990. An update of the enzymology and regulation of sphingomyelin metabolism. *Biochim Biophys Acta,* 1044**,** 1-12.

METSIOS, G. S., STAVROPOULOS-KALINOGLOU, A., SANDOO, A., VAN ZANTEN, J. J., TOMS, T. E., JOHN, H. & KITAS, G. D. 2010. Vascular function and inflammation in rheumatoid arthritis: the role of physical activity. *Open Cardiovasc Med J,* 4**,** 89-96.

MICHEL, T. & VANHOUTTE, P. M. 2010. Cellular signaling and NO production. *Pflugers Arch,* 459**,** 807-16.

MICHELL, B. J., CHEN, Z., TIGANIS, T., STAPLETON, D., KATSIS, F., POWER, D. A., SIM, A. T. & KEMP, B. E. 2001. Coordinated control of endothelial nitric-oxide synthase phosphorylation by protein kinase C and the cAMP-dependent protein kinase. *J Biol Chem,* 276**,** 17625-8.

MICHELL, B. J., HARRIS, M. B., CHEN, Z. P., JU, H., VENEMA, V. J., BLACKSTONE, M. A., HUANG, W., VENEMA, R. C. & KEMP, B. E. 2002. Identification of regulatory sites of phosphorylation of the bovine endothelial nitric-oxide synthase at serine 617 and serine 635. *J Biol Chem,* 277**,** 42344-51.

MICHIELS, C. 2003. Endothelial cell functions. *J Cell Physiol,* 196**,** 430-43.

MIDDLETON, J., AMERICH, L., GAYON, R., JULIEN, D., AGUILAR, L., AMALRIC, F. & GIRARD, J. P. 2004. Endothelial cell phenotypes in the rheumatoid synovium: activated, angiogenic, apoptotic and leaky. *Arthritis Res Ther,* 6**,** 60-72.

MIOSSEC, P., BRIOLAY, J., DECHANET, J., WIJDENES, J., MARTINEZ-VALDEZ, H. & BANCHEREAU, J. 1992. Inhibition of the production of proinflammatory cytokines and immunoglobulins by interleukin-4 in an ex vivo model of rheumatoid synovitis. *Arthritis Rheum,* 35**,** 874-83.

MODUR, V., ZIMMERMAN, G. A., PRESCOTT, S. M. & MCINTYRE, T. M. 1996. Endothelial cell inflammatory responses to tumor necrosis factor alpha. Ceramide-dependent and -independent mitogen-activated protein kinase cascades. *J Biol Chem,* 271**,** 13094-102.

MOGAMI, K., KISHI, H. & KOBAYASHI, S. 2005. Sphingomyelinase causes endothelium-dependent vasorelaxation through endothelial nitric oxide production without cytosolic Ca(2+) elevation. *FEBS Lett,* 579**,** 393-7.

MOHAN, N. & KERR, G. 2000. Spectrum of giant cell vasculitis. *Curr Rheumatol Rep,* 2**,** 390-5.

MORALES, A., GARCIA-RUIZ, C., MIRANDA, M., MARI, M., COLELL, A., ARDITE, E. & FERNANDEZ-CHECA, J. C. 1997. Tumor necrosis factor increases hepatocellular glutathione by transcriptional regulation of the heavy subunit chain of gamma-glutamylcysteine synthetase. *J Biol Chem,* 272**,** 30371-9.

MORGAN, M. D., TURNBULL, J., SELAMET, U., KAUR-HAYER, M., NIGHTINGALE, P., FERRO, C. J., SAVAGE, C. O. & HARPER, L. 2009. Increased incidence of cardiovascular events in patients with antineutrophil cytoplasmic antibody-associated vasculitides: a matched-pair cohort study. *Arthritis Rheum,* 60**,** 3493-500.

MOTLEY, E. D., EGUCHI, K., PATTERSON, M. M., PALMER, P. D., SUZUKI, H. & EGUCHI, S. 2007. Mechanism of endothelial nitric oxide synthase phosphorylation and activation by thrombin. *Hypertension,* 49**,** 577-83.

MOUNT, P. F., KEMP, B. E. & POWER, D. A. 2007. Regulation of endothelial and myocardial NO synthesis by multi-site eNOS phosphorylation. *J Mol Cell Cardiol,* 42**,** 271-9.

MUELLER, A., HOLL-ULRICH, K., LAMPRECHT, P. & GROSS, W. L. 2008. Germinal centre-like structures in Wegener's granuloma: the morphological basis for autoimmunity? *Rheumatology (Oxford),* 47**,** 1111-3.

MUKHTYAR, C., BROGAN, P. & LUQMANI, R. 2009. Cardiovascular involvement in primary systemic vasculitis. *Best Pract Res Clin Rheumatol,* 23**,** 419-28.

MURATE, T., SUZUKI, M., HATTORI, M., TAKAGI, A., KOJIMA, T., TANIZAWA, T., ASANO, H., HOTTA, T., SAITO, H., YOSHIDA, S. & TAMIYA-KOIZUMI, K. 2002. Up-regulation of acid sphingomyelinase during retinoic acid-induced myeloid differentiation of NB4, a human acute promyelocytic leukemia cell line. *J Biol Chem,* 277**,** 9936-43.

MURRAY, R. Z., KAY, J. G., SANGERMANI, D. G. & STOW, J. L. 2005a. A role for the phagosome in cytokine secretion. *Science,* 310**,** 1492-5.

MURRAY, R. Z., WYLIE, F. G., KHROMYKH, T., HUME, D. A. & STOW, J. L. 2005b. Syntaxin 6 and Vti1b form a novel SNARE complex, which is up-regulated in activated macrophages to facilitate exocytosis of tumor necrosis Factor-alpha. *J Biol Chem,* 280**,** 10478-83.

NAKAGAWA, S. 2004. A farewell to Bonferroni: the problems of low statistical power and publication bias. *Behavioural ecology,* 15**,** 1044-1045.

NAKAMURA, H., NAKAMURA, K. & YODOI, J. 1997. Redox regulation of cellular activation. *Annu Rev Immunol,* 15**,** 351-69.

NAKAMURA, M., YOSHIDA, H., ARAKAWA, N., SAITOH, S., SATOH, M. & HIRAMORI, K. 2000. Effects of tumor necrosis factor-alpha on basal and stimulated endothelium-dependent vasomotion in human resistance vessel. *J Cardiovasc Pharmacol,* 36**,** 487-92.

NAKASHIMA, Y., CHEN, Y. X., KINUKAWA, N. & SUEISHI, K. 2002. Distributions of diffuse intimal thickening in human arteries: preferential expression in atherosclerosis-prone arteries from an early age. *Virchows Arch,* 441**,** 279-88.

NAKATSUBO, N., KOJIMA, H., KIKUCHI, K., NAGOSHI, H., HIRATA, Y., MAEDA, D., IMAI, Y., IRIMURA, T. & NAGANO, T. 1998. Direct evidence of nitric oxide production from bovine aortic endothelial cells using new fluorescence indicators: diaminofluoresceins. *FEBS Lett,* 427**,** 263-6.

NARANJO, A., SOKKA, T., DESCALZO, M. A., CALVO-ALEN, J., HORSLEV-PETERSEN, K., LUUKKAINEN, R. K., COMBE, B., BURMESTER, G. R., DEVLIN, J., FERRACCIOLI, G., MORELLI, A., HOEKSTRA, M., MAJDAN, M., SADKIEWICZ, S., BELMONTE, M., HOLMQVIST, A. C., CHOY, E., TUNC, R., DIMIC, A., BERGMAN, M., TOLOZA, S. & PINCUS, T. 2008. Cardiovascular disease in patients with rheumatoid arthritis: results from the QUEST-RA study. *Arthritis Res Ther,* 10**,** R30.

NAWROTH, P. P., BANK, I., HANDLEY, D., CASSIMERIS, J., CHESS, L. & STERN, D. 1986. Tumor necrosis factor/cachectin interacts with endothelial cell receptors to induce release of interleukin 1. *J Exp Med,* 163**,** 1363-75.

NEGISHI, T., CHIK, C. L. & HO, A. K. 1998. Ceramide selectively inhibits calcium-mediated potentiation of beta-adrenergic-stimulated cyclic nucleotide accumulation in rat pinealocytes. *Biochem Biophys Res Commun,* 244**,** 57-61.

NELSON, J. C., JIANG, X. C., TABAS, I., TALL, A. & SHEA, S. 2006. Plasma sphingomyelin and subclinical atherosclerosis: findings from the multi-ethnic study of atherosclerosis. *Am J Epidemiol,* 163**,** 903-12.

NI, X. & MORALES, C. R. 2006. The lysosomal trafficking of acid sphingomyelinase is mediated by sortilin and mannose 6-phosphate receptor. *Traffic,* 7**,** 889-902.

NICOLA, P. J., MARADIT-KREMERS, H., ROGER, V. L., JACOBSEN, S. J., CROWSON, C. S., BALLMAN, K. V. & GABRIEL, S. E. 2005. The risk of congestive heart failure in rheumatoid arthritis: a population-based study over 46 years. *Arthritis Rheum,* 52**,** 412-20.

NILIUS, B. & DROOGMANS, G. 2001. Ion channels and their functional role in vascular endothelium. *Physiol Rev,* 81**,** 1415-59.

NILSEN, E. M., JOHANSEN, F. E., JAHNSEN, F. L., LUNDIN, K. E., SCHOLZ, T., BRANDTZAEG, P. & HARALDSEN, G. 1998. Cytokine profiles of cultured microvascular endothelial cells from the human intestine. *Gut,* 42**,** 635-42.

NIMMEGEERS, S., SIPS, P., BUYS, E., BROUCKAERT, P. & VAN DE VOORDE, J. 2007. Functional role of the soluble guanylyl cyclase alpha(1) subunit in vascular smooth muscle relaxation. *Cardiovasc Res,* 76**,** 149-59.

NORONHA, I. L., KRUGER, C., ANDRASSY, K., RITZ, E. & WALDHERR, R. 1993. In situ production of TNF-alpha, IL-1 beta and IL-2R in ANCA-positive glomerulonephritis. *Kidney Int,* 43**,** 682-92.

NOTO, N., OKADA, T., KARASAWA, K., AYUSAWA, M., SUMITOMO, N., HARADA, K. & MUGISHIMA, H. 2009. Age-related acceleration of endothelial dysfunction and subclinical atherosclerosis in subjects with coronary artery lesions after Kawasaki disease. *Pediatr Cardiol,* 30**,** 262-8.

OGRETMEN, B. & HANNUN, Y. A. 2004. Biologically active sphingolipids in cancer pathogenesis and treatment. *Nat Rev Cancer,* 4**,** 604-16.

ORAL, H., DORN, G. W., 2ND & MANN, D. L. 1997. Sphingosine mediates the immediate negative inotropic effects of tumor necrosis factor-alpha in the adult mammalian cardiac myocyte. *J Biol Chem,* 272**,** 4836-42.

OZGEN, U., SAVASAN, S., BUCK, S. & RAVINDRANATH, Y. 2000. Comparison of DiOC(6)(3) uptake and annexin V labeling for quantification of apoptosis in leukemia cells and non-malignant T lymphocytes from children. *Cytometry,* 42**,** 74-8.

PAGAN, J. K., WYLIE, F. G., JOSEPH, S., WIDBERG, C., BRYANT, N. J., JAMES, D. E. & STOW, J. L. 2003. The t-SNARE syntaxin 4 is regulated during macrophage activation to function in membrane traffic and cytokine secretion. *Curr Biol,* 13**,** 156-60.

PAGNOUX, C., SEROR, R., HENEGAR, C., MAHR, A., COHEN, P., LE GUERN, V., BIENVENU, B., MOUTHON, L. & GUILLEVIN, L. 2010. Clinical features and outcomes in 348 patients with polyarteritis nodosa: a systematic retrospective study of patients diagnosed between 1963 and 2005 and entered into the French Vasculitis Study Group Database. *Arthritis Rheum,* 62**,** 616-26.

PALEOLOG, E. M., DELASALLE, S. A., BUURMAN, W. A. & FELDMANN, M. 1994. Functional activities of receptors for tumor necrosis factor-alpha on human vascular endothelial cells. *Blood,* 84**,** 2578-90.

PAREKH, A. B. 2008a. Ca2+ microdomains near plasma membrane Ca2+ channels: impact on cell function. *J Physiol,* 586**,** 3043-54.

PAREKH, A. B. 2008b. Store-operated channels: mechanisms and function. *J Physiol,* 586**,** 3033.

PAREKH, A. B. & PENNER, R. 1995. Depletion-activated calcium current is inhibited by protein kinase in RBL-2H3 cells. *Proc Natl Acad Sci U S A,* 92**,** 7907-11.

PAREKH, A. B. & PENNER, R. 1997. Store depletion and calcium influx. *Physiol Rev,* 77**,** 901-30.

PARK, C. Y., HOOVER, P. J., MULLINS, F. M., BACHHAWAT, P., COVINGTON, E. D., RAUNSER, S., WALZ, T., GARCIA, K. C., DOLMETSCH, R. E. & LEWIS, R. S. 2009a. STIM1 clusters and activates CRAC channels via direct binding of a cytosolic domain to Orai1. *Cell,* 136**,** 876-90.

PARK, J. Y., SHIN, H. K., CHOI, Y. W., LEE, Y. J., BAE, S. S., HAN, J. & KIM, C. D. 2009b. Gomisin A induces Ca2+-dependent activation of eNOS in human coronary artery endothelial cells. *J Ethnopharmacol,* 125**,** 291-6.

PASCERI, V. & YEH, E. T. 1999. A tale of two diseases: atherosclerosis and rheumatoid arthritis. *Circulation,* 100**,** 2124-6.

PAVOINE, C. & PECKER, F. 2009. Sphingomyelinases: their regulation and roles in cardiovascular pathophysiology. *Cardiovasc Res,* 82**,** 175-83.

PERNEGER, T. 1998. What's wrong with Bonferroni adjustments. *British Medical Journal,* 316**,** 1236-1238.

PETROVIC-RACKOV, L. & PEJNOVIC, N. 2006. Clinical significance of IL-18, IL-15, IL-12 and TNF-alpha measurement in rheumatoid arthritis. *Clin Rheumatol,* 25**,** 448-52.

PINCUS, T. & CALLAHAN, L. F. 1993. What is the natural history of rheumatoid arthritis? *Rheum Dis Clin North Am,* 19**,** 123-51.

POPA, C., NETEA, M. G., VAN RIEL, P. L., VAN DER MEER, J. W. & STALENHOEF, A. F. 2007. The role of TNF-alpha in chronic inflammatory conditions, intermediary metabolism, and cardiovascular risk. *J Lipid Res,* 48**,** 751-62.

POPA, C., VAN TITS, L. J., BARRERA, P., LEMMERS, H. L., VAN DEN HOOGEN, F. H., VAN RIEL, P. L., RADSTAKE, T. R., NETEA, M. G., ROEST, M. & STALENHOEF, A. F. 2009. Anti-inflammatory therapy with tumour necrosis factor alpha inhibitors improves high-density lipoprotein cholesterol antioxidative capacity in rheumatoid arthritis patients. *Ann Rheum Dis,* 68**,** 868-72.

PORTMAN, O. W. & ALEXANDER, M. 1970. Metabolism of sphingolipids by normal and atherosclerotic aorta of squirrel monkeys. *J Lipid Res,* 11**,** 23-30.

POTT, C., STEINRITZ, D., BOLCK, B., MEHLHORN, U., BRIXIUS, K., SCHWINGER, R. H. & BLOCH, W. 2006. eNOS translocation but not eNOS phosphorylation is dependent on intracellular Ca2+ in human atrial myocardium. *Am J Physiol Cell Physiol,* 290**,** C1437-45.

PRESTA, A., LIU, J., SESSA, W. C. & STUEHR, D. J. 1997. Substrate binding and calmodulin binding to endothelial nitric oxide synthase coregulate its enzymatic activity. *Nitric Oxide,* 1**,** 74-87.

PUTNEY, J. W. & BIRD, G. S. 2008. Cytoplasmic calcium oscillations and store-operated calcium influx. *J Physiol,* 586**,** 3055-9.

PUTNEY, J. W., JR. 1986. A model for receptor-regulated calcium entry. *Cell Calcium,* 7**,** 1-12.

QIU, H., EDMUNDS, T., BAKER-MALCOLM, J., KAREY, K. P., ESTES, S., SCHWARZ, C., HUGHES, H. & VAN PATTEN, S. M. 2003. Activation of human acid sphingomyelinase through modification or deletion of C-terminal cysteine. *J Biol Chem,* 278**,** 32744-52.

QUINTERN, L. E., SCHUCHMAN, E. H., LEVRAN, O., SUCHI, M., FERLINZ, K., REINKE, H., SANDHOFF, K. & DESNICK, R. J. 1989a. Isolation of cDNA clones encoding human acid sphingomyelinase: occurrence of alternatively processed transcripts. *EMBO J,* 8**,** 2469-73.

QUINTERN, L. E., ZENK, T. S. & SANDHOFF, K. 1989b. The urine from patients with peritonitis as a rich source for purifying human acid sphingomyelinase and other lysosomal enzymes. *Biochim Biophys Acta,* 1003**,** 121-4.

RAINES, M. A., KOLESNICK, R. N. & GOLDE, D. W. 1993. Sphingomyelinase and ceramide activate mitogen-activated protein kinase in myeloid HL-60 cells. *J Biol Chem,* 268**,** 14572-5.

RAMAN, C. S., LI, H., MARTASEK, P., KRAL, V., MASTERS, B. S. & POULOS, T. L. 1998. Crystal structure of constitutive endothelial nitric oxide synthase: a paradigm for pterin function involving a novel metal center. *Cell,* 95**,** 939-50.

RASHIDI, A., SEHGAL, A. R., RAHMAN, M. & O'CONNOR, A. S. 2008. The case for chronic kidney disease, diabetes mellitus, and myocardial infarction being equivalent risk factors for cardiovascular mortality in patients older than 65 years. *Am J Cardiol,* 102**,** 1668-73.

RATHEL, T. R., LEIKERT, J. J., VOLLMAR, A. M. & DIRSCH, V. M. 2003. Application of 4,5-diaminofluorescein to reliably measure nitric oxide released from endothelial cells in vitro. *Biol Proced Online,* 5**,** 136-142.

RAVI, K., BRENNAN, L. A., LEVIC, S., ROSS, P. A. & BLACK, S. M. 2004. S-nitrosylation of endothelial nitric oxide synthase is associated with monomerization and decreased enzyme activity. *Proc Natl Acad Sci U S A,* 101**,** 2619-24.

RAY, J. G., MAMDANI, M. M. & GEERTS, W. H. 2005. Giant cell arteritis and cardiovascular disease in older adults. *Heart,* 91**,** 324-8.

RAZA, K., CARRUTHERS, D. M., STEVENS, R., FILER, A. D., TOWNEND, J. N. & BACON, P. A. 2006. Infliximab leads to a rapid but transient improvement in endothelial function in patients with primary systemic vasculitis. *Ann Rheum Dis,* 65**,** 946-8.

RAZA, K., THAMBYRAJAH, J., TOWNEND, J. N., EXLEY, A. R., HORTAS, C., FILER, A., CARRUTHERS, D. M. & BACON, P. A. 2000. Suppression of inflammation in primary systemic vasculitis restores vascular endothelial function: lessons for atherosclerotic disease? *Circulation,* 102**,** 1470-2.

REEFMAN, E., KAY, J. G., WOOD, S. M., OFFENHAUSER, C., BROWN, D. L., ROY, S., STANLEY, A. C., LOW, P. C., MANDERSON, A. P. & STOW, J. L. 2010. Cytokine secretion is distinct from secretion of cytotoxic granules in NK cells. *J Immunol,* 184**,** 4852-62.

REINHOLD-KELLER, E., HERLYN, K., WAGNER-BASTMEYER, R. & GROSS, W. L. 2005. Stable incidence of primary systemic vasculitides over five years: results from the German vasculitis register. *Arthritis Rheum,* 53**,** 93-9.

REUMAUX, D., KUIJPERS, T. W., HORDIJK, P. L., DUTHILLEUL, P. & ROOS, D. 2003. Involvement of Fcgamma receptors and beta2 integrins in neutrophil activation by anti-proteinase-3 or anti-myeloperoxidase antibodies. *Clin Exp Immunol,* 134**,** 344-50.

RIDKER, P. M., DANIELSON, E., FONSECA, F. A., GENEST, J., GOTTO, A. M., JR., KASTELEIN, J. J., KOENIG, W., LIBBY, P., LORENZATTI, A. J., MACFADYEN, J. G., NORDESTGAARD, B. G., SHEPHERD, J., WILLERSON, J. T. & GLYNN, R. J. 2008. Rosuvastatin to prevent vascular events in men and women with elevated C-reactive protein. *N Engl J Med,* 359**,** 2195-207.

ROMITI, E., VASTA, V., MEACCI, E., FARNARARO, M., LINKE, T., FERLINZ, K., SANDHOFF, K. & BRUNI, P. 2000. Characterization of sphingomyelinase activity released by thrombin-stimulated platelets. *Mol Cell Biochem,* 205**,** 75-81.

ROSS, R. 1999. Atherosclerosis is an inflammatory disease. *Am Heart J,* 138**,** S419-20.

RUGER, B., GIUREA, A., WANIVENHAUS, A. H., ZEHETGRUBER, H., HOLLEMANN, D., YANAGIDA, G., GROGER, M., PETZELBAUER, P., SMOLEN, J. S., HOECKER, P. & FISCHER, M. B. 2004. Endothelial precursor cells in the synovial tissue of patients with rheumatoid arthritis and osteoarthritis. *Arthritis Rheum,* 50**,** 2157-66.

SAMAD, F., HESTER, K. D., YANG, G., HANNUN, Y. A. & BIELAWSKI, J. 2006. Altered adipose and plasma sphingolipid metabolism in obesity: a potential mechanism for cardiovascular and metabolic risk. *Diabetes,* 55**,** 2579-87.

SANDOVAL, R., MALIK, A. B., MINSHALL, R. D., KOUKLIS, P., ELLIS, C. A. & TIRUPPATHI, C. 2001. Ca(2+) signalling and PKCalpha activate increased endothelial permeability by disassembly of VE-cadherin junctions. *J Physiol,* 533**,** 433-45.

SANGLE, S. R., DAVIES, R. J., MORA, M., BARON, M. A., HUGHES, G. R. & D'CRUZ, D. P. 2008. Ankle-brachial pressure index: a simple tool for assessing cardiovascular risk in patients with systemic vasculitis. *Rheumatology (Oxford),* 47**,** 1058-60.

SANTANA, A. N. 2009. Circulating endothelial progenitor cells in ANCA-associated vasculitis: the light at the end of the tunnel? *Rheumatology (Oxford),* 48**,** 1183-4.

SANTANA, P., PENA, L. A., HAIMOVITZ-FRIEDMAN, A., MARTIN, S., GREEN, D., MCLOUGHLIN, M., CORDON-CARDO, C., SCHUCHMAN, E. H., FUKS, Z. & KOLESNICK, R. 1996. Acid sphingomyelinase-deficient human lymphoblasts and mice are defective in radiation-induced apoptosis. *Cell,* 86**,** 189-99.

SARBAN, S., KOCYIGIT, A., YAZAR, M. & ISIKAN, U. E. 2005. Plasma total antioxidant capacity, lipid peroxidation, and erythrocyte antioxidant enzyme activities in patients with rheumatoid arthritis and osteoarthritis. *Clin Biochem,* 38**,** 981-6.

SASAKI, T., HAZEKI, K., HAZEKI, O., UI, M. & KATADA, T. 1995. Permissive effect of ceramide on growth factor-induced cell proliferation. *Biochem J,* 311 ( Pt 3)**,** 829-34.

SATHISHKUMAR, S., BOYANOVSKY, B., KARAKASHIAN, A. A., ROZENOVA, K., GILTIAY, N. V., KUDRIMOTI, M., MOHIUDDIN, M., AHMED, M. M. & NIKOLOVA-KARAKASHIAN, M. 2005. Elevated sphingomyelinase activity and ceramide concentration in serum of patients undergoing high dose spatially fractionated radiation treatment: implications for endothelial apoptosis. *Cancer Biol Ther,* 4**,** 979-86.

SAULSBURY, F. T. 1999. Henoch-Schonlein purpura in children. Report of 100 patients and review of the literature. *Medicine (Baltimore),* 78**,** 395-409.

SAVAGE, C. O. 2002. The evolving pathogenesis of systemic vasculitis. *Clin Med,* 2**,** 458-64.

SAWADA, M., NAKASHIMA, S., KIYONO, T., YAMADA, J., HARA, S., NAKAGAWA, M., SHINODA, J. & SAKAI, N. 2002. Acid sphingomyelinase activation requires caspase-8 but not p53 nor reactive oxygen species during Fas-induced apoptosis in human glioma cells. *Exp Cell Res,* 273**,** 157-68.

SCHACHINGER, V., BRITTEN, M. B. & ZEIHER, A. M. 2000. Prognostic impact of coronary vasodilator dysfunction on adverse long-term outcome of coronary heart disease. *Circulation,* 101**,** 1899-906.

SCHEEL-TOELLNER, D., WANG, K., ASSI, L. K., WEBB, P. R., CRADDOCK, R. M., SALMON, M. & LORD, J. M. 2004. Clustering of death receptors in lipid rafts initiates neutrophil spontaneous apoptosis. *Biochem Soc Trans,* 32**,** 679-81.

SCHISSEL, S. L., JIANG, X., TWEEDIE-HARDMAN, J., JEONG, T., CAMEJO, E. H., NAJIB, J., RAPP, J. H., WILLIAMS, K. J. & TABAS, I. 1998a. Secretory sphingomyelinase, a product of the acid sphingomyelinase gene, can hydrolyze atherogenic lipoproteins at neutral pH. Implications for atherosclerotic lesion development. *J Biol Chem,* 273**,** 2738-46.

SCHISSEL, S. L., KEESLER, G. A., SCHUCHMAN, E. H., WILLIAMS, K. J. & TABAS, I. 1998b. The cellular trafficking and zinc dependence of secretory and lysosomal sphingomyelinase, two products of the acid sphingomyelinase gene. *J Biol Chem,* 273**,** 18250-9.

SCHISSEL, S. L., SCHUCHMAN, E. H., WILLIAMS, K. J. & TABAS, I. 1996a. Zn2+-stimulated sphingomyelinase is secreted by many cell types and is a product of the acid sphingomyelinase gene. *J Biol Chem,* 271**,** 18431-6.

SCHISSEL, S. L., TWEEDIE-HARDMAN, J., RAPP, J. H., GRAHAM, G., WILLIAMS, K. J. & TABAS, I. 1996b. Rabbit aorta and human atherosclerotic lesions hydrolyze the sphingomyelin of

retained low-density lipoprotein. Proposed role for arterial-wall sphingomyelinase in subendothelial retention and aggregation of atherogenic lipoproteins. *J Clin Invest,* 98**,** 1455-64.

SCHMIDT, T. S. & ALP, N. J. 2007. Mechanisms for the role of tetrahydrobiopterin in endothelial function and vascular disease. *Clin Sci (Lond),* 113**,** 47-63.

SCHMITZ-HUEBNER, U. & KNOP, J. 1984. Evidence for an endothelial cell dysfunction in association with Behcet's disease. *Thromb Res,* 34**,** 277-85.

SCHNEIDER, P. B. & KENNEDY, E. P. 1967. Sphingomyelinase in normal human spleens and in spleens from subjects with Niemann-Pick disease. *J Lipid Res,* 8**,** 202-9.

SCHNEIDER-BRACHERT, W., TCHIKOV, V., NEUMEYER, J., JAKOB, M., WINOTO-MORBACH, S., HELD-FEINDT, J., HEINRICH, M., MERKEL, O., EHRENSCHWENDER, M., ADAM, D., MENTLEIN, R., KABELITZ, D. & SCHUTZE, S. 2004. Compartmentalization of TNF receptor 1 signaling: internalized TNF receptosomes as death signaling vesicles. *Immunity,* 21**,** 415-28.

SCHNITTLER, H. J. 1998. Structural and functional aspects of intercellular junctions in vascular endothelium. *Basic Res Cardiol,* 93 Suppl 3**,** 30-9.

SCHUBERT, K. M., SCHEID, M. P. & DURONIO, V. 2000. Ceramide inhibits protein kinase B/Akt by promoting dephosphorylation of serine 473. *J Biol Chem,* 275**,** 13330-5.

SCHUCHMAN, E. H. 2010. Acid sphingomyelinase, cell membranes and human disease: lessons from Niemann-Pick disease. *FEBS Lett,* 584**,** 1895-900.

SCHUCHMAN, E. H., LEVRAN, O., PEREIRA, L. V. & DESNICK, R. J. 1992. Structural organization and complete nucleotide sequence of the gene encoding human acid sphingomyelinase (SMPD1). *Genomics,* 12**,** 197-205.

SCHUCHMAN, E. H., SUCHI, M., TAKAHASHI, T., SANDHOFF, K. & DESNICK, R. J. 1991. Human acid sphingomyelinase. Isolation, nucleotide sequence and expression of the full-length and alternatively spliced cDNAs. *J Biol Chem,* 266**,** 8531-9.

SCHUTZE, S., MACHLEIDT, T., ADAM, D., SCHWANDNER, R., WIEGMANN, K., KRUSE, M. L., HEINRICH, M., WICKEL, M. & KRONKE, M. 1999. Inhibition of receptor internalization by monodansylcadaverine selectively blocks p55 tumor necrosis factor receptor death domain signaling. *J Biol Chem,* 274**,** 10203-12.

SCHUTZE, S., POTTHOFF, K., MACHLEIDT, T., BERKOVIC, D., WIEGMANN, K. & KRONKE, M. 1992. TNF activates NF-kappa B by phosphatidylcholine-specific phospholipase C-induced "acidic" sphingomyelin breakdown. *Cell,* 71**,** 765-76.

SCHWANDNER, R., WIEGMANN, K., BERNARDO, K., KREDER, D. & KRONKE, M. 1998. TNF receptor death domain-associated proteins TRADD and FADD signal activation of acid sphingomyelinase. *J Biol Chem,* 273**,** 5916-22.

SCOTT, D. L. 2000. Prognostic factors in early rheumatoid arthritis. *Rheumatology (Oxford),* 39 Suppl 1**,** 24-9.

SEGUI, B., ANDRIEU-ABADIE, N., ADAM-KLAGES, S., MEILHAC, O., KREDER, D., GARCIA, V., BRUNO, A. P., JAFFREZOU, J. P., SALVAYRE, R., KRONKE, M. & LEVADE, T. 1999. CD40

signals apoptosis through FAN-regulated activation of the sphingomyelin-ceramide pathway. *J Biol Chem,* 274**,** 37251-8.

SEPAROVIC, D., PINK, J. J., OLEINICK, N. A., KESTER, M., BOOTHMAN, D. A., MCLOUGHLIN, M., PENA, L. A. & HAIMOVITZ-FRIEDMAN, A. 1999. Niemann-Pick human lymphoblasts are resistant to phthalocyanine 4-photodynamic therapy-induced apoptosis. *Biochem Biophys Res Commun,* 258**,** 506-12.

SEVEN, A., GUZEL, S., ASLAN, M. & HAMURYUDAN, V. 2008. Lipid, protein, DNA oxidation and antioxidant status in rheumatoid arthritis. *Clin Biochem,* 41**,** 538-43.

SEYAHI, E., UGURLU, S., CUMALI, R., BALCI, H., SEYAHI, N., YURDAKUL, S. & YAZICI, H. 2006. Atherosclerosis in Takayasu arteritis. *Ann Rheum Dis,* 65**,** 1202-7.

SHAH, C., YANG, G., LEE, I., BIELAWSKI, J., HANNUN, Y. A. & SAMAD, F. 2008. Protection from high fat diet-induced increase in ceramide in mice lacking plasminogen activator inhibitor 1. *J Biol Chem,* 283**,** 13538-48.

SHAUL, P. W., SMART, E. J., ROBINSON, L. J., GERMAN, Z., YUHANNA, I. S., YING, Y., ANDERSON, R. G. & MICHEL, T. 1996. Acylation targets endothelial nitric-oxide synthase to plasmalemmal caveolae. *J Biol Chem,* 271**,** 6518-22.

SHIMOKAWA, H., FLAVAHAN, N. A. & VANHOUTTE, P. M. 1991. Loss of endothelial pertussis toxin-sensitive G protein function in atherosclerotic porcine coronary arteries. *Circulation,* 83**,** 652-60.

SHIREMAN, P. K. & PEARCE, W. H. 1996. Endothelial cell function: biologic and physiologic functions in health and disease. *AJR Am J Roentgenol,* 166**,** 7-13.

SHOENFELD, Y., GERLI, R., DORIA, A., MATSUURA, E., CERINIC, M. M., RONDA, N., JARA, L. J., ABU-SHAKRA, M., MERONI, P. L. & SHERER, Y. 2005. Accelerated atherosclerosis in autoimmune rheumatic diseases. *Circulation,* 112**,** 3337-47.

SIDDHANTA, U., PRESTA, A., FAN, B., WOLAN, D., ROUSSEAU, D. L. & STUEHR, D. J. 1998. Domain swapping in inducible nitric-oxide synthase. Electron transfer occurs between flavin and heme groups located on adjacent subunits in the dimer. *J Biol Chem,* 273**,** 18950-8.

SIDIROPOULOS, P. I., SIAKKA, P., PAGONIDIS, K., RAPTOPOULOU, A., KRITIKOS, H., TSETIS, D. & BOUMPAS, D. T. 2009. Sustained improvement of vascular endothelial function during anti-TNFalpha treatment in rheumatoid arthritis patients. *Scand J Rheumatol,* 38**,** 6-10.

SIVALINGAM, S. P., THUMBOO, J., VASOO, S., THIO, S. T., TSE, C. & FONG, K. Y. 2007. In vivo pro- and anti-inflammatory cytokines in normal and patients with rheumatoid arthritis. *Ann Acad Med Singapore,* 36**,** 96-9.

SMITH, E. L. & SCHUCHMAN, E. H. 2008a. Acid sphingomyelinase overexpression enhances the antineoplastic effects of irradiation in vitro and in vivo. *Mol Ther,* 16**,** 1565-71.

SMITH, E. L. & SCHUCHMAN, E. H. 2008b. The unexpected role of acid sphingomyelinase in cell death and the pathophysiology of common diseases. *FASEB J,* 22**,** 3419-31.

SMOLEN, J. S., BEAULIEU, A., RUBBERT-ROTH, A., RAMOS-REMUS, C., ROVENSKY, J., ALECOCK, E., WOODWORTH, T. & ALTEN, R. 2008. Effect of interleukin-6 receptor inhibition with

tocilizumab in patients with rheumatoid arthritis (OPTION study): a double-blind, placebo-controlled, randomised trial. *Lancet,* 371**,** 987-97.

SODERDAHL, T., ENOKSSON, M., LUNDBERG, M., HOLMGREN, A., OTTERSEN, O. P., ORRENIUS, S., BOLCSFOLDI, G. & COTGREAVE, I. A. 2003. Visualization of the compartmentalization of glutathione and protein-glutathione mixed disulfides in cultured cells. *FASEB J,* 17**,** 124-6.

SOLOMON, D. H., KARLSON, E. W., RIMM, E. B., CANNUSCIO, C. C., MANDL, L. A., MANSON, J. E., STAMPFER, M. J. & CURHAN, G. C. 2003. Cardiovascular morbidity and mortality in women diagnosed with rheumatoid arthritis. *Circulation,* 107**,** 1303-7.

SOT, J., BAGATOLLI, L. A., GONI, F. M. & ALONSO, A. 2006. Detergent-resistant, ceramide-enriched domains in sphingomyelin/ceramide bilayers. *Biophys J,* 90**,** 903-14.

SPENCE, M. W., BYERS, D. M., PALMER, F. B. & COOK, H. W. 1989. A new Zn2+-stimulated sphingomyelinase in fetal bovine serum. *J Biol Chem,* 264**,** 5358-63.

SPIEGEL, S. & MILSTIEN, S. 2003. Sphingosine-1-phosphate: an enigmatic signalling lipid. *Nat Rev Mol Cell Biol,* 4**,** 397-407.

STAHMANN, N., WOODS, A., CARLING, D. & HELLER, R. 2006. Thrombin activates AMP-activated protein kinase in endothelial cells via a pathway involving Ca2+/calmodulin-dependent protein kinase kinase beta. *Mol Cell Biol,* 26**,** 5933-45.

STANLEY, A. C. & LACY, P. 2010. Pathways for cytokine secretion. *Physiology (Bethesda),* 25**,** 218-29.

STATHOPULOS, P. B., ZHENG, L., LI, G. Y., PLEVIN, M. J. & IKURA, M. 2008. Structural and mechanistic insights into STIM1-mediated initiation of store-operated calcium entry. *Cell,* 135**,** 110-22.

STOFFEL, W., JENKE, B., HOLZ, B., BINCZEK, E., GUNTER, R. H., KNIFKA, J., KOEBKE, J. & NIEHOFF, A. 2007. Neutral sphingomyelinase (SMPD3) deficiency causes a novel form of chondrodysplasia and dwarfism that is rescued by Col2A1-driven smpd3 transgene expression. *Am J Pathol,* 171**,** 153-61.

STOW, J. L., LOW, P. C., OFFENHAUSER, C. & SANGERMANI, D. 2009. Cytokine secretion in macrophages and other cells: pathways and mediators. *Immunobiology,* 214**,** 601-12.

SUPPIAH, R. J., A. BATRA, R. FLOSSMANN, O. HAPRER, L. HOGLUND, P. JAVAID, MK. JAYNE, D. MUKHTYAR, C. WESTMAN, K. DAVIS, JC JR. HOFFMAN, GS. MCCUNE, WJ. MERKEL, PA. ST CLAIR, EW. SEO, P. SPIERA, R. STONE, JH. LUQMANI, R. 2011. A model to predict cardiovascular events in patients with newly diagnosed Wegener's granulomatosis and microscopic polyangiitis. *Arthritis Care Res (Hoboken),* 63**,** 588-596.

SURKS, H. K., MOCHIZUKI, N., KASAI, Y., GEORGESCU, S. P., TANG, K. M., ITO, M., LINCOLN, T. M. & MENDELSOHN, M. E. 1999. Regulation of myosin phosphatase by a specific interaction with cGMP- dependent protein kinase Ialpha. *Science,* 286**,** 1583-7.

SZEKANECZ, Z., BESENYEI, T., SZENTPETERY, A. & KOCH, A. E. 2010. Angiogenesis and vasculogenesis in rheumatoid arthritis. *Curr Opin Rheumatol,* 22**,** 299-306.

TABAS, I. 1999. Secretory sphingomyelinase. *Chem Phys Lipids,* 102**,** 123-30.

TABAS, I., LI, Y., BROCIA, R. W., XU, S. W., SWENSON, T. L. & WILLIAMS, K. J. 1993. Lipoprotein lipase and sphingomyelinase synergistically enhance the association of atherogenic lipoproteins with smooth muscle cells and extracellular matrix. A possible mechanism for low density lipoprotein and lipoprotein(a) retention and macrophage foam cell formation. *J Biol Chem,* 268**,** 20419-32.

TABAS, I., WILLIAMS, K. J. & BOREN, J. 2007. Subendothelial lipoprotein retention as the initiating process in atherosclerosis: update and therapeutic implications. *Circulation,* 116**,** 1832-44.

TAKAHASHI, I., TAKAHASHI, T., MIKAMI, T., KOMATSU, M., OHURA, T., SCHUCHMAN, E. H. & TAKADA, G. 2005. Acid sphingomyelinase: relation of 93lysine residue on the ratio of intracellular to secreted enzyme activity. *Tohoku J Exp Med,* 206**,** 333-40.

TAKAHASHI, T., ABE, T., SATO, T., MIURA, K., TAKAHASHI, I., YANO, M., WATANABE, A., IMASHUKU, S. & TAKADA, G. 2002. Elevated sphingomyelinase and hypercytokinemia in hemophagocytic lymphohistiocytosis. *J Pediatr Hematol Oncol,* 24**,** 401-4.

TAKEMURA, H., HUGHES, A. R., THASTRUP, O. & PUTNEY, J. W., JR. 1989. Activation of calcium entry by the tumor promoter thapsigargin in parotid acinar cells. Evidence that an intracellular calcium pool and not an inositol phosphate regulates calcium fluxes at the plasma membrane. *J Biol Chem,* 264**,** 12266-71.

TAM, C., IDONE, V., DEVLIN, C., FERNANDES, M. C., FLANNERY, A., HE, X., SCHUCHMAN, E., TABAS, I. & ANDREWS, N. W. 2010. Exocytosis of acid sphingomyelinase by wounded cells promotes endocytosis and plasma membrane repair. *J Cell Biol,* 189**,** 1027-38.

TANG, W. H., TONG, W., TROUGHTON, R. W., MARTIN, M. G., SHRESTHA, K., BOROWSKI, A., JASPER, S., HAZEN, S. L. & KLEIN, A. L. 2007. Prognostic value and echocardiographic determinants of plasma myeloperoxidase levels in chronic heart failure. *J Am Coll Cardiol,* 49**,** 2364-70.

TANI, M., ITO, M. & IGARASHI, Y. 2007. Ceramide/sphingosine/sphingosine 1-phosphate metabolism on the cell surface and in the extracellular space. *Cell Signal,* 19**,** 229-37.

TELLIER, E., NEGRE-SALVAYRE, A., BOCQUET, B., ITOHARA, S., HANNUN, Y. A., SALVAYRE, R. & AUGE, N. 2007. Role for furin in tumor necrosis factor alpha-induced activation of the matrix metalloproteinase/sphingolipid mitogenic pathway. *Mol Cell Biol,* 27**,** 2997-3007.

TESAR, V., MASEK, Z., RYCHLIK, I., MERTA, M., BARTUNKOVA, J., STEJSKALOVA, A., ZABKA, J., JANATKOVA, I., FUCIKOVA, T., DOSTAL, C. & BECVAR, R. 1998. Cytokines and adhesion molecules in renal vasculitis and lupus nephritis. *Nephrol Dial Transplant,* 13**,** 1662-7.

THERADE-MATHARAN, S., LAEMMEL, E., CARPENTIER, S., OBATA, Y., LEVADE, T., DURANTEAU, J. & VICAUT, E. 2005. Reactive oxygen species production by mitochondria in endothelial cells exposed to reoxygenation after hypoxia and glucose depletion is mediated by ceramide. *Am J Physiol Regul Integr Comp Physiol,* 289**,** R1756-62.

THOMAS, F., BEAN, K., PROVOST, J. C., GUIZE, L. & BENETOS, A. 2001. Combined effects of heart rate and pulse pressure on cardiovascular mortality according to age. *J Hypertens,* 19**,** 863-9.

THORS, B., HALLDORSSON, H., JONSDOTTIR, G. & THORGEIRSSON, G. 2008. Mechanism of thrombin mediated eNOS phosphorylation in endothelial cells is dependent on ATP levels after stimulation. *Biochim Biophys Acta,* 1783**,** 1893-902.

THORS, B., HALLDORSSON, H. & THORGEIRSSON, G. 2004. Thrombin and histamine stimulate endothelial nitric-oxide synthase phosphorylation at Ser1177 via an AMPK mediated pathway independent of PI3K-Akt. *FEBS Lett,* 573**,** 175-80.

TILG, H. & MOSCHEN, A. R. 2008. Inflammatory mechanisms in the regulation of insulin resistance. *Mol Med,* 14**,** 222-31.

TITIEVSKY, A., TITIEVSKAYA, I., PASTERNACK, M., KAILA, K. & TORNQUIST, K. 1998. Sphingosine inhibits voltage-operated calcium channels in GH4C1 cells. *J Biol Chem,* 273**,** 242-7.

TOBOREK, M., BARGER, S. W., MATTSON, M. P., MCCLAIN, C. J. & HENNIG, B. 1995. Role of glutathione redox cycle in TNF-alpha-mediated endothelial cell dysfunction. *Atherosclerosis,* 117**,** 179-88.

TOMIUK, S., HOFMANN, K., NIX, M., ZUMBANSEN, M. & STOFFEL, W. 1998. Cloned mammalian neutral sphingomyelinase: functions in sphingolipid signaling? *Proc Natl Acad Sci U S A,* 95**,** 3638-43.

TORNQUIST, K., MALM, A. M., PASTERNACK, M., KRONQVIST, R., BJORKLUND, S., TUOMINEN, R. & SLOTTE, J. P. 1999. Tumor necrosis factor-alpha, sphingomyelinase, and ceramide inhibit store-operated calcium entry in thyroid FRTL-5 cells. *J Biol Chem,* 274**,** 9370-7.

TRACEY, K. J., FONG, Y., HESSE, D. G., MANOGUE, K. R., LEE, A. T., KUO, G. C., LOWRY, S. F. & CERAMI, A. 1987. Anti-cachectin/TNF monoclonal antibodies prevent septic shock during lethal bacteraemia. *Nature,* 330**,** 662-4.

TSOU, T. C., YEH, S. C., TSAI, F. Y., CHEN, J. W. & CHIANG, H. C. 2007. Glutathione regulation of redox-sensitive signals in tumor necrosis factor-alpha-induced vascular endothelial dysfunction. *Toxicol Appl Pharmacol,* 221**,** 168-78.

TURESSON, C., JACOBSSON, L. & BERGSTROM, U. 1999. Extra-articular rheumatoid arthritis: prevalence and mortality. *Rheumatology (Oxford),* 38**,** 668-74.

TURESSON, C., JACOBSSON, L. T., STURFELT, G., MATTESON, E. L., MATHSSON, L. & RONNELID, J. 2007. Rheumatoid factor and antibodies to cyclic citrullinated peptides are associated with severe extra-articular manifestations in rheumatoid arthritis. *Ann Rheum Dis,* 66**,** 59-64.

TURESSON, C. & MATTESON, E. L. 2009. Vasculitis in rheumatoid arthritis. *Curr Opin Rheumatol,* 21**,** 35-40.

TURESSON, C., O'FALLON, W. M., CROWSON, C. S., GABRIEL, S. E. & MATTESON, E. L. 2002. Occurrence of extraarticular disease manifestations is associated with excess mortality in a community based cohort of patients with rheumatoid arthritis. *J Rheumatol,* 29**,** 62-7.

VAN BLITTERSWIJK, W. J., VAN DER LUIT, A. H., VELDMAN, R. J., VERHEIJ, M. & BORST, J. 2003. Ceramide: second messenger or modulator of membrane structure and dynamics? *Biochem J,* 369**,** 199-211.

VAN DER ZEE, J. M., HEURKENS, A. H., VAN DER VOORT, E. A., DAHA, M. R. & BREEDVELD, F. C. 1991. Characterization of anti-endothelial antibodies in patients with rheumatoid arthritis complicated by vasculitis. *Clin Exp Rheumatol,* 9**,** 589-94.

VAN DOORNUM, S., MCCOLL, G. & WICKS, I. P. 2002. Accelerated atherosclerosis: an extraarticular feature of rheumatoid arthritis? *Arthritis Rheum,* 46**,** 862-73.

VAN DOORNUM, S., MCCOLL, G. & WICKS, I. P. 2005. Tumour necrosis factor antagonists improve disease activity but not arterial stiffness in rheumatoid arthritis. *Rheumatology (Oxford),* 44**,** 1428-32.

VAN LEUVEN, S. I., KASTELEIN, J. J., D'CRUZ, D. P., HUGHES, G. R. & STROES, E. S. 2006. Atherogenesis in rheumatology. *Lupus,* 15**,** 117-21.

VANHOUTTE, P. M., SHIMOKAWA, H., TANG, E. H. & FELETOU, M. 2009. Endothelial dysfunction and vascular disease. *Acta Physiol (Oxf),* 196**,** 193-222.

VAUDO, G., MARCHESI, S., GERLI, R., ALLEGRUCCI, R., GIORDANO, A., SIEPI, D., PIRRO, M., SHOENFELD, Y., SCHILLACI, G. & MANNARINO, E. 2004. Endothelial dysfunction in young patients with rheumatoid arthritis and low disease activity. *Ann Rheum Dis,* 63**,** 31-5.

VENKATARAMAN, K. & FUTERMAN, A. H. 2000. Ceramide as a second messenger: sticky solutions to sticky problems. *Trends Cell Biol,* 10**,** 408-12.

VILLENA, J., HENRIQUEZ, M., TORRES, V., MORAGA, F., DIAZ-ELIZONDO, J., ARREDONDO, C., CHIONG, M., OLEA-AZAR, C., STUTZIN, A., LAVANDERO, S. & QUEST, A. F. 2008. Ceramide-induced formation of ROS and ATP depletion trigger necrosis in lymphoid cells. *Free Radic Biol Med,* 44**,** 1146-60.

VOLLERTSEN, R. S. & CONN, D. L. 1990. Vasculitis associated with rheumatoid arthritis. *Rheum Dis Clin North Am,* 16**,** 445-61.

VON FELDT, J. M. 2008. Premature atherosclerotic cardiovascular disease and systemic lupus erythematosus from bedside to bench. *Bull NYU Hosp Jt Dis,* 66**,** 184-7.

VOSKUYL, A. E., EMEIS, J. J., HAZES, J. M., VAN HOGEZAND, R. A., BIEMOND, I. & BREEDVELD, F. C. 1998a. Levels of circulating cellular fibronectin are increased in patients with rheumatoid vasculitis. *Clin Exp Rheumatol,* 16**,** 429-34.

VOSKUYL, A. E., VAN DUINEN, S. G., ZWINDERMAN, A. H., BREEDVELD, F. C. & HAZES, J. M. 1998b. The diagnostic value of perivascular infiltrates in muscle biopsy specimens for the assessment of rheumatoid vasculitis. *Ann Rheum Dis,* 57**,** 114-7.

WAHE, A., KASMAPOUR, B., SCHMADERER, C., LIEBL, D., SANDHOFF, K., NYKJAER, A., GRIFFITHS, G. & GUTIERREZ, M. G. 2010. Golgi-to-phagosome transport of acid sphingomyelinase and prosaposin is mediated by sortilin. *J Cell Sci,* 123**,** 2502-11.

WANG, P., BA, Z. F. & CHAUDRY, I. H. 1994. Administration of tumor necrosis factor-alpha in vivo depresses endothelium-dependent relaxation. *Am J Physiol,* 266**,** H2535-41.

WATSON, D. J., RHODES, T. & GUESS, H. A. 2003. All-cause mortality and vascular events among patients with rheumatoid arthritis, osteoarthritis, or no arthritis in the UK General Practice Research Database. *J Rheumatol,* 30**,** 1196-202.

WATTS, R., LANE, S., HANSLIK, T., HAUSER, T., HELLMICH, B., KOLDINGSNES, W., MAHR, A., SEGELMARK, M., COHEN-TERVAERT, J. W. & SCOTT, D. 2007. Development and validation of a consensus methodology for the classification of the ANCA-associated vasculitides and polyarteritis nodosa for epidemiological studies. *Ann Rheum Dis,* 66**,** 222-7.

WATTS, R. A. & SCOTT, D. G. 2004. Epidemiology of the vasculitides. *Semin Respir Crit Care Med,* 25**,** 455-64.

WATTS, R. A., SUPPIAH, R., MERKEL, P. A. & LUQMANI, R. 2010. Systemic vasculitis--is it time to reclassify? *Rheumatology (Oxford)*.

WATTS, V. L. & MOTLEY, E. D. 2009. Role of protease-activated receptor-1 in endothelial nitric oxide synthase-Thr495 phosphorylation. *Exp Biol Med (Maywood),* 234**,** 132-9.

WESTEDT, M. L., HERBRINK, P., MOLENAAR, J. L., DE VRIES, E., VERLAAN, P., STIJNEN, T., CATS, A. & LINDEMAN, J. 1985. Rheumatoid factors in rheumatoid arthritis and vasculitis. *Rheumatol Int,* 5**,** 209-14.

WESTERWEEL, P. E. & VERHAAR, M. C. 2009. Endothelial progenitor cell dysfunction in rheumatic disease. *Nat Rev Rheumatol,* 5**,** 332-40.

WIEGMANN, K., SCHUTZE, S., MACHLEIDT, T., WITTE, D. & KRONKE, M. 1994. Functional dichotomy of neutral and acidic sphingomyelinases in tumor necrosis factor signaling. *Cell,* 78**,** 1005-15.

WIEGMANN, K., SCHWANDNER, R., KRUT, O., YEH, W. C., MAK, T. W. & KRONKE, M. 1999. Requirement of FADD for tumor necrosis factor-induced activation of acid sphingomyelinase. *J Biol Chem,* 274**,** 5267-70.

WILLIAMS, J. M., KAMESH, L. & SAVAGE, C. O. 2005. Translating basic science into patient therapy for ANCA-associated small vessel vasculitis. *Clin Sci (Lond),* 108**,** 101-12.

WILLIAMS, K. J. & TABAS, I. 1995. The response-to-retention hypothesis of early atherogenesis. *Arterioscler Thromb Vasc Biol,* 15**,** 551-61.

WILLIAMS, R. O., FELDMANN, M. & MAINI, R. N. 1992. Anti-tumor necrosis factor ameliorates joint disease in murine collagen-induced arthritis. *Proc Natl Acad Sci U S A,* 89**,** 9784-8.

WILLIAMS, R. T., SENIOR, P. V., VAN STEKELENBURG, L., LAYTON, J. E., SMITH, P. J. & DZIADEK, M. A. 2002. Stromal interaction molecule 1 (STIM1), a transmembrane protein with growth suppressor activity, contains an extracellular SAM domain modified by N-linked glycosylation. *Biochim Biophys Acta,* 1596**,** 131-7.

WIMALASUNDERA, R., FEXBY, S., REGAN, L., THOM, S. A. & HUGHES, A. D. 2003. Effect of tumour necrosis factor-alpha and interleukin 1beta on endothelium-dependent relaxation in rat mesenteric resistance arteries in vitro. *Br J Pharmacol,* 138**,** 1285-94.

WISEMAN, H. & HALLIWELL, B. 1996. Damage to DNA by reactive oxygen and nitrogen species: role in inflammatory disease and progression to cancer. *Biochem J,* 313 ( Pt 1)**,** 17-29.

WOLFE, F. & MICHAUD, K. 2004. Heart failure in rheumatoid arthritis: rates, predictors, and the effect of anti-tumor necrosis factor therapy. *Am J Med,* 116**,** 305-11.

WONG, M. L., XIE, B., BEATINI, N., PHU, P., MARATHE, S., JOHNS, A., GOLD, P. W., HIRSCH, E., WILLIAMS, K. J., LICINIO, J. & TABAS, I. 2000. Acute systemic inflammation up-regulates

secretory sphingomyelinase in vivo: a possible link between inflammatory cytokines and atherogenesis. *Proc Natl Acad Sci U S A,* 97**,** 8681-6.

WRIGLEY, B. J., LIP, G. Y. & SHANTSILA, E. 2010. Coronary atherosclerosis in rheumatoid arthritis: could endothelial progenitor cells be the missing link? *J Rheumatol,* 37**,** 479-81.

WU, M. M., BUCHANAN, J., LUIK, R. M. & LEWIS, R. S. 2006. Ca2+ store depletion causes STIM1 to accumulate in ER regions closely associated with the plasma membrane. *J Cell Biol,* 174**,** 803-13.

XIA, Z., LIU, M., WU, Y., SHARMA, V., LUO, T., OUYANG, J. & MCNEILL, J. H. 2006. N-acetylcysteine attenuates TNF-alpha-induced human vascular endothelial cell apoptosis and restores eNOS expression. *Eur J Pharmacol,* 550**,** 134-42.

XING, Z., GAULDIE, J., COX, G., BAUMANN, H., JORDANA, M., LEI, X. F. & ACHONG, M. K. 1998. IL-6 is an antiinflammatory cytokine required for controlling local or systemic acute inflammatory responses. *J Clin Invest,* 101**,** 311-20.

XU, X. X. & TABAS, I. 1991. Sphingomyelinase enhances low density lipoprotein uptake and ability to induce cholesteryl ester accumulation in macrophages. *J Biol Chem,* 266**,** 24849-58.

YANG, J. J., PRESTON, G. A., PENDERGRAFT, W. F., SEGELMARK, M., HEERINGA, P., HOGAN, S. L., JENNETTE, J. C. & FALK, R. J. 2001. Internalization of proteinase 3 is concomitant with endothelial cell apoptosis and internalization of myeloperoxidase with generation of intracellular oxidants. *Am J Pathol,* 158**,** 581-92.

YIU, K. H., WANG, S., MOK, M. Y., OOI, G. C., KHONG, P. L., LAU, C. P., LAI, W. H., WONG, L. Y., LAM, K. F., LAU, C. S. & TSE, H. F. 2010. Role of circulating endothelial progenitor cells in patients with rheumatoid arthritis with coronary calcification. *J Rheumatol,* 37**,** 529-35.

YOSHIZUMI, M., PERRELLA, M. A., BURNETT, J. C., JR. & LEE, M. E. 1993. Tumor necrosis factor downregulates an endothelial nitric oxide synthase mRNA by shortening its half-life. *Circ Res,* 73**,** 205-9.

ZAVADA, J., KIDERYOVA, L., PYTLIK, R., HRUSKOVA, Z. & TESAR, V. 2009. Reduced number of endothelial progenitor cells is predictive of early relapse in anti-neutrophil cytoplasmic antibody-associated vasculitis. *Rheumatology (Oxford),* 48**,** 1197-201.

ZAVADA, J., KIDERYOVA, L., PYTLIK, R., VANKOVA, Z. & TESAR, V. 2008. Circulating endothelial progenitor cells in patients with ANCA-associated vasculitis. *Kidney Blood Press Res,* 31**,** 247-54.

ZEIDAN, Y. H. & HANNUN, Y. A. 2007. Activation of acid sphingomyelinase by protein kinase Cdelta-mediated phosphorylation. *J Biol Chem,* 282**,** 11549-61.

ZEIDAN, Y. H. & HANNUN, Y. A. 2010. The Acid sphingomyelinase/ceramide pathway: biomedical significance and mechanisms of regulation. *Curr Mol Med,* 10**,** 454-66.

ZEIHER, A. M., DREXLER, H., WOLLSCHLAGER, H. & JUST, H. 1991. Endothelial dysfunction of the coronary microvasculature is associated with coronary blood flow regulation in patients with early atherosclerosis. *Circulation,* 84**,** 1984-92.

ZERIMECH, F., HUET, G., BALDUYCK, M. & DEGAND, P. 1993. Cysteine proteinase activity in synovial fluids measured with a centrifugal analyzer. *Clin Chem,* 39**,** 1751-3.

ZHANG, A. Y., TEGGATZ, E. G., ZOU, A. P., CAMPBELL, W. B. & LI, P. L. 2005a. Endostatin uncouples NO and Ca2+ response to bradykinin through enhanced O2*- production in the intact coronary endothelium. *Am J Physiol Heart Circ Physiol,* 288**,** H686-94.

ZHANG, A. Y., YI, F., JIN, S., XIA, M., CHEN, Q. Z., GULBINS, E. & LI, P. L. 2007. Acid sphingomyelinase and its redox amplification in formation of lipid raft redox signaling platforms in endothelial cells. *Antioxid Redox Signal,* 9**,** 817-28.

ZHANG, D. X., YI, F. X., ZOU, A. P. & LI, P. L. 2002. Role of ceramide in TNF-alpha-induced impairment of endothelium-dependent vasorelaxation in coronary arteries. *Am J Physiol Heart Circ Physiol,* 283**,** H1785-94.

ZHANG, D. X., ZOU, A. P. & LI, P. L. 2001. Ceramide reduces endothelium-dependent vasodilation by increasing superoxide production in small bovine coronary arteries. *Circ Res,* 88**,** 824-31.

ZHANG, D. X., ZOU, A. P. & LI, P. L. 2003. Ceramide-induced activation of NADPH oxidase and endothelial dysfunction in small coronary arteries. *Am J Physiol Heart Circ Physiol,* 284**,** H605-12.

ZHANG, H., ZHANG, J., UNGVARI, Z. & ZHANG, C. 2009a. Resveratrol improves endothelial function: role of TNF{alpha} and vascular oxidative stress. *Arterioscler Thromb Vasc Biol,* 29**,** 1164-71.

ZHANG, S. L., YU, Y., ROOS, J., KOZAK, J. A., DEERINCK, T. J., ELLISMAN, M. H., STAUDERMAN, K. A. & CAHALAN, M. D. 2005b. STIM1 is a Ca2+ sensor that activates CRAC channels and migrates from the Ca2+ store to the plasma membrane. *Nature,* 437**,** 902-5.

ZHANG, Y., LI, X., BECKER, K. A. & GULBINS, E. 2009b. Ceramide-enriched membrane domains--structure and function. *Biochim Biophys Acta,* 1788**,** 178-83.

ZHANG, Y., LI, X., CARPINTEIRO, A. & GULBINS, E. 2008. Acid sphingomyelinase amplifies redox signaling in Pseudomonas aeruginosa-induced macrophage apoptosis. *J Immunol,* 181**,** 4247-54.

ZHOU, H., SUMMERS, S. A., BIRNBAUM, M. J. & PITTMAN, R. N. 1998. Inhibition of Akt kinase by cell-permeable ceramide and its implications for ceramide-induced apoptosis. *J Biol Chem,* 273**,** 16568-75.

ZHOU, Y., MANCARELLA, S., WANG, Y., YUE, C., RITCHIE, M., GILL, D. L. & SOBOLOFF, J. 2009. The short N-terminal domains of STIM1 and STIM2 control the activation kinetics of Orai1 channels. *J Biol Chem,* 284**,** 19164-8.

ZOELLNER, H., HOFLER, M., BECKMANN, R., HUFNAGL, P., VANYEK, E., BIELEK, E., WOJTA, J., FABRY, A., LOCKIE, S. & BINDER, B. R. 1996. Serum albumin is a specific inhibitor of apoptosis in human endothelial cells. *J Cell Sci,* 109 ( Pt 10)**,** 2571-80.

ZUMBANSEN, M. & STOFFEL, W. 1997. Tumor necrosis factor alpha activates NF-kappaB in acid sphingomyelinase-deficient mouse embryonic fibroblasts. *J Biol Chem,* 272**,** 10904-9.